Physicochemical
Problems
of Mineral Processing
37 (2003)

Instructions for preparation of manuscripts

It is recommended that the following guidelines be followed by the authors of the manuscripts:

- Original papers dealing with the principles of mineral processing and papers on technological aspects of mineral processing will be published in the journal which appears once a year.
- The manuscript should be sent to the Editor for reviewing before February 15 each year.
- The manuscript should be written in English. For publishing in other languages on approval of the editor is necessary.
- Contributors whose first language is not the language of the manuscript are urged to have their manuscript competently edited prior to submission.
- The manuscript should not exceed 10 pages.
- Two copies of the manuscript along with an electronic should be submitted for publication before April 15.
- There is a 80 USD fee for printing the paper. No fee is required for the authors participating in the Annual Symposium on Physicochemical Problems on Mineral Processing.
- Manuscripts and all correspondence regarding the symposium and journal should be sent to the editor.

Address of the Editorial Office
Wrocław University of Technology
Wybrzeże Wyspiańskiego 27, 50-370 Wrocław, Poland
Institute of Mining Engineering
Laboratory of Mineral Processing

Location of the Editiorial Office:
Pl. Teatralny 2, Wrocław, Poland
Phone: (071) 320 68 79, (071) 320–68–78
Fax: 3448123, telex: 0712254 pwr.pl
andrew@.ig.pwr.wroc.pl
jd@iic.pwr.wroc.pl
http://www.ig.pwr.wroc.pl/conference/conf uk.html

Physicochemical Problems of Mineral Processing 37 (2003)

Z. SADOWSKI
(EDITORS)

WROCŁAW 2003

Editors

Zygmunt Sadowski, Jan Drzymala, Andrzej Łuszczkiewicz

Editional Board

Zofia Blaschke, Wiesław Blaschke, Marian Brożek, Stanisław Chibowski, Witold Charewicz, Tomasz Chmielewski, Beata Cwalina, Janusz Girczys, Andrzej Heim, Jan Hupka, Andrzej Krysztafkiewicz, Janusz Laskowski, Janusz Lekki, Kazimierz Małysa, Pawel Nowak, Andrzej Pomianowski (honorary chairman), Stanisława Sanak-Rydlewska, Jerzy Sablik, Jan Szymanowski, Kazimierz Sztaba (chairman)

Reviewers

postoluk, M. Brożek, W. Charewicz, B. Cwalina, J. Drzymala, T. Farbiszewska, A. Haim, J. Hupka, J. Kowalczyk, A. Krysztafkiewiez, Z. Sadowski, S. Sanak-Rydlewska, A. Skłodowska, A. Sokołowski, J. Szymanowski, T. Tumidajski, P. Wodziński

Technical assistance

Stefan Zawadzki

The papers published in Physicochemical Problems of Minercal Processing are abstracted in Chemical Abstracts, Metals Abstracts, Реферативныи Журал and other sources

ISSN 0137-1282

OFICYNA WYDAWNICZA POLITECHNIKI WROCŁAWSKIEJ, WYBRZEŻE WYSPIAŃSKIEGO 27, 50-370 WROCLAW, POLAND

CONTENTS

Physicochemical Problems of Mineral Processing, 37 (2003) 5-17
Fizykochemiczne Problemy Mineralurgii, 37 (2003) 5-17

Kazimierz St. SZTABA*)

SELECTED PROBLEMS OF DETERMINING THE EFFECTIVENESS OF THE SEPARATION TECHNOLOGICAL PROCESSES OF MINERAL ENGINEERING

Received March 2003, reviewed, and accepted May 15, 2003

Evaluating the rate of reaching the assumed aim of any activity is the ground of verification of correctness of conduct assumed for its implementation. This evaluation is also the basis of verification of the algorithm of this conduct, including its modifying in order to reach the optimum state of the assumed goal. The procedures used for such an evaluation used to be described as a study of effectiveness of activities in question and its result directly as effectiveness. In case of technological processes, including the basic group of operations of mineral engineering, effectiveness is usually determined as a numerically expressed relation of really obtained process results to the results assumed, forecast or theoretically possible to be obtained. The variety of formulations of detailed assumptions of processes occurring in this discipline formulate the need of significant differentiation not only of the methods of evaluating its effectiveness but also precise determination of the very notion of effectiveness in the concrete conditions of implementation of the technological process. The work contains a discussion of this problem.

Key words: technological process, process aim, process effectiveness

BASIC CONDITIONS OF TECHNOLOGICAL PROCESSES, THEIR AIMS AND EVALUATION

Heterogeneity of tasks performed by means of operations and processes (sets of operations)[1] of mineral engineering requires the application of not only a very well developed range of technological procedures based upon the use of numerous properties of the material subjected to processing but also a differentiated approach to

*) Department of Mineral Processing, Environment Protection and Waste Utilization, AGH University, Al. Mickiewicza 30, 30-059 Kraków, Poland; e-mail: sztaba@uci.agh.edu.pl

[1] the term „process" will be still uniformly used, taking into account the fact that a single operation can be treated as a set composed of just one operation, which happens in practice

determining the aims of this processing as well as the evaluation of the obtained results.

The subject matter of these remarks is constituted by separation processes, which result in obtaining at least two products of mutually differentiated properties from the feed. This group comprises the majority of processes determining the economic application of almost all mineral raw materials, i.e. primary and secondary.

The above description of separation processes is sufficient for the most general approach yet it is highly imprecise in relation to detailed requirements, which are formulated as implementation aims[2]. It should be remarked here that all rational considerations concerning mineral engineering must take into account its utilitarian character and the mentioned various solutions, necessary to achieve the assumed aims. The latter ones, unit by unit, can be formulated as:

- obtaining products of assumed properties, most often the contents of certain components (elements, grain classes, other phases differentiated in a certain way) which are concentrated (selectively or collectively) in concentrates (components differentiated due to the chemical composition – metals, combustible substances and others), grain size fractions (grain classes), and also the minimizing of these contents in a given product not apt for further processing or, generally – at least now – useless (secondary materials, waste),
- maximization of recovery of these components by means of introducing them into appropriate concentrates – increase of the utilization rate of the raw material,
- eliminating a certain component (components) from the concentrate of another component – obtaining the required effectiveness of separation of concentrates,
- obtaining a possibly large number of useful components of the multi-component raw material – complex (full) utilization of the raw material (Sztaba 1970),
- maximization of economic effects of the raw material utilization – obtaining the highest profits while providing the assumed product properties,

and also many other variants of the assumed aims, in particular different listings of unit aims, given as examples. The need of constructing such listings occurs first of all in the cases of multi-product processing of raw materials. This concerns mainly the multi-component raw materials, for example the polymetallic metal ores, but also the complex utilization of any other raw materials and producing from the material with one separated component a few concentrates of different uses and thus differentiated properties, for instance a rich metal concentrate for pyrometallurgical processing and a poorer one for hydrometallurgy. It should be observed that when more than one "useful" product is obtained, their yields, costs of obtaining and also commercial values are generally different which requires taking into account the process results, especially when evaluating the economic effects.

The outlined conditionings of mineral engineering processing significantly affect the possibilities of evaluating their results and the choice of the method of such an

[2] formal descriptions of separation and non-separation processes in (Sztaba 2002b)

evaluation. It should be stressed that a limited range of information is left to be the starting point of such an evaluation. It usually comprises the qualitative characteristics and content of separated components in the feed and at least in the selected products, sometimes also in their separate fractions (e.g. grain classes); rarely direct information about mass expenditures (yields) of products, unit costs of process execution and commercial values of products. Gaining additional information, though more and more possible, results in additional costs, not always to be confirmed by reaching the increased value of production[3].

PRINCIPLES OF DETERMINING THE PROCESS EFFECTIVENESS

As it has been already mentioned, every technological process is performed with the assumed aim and determining the effectiveness of this process is used to evaluate the degree of this aim. Determining the effectiveness of processes and methods of its evaluation have been studied theoretically and practically by mineral engineering (mineral processing).

The notion as such was named differently (Drzymała 2002, previously many others), many methods of calculating the effectiveness were proposed (often adapted to single cases) (Barskij, Plaksin 1967, Barskij, Rubinštejn 1970, Stępiński 1964 and others). The terminology standard introduced in Poland (Polska Norma 1999) recommends univocally the use of the notion of effectiveness.

In case of the principal group of mineral engineering processes effectiveness was assumed to be determined as a numerically expressed relation of really obtained process results to the assumed, forecast or theoretically possible results.

The general definition of effectiveness can be presented as (Sztaba 2002b)[4]:

$$S = E = \frac{W_r}{W_0} \tag{1}$$

where:
W_r – obtained result,
W_0 – expected or theoretically possible result.

Equation (1) can be treated as a general definition of effectiveness. In technological applications only these cases are considered in which the values W_r and W_0 assume numerical values. Practically, most often the value of effectiveness, calculated in such a way, is assumed to be a percent evaluation of success in aiming at reaching the value of W_0, multiplying the fraction in expression (1) by 100.

[3] the problem of evaluation of the economic value of information has not been practically solved despite a general statement, given here; it is of a very broad range, concerns not only the discussed processes and is not the subject-matter of the present considerations,

[4] in the definition formulas (1), (2.1), (2.2) and in descriptions the author applied a more general designation of effectiveness – S, beside the more popular one – E and, next, he uses E all the time.

THE CHOICE OF THE BASE OF REFERENCE AND THE SUBJECT OF EFFECTIVENESS CALCULATION

The assumption of the value W_0 is of principal significance for the result of calculations of the numerical value of effectiveness (further on, shortly, effectiveness). The majority of the applied and proposed methods of effectiveness calculating assume openly or more often assumingly that the aim of the process is to obtain that an ideal result; in case of the discussed separation processes, the ideal accurate separation of the selected feed components, i.e., among others, the maximum content of these components in their corresponding products. All known formulations of the theory of separation indicate agreeably that reaching such a result would occur at a very high outlay of energy (practically limitlessly high). In all separation processes the increase of separation accuracy is obtained at the cost of the progressively growing expenditure of energy, i.e. also the costs. Therefore, in real circumstances, such requirements are never applied, even at the separation of products of high quality standards, such as abrasive micropowders. Thus it should be assumed that the value W_0 should be, except for totally exceptional cases, the expected result of the process. This variant is generally taken into consideration in the applied methods of calculating the effectiveness by means of introducing the tolerance ranges for the obtained results of its evaluation.

Determining the subject-matter of effectiveness evaluation creates another problem. To present this, it is possible to use the simplest case of effectiveness evaluation according to the content – a_1 – of the selected component in the appropriate product. Then $S = a_1$. Attributing this expression the features of effectiveness equals an assumption that it represents the results of applying formula (1) and thus that, in fact, it is the expression $S = a_1 / 1$ and, consequently, $W_0 = 1$. It can be accepted, for instance, in case of the process of grain classification where such grains are separated which can belong only to one of a few mutually separable classes, or, for example, in case of coal enrichment, if we assume the occurrence of grains of pure mineral substance and a_1 is its content. On the other hand, such an assumption for the evaluation of effectiveness of producing the metal concentrate would mean that obtaining pure metal in the enrichment process could be assumed. This can be attributed only to the entire processing process whose evaluation is not grounded according to the results of enrichment exclusively. Such an assumption would be grounded in this case:

$$S = E = \frac{a_1}{a_{max}}, \tag{2.1}$$

where a_{max} – metal content in the mineral being its carrier.

Taking into account all simplifications and conventionalities of this example it can be stated according to it that the phase significantly subjected to separation, i.e. the grain class, metal-bearing mineral, “pure” grains of crude coal, should be a real

subject of separation effectiveness evaluation. It contains the minimum impurities of mineral substance (and the grains and waste rock – of combustible substance). On the other hand, however, introducing the expected, e.g. required by the buyer, value of a_{prod} into the denominator of the expression for S results in the simplest and practically applied principle of agreement between the real concentrate quality with the assumed one.

$$S = E = \frac{a_1}{a_{prod}}, \tag{2.2}$$

from which the lack of purpose of concentrate production appears $a_1 > a_{prod}$ then $S > 1$ with the unnecessary outlay of energy.

ASSUMPTIONS OF SYSTEMATIZATION OF EFFECTIVENESS EVALUATIONS

The formerly stressed various requirements concerning both the shaping of the process results and rules of evaluation resulted in the origin of very many methods and means of such an evaluation (Barskij, Plaksin 1967; Barskij, Rubinštejn 1970; Stępiński 1961, 1964; Sztaba 1983-2001, 1998a, 2000a, 2000b, 2000c,2002a and others). A mainly practical significance of these methods is the cause of a few attempts of a purely formal approach to its forming (Drzymała 2002), separated from a very differentiated demand.

Many authors, including the above ones, pointed out the possibility of differentiating a few basic groups of the discussed methods, assuming as a selecting criterion the variant interpretation of the basic notion of effectiveness, generating the origin and development of the methods of approach with the application, of course, of the formerly discussed range of information about the results[5]. The basic evaluation groups (evaluation criteria) were differentiated:

- principal (very vast literature, despite the previously quoted: Sztaba 1956a, 1956b, 1983, 1993a, 1993b, 2001; Tumidajski 1993 and many others)
  - technological,
  - statistical,
  - economic,
- but also
  - power engineering (Sztaba, Tora 1987; Tora, Sztaba 1983) and
  - thermodynamic (Barskij, Plaksin 1967; Barskij, Rubinštejn 1970),
- stressing the approaches (Barskij, Plaksin 1967; Barskij, Rubinštejn 1970 and others):
  - static and
  - kinetic.

[5] the information about the process results does not exhaust the description of its course conditions, they both constitute jointly a basic for the construction of process models which, among others, formulate the foundation to create specific effectiveness evaluations and which are not the subject-matter of this paper

The basic characteristics of the mentioned groups are widely presented in the quoted works, which grounds its neglecting in the present one. Following, certain additional features of the selected effectiveness evaluations will be indicated and discussed, mainly technological, which are most often applied both in industry and science.

SELECTED REMARKS ON THE PROCESS EFFECTIVENESS EVALUATION METHODS

TECHNOLOGICAL EVALUATIONS FOR THE ENTIRE PROCESS MATERIAL

The requirements of industry contributed to the most intensive development of effectiveness evaluation methods in the "technological" group, i.e. using the values directly corresponding to the methods of presenting technological characteristics of the feed and process products. They are used both for the evaluation of quality of products and the rate of utilization of feed components. They also constitute the base of evaluation of operations of mineral processing plants. The heterogeneity of detailed aspects of performing such evaluations resulted in their specific specialization, i.e. a possibility of differentiating three distinct subgroups of evaluations:

a) qualitative,
b) quantitative,
c) general.

The results of the performed process, determined for the entire processed material, are most often the subject of evaluation, as it is indicated by the title of this subchapter. Yet, in case of a more precise process study, and, especially, when statistical descriptions and evaluations are introduced, it is necessary to trace the behaviour of the feed grains during the process, differentiated according to certain qualitative criteria (grain size, rarely shape, density and possibly other distinctive features). Subchapter 3.2 contains general remarks concerning methods of conduct in such cases.

The elementary separation process of the feed with one distinctive component was assumed to be an example for discussing the characteristics of selected evaluations. The component content in the feed was a_0. There were two products, 1 (e.g. "concentrate" of a_1 content) and 2. (e.g. waste of a_2 content) in the feed – $a_1 > a_0 > a_2$. The yields (γ) of products are calculated in the well-known way according to the component balance (Stępiński 1964):

$$\gamma_1 = \frac{a_0 - a_2}{a_1 - a_2} \tag{3.1}$$

$$\gamma_2 = 1 - \gamma_1 . \tag{3.2}$$

All values are given in fractions. Practically, percent values are used, the method of mutual transformations is obvious. In the formulas used as examples the most popular denotation E ≡ S is used, adding differentiating numbers.

Note a) This is the most numerous subgroup (conventional denotation E'), using mainly the qualitative features of products. They comprise the following evaluation methods:

- only quality of products, out of which each one is evaluated separately, here the examples are simple evaluation methods, described in chapter 2.2 with formulas (2.1) and (2.2),
- methods of separation selectivity – applied for the differentiation rate of products quality – their construction is based on the non-negative difference of content, e.g.:

$$E'_5 = a_1 - a_2\,, \tag{4}$$

or $$E'_7 = \frac{a_1 - a_2}{a_0}$$ ("Truszlewicz's index"), (5)

or their quotient (>1), for instance:

$$E'_6 = a_1 / a_2\,, \tag{6}$$

or $$E'_8 = \frac{a_1}{a_2} \cdot \frac{1 - a_2}{1 - a_1}$$; ("Gaudin's index") (7)

- methods of rate of approximation to the largest possible differentiation of content in the selected product and feed:

for product 1.: $$E'_{9_1} = \frac{a_1 - a_0}{a_{max} - a_0} \tag{8.1}$$

for product 2.: $$E'_{9_2} = \frac{a_0 - a_2}{a_0 - a_{min}} \tag{8.2}$$

where a_{min} – the least possible content in product 2. (e.g. the so-called value of background).

Formula (2.1) shows the formerly mentioned justification of including permissible deviations of value a_1 from a_{max} (or a_{min}) in the effectiveness evaluation. If product 1. is allowed to control "impurity" caused by a separate material in the amount δ_1 and, analogically, product 2. contains it in the amount δ_2, this formula is transformed:

for product 1. in the form: $$E'^{\delta}_{1_1} = \frac{a_1}{a_{max} - \delta_1} > E'_{1_1} = \frac{a_1}{a_{max}}, \tag{9.1}$$

for product 2. in the form: $$E'^{\delta}_{1_2} = \frac{(a_{max} - \delta_2) \cdot a_2}{a_{max}} < E'_{1_2} = \frac{a_2}{a_{max}}. \tag{9.2}$$

Similarly, other formulas can also be transformed and values δ_1 and δ_2 can be taken into consideration.

Note b) Practically, the only evaluation in the quantitative group (conventional symbol E") is the recovery, $E''_1 \equiv \varepsilon$, representing the utilization rate of the certain part of the component included in the feed. Therefore it is the most important indicator of evaluation of the raw material utilization rate, used to evaluate the quality of operating of the system of the processing plant. The well-known formula is used to calculate the recovery:

$$\varepsilon_1 = E''_1 = \frac{a_1 \cdot (a_0 - a_2)}{a_0 \cdot (a_1 - a_2)} = \gamma_1 \cdot \frac{a_1}{a_0}. \tag{10}$$

The recovery calculation can be disturbed when there is a partial change of the material characteristics in the process course. A good example is constituted by a part of flow classification processes, more seldom by sieving, in which there are significant tangential forces between material grains and machine elements (e.g. hydrocyclones, sedimentation centrifuges, high-movement sieves, etc). In these cases the total number of fine classes in the sum of product is larger than in the feed at the cost of coarser classes. If the total increase of the content of the fine class (evaluated component) in relation to the feed is Δ, then its resulting content in the feed is $a_0 + \Delta = a_0^*$ and the formula of recovery will be:

$$\varepsilon_1^* = E''^*_1 = \frac{a_1 \cdot (a_0^* - a_2)}{a_0^* \cdot (a_1 - a_2)} = \gamma_1^* \cdot \frac{a_1}{a_0}, \tag{10.1}$$

where γ_1^* – corrected value of yield of product 1.

The group of quantitative evaluations comprises also a more complex evaluation of separation accuracy of respective material components, separated to appropriate concentrates. Here the selection indexes are used which are calculated as geometric means of the relations of recovery and rejection (filling up recovery $(1 - \varepsilon)$ determine which part of the total amount of the given component contained in the feed is found outside the appropriate concentrate) of both considered components. If we assume that two components, A and B, are separated into appropriate concentrates and their recovery are marked in the component A concentrate as ε_{AA} and ε_{AB} respectively, then the selection of component A off component B is described by the expression:

$$E''_{2_{AB}} = \sqrt{\frac{\varepsilon_{AA}}{1-\varepsilon_{AA}} \cdot \frac{1-\varepsilon_{AB}}{\varepsilon_{AB}}}. \tag{11}$$

There are still other methods of calculating the selection index, depending on the evaluation variant of the technological system (Stępiński 1964).

Note c) The method presented by *Hancock* in 1918 and usually connected with his name has the principal significance in the subgroup of general evaluations – symbol E. Regardless Hancock's propositions, there are at least several independent works (Barskij, Rubinštejn 1970; Sztaba 1993b) whose authors, starting from seemingly different assumptions, obtained the same result in the form of the formula:

$$E_1 = \frac{(a_0 - a_2)\cdot(a_1 - a_0)}{a_0 \cdot (a_1 - a_2)\cdot(a_{max} - a_0)}, \tag{12}$$

in which, especially in case of applying in the grain classification processes and when there are no precise data, $a_{max} = 1$ is often assumed. The relation between evaluation (12) with recovery (10) makes this evaluation susceptible to changes of material composition in the course of the separation process. Taking into account the same assumptions of this conditioning as in the case of recovery, it is obtained, analogically to formula (10.1):

$$E_1^* = \frac{(a_0^* - a_2)\cdot(a_1 - a_0^*)}{a_0^* \cdot (a_1 - a_2)\cdot(a_{max} - a_0^*)}. \tag{12.1}$$

TECHNOLOGICAL EVALUATION FOR FRACTIONS OF THE PROCESSED MATERIAL

As it was mentioned in the introduction to subchapter 3.1, there is a need (in some research projects, in the application of some statistical evaluation methods) of studying the behaviour of separate fractions during the process and these are numbered successively 1, 2, ..., i, ..., n, which can be separated in the processed material. The mechanisms of such behaviours are in agreement with the behaviour of non-fraction products. Therefore for their evaluation the methods of process effectiveness evaluation are applied with the application of values used during the technological process evaluation as input ones. These values concern the fractions being separated. It is assumed that such evaluations are marked with small letters; e_i – for the i-th fraction, with other discriminants as for process evaluations. For instance, formulas (7), (10) and (12) take the forms:

$$e'_{8_i} = \frac{a_{1_i}}{a_{2_i}} \cdot \frac{1-a_{2_i}}{1-a_{1_i}} \tag{7.1}$$

$$\varepsilon_{1_i} = e''_{1_i} = \frac{a_{1_i} \cdot (a_{0_i} - a_{2_i})}{a_{0_i} \cdot (a_{1_i} - a_{2_i})} = \gamma_1 \cdot \frac{a_{1_i}}{a_{0_i}}. \tag{10.2}$$

$$e_{1_i} = \frac{(a_{0_i} - a_{2_i}) \cdot (a_{1_i} - a_{0_i})}{a_{0_i} \cdot (a_{1_i} - a_{2_i}) \cdot (a_{max_i} - a_{0_i})}, \tag{12.2}$$

where a_{x_i} – value a_x for the i-th fraction.

Special attention should be paid to the recovery of the i-th fraction in the selected product (10.2), identical to the number of separation – $\varepsilon_i \equiv \tau_i$ – the basic value occurring in statistical descriptions and evaluations of results of separation processes, determining the possibility of transfer of grains of certain properties to the chosen product (among others: Sztaba 1956a, 1956b, 1983-2001, 1993b; Stępiński 1964; Tumidajski 1993).

OTHER SELECTED REMARKS ON THE CONSTRUCTION OF EFFECTIVENESS EVALUATIONS

Certain separation processes include limitations for a free separation of certain grain groups. "Difficult grains", taken into consideration in the sieving process, are such an example. Their occurrence, significant for the process course, requires including the evaluation methods in construction (Sztaba 1993b and others).

At the beginning of the nineties of the previous century the notional identity of the results of separation processes with the phenomenon of natural segregation of grained materials was pointed out. The latter ones were heterogeneous due to at least one feature, which could be a separation feature[6]. It enables the application of the segregation rate achieved in the products of such processes for the evaluation of their effectiveness (Sztaba 1993a, 1998a, 2000a).

The significance of complex utilization of mineral raw materials, stressed in the introduction, being one of important conditions of reaching the sustained economic and social development, evoked the need of determining the principles and methods of evaluation of multi-product separation processes, most often the multi-component input raw materials, including the secondary ones. The present propositions assume the calculation of effectiveness of such processes according to partial evaluations, performed for selected material components, taking into account their participation in the feed and also weights considering their economic value, including the quality values, market unit values of respective concentrates as well as the costs of their production and possibilities and costs of managing the resulting secondary products or waste (Sztaba 1983, 2000b, 2000c, 2001, 2002a). The research to solve this group of

[6] the feature, most often physical, of grains whose differentiated values condition directing them to respective products of the process

tasks requires special attention; especially that one should foresee the necessity of considering additional evaluation elements in the form of environmental, social and other conditionings of the sustained development.

The present work was performed within the framework of the research project no 9 T12A 032 19 in the years 2000-2003, sponsored by the Polish Committee of Scientific Research.

REFERENCES – SELECTED TITLES

БАРСКИЙ, Л. А., ПЛАКСИН, И. Н. (1967), *Критерии оптимизации разделительных процессов* (*Criteria of Optimization of Separation Processes*), „Наука" Москва, *in Russian.*

БАРСКИЙ, Л. А., РУБИНШТЕЙН, Ю. Б. (1970), *Кибернетические методы в обогащении полезных ископаемых* (*Cybernetic Methods in Mineral Processing*), „Недра" Москва, *in Russian.*

DRZYMAŁA, J. (2002), *Tworzenie i kategoryzacja parametrów separacji* (*Craeting and Categorizing of Separation Parameters*), Inżynieria Mineralna v. 3 2002, no 1(5), pp.11-19, *in Polish.*

Polska Norma 1999 – PN-G-01061, *Przeróbka rud metali nieżelaznych. Terminologia – Polski Komitet Normalizacyjny* (*Non-ferrous Metal Ore Processing. Terminology,* Polish Standard Committee), *in Polish.*

STĘPIŃSKI, W. (1961), *Ekonomika procesów wzbogacania rud i węgli* (*Economics of Enrichment Processes of Ores and Coals*), Wydawnictwo Górniczo-Hutnicze Katowice, *in Polish.*

STĘPIŃSKI, W. (1964), *Wzbogacanie grawitacyjne* (*Gravitational Enrichment*), PWN Łódź – Warszawa – Kraków, *in Polish.*

SZTABA, K. (1956a), *Metoda statystyczna badania procesu klasyfikacji mokrej* (*Statistical Method of Wet Classification Research*), Archiwum Górnictwa t.I. v.1. pp.33-54, *in Polish.*

SZTABA, K. (1956b), *Krzywe rozdziału w procesie klasyfikacji mokrej* (*Separation Curves of the Wet Classification*), Archiwum Górnictwa t.I v.2. pp.167-197, *in Polish.*

SZTABA, K. (1970), *Problemy kompleksowej utylizacji surowców mineralnych* (*Problems of Complex Utilization of Minerals*) – Zeszyty Naukowe Politechniki Wrocławskiej, Prace Naukowe Instytutu Górnictwa Politechniki Wrocławskiej no 5 pp.83-91, *in Polish.*

SZTABA, K. (1983), *W poszukiwaniu najwłaściwszej metody oceny skuteczności technologicznej procesów przeróbczych* (*For the Best Method of Evaluation of Effectiveness of Technological Processes*)*, Materiały* XVII Krakowskiej Konferencji naukowo-technicznej przeróbki kopalin AGH – SITG, Kraków – Zakopane pp.5-10, *in Polish.*

SZTABA, K. (1983-2001), Kontrola procesów technologicznych; działy: pobieranie próbek oraz *ocena skuteczności procesów technologicznych* (*Control of Technological Processes, sections: sampling and evaluation of effectiveness of technological processes*)*,* lectures for students of mining of AGH, specialization: mineral processing, unpublished, *in Polish.*

SZTABA, K. (1993a), *Segregation of Grained Material – Conditions and Possibilities of Evaluation*, Proceedings of the XVIII International Mineral Processing Congress, Sydney (Australia) 1993, vol.2, pp.505-509, *in Polish.*

SZTABA, K. (1993b), *Przesiewanie (Sieving),* Śląskie Wydawnictwo Techniczne Katowice, *in Polish.*

SZTABA, K. (1998a), *Stopień segregacji jako podstawa oceny skuteczności technologicznej procesów przeróbki kopalin i jakości jej produktów* (*Segregation Rate as the Basis of Evaluation of Technological Effectiveness of Mineral Processing and Its Product Quality*)*,* Fizykochemiczne Problemy Mineralurgii v.32, 1998, pp.57-67, *in Polish.*

SZTABA, K. (1998b), *Próba systematyzacji uwarunkowań oraz kryteriów oceny ekonomicznej automatyzacji zakładów przeróbki kopalin* (*Attempt of Systematization of Conditionings and Criteria of Economic Evaluation of Automation of Processing Plants*) – Mechanizacja i Automatyzacja Górnictwa 1998 no 11, pp.20-26, *in Polish.*

SZTABA, K. S. (2000a), *Evaluation of the Effectiveness of Separation Processes according to the Obtained Feed-Segregation Rate,* Proceedings of the XXI International Mineral Processing Congress, Rome, Italy July 23-27, 2000, Elsevier Science B.V. Amsterdam, Vol.A, pp.A7-1-7.

SZTABA, K. S. (2000b), *Описание и оценка многопродуктовых технологических операций в технологии минералов* (*Description and Evaluation of Multi-product Technological Operations of Mineral Processing*), *Тезисы докладов юбилейных „Плаксинских Чтений”*: „Развитие идей И. Н. Плаксина в области обогащения полезных ископаемых и гидрометаллургии”, Москва 10-14 октября 2000 г. p.103, *in Russian.*

SZTABA, K. S. (2000c), *Podstawowe problemy opisu i oceny wieloproduktowych operacji technologicznych inżynierii mineralnej* (*Basic Problems of Description and Evaluation of Multiproduct Technological Operations of Mineral Engineering*), Zeszyty Naukowe Politechniki Łódzkiej no 838, Inżynieria Chemiczna i Procesowa v. 27, Łódź, pp.235-243, *in Polish.*

SZTABA, K. S. (2001), *Koncepcje oceny wieloproduktowych procesów rozdzielczych* (*Concepts of Evaluation of Multi-product Separation Processes*)*,* VI Międzynarodowa Konferencja Przeróbki Rud Metali Nieżelaznych (ICNOP ‘2001), Instytut Metali Nieżelaznych – Gliwice, KGHM „Polska Miedź” S.A., CBPM „Cuprum” Sp. z o. o., Szklarska Poręba 16-18.05.2001 r: *Conference materials* pp.1-19, *in Polish.*

SZTABA, K. S. (2002a), *Concepts of the Evaluation of Multi-product Separation Processes of Mineral Engineering,* Archives of Mining Sciences (Archiwum Górnictwa) PAN, y. 47 v.1, pp.51-67.

SZTABA, K. S. (2002b), *Evaluation of Non-separation Operations of Mineral Engineering*, Physicochemical Problems of Mineral Processing, 36 (2002), pp.135-146.

SZTABA, K., Tora, B. (1987), *Analiza skuteczności odwadniania koncentratu miedziowego* (*Analysis of Dewatering Effectiveness of Cu Concentrate*), Zeszyty Naukowe Politechniki Śląskiej nr 919, Seria Energetyka v.100, Gliwice pp.241-248, *in Polish.*

TORA, B., SZTABA, K. (1983), *Problemy oceny efektywności odwadniania koncentratów flotacyjnych na przykładzie koncentratu miedziowego* (*Problems of Evaluation of Effectiveness of Dewatering of Flotation Concentrates Exemplified by Cu Concentrate*)*, Materiały* XVII Krakowskiej Konferencji naukowo-technicznej przeróbki kopalin AGH – SITG, Kraków – Zakopane, pp.83-90, *in Polish.*

TUMIDAJSKI, T. (1993), *Zastosowanie metod statystycznych w analizie procesów przeróbki surowców mineralnych* (*Application of Statistical Methods in Analysis of Mineral Processing*), Śląskie Wydawnictwo Techniczne Katowice, *in Polish.*

Sztaba K., *Wybrane problemy określania skuteczności rozdzielczych procesów technologicznych inżynierii mineralnej,* Physicochemical Problems of Mineral Processing, 37, (2003), 5-17 (w jęz. ang.).

Ocena stopnia osiągnięcia założonego celu dowolnej działalności jest podstawą weryfikacji prawidłowości algorytmu postępowania przyjętego do jej realizacji. Jest ona także jednym z głównych warunków modyfikowania zarówno tego algorytmu, jak szczegółowego określenia owego celu, z zamiarem osiągnięcia jego stanu optymalnego. Procedury stosowane do takiej oceny zwykło się najczęściej określać badaniem skuteczności odnośnych działań, a jego wynik wprost skutecznością. W przypadku procesów technologicznych skuteczność określa się zwykle jako wyrażony liczbowo stosunek rzeczywiście otrzymanych wyników procesu do wyników założonych, przewidywanych lub teoretycznie możliwych do osiągnięcia. W szczególnym stopniu zadanie określania i badania skuteczności występuje w przypadku procesów inżynierii mineralnej, zwłaszcza podstawowej grupy tych operacji, decydujących o końcowym wyniku procesu i stopniu osiągnięcia jego założonych rezultatów. Wśród tych procesów zdecydowaną większość stanowią procesy rozdzielcze – przede wszystkim wzbogacania i klasyfikacji ziarnowej. Różnorodność właściwości surowców mineralnych, zarówno pierwotnych –naturalnych – jak i wtórnych – powstałych w wyniku wcześniejszego przeprowadzenia operacji technologicznych wydzielenia części materiału pierwotnego i zmiany jego cech charakterystycznych – oraz nie mniejsza różnorodność wymagań co do właściwości produktów procesów inżynierii mineralnej – przeróbki kopalin

i surowców wtórnych – użytkowanych praktycznie we wszystkich gałęziach produkcji przetwórczej z ich niezliczonymi wariantami założeń i celów szczegółowych, wywołuje potrzebę znacznego różnicowania nie tylko metod oceny ich skuteczności, lecz też modyfikowania interpretacji podstawowego pojęcia skuteczności w konkretnych warunkach założeń i przebiegu praktycznie każdego procesu technologicznego. Opracowanie zawiera przegląd podstawowych wariantów takich wymagań i przedstawia propozycje – w części już wykorzystywane – dostosowywania do nich sposobów szczegółowych określania skuteczności procesów. Przedstawia również wybrane, rzadziej zauważane okoliczności wpływające na ocenę skuteczności procesów, w tym dyskusję poziomu odniesienia takiej oceny, uwzględniania dopuszczalnych tolerancji jakości produktów, przypadków zmiany w trakcie procesu niektórych właściwości pierwotnych nadawy. Ograniczając rozważania do wybranych zagadnień tzw. ocen technologicznych, wskazuje się na ich związki z innymi podstawowymi grupami ocen: statystycznych i ekonomicznych, a także na kierunki rozwoju metod oceny niezbędnego dla sprostania zadaniom kompleksowego wykorzystania surowców, warunkującego między innymi realizację zasad zrównoważonego rozwoju gospodarki i społeczeństwa.

Physicochemical Problems of Mineral Processing, 37 (2003) 19-26
Fizykochemiczne Problemy Mineralurgii, 37 (2003) 19-26

Jan DRZYMAŁA*

SORTING AS A PROCEDURE OF EVALUATING AND COMPARING SEPARATION RESULTS

Received March 2003, reviewed, and accepted May 15, 2003

Results of separation of the same feed into products can be evaluated by different procedures. Relatively well known are product-separation, upgrading, and classification. The procedure of product separation relies on determination of the mass or yield of products, upgrading is based on determination of mass or concentration of a feed component (chemical component, particle, fraction) in products while classification relies on analytical determination of content of various fractions present in the feed and products and takes into account the value of the feature responsible for separation. In this paper another approach is described, which was named sorting. This procedure utilizes the results of analysis of the quality of separation products and the feed based on the determination of the value of the property utilized for separation (or related feature) of individual particles (or a group of particles) and assigning it to different sorting groups of similar properties. The sorting curves are plotted as a selected separation parameter versus the group number. There are many sorting-separation parameters including contents, yields, and their combinations. The simplest parameter of sorting is probably the recovery of a group of particles, which provides sorting curves similar to the Tromp curve used in classification. The separation results can be plotted either in a form of two lines, one line, or a point. However, a meaningful comparison of the separation results by means of sorting curves is possible when the separation tests are performed for a given feed quality and given magnitude of ordering forces while the position of the splitting forces changes. A family of sorting curves can be obtained for tests performed at different levels of the ordering forces.

key words: separation, splitting, upgrading, classification, sorting

INTRODUCTION

Separation relies on physical or virtual splitting of a starting material into real or virtual products that differ in quantity, quality or both. The separation takes place after exposure the feed to the separating forces. The separating forces are ordering, disordering and splitting forces (Fig.1). These forces significantly influence the results of separation. To evaluate the degree of separation, the products of the process have to be analyzed. The determination of quantity of the products of separation is performed

* Technical University of Wroclaw, Wybrzeze Wyspianskiego 27, 50-370 Wroclaw, Poland; e-mail jd@ig.pwr.wroc.pl

using such analytical procedures as weighing, counting, volume measurement, etc. They provide the yield of the products. If the quality of the products is identical or we are not interested in the quality the separation products, the process can be characterized by the yield of the products or dependent parameters such as recovery of a component only. This procedure can be called the product-separation (Drzymała, 2001a).

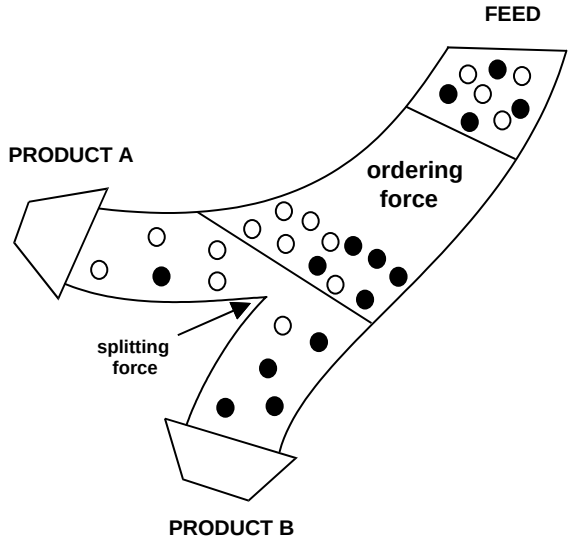

Fig.1. For a given property of the feed the result of separation depend on separating forces including ordering, splitting and other, for instance disordering, forces

The quality of the products can be established by different analytical methods (chemical, optical, screening, etc.). Presently two approaches, called upgrading and classification, are commonly applied for qualitative analyses of materials and samples, and next for characterization of separation. The upgrading relies on mass or content of a component in another components of the feed while classification on the value of the main feature used for separation (Drzymała, 2001a). Mentioned above product-separation procedure is based on the mass of the products of separation.

It seems obvious that other properties of the main feature used for separation may provide additional means of evaluation of the separation results. In this paper a property of the main feature that is belonging to a certain group of particles of similar properties will be used as an analytical procedure for determination of the quality of the products. It will be called sorting, because assignment of particles to a certain group is based on similarity of individual particles. In same cases the sorting into groups can be accomplished according to similarity of feature of a group, instead of individual, particles. The methods which can be used for evaluation and characterizing results of separation are briefly described in Table 1.

Table 1. List of methods of evaluation and characterizing results of separation

Parameter	Aspect of separation
mass of products	product-separation
mass of a component of feed and products of separation determined analytically in representative samples. Typical components: chemical components (elements, minerals, etc.), particles, fractions, etc.	upgrading (enrichment)
real or mean **value of feature** utilized for analytical separation of samples of feed and separation products into portion of matter (fractions also called classes, individual particles , etc.). The feature of analytical separation is the same (or related) as the feature of separation of feed into products	classification
consecutive **number** of a component (individual particle or group of particles) of feed and separation products assigned to the component during analytical procedure of sorting of particles according to the value of feature utilized for separation into products or related features	sorting

EVALUATION OF RESULTS OF SEPARATION BY SORTING

A hypothetical process will be considered here in which the feed was split into two products, that is, concentrate (product A) and tailing (product B). The samples of the feed and products of separation were sent to a mineralogical laboratory. The particles in the samples were observed under optical microscope and assigned to 10 different groups containing visually 10%, 20%, 30%, 40%, 50%, 60%, 70%, 80%, 90%, and 100% of a black mineral. The black mineral was the useful mineral and the separation of the feed into products A and B took place due to the value of a property (let us assume that it was magnetic susceptibility) proportional to the content of the black mineral in the particle. The groups were named 1, 2, ..., and 10, respectively. The mass and content of each group in the feed and products of separation was determined by counting the particles and then taking into account their density and volume. The mass can also be determined directly by weighing. The results of the mineralogical sorting analysis are given in Table 2. The numerical values were further used for calculation of other separation parameters including recovery of each group, and Hancock's parameter (Tarjan, 1986) for each group (Table 3). The separation parameters can be used for plotting different sorting curves. Two of them are shown in Figs 2a and 2b. Since there are infinitive number of sorting parameters, which can be generated (Drzymala, 2001b) from the content of a group in the feed (α), content of a group in product (λ), and yield of the product (γ), the number of sorting curves is also unlimited (Drzymala, 2002). In addition to that, each sorting curves can be plotted either in cumulative or non-cumulative form on normal, logarithmic or multi-logarithmic scale.

Table 2. Results of separation based on mineralogical sorting analysis. Yield of product A (γ_A) was 32.1% and product B γ_B = 67.9%

Group of particles No.	Feed		Product A		Product B	
	content	cumulative content	content	cumulative content	content	cumulative content
n_i	α_i %	$\Sigma\alpha_i$ %	$\lambda_{i,A}$ %	$\Sigma\lambda_{i,A}$ %	$\lambda_{i,B}$ %	$\Sigma\lambda_{i,B}$ %
1	0.01	0.01	0	0	0.015	0.010
2	2.45	2.46	0	0	3.61	3.62
3	12.32	14.78	2.51	2.51	16.96	20.58
4	24.05	38.83	8.39	10.90	31.45	52.03
5	21.16	59.99	16.21	27.11	23.50	75.53
6	13.12	73.11	16.02	43.13	11.75	87.28
7	11.45	84.56	19.66	62.79	7.57	94.85
8	7.78	92.34	16.54	79.33	3.64	98.49
9	3.86	96.20	9.42	88.75	1.23	99.72
10	3.80	100.00	11.25	100.00	0.28	100.00

Table 3. Calculated parameters of separation based on mineralogical (sorting) analysis. Yield of product A (γ_A) was 32.1% and product B γ_B = 67.9%. Recovery is calculated according to Eq. 1

Group of particles n_i *(No.)*	Selected separation parameters			Pairs of parameters of sorting curve			
	Recovery of group n_i of particles in product A, ε_i, %	Hancock parameter H=$\varepsilon_{i,A}$ - $\varepsilon_{i,B}$ %	others	recovery sorting curve	recovery sorting curve	Hancock sorting curve $(H_{75}-H_{-75})/2$	Hancock sorting curve
1	0	-100.00	....				
2	0	-100.00	....				
3	6.54	-86.92	....				
4	11.20	-77.6	....	$n_{\varepsilon 50}$ = 6.7	$n_{\varepsilon 50}$ = 6.7	$n_{\varepsilon 50}$ = 6.7	$n_{\varepsilon 50}$ = 6.7
5	24.59	-50.82	....				
6	39.20	-21.6	....	E_n = 1.6	O_s = 15.4	H_n = 2.5	O_s = 10.0
7	55.11	10.22	....				
8	68.24	36.48	....				
9	78.34	56.68	....				
10	95	90.00	....				

TYPES OF SORTING CURVES

The simplest sorting curve represents the results of separation in the form of content of various groups of particles as a function of the group number (Fig. 2a). To show adequately the separation results using the group content as separation parameter, two sorting curves have to be plotted. One curve can be drawn for the feed and the other for separation products or the two curves can be for the products of separation. In Fig. 2a one line was plotted as a dashed line to emphasize that it provides an excess information and it can be omitted. The sorting curves from Fig. 2a are not particularly convenient because there are two lines. It is more convenient to combine the two curves into one. It can be accomplished by choosing an appropriate separation parameter, which used alone would provide full information about the separation. Recovery, for instance, is such a parameter (Barski, and Rubinstein, 1970). In our case the recovery is defined as:

recovery of a group of particles in product A ($\varepsilon_{i,A}$) = content of a group in product A ($\lambda_{i,A}$) x yield of product A (γ_A) / content of a group in feed (α_i) (1)

The sorting curve ($\varepsilon_{i,A}$) = f($n_{i,A}$), where n_i is the group number, used alone characterizes well the results of separation because the sorting curve for product B is a mirror image of curve for product A, because:

$$\varepsilon_{i,B} = 100\% - \varepsilon_{i,A} \tag{2}$$

The recovery-sorting curve is plotted in Fig. 2b, and the sorting curve for product B, as a line which can be omitted, was plotted as a dashed line. It should be noted that the recovery-sorting curve is similar to the Tromp or separation curve (Kelly and Spottiswood, 1982) used for delineation of separation as a classification. The difference between the recovery-sorting and recovery-classification curves is that the former is plotted as a function of the number of a group of particle, not as a function of the numerical values of the feature of the fraction.

The recovery-sorting curve can be further reduced to a point by replacing the curve with its shape parameters. For the Tromp plot the most frequently used are such shape parameters as $n_{\varepsilon 50}$ and E_n. We will use here the same approach. The $n_{\varepsilon 50}$ and E_n parameters are defined as follows:

$n_{\varepsilon 50}$ = number of group of particles of similar feature used for separation (or related) for which the recovery of the group in a product is equal to 50% (3)

$$E_n = (n_{\varepsilon=75\%} - n_{\varepsilon=25\%})/2 \tag{4}$$

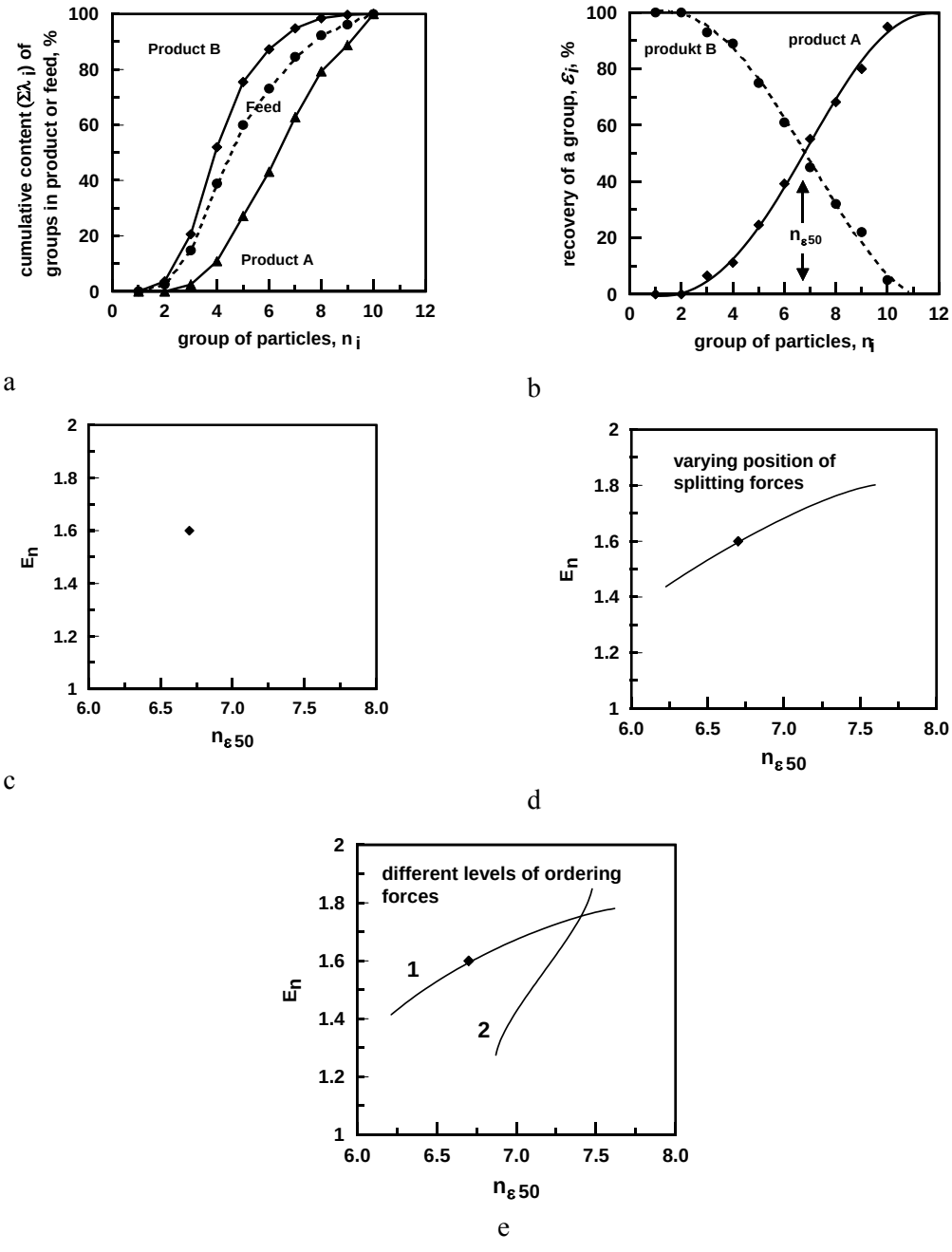

Fig. 2. Sorting curves: a) cumulative content vs. group number, b) recovery of a group vs. group number, c) E_n vs. $n_{\varepsilon 50}$, d) E_n vs. $n_{\varepsilon 50}$ for varying positions of splitting force, e) E_n vs. $n_{\varepsilon 50}$ for varying positions of splitting force and at two different levels (1 and 2) of ordering forces

It should be noticed that any pair of parameters, which are capable to characterize more or less accurately the recovery curve could be used. Another pair could be $n_{\varepsilon 50}$ and the sharpness of separation O_s, which is the slope of the recovery-sorting curve near $n_{\varepsilon 50}$ (Barski and Rubinstein, 1970; Wills, 1970). The plot of E_n vs. $n_{\varepsilon 50}$ is shown in Fig. 2c. For one separation test carried out for the same feed at a constant position of the ordering and splitting forces the plot of E_n vs. $n_{\varepsilon 50}$ (or O_s vs. $n_{\varepsilon 50}$) contains only one experimental point. To create a sorting curve containing more experimental points we have to run more separation tests at different positions of the splitting force. This procedure, after mineralogical (sorting) analysis of the products of separation, provides additional points on the sorting curve (Fig. 2d). Another sorting curve can be plotted for another level of the ordering force (Fig. 2e). Having two sorting curves it becomes possible to compare the results of different separation tests with the same feed.

CONCLUSIONS

It was shown in this paper that sorting could be used as another procedure of characterizing separation. It is different from the product-separation, upgrading, and classification procedures, which are frequently used for characterization and comparing separation results. The sorting method relies on sorting individual particles into groups according to their similarity of the property used for separation or related properties. There are many sorting parameters. The sorting parameters can be used for plotting sorting curves. Depending on the sorting parameters the result of one separation can provide two sorting lines, one line, or a point. A meaningful comparison of separation results by sorting is possible provided that separation tests for a given feed are performed at a given magnitude of the ordering forces and at varying position of the splitting forces. Further test can be carried out at different levels of the ordering forces.

Very likely there are other methods of evaluation of separation results but they should not be much different from those already presented in this paper.

REFERENCES

BARSKI, L.A., RUBINSTEIN, J.B., (1970), *Cybernetic methods in mineral processing,* Nedra, Moscow (in Russian).

DRZYMAŁA, J., (2001a), *Podstawy Mineralurgii (Principles of Mineral Processing)*, Oficyna Wydawnicza Pol. Wrocł., Wrocław.

DRZYMAŁA, J., (2001b), *Generating upgrading curve used for characterizing separation processes,* Inżynieria Mineralna - J. Polish Min. Soc., vol. II, nr 2(4), 35-40.

DRZYMAŁA, J., (2002), *Creation and categorization of separation parameters,* Inżynieria Mineralna - J. Polish Min. Soc., vol. III, nr 1(5), 11-20.

KELLY, E.G., SPOTTISWOOD, D.J., (1982), *Introduction to Mineral Processing,* Wiley, New York.

TARJAN, G., 1981, *Mineral Processing*, Vol., Akademiai Kiado, Budapest.

WILLS, B., 1979, *Mineral Processing Technology*, Pergamon, London.

Drzymała J., *Sortowanie jako sposób oceny i porównywania wyników separacji,* Physicochemical Problems of Mineral Processing, 37, (2003) 19-26 (w jęz. ang.).

Oceny wyników rozdziału separacji na produkty nadawy o tym samym składzie można dokonać w oparciu o różne procedury. Dobrze znane są metody polegające na opisie separacji jako rozdział na produktu, wzbogacanie, czy też klasyfikacja. Opis separacji polegającej na rozdziale na produkty polega na ilościowym określeniu wychodu produktów (np. masy), podczas gdy wzbogacanie jest oparte na określeniu ilości (np. masy) i jakości produktów w oparciu o zawartość składników (chemicznych, ziarn, frakcji) w nadawie i produktach. Z kolei klasyfikacja polega na analitycznym określeniu zawartości pewnych frakcji obecnych w nadawie i produktach separacji biorąc pod uwagę cechę, dzięki której nastąpiła separacja. W tej pracy opisano jeszcze inną procedurę, którą nazwano sortowaniem. Metoda ta wykorzystuje wyniki analizy jakości produktów separacji i nadawy oparte na określaniu wartości cechy, która została użyta do separacji, lub cechy od niej zależnej, dla indywidualnych ziarn lub grupy ziarn i przypisanie jej do różnych grup o podobnych właściwościach. Wyniki charakteryzowania procesu pod kątem sortowania mogą być wykreślane w postaci: wybrany parametr separacji względem numeru grupy. Istnieje wiele parametrów procesu separacji opisywanego jako sortowanie i są one oparte o zawartość i wychód oraz ich kombinacje. Najprostszym parametrem sortownia opartym o zawartość i wychód jest prawdopodobnie uzysk grupy ziarn, który dostarcza danych do wykreślenia krzywej sortowania podobnej do krzywej Trompa stosowanej przy opisie separacji jako klasyfikacji. Wyniki separacji jako sortowanie mogą być wykreślane w postaci dwóch linii, jednej linii lub punktu. Pełne porównanie wyników separacji za pomocą krzywych sortowania jest możliwe wtedy, gdy wyniki separacji dotyczą stałej jakości nadawy i danego poziomu sił porządkujących zastosowanych do separacji, podczas gdy położenie sił rozdzielających ulega zmianie. Z kolei rodzinę krzywych separacji można uzyskać prowadząc separacje przy różnych wartościach sił porządkujących.

Physicochemical Problems of Mineral Processing, 37 (2003) 27-36
Fizykochemiczne Problemy Mineralurgii, 37 (2003) 27-36

Tomasz SZYMAŃSKI, Piotr WODZIŃSKI*

SCREENING ON A SCREEN WITH A VIBRATING SIEVE

Received March 2003, reviewed, and accepted May 15, 2003

This paper, dedicated to membrane screens with vibrating sieves, is one of the series prepared at the Technical University of Lodz. The membrane screens are the machines with a specific sieve motion, which is forced in points. Only the sieve in the form of a membrane stretched over an immobile riddle, vibrates. This sieve is characterized by a non-uniform distribution of amplitudes on the vibrating surface. This is a property that distinguishes these screens from other industrial screens. In connection with the above mentioned feature, the method of screening is not the same as in other screens. The present paper describes these differences and the methods of their characterization. Results of investigations on the screening efficiency depending on the process capacity are analyzed.

Key words: membrane screen, oversize, particle material, recovery, screening, sieve, undersize, vibrating sieve

INTRODUCTION

This paper is next in the series devoted to screens with vibrating sieves. In the previous papers the screen construction, drive and sieve motion characteristics were discussed, while in the present one the authors wish to present differences in the process of screening as compared to the process carried out in other screens. The most important characteristic feature of membrane screens is the excitation of sieve vibrations by the so-called pushing rods (Szymański, Wodziński 2001). This causes a non-uniform amplitude distribution on the sieve surface. It is known that the sieve vibrations are a driving force of feed motion, i.e. screened material motion, and one of the most significant parameters on which the success of screening depends. The screening is successful if the finer fraction is screened off at the highest efficiency possible. We mean here the so-called recovery or efficiency of the undersize fraction, i.e. the ratio of the mass of undersize particles screened off to the mass of particles of the finer fraction present in the feed.

* Lodz Technical University, Faculty of Process and Environmental Engineering, Department of Process Equipment, Wólczańska 213, 93-005 Lodz, Poland, e-mail wodzinsk@wipos.p.lodz.pl

$$\eta=\eta_f = \frac{\text{the mass of finer fraction which passed through the mesh}}{\text{total mass of finer fraction in the feed}} \quad (1)$$

For typical screening the recovery of coarser fraction η_c in the oversize product is 100%, therefore solely η_f can be used for characterization and comparison of screening results.

Usually, the process technology specifies the accepted level of finer fraction that can remain in the oversize product. So, it means that we know the efficiency of screening. This is a basis for designing of screens. One of the methods to determine the sieve surface on which the process is to be performed at a given efficiency, is a model with the discharge function. The authors propose to replace the exponential discharge function by a straight line because of a specific screening in the screens with vibrating sieves.

The screens with vibrating sieves are designed first of all for screening of fine and very fine granular materials. They are characterized by relatively high dynamic factors. That is why in these machines layers on the sieve are well segregated and high screening efficiency is achieved. The screens with vibrating sieves are characterized by high frequency of vibrations and small amplitudes. In the screen tested by the authors, the frequency is 50 Hz and a maximum amplitude is 2 mm. The angle of sieve inclination can be changed in the range from 0 to 35°, i.e. twice as large inclination is obtained as compared to the screens with stable sieves. So large angles and high accelerations induce significant velocities of the material on the sieve, reaching 0.5 to 1.0 m/s (Wodziński 1997).

CONSTRUCTION OF SCREENS WITH VIBRATING SIEVES

Among many design solutions of industrial screens with vibrating sieves the most advantageous seems to be the screen with a driving frame (Fig. 1). This screen was designed and built at Lodz Technical University. It is a subject of the present paper. Figure 1 shows two ways in which the frame drive was designed. The first one is a system driven by a single electromagnetic vibrator placed in the center (broken line), the second one – by two electromagnetic vibrators located on two ends of the driving frame.

In this screen, the driving frame (R_n) is excited to vibrations by a vibrator, or electromagnetic vibrators (WEM) and the frame vibrations are transferred onto the sieve (S) by means of connectors called pushing rods (P). The riddle (R_z) remains immobile. In the tested system, double-action pushing rods that transfer full vibrations onto the sieve were applied (Szymański, Wodziński 2001). This means that the sieve motion is forced on both sides of the equilibrium position (downward and upward). At present, only a few manufacturers in the world produce membrane screens with one-sided excitation, i.e. such where the sieve is only tossed upward. Actually, this

facilitates the exchange of sieves but much deteriorates the process of screening. Taking into account a growing durability of sieves produced now, the system with double-sided excitation of the sieve motion seems to be more recommendable.

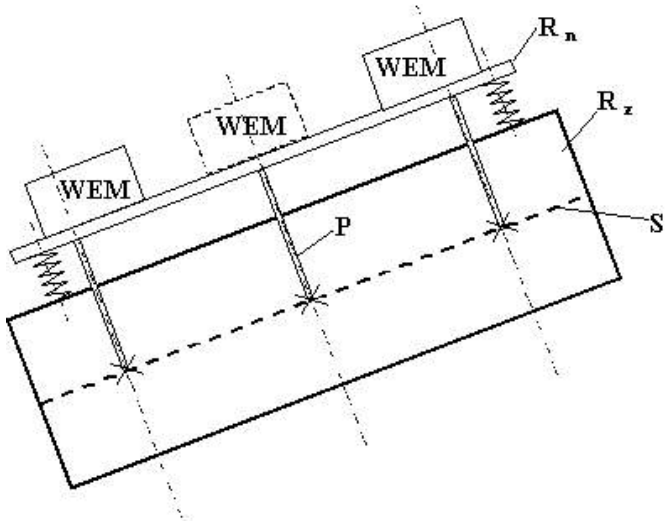

Fig. 1. Frame screen with a vibrating sieve

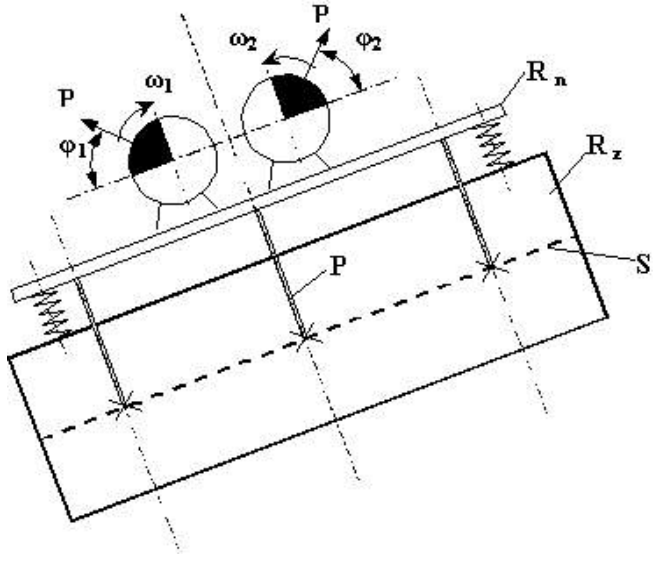

Fig. 2. A system with rotating vibrators

The system with a driving frame is a universal solution, where without any significant changes of design, beside electromagnetic vibrators, two engines with unbalanced shafts can be used (Fig. 2).

When one electromagnetic vibrator placed in the axis of symmetry of the screen is used, a risk of torsional vibrations of the frame around the center of gravity may appear. This is not advantageous and can be eliminated by a system with two electromagnetic vibrators (Szymański, Wodziński 2001).

In the system with two rotary vibrators (unbalanced engines), they work in the conditions of a counter-current self-synchronization. Such driving system guarantees that a linear trajectory of vibrations is obtained, the trajectory being perpendicular to the sieve surface, i.e. to the driving frame as well (Szymański, Wodziński 2001).

THE PROCESS OF SCREENING THIN LAYERS ON VIBRATING SIEVES

Screening on screens with vibrating sieves is carried out with thin material layers. The thickness of material layer on the sieve is as small as possible. It would be ideal if the layer thickness could be equal to the dimension of the particle classified. However, in practice it is assumed that this thickness can reach several diameters of the classified particles.

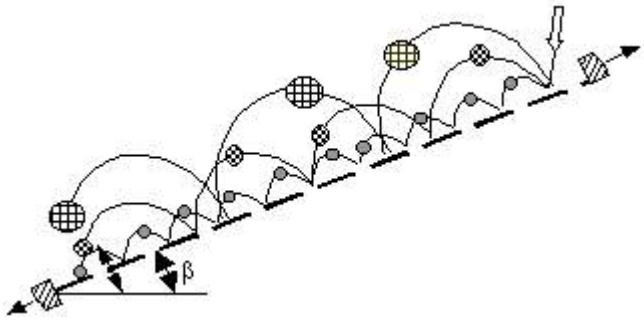

Fig. 3. Behavior of particles in a thin layer

Thin layer screening takes place when material (layer) on the vibrating sieve moves along at high speed, which means that at the same feed rate, the layer thickness decreases. In such conditions there is no segregation resistance during screening, however, individual particles move in a “restrained” way (Fig. 3). This provides very good stratification conditions, which in turn enable very high efficiency reaching 100%.

A MODEL WITH DISCHARGE FUNCTION FOR THE SCREEN WITH VIBRATING SIEVES

In practice, a sieve design is limited to the determination of surfaces of the sieves. In most cases the sieve width and efficiency are imposed and then a designer is to calculate such sieve length that guarantees the desired efficiency. For this purpose a model with discharge function can be used (Sztaba 1993). The external surface of the granular layer screened on the sieve has the shape of an exponential curve (in longitudinal section). This follows from numerous studies on the distribution of the mass of finer fraction screened off from the layer on the sieve, along the sieve. This curve is shown in Fig. 4, in the following reference system: X axis – time or sieve length, Y axis – the height of the layer on the sieve or the mass of material that remained on the sieve.

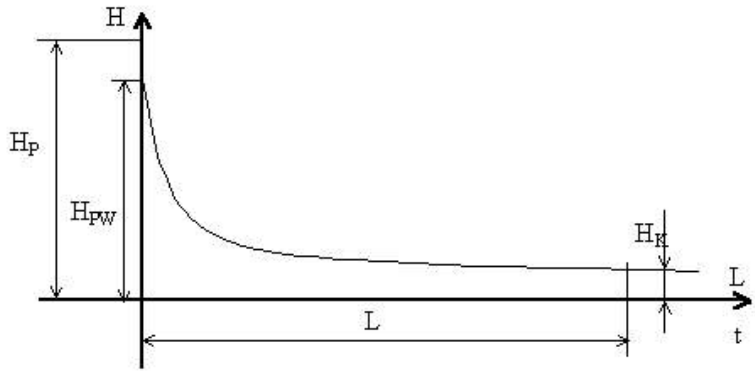

Fig. 4. Discharge function

This shape of the discharge function occurs in thick-layer screening. In the case of thin-layer screening, the authors propose to replace the exponential curve by a straight line (Fig. 5). At the initial stage of the process, in the screen with a vibrating sieve, the layer thickness is equal to several diameters of the classified particles at most. At the final stage of the screening, the layer is equal to the mean diameter of the coarser particles. It is obvious that these are not layers in the exact meaning of the word. Particles move in the way shown in Fig. 3 and by the thickness of these particles we mean a model method of presenting the amount of these particles.

A characteristic feature of the proposed model is an assumption that the real discharge function is replaced by an approximated discharge function which is a straight line. This assumption is possible because in thin-layer screening we observe a relatively small change in the height of the layer on the sieve. The process is carried out so that the layer thickness does not exceed several (2 to 3) diameters of the average particle in the feed.

As in the case of a normal discharge function, we will use the following relations:

$$H = H(L) \tag{2}$$

$$H = H(t) \tag{3}$$

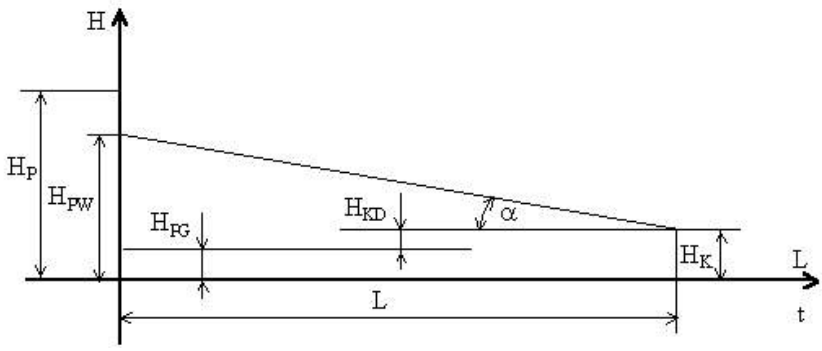

Fig. 5. Discharge function for thin-layer screening

At the beginning of the process (hence, at the beginning of the sieve) the layer heights are: H_P (resulting from the mass flux of feed onto the sieve) and H_{PW} – after the first gravitational discharge, without any machine vibrations. It is obvious that the initial layer thickness H_P is the sum of the initial height of the oversize H_{PG} and undersize product H_{PD}:

$$H_P = H_{PG} + H_{PD} \tag{4}$$

At the end of the sieve, the final height of the oversize fraction stream H_{KG} and the final height of the stream of finer particles that still remained on the sieve H_{KD}. The two values give altogether the value of H_K.

$$H_K = H_{KG} + H_{KD} \tag{5}$$

For a normally working screen, i.e. when the sieve is not damaged and particles of the oversize fraction do not get to the undersize product, the height of the layer of the oversize fraction is the same at the beginning and at the end of the process.

$$H_{KG} = H_{PD} \tag{6}$$

For thin-layer screening, equations (2) and (3) assume the form:

$$H_K = H_{PW} - a \cdot L \tag{7}$$

$$H_K = H_{PW} - a \cdot t \tag{8}$$

These equations are interrelated by the velocity of material layer sliding on the sieve:

$$u_m = L / t \tag{9}$$

In the equations that describe the discharge function there is one empirical factor a (straight line inclination a = tgα), which includes:

- machine motion,
- properties of the granular material,
- moisture content of the feed,
- screening efficiency,

and also other parameters which can be considered significant for the process of screening.

At present, research is carried out to justify the applicability of the discharge function in the form of a straight line.

RESULTS OF STUDIES ON THE EFFICIENCY OF THIN-LAYER SCREENING

Below, results of research on the screening efficiency in the screens with vibrating sieves will be discussed. As mentioned in the introduction, the efficiency denotes here the efficiency of the undersize fraction, i.e. the ratio of the mass of material that should be in the undersize product to the mass of material which was actually screened off (Banaszewski 1990).

The investigations were carried out in a frame screen driven by two engines with unbalanced shafts (Fig. 6).

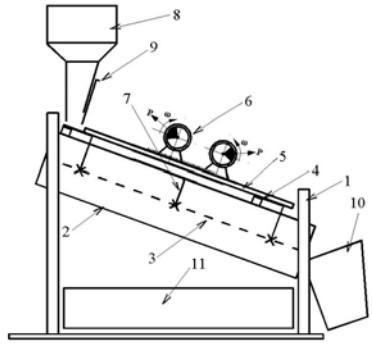

Fig. 6. Experimental setup

Supporting structure 1 is the machine frame. Riddle 2 inclined at different angles which remains immobile during the screen operation, is mounted in the frame. Sieve 3 is stretched on the riddle. Flat springs 4, on which driving frame 5 rests, are mounted on the riddle. Inertial vibrators 6 are installed on the driving frame. It is also possible to use electromagnetic vibrator or vibrators. The driving frame is connected to the sieve by means of rigid pushing rods 7. The feed is in tank 8 with valve 9 which controls the size of the discharge hole. The coarser fraction is collected to vessel 10, while the finer one to container 11. Dimensions of the tested screen are L = 1500 mm and B = 500 mm. In the case of screening of fine materials this is a typical industrial-scale screen. Such are the sieve surfaces of machines used for screening of fine- and very fine-grained materials.

Two types of material were used in the investigation. These were marble aggregate that represented sharp-edged particles, and agalite representing spherical particles. The tested material was dry, with no transient moisture. Both agalite and aggregate were screened preliminarily, impurities were removed and the material was classified into fractions depending on particle diameters. Half of the material were the particles which represented the undersize fraction. Tests were performed on a sieve of mesh size 0.63 mm. The sieve was inclined at 15°, 20°, 25° and 30° to the level.

Results are given in the form of diagrams illustrating the dependence of screening capacity on process efficiency $\eta=f(Q)$. The efficiency was selected so as to carry out the process as a thin-layer screening.

Figures 7 and 8 show curves $\eta=f(Q)$ for angles of sieve inclination given above for agalite, and for marble aggregate, respectively.

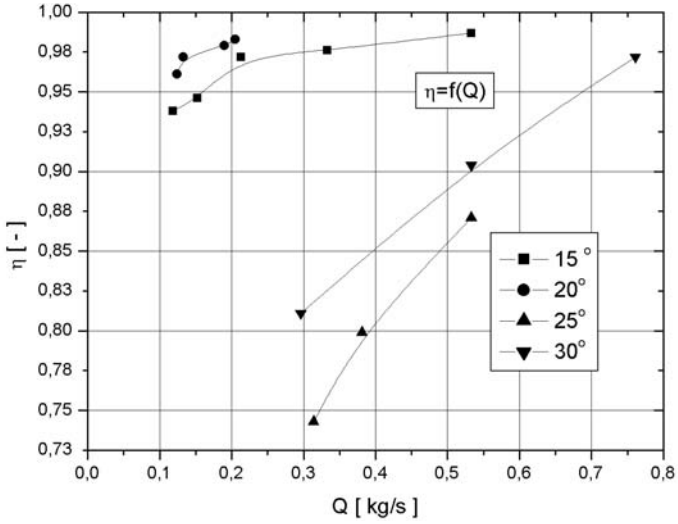

Fig. 7. Dependence of screening efficiency on capacity for agalite

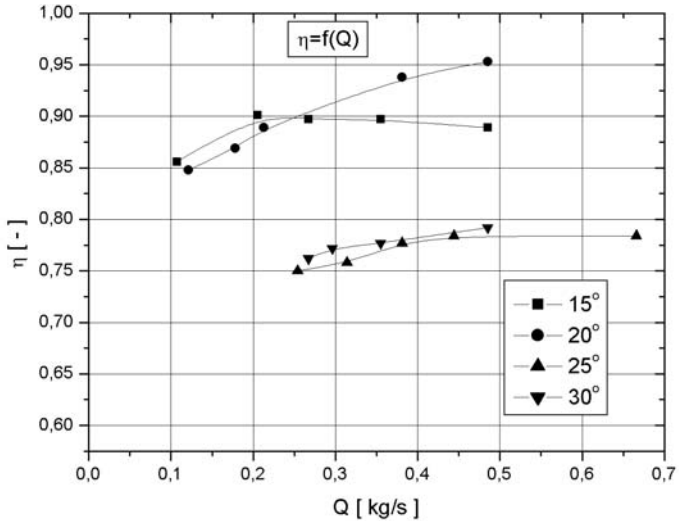

Fig. 8. Dependence of screening efficiency on capacity for marble aggregate

CONCLUSIONS

The aim of the above presented research was to determine experimentally the operating parameters of a frame screen with a vibrating sieve in the process of industrial screening of loose materials with model particle shapes. The subject of studies were two parameters: screening efficiency and capacity. These parameters determine the process; they also form a basis for defining the criterion of estimation of the device operation quality.

The analysis of results leads to the following detailed conclusions:

1. The character of curves shown in the diagrams suggests that high screening efficiency can be achieved at properly chosen process parameters.
2. An increase of efficiency in some cases may provide the evidence that at a further growth of process efficiency, a point will be reached that corresponds to a maximum screening efficiency. The screening should be carried out for such conditions.
3. Also the angle of sieve inclination is an important factor that determines if the screening is correct.
4. It follows from the presented graphs that the conditions of grain classification should be determined taking into account the type of material screened. Different shapes of screened particles have different abilities of passing through the mesh.
5. It is possible to achieve high screening efficiency when the sieve, while vibrating in a non-uniform way on its whole surface, has an ability of self-cleaning, i.e. to release blocked particles.

A screen construction with a driving frame offered a possibility of applying different configurations of the driving system. The frame screen discussed in the paper, because of a simple construction, can be used in almost all industrial conditions.

REFERENCES

1. BANASZEWSKI T. (1990), *Przesiewacze*, Śląsk, Katowice.
2. SZTABA K.(1993), *Przesiewanie*, Śląsk, Wyd. Techniczne, Katowice.
3. SZYMAŃSKI T., WODZIŃSKI P.(2001), *Membrane screens with vibrating sieves, Physicochemical Problems of Mineral Procesing*, 35, s.113-123.1
4. SZYMAŃSKI T., WODZIŃSKI P. (2002), *Rozkład amplitudy na sicie przesiewacza membranowego z sitem drgającym*, ZN Polit. Śląskiej nr 1564, s.601-614.
5. WODZIŃSKI P.(1997), *Przesiewanie i przesiewacze*, Monografie, Wyd. P.Ł., Łódź.

This study is next in a series devoted to membrane screens and is part of the research program on „The classification of granular materials" carried out within Basic Research Project no. Dz.St.12.

Szymański T., Wodński P., *Proces przesiewania na przesiewaczu z sitem drgającym*, Physicochemical Problems of Mineral Processing, 37 (2003) 27-36 (w jęz. ang.).

Niniejszy artykuł dotyczy przesiewaczy membranowych z sitem drgającym i jest kolejną pracą z tego cyklu, wykonywaną w Politechnice Łódzkiej. Przesiewacze membranowe są to maszyny o specyficznym ruchu sita, bowiem wymuszany jest punktowo ruch samego sita, przeponowo rozpiętego w nieruchomym rzeszocie. Sito to charakteryzuje się nierównomiernym rozkładem amplitudy na powierzchni drgającej. Jest to cecha wyróżniająca tego typu przesiewacze od innych spotykanych w przemyśle. W związku z wyżej wymienioną cechą sposób prowadzenia procesu przesiewania nie jest taki sam jak na innych przesiewaczach. Poniższy artykuł dotyczy tychże różnic, jak również sposobu ich opisu. W artykule przedstawiono wyniki badań nad skutecznością przesiewania w zależności od wydajności procesu. Znamienną cechą klasyfikacji na przesiewaczach z sitami drgającymi jest cienka warstwa materiału na sicie, której grubość równa jest wymiarowi ziarna podziałowego lub jest najwyżej dwukrotnie większa. Stwarza to bardzo korzystne warunki dla przebiegu klasyfikacji. Dlatego uzyskuje się bardzo wysokie sprawności, dochodzące do 100%, co nie jest możliwe do osiągnięcia na przesiewaczach klasycznych. Również wydajności procesu są znacznie większe od osiąganych na innych maszynach przesiewających. W artykule przedstawiony został nowy sposób opisu procesu przesiewania na przesiewaczach z sitami drgającymi. Dla przesiewania cienkowarstwowego, autorzy poniższego artykułu proponują zastąpić eksponencjalną krzywą wysypu - linią prostą. Na sicie przesiewacza z sitem drgającym w początkowym okresie procesu znajduje się warstwa o grubości równej co najwyżej kilku wymiarom ziarna podziałowego. Natomiast w końcowym etapie przesiewania warstwa o grubości równej średniemu wymiarowi ziaren klasy górnej. Spośród wielu rozwiązań konstrukcyjnych przesiewaczy z sitami drgającymi najbardziej korzystny wydaje się układ z ramą napędową, który opracowany został w Politechnice Łódzkiej. W przesiewaczu tym rama napędowa wzbudzana jest do drgań, które z kolei przenoszone są na sito za pomocą łączników zwanych popychaczami. W badanych układach zastosowano popychacze dwustronnego działania, które charakteryzują się tym, że przenoszą pełne drgania na sito przesiewacza. Układ z ramą napędową jest rozwiązaniem uniwersalnym, w którym bez większych zmian konstrukcyjnych można zastosować jeden lub dwa wibratory elektromagnetyczne, jak również napęd składający się z dwóch silników z wałami niewyważonymi pracujących w synchronizacji przeciwbieżnej. Zalety i uniwersalność budowy przesiewacza ramowego powodują, że może on znaleźć i znajduje szerokie zastosowanie w przemyśle. Rezultaty badań mogą być bezpośrednio wykorzystane do celów projektowych, ponieważ omawiany przesiewacz jest wykonany w skali przemysłowej dla materiałów drobno uziarnionych.

Physicochemical Problems of Mineral Processing, 37 (2003) 37-50
Fizykochemiczne Problemy Mineralurgii, 37 (2003) 37-50

Marta KRASOWSKA*, Marcel KRZAN*, Kazimierz MAŁYSA*

BUBBLE COLLISIONS WITH HYDROPHOBIC AND HYDROPHILIC SURFACES IN α-TERPINEOL SOLUTIONS

Received March 2003, reviewed, and accepted May 15, 2003

Influence of α-terpineol on phenomena occurring when a gas bubble approaches (collides with) hydrophilic (glass) and hydrophobic (Teflon) solid surfaces was revealed using high-speed camera (1182 frames/s). It was found that the bubble approaching the solid surface bounced backwards from the surface and its shape pulsated rapidly with frequency over 1000Hz. Number of the bouncing cycles and magnitude of the shape pulsations were decreasing with increasing α-terpineol concentrations. In distilled water the amplitude, frequency and number of the "approach-bouncing" cycles were identical at Teflon and glass interface. In of α-terpineol solutions a "necking" formation was recorded at Teflon surface, but not at the glass. The "necking" formation is a straightforward indication that the three-phase contact was formed. We found the most intriguing that a small amount of α-terpineol (adsorption coverage of 0.6%) sped-up and affected in such significant degree the bubble attachment to the hydrophobic surface. It was found that the induction time of the bubble attachment to Teflon was 5 milliseconds in α-terpineol presence. The average thickness of the thin liquid film separating the bubble and Teflon was estimated to be ca. 2,7 μm at the film rupture.

Key words:gas bubble, glas, Teflon, collision, α-terpineol

INTRODUCTION

Attachment of solid grains to air bubbles is a necessary condition of flotation, because the bubbles act as carriers transporting grains of useful ore component(s) to the froth layer. During flotation the bubbles and particles (independent of their nature, i.e. both hydrophobic and hydrophilic) are repeatedly brought together within the cell into positions of close encounters and/or collisions, necessary for formation of the

* Institute of Catalysis and Surface Chemistry Polish Academy of Sciences, ul. Niezapominajek 8, 30-239 Krakow, Poland, ncmalysa@cyf-kr.edu.pl

bubble-grain aggregates. Collectors and frothers are two essential types of the reagents added into flotation system to modify properties of the solid/liquid and liquid/gas interfaces and enable separation of the useful grains of the ore from gangue minerals. Schulman and Leja (Schulman and Leja, 1954; Leja, 1956-57) pointed out the importance of the proper choice of the collector and frother because their molecules should interact to facilitate rupture of the liquid film and enable formation of the three-phase contact. Probability, P, of formation of a stable bubble-grain aggregate can be considered (Derjaguin and Dukhin, 1960; Schimmoler et. al., 1993; Ralston and Dukhin, 1999) as:

$$P = P_c P_a P_d \tag{1}$$

where P_c is the probability of collision, P_a is the probability of attachment (formation of the tree phase contact) and P_d is the probability that detachment would not subsequently occur.

Probability of the collision is determined mainly by hydrodynamic conditions of the bubbles and particles motion. Surface properties of the solid/liquid and liquid/gas interfaces are decisive for attachment and detachment efficiencies. Thus, the differentiation between hydrophobic and hydrophilic particles occurs at these stages of the bubble-particle interactions (Leja, 1982). For formation of a stable bubble-particle aggregate the following processes have to take place (after particle and bubble collision): i) the syneresis and thinning of the liquid layer separating the bubble and particle to a critical rupture thickness, ii) the rupture of the liquid film and formation of a "hole" of the three phase contact, and iii) the expansion of the "hole" and formation of the perimeter of the three phase contact assuring stability of the bubble-particle aggregate. It is well-known that the hydrophobization of the surface of grains of useful component of the ore is a key factor for successful flotation separation. However, there is still a lot of unanswered questions and discussion related to the mechanism and time scale of the particle attachment to bubble, despite numerous studies addressing this problem (Nguyen et.al., 1997; Stechemesser and Nguyen, 1998; Schulze et.al., 2001; Yoon, 2000; Wang et.al., 2003; Gu et.al., 2003 - to mention only a few of the recent papers).

The paper presents results of studies of the influence of α–terpineol concentration on phenomena occurring when the bubble collides with solid hydrophilic and hydrophobic surfaces, and with free surface of the solution, as well. Rapid bubble pulsations ($f > 1000$ Hz) and bouncing from the solid surfaces and also the solution free surface were recorded and are described. Timescale of the bubble collisions, bouncing and attachment (when occurs) is presented for the interfaces studied.

EXPERIMENTAL

The experimental set-up is presented in Fig.1. It consists of the following main parts: i) a glass column with capillary and gas supply system, ii) recording camera, and iii) system of the movie transferring, splitting into single frames and image analysis.

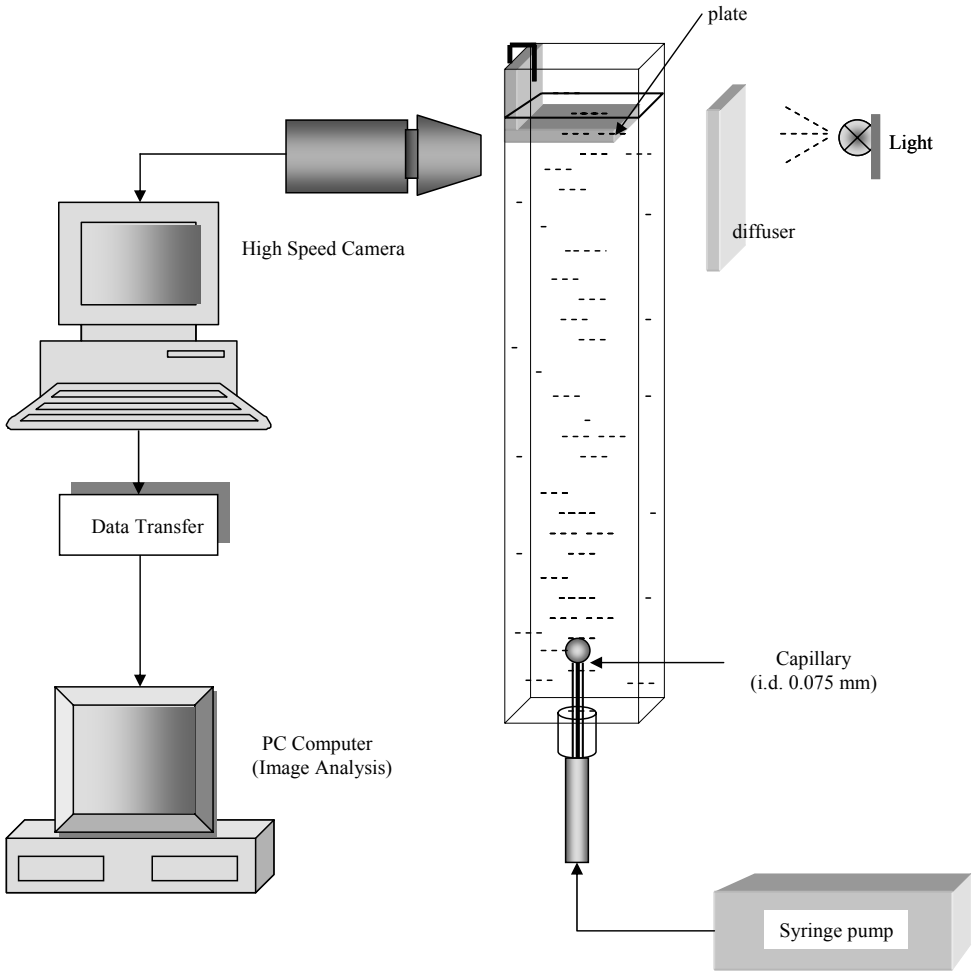

Fig. 1. Schematic of the experimental set-up

To avoid optical distortions the square glass column (50x50 mm) having at the bottom a capillary of inner diameter 0.075mm was used in the experiments. Bubbles were formed at the capillary orifice using the high precision (Cole-Parmer) syringe pump. At distance of ca. 30 cm from the capillary orifice (just beneath the solution surface) a glass (hydrophilic surface) or Teflon (hydrophobic surface) plate was mounted. Phenomena occurring when the bubble approached the solid surfaces and free surface of the solution were recorded. The movies were recorded using the high-speed (1182 frames per second) camera (with Cosmicar objective and rings for higher magnification). The movies obtained were transformed into BMP pictures and analyzed using a PC with SigmaScanPro Image Analysis Software. The distances between interface and bubble, subsequent positions of the bubble, and the bubble diameters were measured as a function of time. During collisions of the bubble with solid surface the bubble velocity variations were determined on the basis of measurements of the positions of the bottom pole of the bubble. To get absolute dimensions the image of nylon sphere of 3.89mm diameter was recorded after each experiment. The entire set-up was located on a vibration isolated laboratory table with an automatic levelling system.

Four-times distilled water and high purity α-terpineol were used for solution preparation. The glass and Teflon plates were cleaned with a chromic mixture and carefully washed-out with distilled water. The plates were immersed into solution studied for at least a few minutes (to have adsorption equilibrium) prior to the experiment. The experiments were carried out in room temperature.

RESULTS AND DISCUSSION

Figure 2 shows the sequences of frames illustrating the phenomena occurring when the rising bubble approaches Teflon (Fig. 2A) and glass (Fig. 2B) surface in α-terpineol solution of concentration $1 \cdot 10^{-5}$ M. Each subsequent picture shows the bubble position and its shape after time interval of 0.845 ms. Comparing both sets of the pictures one can immediately notice similarities and differences in the sequences of phenomena occurring during the bubble collision with Teflon and glass surfaces. In both cases: i) the bubble approaching the solids surfaces did not „stay " immediately at the surface, but started to move backward, i.e. opposite to the direction of the buoyancy force, ii) the bubble shape pulsated rapidly, changing its shape during time intervals shorter than 0.845ms. The distinct difference in the collision course can clearly be noted on the frames showing the second approach of the bubble to these solid surfaces. In the case of glass (hydrophilic surface) the phenomena occurring during the bubble second approach are qualitatively similar as during the first one, i.e. the bubble bounced after collision and simultaneously its shape pulsated rapidly. However, in the case of Teflon (hydrophobic surface) a "necking" formation can be clearly seen after the bubble second approach. Such necking formation was described some time ago by Schulman and Leja (1958).

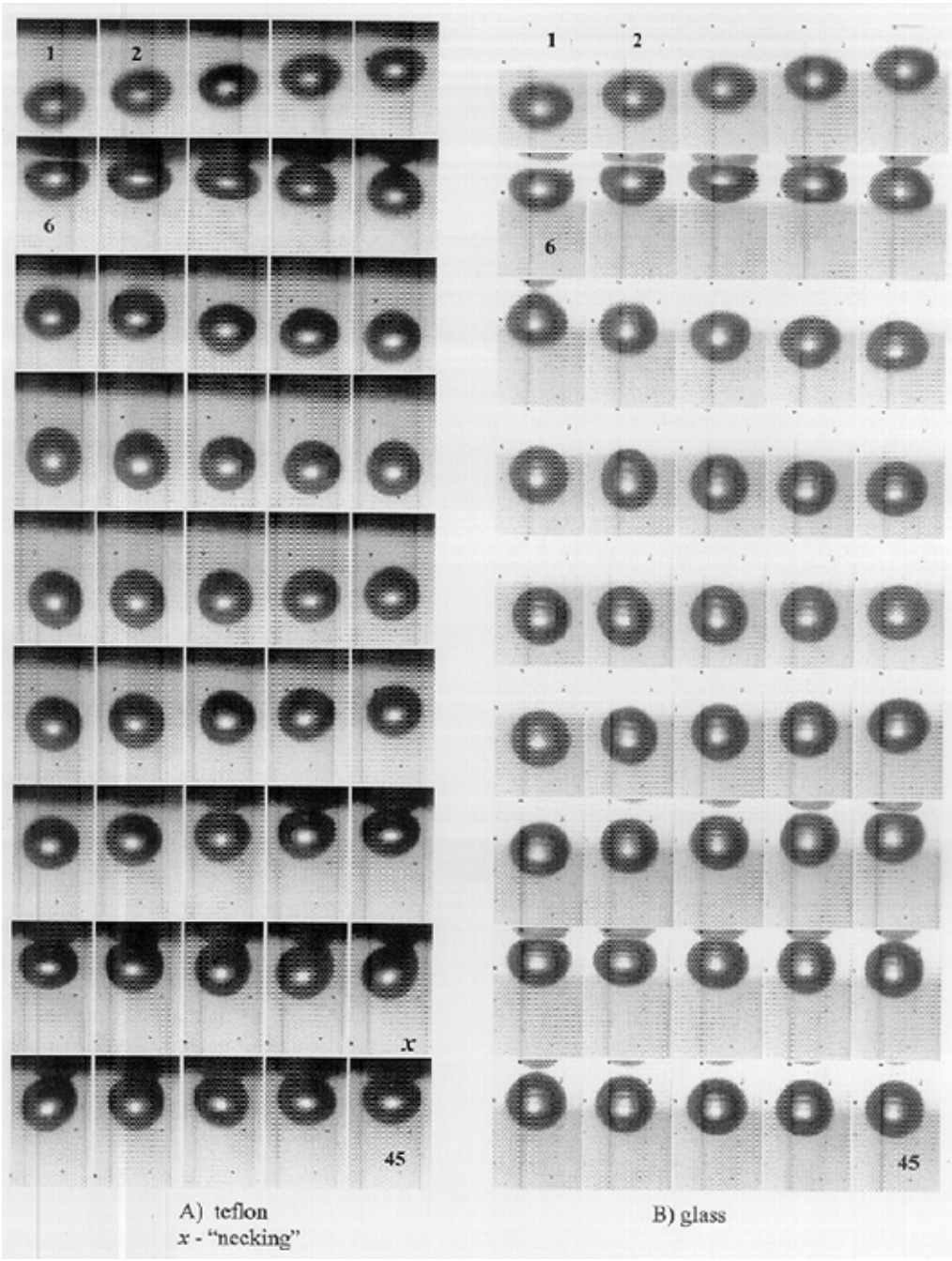

Fig. 2. Images of the bubble bouncing and pulsations in $1 \cdot 10^{-5}$ M α-terpineol solutions at the solid surfaces: A) Teflon, and B)glass. Time interval between every frame is 0.846 ms

Formation of this "necking" is a straightforward indication that the three phase contact solution-gas-Teflon was formed. As a result of the three phase contact formation the bubble was attached to Teflon surface and it's bouncing was stopped.

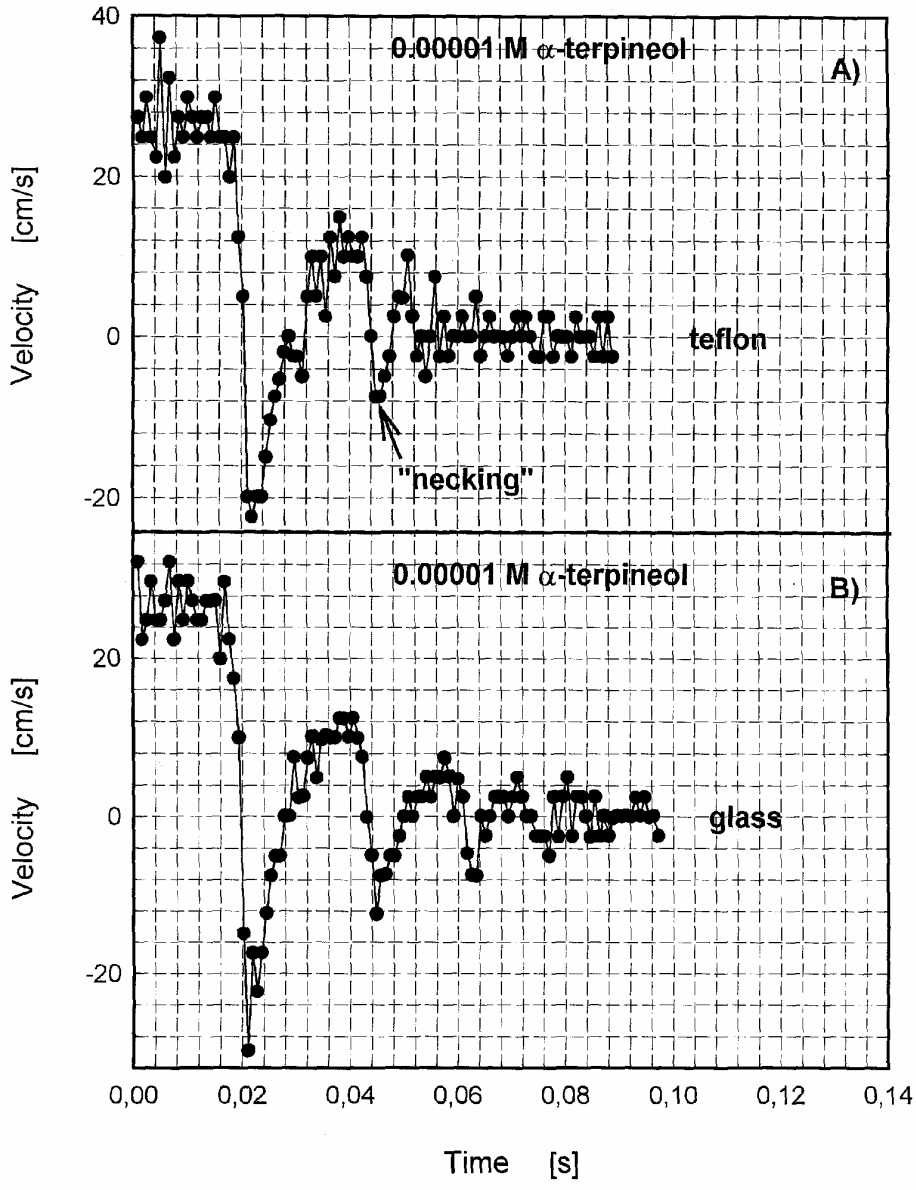

Fig. 3. Variations of the bubble velocity in $1 \cdot 10^{-5}$ M α-terpineol solution during the "approach-bouncing" cycles at: A) Teflon, and B) glass surface

The results of analysis of variations of the bubble velocity during collisions with solid hydrophobic (Teflon) and hydrophilic (glass) surfaces in $1 \cdot 10^{-5}$ M α-terpineol solution are presented in Fig. 3. As seen there the velocity of the bubble approach to the solid surfaces was constant (ca. 26.5 cm). On collision with Teflon (Fig.3A) or glass (Fig.3B) surface the bubble velocity was rapidly slowed down and then, the bubble moved backwards reaching the velocity up to 22-28 cm/s. Next, the bubble started second approach to the solid surface. It is worthy to underline how rapid this cycle was. As can be seen in Fig.3 the timescale of the bubble velocity changing from +20 cm/s to –20 cm/s was 3-4 ms. Next, the bubble started its second approach to the surface, but the velocity of the second approach was lower (ca. 12 cm/s) as a result of the energy dissipation. During this second approach the bubble formed the three-phase contact with Teflon surface and, as a result of the bubble attachment to Teflon surface, the "necking" could be noticed (see Fig. 2A). In the case of glass, the three-phase contact was not formed and the bubble bounced again – there was no "necking" (see Fig. 2B). From the moment of the "necking" formation at Teflon surface there is clearly seen difference in the profiles of the bubble velocity variations at Teflon and glass surfaces (compare Fig. 3A and 3B). Attachment of the bubble to Teflon surface caused rapid damping of the bubble bouncing, while in the case of glass at least 2 additional cycles "approach-bouncing" were still detected (see Fig. 3B). As described above (Experimental) the instantaneous values of the bubble velocity were determined from measurement of the positions of the bottom pole of the bubble. Therefore, we believe that the velocity changes which can still be noted after the "necking formation" at Teflon surface (Fig. 3A) are in reality the bubble shape pulsations only. This is also confirmed by the fact that these velocity fluctuations are of significantly higher frequency than the real approach-bouncing cycles observed at the glass surface.

Data presented in Figs. 2 and 3 show straightforward that - as one could expect - the bubble attachment occurred at the hydrophobic surface, but not at the hydrophilic one. Moreover, they show that the timescale of the liquid film rupture and formation of the three-phase contact is of an order of a few milliseconds only. However, the importance of α-terpineol presence for the attachment to occur is rather unexpected and most intriguing. We have just found that without α-terpineol presence, i.e. in distilled water, the bubble attachment to Teflon surface was strongly hindered or at least slowed down.

Figure 4 presents the pictures of the bubble "approach-bouncing" cycles and its shape pulsations on collisions with Teflon (Fig. 4A) and glass (Fig. 4B) in distilled water. Variations of the bubble instantaneous velocities during the collisions are presented in Fig. 5 for Teflon (Fig. 5A) and glass (Fig. 5B). In distilled water the velocity variations of the "approach-bouncing" cycles are identical for Teflon and glass. Four distinct "approach-bouncing" cycles were detected both at Teflon and glass surfaces. Moreover, the amplitude and frequency of the velocity variations were identical on collisions with the hydrophobic and hydrophilic surfaces. There was no "necking" with the hydrophobic Teflon surface. Lack of the "necking" formation in

distilled water is also clearly seen on sequences of photos presented in Fig. 4. There are presented variations of the bubble shape and positions during 3 "approach-bouncing" cycles and no difference between collisions with Teflon and glass can be spotted.

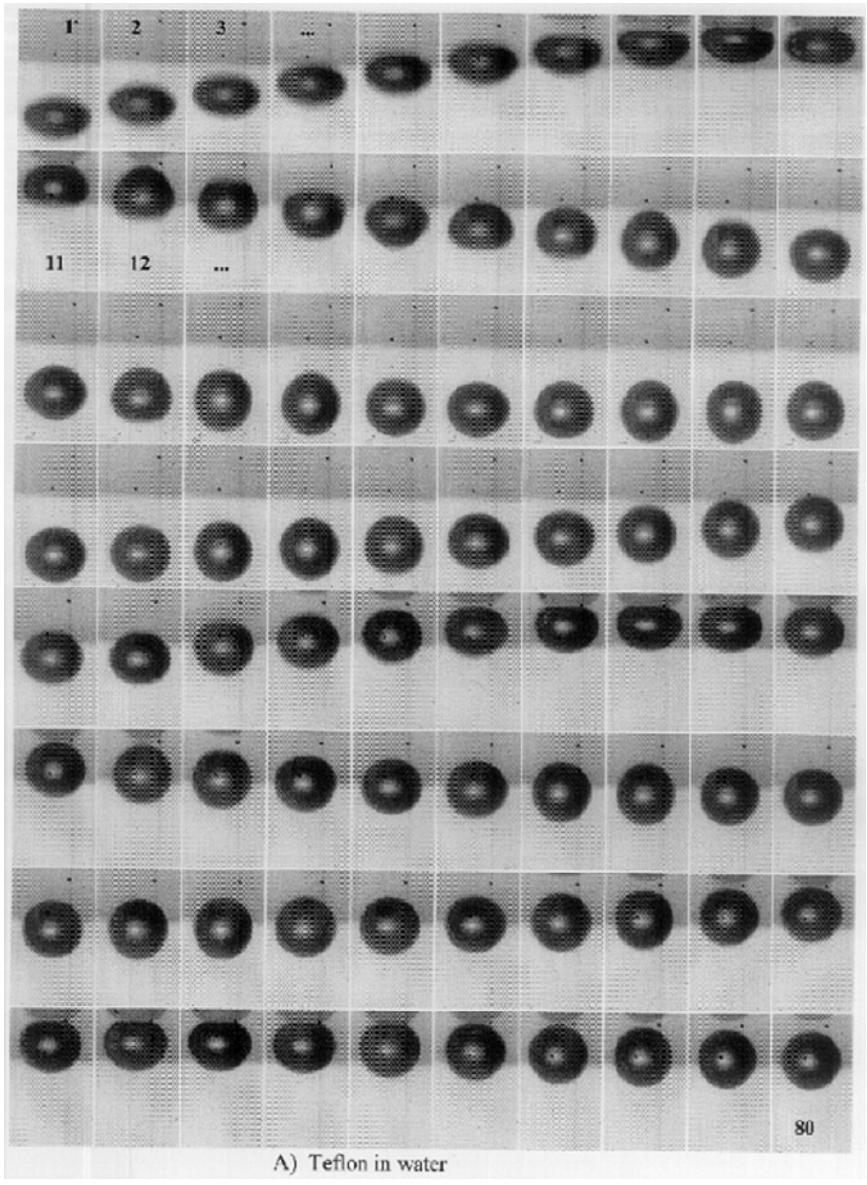

Fig. 4. Images of the bubble bouncing and pulsations in distilled water at: A) Teflon, and B) glass. Time interval between every frame is 0.846 ms

Certainly, we do not intend to claim that at longer time of contact the bubble will not be attached to the hydrophobic surface of Teflon. Surely, there will be formation of the three-phase contact and the bubble attachment to Teflon surface. However, we found it really fascinating how even this small amount of α-terpineol affected and sped-up the bubble attachment to the hydrophobic surface. At α-terpineol concentration of $1 \cdot 10^{-5}$ M the average adsorption coverage at bubble surface was 0.6% (Krzan and Malysa, 2002). Increasing α-terpineol concentration to $3 \cdot 10^{-5}$ M only (adsorption coverage - 1.8%) caused formation of the "necking" during the bubble first approach to Teflon surface, as showed in Fig. 6. There was no "necking" in the case of the glass surface (Fig.6B) and the bubble bounced backwards. This effect of α-terpineol presence on kinetics of the three phase contact formation with hydrophobic surface is really astonishing and confirms the Schulman-Leja theory (Schulman and Leja, 1954; Leja, 1956-57) about importance of frother in attachment of grains to bubble surface.

Data presented in Figs 2, 3 and 6 enable estimation of values of the induction time (Sven-Nilsson, 1934) for Teflon. The induction time is defined, generally speaking, as a minimum time of contact of the bubble and grain necessary to attach the grain to the bubble. Commonly, the induction time is measured by moving either a captive bubble in a solution toward and away of a bed of mineral grains or by moving the beds of grains toward and away from the bubble. In such measurements the induction time includes the times of: i) approach (collision), ii) film thinning, iii) film rupture, and iv) formation and spreading of the three phase contact. If we include all these stages into values of the induction time, which can be called $t_{ind.(max)}$, then we have the values of 26 and 5 ms for α-terpineol concentrations $1 \cdot 10^{-5}$ and $3 \cdot 10^{-5}$ M (see Figs. 3A and 6A), respectively. However, it seems more appropriate to consider, as was recently discussed by Gu et. al (2003) and Nguyen et. al. (1997), that the induction time consists only of the time required for film thinning, rupture and three phase contact expansion.

Bubble velocity profiles are an indication of the processes taking place during our experiments at solid surface. Far away from the interface the bubble moved with a constant terminal velocity in α-terpineol solutions (Krzan and Malysa, 2002). Decreasing and reversal of the bubble velocity means that the bubble was slowed down, stopped and bounced back as a result of the processes occurring in a thin liquid layer separating the bubble from solid surface. If the bubble did not bounce back but the "necking" formation was observed, then, during this time period the following processes occurred: i) drainage of the thin liquid film to a critical thickness of rupture, ii) rupture of the film and formation of the three phase contact, and iii) spreading of the tree phase contact spreading to a minimum radius required for a stable attachment. When the bubble bounces back without the "necking" formation it means that thin liquid film did not rupture and the three-phase contact was not formed. As seen from Figs. 2-6 only at the hydrophobic Teflon surface and in presence of α-terpineol the bubble attachment was observed. According to the discussion presented above the

time of the first approach-bouncing cycle in $1 \cdot 10^{-5}$ M α-terpineol solution should not be included in evaluation of the induction time values. Thus, as seen from Figs. 3 and 6 the real values of the induction time are 5 milliseconds, both for $1 \cdot 10^{-5}$ and $3 \cdot 10^{-5}$ M α-terpineol solutions.

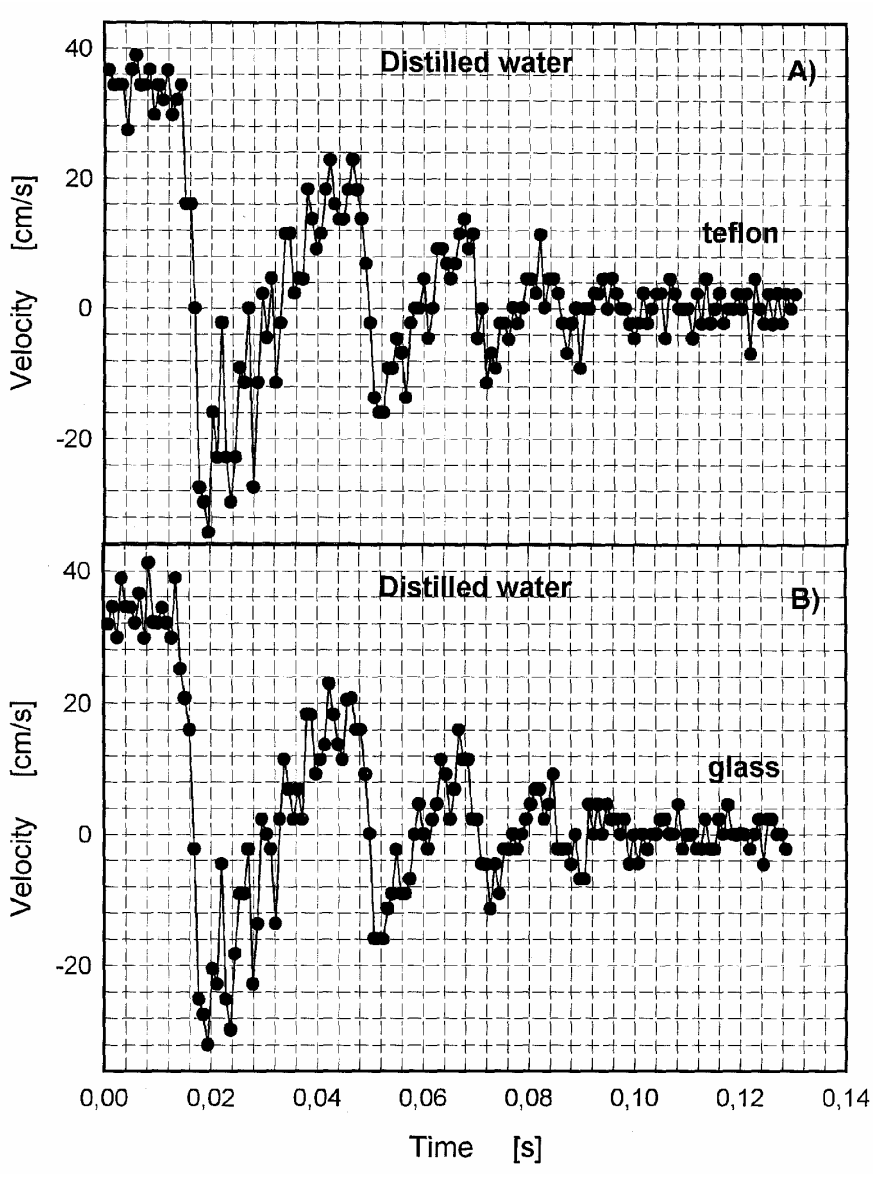

Fig. 5. Variations of the bubble velocity in distilled water during the "approach-bouncing" cycles at: A) Teflon, and B) glass surface

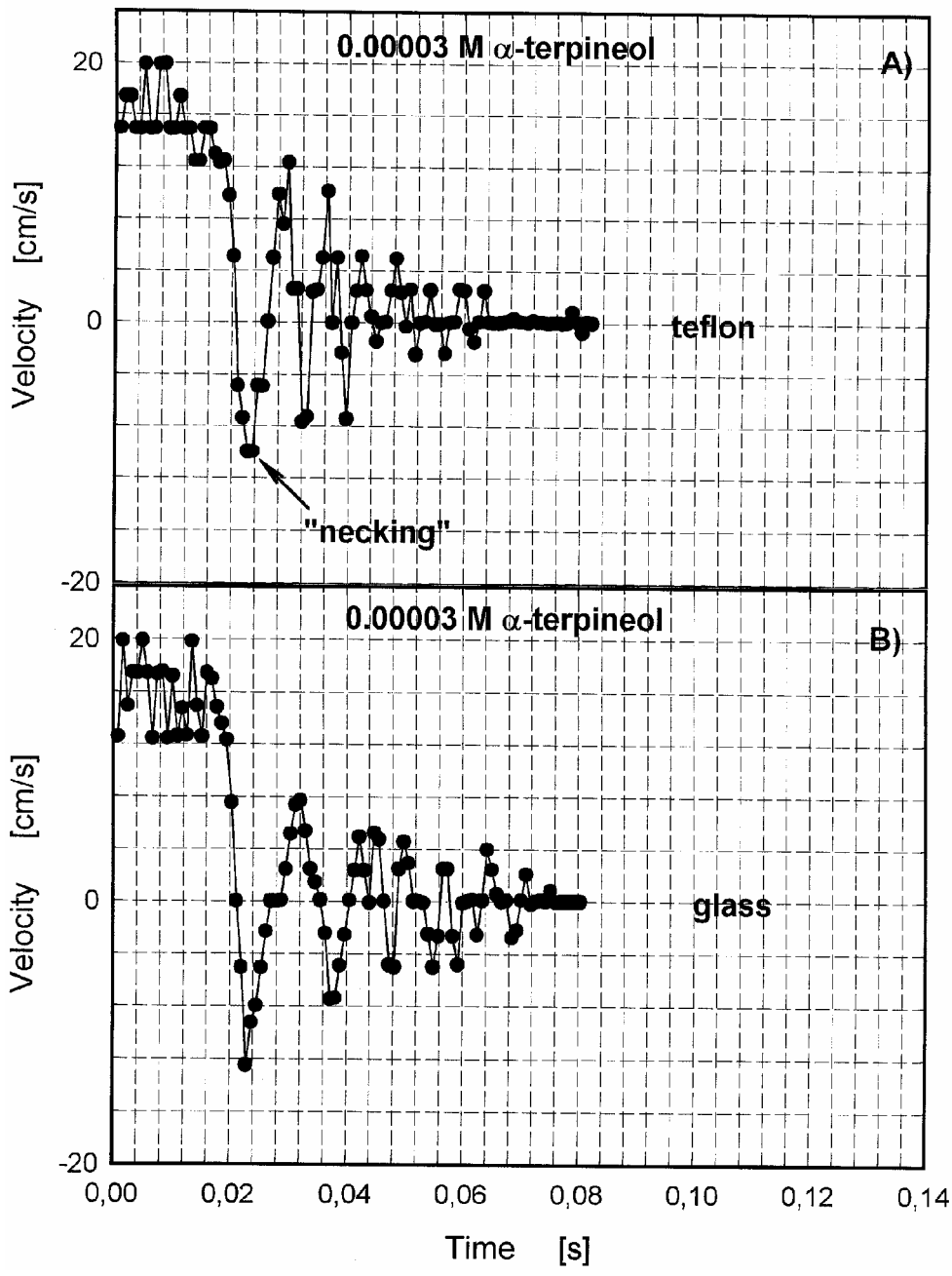

Fig. 6. Variations of the bubble velocity in $3 \cdot 10^{-5}$ M α-terpineol solution during the "approach-bouncing" cycles at: A) Teflon, and B) glass surface

We can also estimate an average thickness of the thin liquid film prior to its rupture at Teflon surface. According to Scheludko (1967) the thinning of the circular plane parallel film between a solid wall (non-slip conditions) and free surface (full mobility) can be described by the following relation:

$$\frac{d(1/h^2)}{dt} = \frac{16}{3\eta R_F^2}\Delta P \tag{2}$$

where h is the film thickness, t time, η viscosity, R_F radious of the film and ΔP difference between pressure in the thin film and preassure in bulk phase. After integration and assuming that at t=0, $h \Rightarrow \infty$ we obtain:

$$\frac{1}{h^2} = \frac{16}{3}\frac{\Delta P}{\eta R_F^2}t \tag{3}$$

From relation (4) the effective radius of the film formed by a bubble at interface can be found (Princen, 1969; Jachimska et al., 1998):

$$R_F^2 = \frac{FR_b}{\pi\sigma_{eq}} \tag{4}$$

where R_B is the bubble radius, σ_{eq} is the soluton surface tension, and F is the total force causing the film thinning (buoyancy force, disjoining pressure, capillary force). Taking into account that:

$$\Delta P = \frac{2\sigma_{eq}}{R_b} \tag{5}$$

$$F = \frac{4}{3}\pi R_b^3 \rho g \tag{6}$$

we can obtain finally from Eqs. 3-6 that:

$$\frac{1}{h^2} = 8\frac{\sigma_{eq}^2}{\eta\rho g R_b^5}t \tag{7}$$

where ρ is solution density and g gravity acceleration.

In the case of α-terpineol solution of concentration $1 \cdot 10^{-5}$ M the bubble radius R_b = 0,07 mm, σ = 72.6 mN/m, g=9.81 m/s, η = 0.001 Nsm^{-2}. Assuming, that the thinning time is equal to the induction time, i.e. $t = 5 \cdot 10^{-3}$ s we will obtain (Eq. 7) that the average thickness of the rupturing film was ca. 2.7 μm. This value seems to be reasonable and of similar order as that one reported elsewhere (Malysa, 1998) for the rupture thickness of foam films in top layer of α-terpineol foams. Please, take into account that these values refer to the average thickness of the films. Certainly, in reality the thinning films are not plane parallel - there is a lot of thickness fluctuations and as a result locally, at the area of hole nuclei of the three phase contact formation, this rupture thickness can be smaller. Thus, the estimated average thickness should be treated as the highest limit of the thickness of the film rupture.

CONCLUSIONS

Bubble colliding with solid surface is not stopped immediately, but bounces backwards within timescale of a few milliseconds. Simultaneously, its shape pulsates rapidly with frequency over 1000Hz. Number of the bouncing cycles and magnitude of the shape pulsations was the highest in distilled water and was decreasing with increasing α-terpineol concentrations

In distilled water the amplitude, frequency and number of the "approach-bouncing" cycles were identical at hydrophobic (Teflon) and hydrophilic (glass) surfaces.

In α-terpineol a presence of "necking" formation was observed at the Teflon surface, but not at glass. The "necking" formation is a straightforward proof that the three-phase contact was formed. The induction time of the bubble attachment to Teflon was 5 milliseconds.

It was estimated, on the basis of the induction time determined, that the average thickness of the thin liquid film separating the bubble and Teflon was ca. 2.7 μm prior to the film rupture.

ACKNOWLEDGEMENTS

Skilful assistance of Eng. M. Baranska with the experiments is gratefully acknowledged. The authors thank Dr. K. Lunkenheimer and MPI fur Kolloid- und Grenzflachenforschung for making available the SpeedCam512+ for this study.

REFERENCES

DERJAGUIN, B.V. and DUKHIN S.S., (1960), "*Theory of flotation of small and medium-size particles"*, Trans. Inst. Min. Metall, 70, 221-246.

GU, G., XU, Z., NADAKUMAR, K., MASLIYAH, J., (2003), *"Effects of physical environment on induction time of air-bitumen attachment"*, Int. J. Miner. Process., 69, 235-250.

JACHIMSKA, B., WARSZYNSKI, P., MAŁYSA, K., (1998), *"Effect of motion on lifetime of bubbles at n-butanol solution surface",* Colloids & Surfaces A:, 143, 429-440.

KRZAN, M, MALYSA, K., (2002), *"Influence of frother concentration on bubble dimensions and rising velocities",* Physicochem. Problems Mineral Process., 36, 65-76.

LEJA, J., (1956-1957), *"Mechanism of collector adsorption and dynamic attachment of particles to air bubbles as derived from surface-chemical studies"*, Inst. Mineral. Metal. Trans., 66 (9) 425-437.
LEJA, J., *Surface Chemistry of Froth Flotation.* Plenum Press, New York and London, 1982, chap. 9.
MALYSA, K., (1998), "*Water contents and distribution in flotation froth"* in *"Frothing in Flotation - II*." (J.Laskowski and E.T.Woodburn - Eds.), Gordon and Breach Publishers, chap.3, pp. 81-108.
NGUYEN, A.V., SCHULZE, H.J., STECHEMESSER, H., ZOBEL, G., (1997), *"Contact time during impact of a spherical particle against a plane gas-liquid interface: experiment*", Int. J. Miner. Process., 150, 113-125.
PRINCEN, H. M., (1969), *in* "*Surface and Colloid Science*" (E. Matijevic and F. E. Eirich - Eds.), vol. 2, p. 45.
RALSTON, J. and DUKHIN S.S., (1999), *"The interaction between particles and bubbles"*, Colloids & Surfaces A:, 151, 3-14.
SCHELUDKO, A., (1967), "*Thin liquid films"*, Advances Coll. Interface Sci., 1, 391-464.
SCHIMMOLER B.K., LUTRELL G.H., YOON R.-H., (1963), *"A combined hydrodynamic-surface force model for bubble-particle collection*". Proc. XVIII Intern. Miner. Process. Congress, Sydney, vol. **3**, pp. 751-756.
SCHULMAN, J.H. and LEJA, J., (1954), *"Molecular interactions at the solid-liquid interface with special reference flotation and solid stabilised emulsions*", Kolloid-Z., 136 (3/4), 107-120.
SCHULMAN, J.H. and LEJA, J., (1958), *"Static and dynamic attachment of air bubbles to solid surfaces",* in *"Surface Phenomena in Chemistry and Biology*.", (J.F. Danielli, K.G.A. Pankhurst, A.C. Riddiford - Eds.), Pergamon Press, pp. 236-245.
SCHULZE, H.J., STOCKELHUBER, K.W., WENGER, A., (2001), *The influence of acting forces on the rupture mechanism of wetting films – nucleation or capillary waves,* Coll. & Surfaces A:, 192, 61-72.
STECHEMESSER, H., NGUYEN, A.V., (1998), *"Dewetting kinetics between a gas bubble and a flat solid surface and the effect of three-phase solid-gas-liquid contact line tension"*, Colloids & Surfaces A:, 142, 257-264.
SVEN-NILSSON, I., (1934), *"Effect of contact time between mineral and air bubbles on flotation"*, Kolloid-Z., 69 (2) 230-232 (according to Gu et.al., 2003).
WANG, W., ZHOU, Z., NADAKUMAR, K., XU, Z., MASLIYAH, J.H., (2003), *"Attachment of individual particles to a stationary air bubble in model systems"*, Int. J. Miner. Process., 68, 47-69.
YOON R.-H., (2000), "*The role of hydrodynamic and surface forces in bubble-particle interaction"*, Int. J. Miner. Process., 58, 129-143.

Krasowska M., Krzan M., Małysa K., *Kolizje baniek powietrza z hydrofobowymi i hydrofilnymi powierzchniami w roztworach α-terpinolu*, Physicochemical Problems of Mineral Processing, 37 (2003) 37-50 (w jęz. ang.).

Wyznaczono wpływ α-terpineolu (spieniacz) na przebiegi procesów zachodzących w trakcie kolizji baniek powietrza z hydrofilową (szkło) oraz hydrofobową powierzchnia (teflon) ciała stałego. Uzyskano za pomocą szybkiej kamery (1182 klatki/s), zdjęcia procesów zachodzących podczas zderzenia bańki z powierzchnią ciała stałego o skrajnie różnych właściwościach hydrofobowo-hydrofilowych. Stwierdzono, że bańka dochodząca do powierzchni ciała stałego nie zostaje unieruchomiona, lecz może ulegać wielokrotnemu odbiciu i równocześnie jej kształt pulsuje z częstotliwością powyżej1000 Hz. Pulsacje, liczba odbić i ich amplituda maleją wraz ze wzrostem stężenia α-terpineolu. W wodzie destylowanej liczba odbić i ich amplituda są identyczne zarówno przy powierzchni szkła jak i przy powierzchni teflonu. Natomiast w roztworach α-terpineolu zaobserwowano tzw. „necking" przy powierzchni teflonu, który dowodzi powstania trójfazowego kontaktu. Interesujący jest też fakt, że tak minimalne stężenie α-terpineolu (dające pokrycie adsorpcyjne 0.6%) umożliwiło i przyspieszyło utworzenie trójfazowego kontaktu z powierzchnia hydrofobową. Stwierdzono, że w badanych roztworach α-terpineolu czas indukcji w układzie bańka-teflon wynosił 5 ms. W oparciu o wyznaczony czas indukcji oszacowano, że średnia grubość filmu ciekłego rozdzielającego bańkę i teflon (w momencie jego przerwania) wynosiła ok. 2.7 μm.

Physicochemical Problems of Mineral Processing, 37 (2003) 51-56
Fizykochemiczne Problemy Mineralurgii, 37 (2003) 51-56

Teresa FARBISZEWSKA[*], Jadwiga FARBISZEWSKA-KICZMA[**],
Mirosław BĄK[**]

BIOLOGICAL EXTRACTION OF METALS FROM A POLISH BLACK SHALE

Received March 2003, reviewed, and accepted May 15, 2003

The black shale ore is characterized by variable content of metals. In black shale metals occur in form of sulphides and sandwich compounds in which metals create organometalic connections with hydrocarbons. The method of flotation is successfully used to enriching sandstone and carbonate ores but this method is not effective for the shale ore. In existing technology of shale ore enriching, this ore is in considerable degree not used and passes to waste material. In this study, the bioextraction process was carried out with a Polish cupriferous black shale ore coming from Lubin-Głogów region on a large laboratory scale. This process was carried out in the „Biomel" batch reactor during 28 days with temperature control (40^{o} C), continuous aeration and mixing (300 r.p.m.). There were used two bacterial cultures *A.ferooxidans* F7-01 and *A.thiooxidans* T1- 01. Simultaneously, a control test was performed with thymol as a bacteriostatic substance. A concentration of Cu, Ni, Zn, Pb ions was determined by ASA method every three-four days. The results of investigations confirm our assumptions that Polish black shale ore could be a source of many metals by bioleaching in acid medium. We can suggest that 50% of copper contained in shale is a chalcocite because bioleaching of them was the most effective. The effect of bioleaching sphalerite contained in black shale ore was very low. We have not succeed in bioleaching galena. The following conclusion can be drown: batch strains used in our study convert PbS into $PbSO_4$, which is sparingly soluble and forms precipitate.

Key words: bioleaching, black shale ore

INTRODUCTION

The Lubin deposits of a black shale ore are structured from three litological forms: carbonate, sandstone, shale. The most interesting one and the most rich in copper and many of other metals is the shale layer.

[*]Uniwersytet Opolski, Wydział Przyrodniczo-Techniczny, Katedra Biologii Stosowanej i Eksperymentalnej, ul. Kominka 4, 45-032 Opole, Poland
**Uniwersytet Opolski, Wydział Przyrodniczo-Techniczny, Katedra Inżynierii Procesowej, ul. Dmowskiego 7/9, 45-365 Opole, Poland, gaga@uni.opole.pl

The black shale ore is characterized by variable content of metals and contains on average 5,5% Cu and also, among other metals, about 0,01% Ag, 0,03% V. This ore is created with bituminous shale, which consists mostly from clay minerals, carbonates, organic matter and detritus quartz (Kucha, Mayer, 1996).

In bituminous shale metals occur in form of sulphides and sandwich compounds in which metals create organometalic connections with hydrocarbons (Sawłowicz, Speczik, 1996).

The method of flotation is successfully used to enriching of sandstone and carbonate ores but this method is not effective for shale ore because of its properties. In existing technology of shale ore enriching, this ore is in considerable degree not used and passes to waste material. From several years it has been known, that shale ore should be enriched separately with usage of a new method.

MATERIALS AND METHODS

In this study, the bioextraction process was carried out with a Polish cupriferous black shale ore coming from Lubin-Głogów region. Our initial treatment of shale by sulphuric acid were aimed for removing base-forming minerals. After pre-treatment this shale contained 5,6% Cu, 0,017% Ni, 0,67% Pb, 0,2% Zn, 0,014% Mo, 0,035% V, 0,03% As. Samples of autochthonous *Acidithiobacillus* bacterial strains were isolated and adapted to Cu, Ni, As, Ag cations (Kelly et al. 2000). There were used two bacterial cultures *A.ferrooxidans* F7-01 and *A.thiooxidans* T1-01 stored in Practical and Experimental Biology Department of University of Opole (Farbiszewska et al. 2002).

Bioleaching process was carried out by 28 days in the „Biomel" batch reactor with temperature control (40^{o} C), continuous aeration and mixing (300 r.p.m.). There was placed 800 g black shale ore into 3200 cm^3 leaching medium (Mg^{2+}, SO_4^{2-}, K^+, HPO_4^{2-}, NH_4^+, Fe^{2+}) and 800 cm^3 inoculum. The active bacteria strains presented in culture were F7-01 and T1-01 in ratio 1:1. The concentration of ions in medium was determined as 5g in 1 dm^3. All pH measurements were performed at the reaction temperature and it held on a level pH 2.

Simultaneously there were two control systems, designing as K_1 and K_2. Control tests were performed with 800 g of a black shale ore and 4000 cm^3 leaching medium. There was introduced 25g thymol as a bacteriostatic substance to K_2. A concentration of Cu, Ni, Zn, Pb ions was determined by ASA method every three-four days.

RESULTS AND DISCUSSION

Bioleaching process of cupriferous shale was carried out in acid medium on a large laboratory scale. There were compared amounts (in percentages) of extracted Cu, Ni, Zn, Pb in succeeding days of process duration.

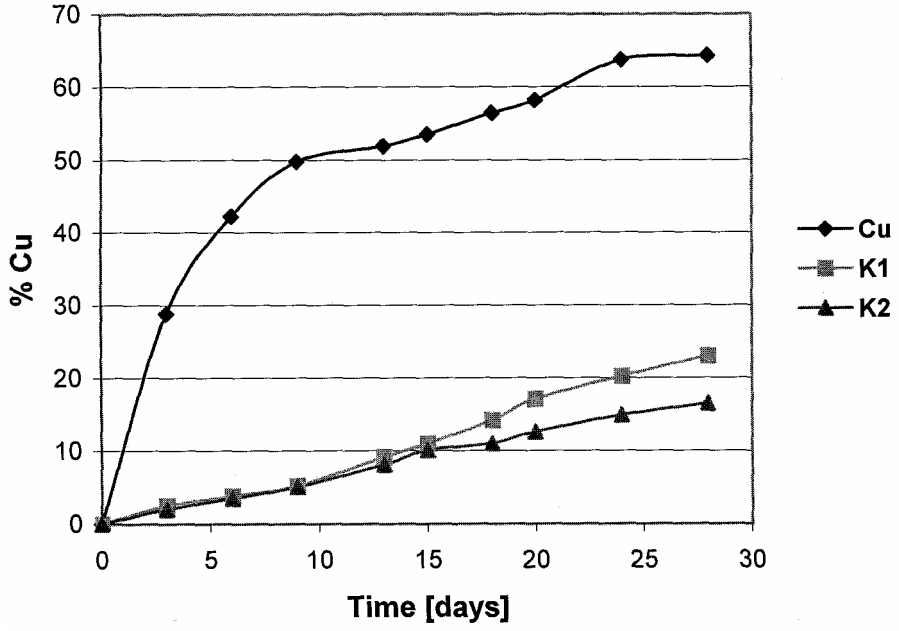

Fig. 1. Percent of copper leached with *A.ferrooxidans* F7-01 and *A.thiooxidans* T1-01

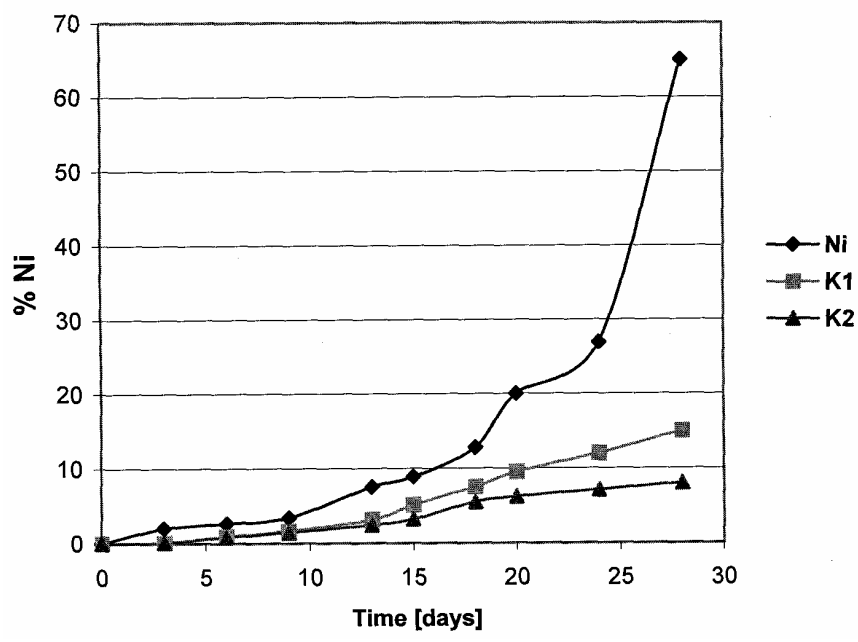

Fig. 2. Percent of nickel leached with *A.ferrooxidans* F7-01 and *A.thiooxidans* T1-01

Figure 1 shows extension of the leaching process in the batch and control systems. These results indicate that the process run most intensely in first six days of its duration. In this period 42,23% of copper contained in shale ore was leached. In simultaneous control test K_1 only 5,1 % of copper was extracted that imply a bioleaching character of this process. For next 22 days the dynamics of process grew smaller. In the batch system, control systems K_1 and K_2 adequate 64,3%, 23% and 16,5% of copper were extracted. We can conclude that 47,8% of copper in the batch system was obtained in a bioleaching process and 16,5% of copper obtained in K_2 system were chemically leached. The leaching process in the first phase coursed in K_1 control system similarly as in system K_2 and had a chemical character. Since thirteenth day a intensive growth of the leaching rate of copper was observed in K_1. We can state that considerably grew larger activity of chemolithoautotrophs batch delivered to system together with black shale ore. The initial activity of them was not large and their development occurred after dozen days.

Nickel bioleaching kinetics (see Figure 2) show quite different courses than copper bioleaching kinetics. In this case, leaching process in the batch system increases very slowly during first 13 days. When 50% of copper was extracted, impetuous nickel bioleaching begun than in creases. In 28 day of process duration 65% of nickel included in black shale ore was removed. Similar results, only with low efficiency were obtained in control system K_1. Comparing course of process in K_1 to changes in control system K_2 we could observe in this control test the bioleaching process by autochthonous bacteria strains besides chemical leaching.

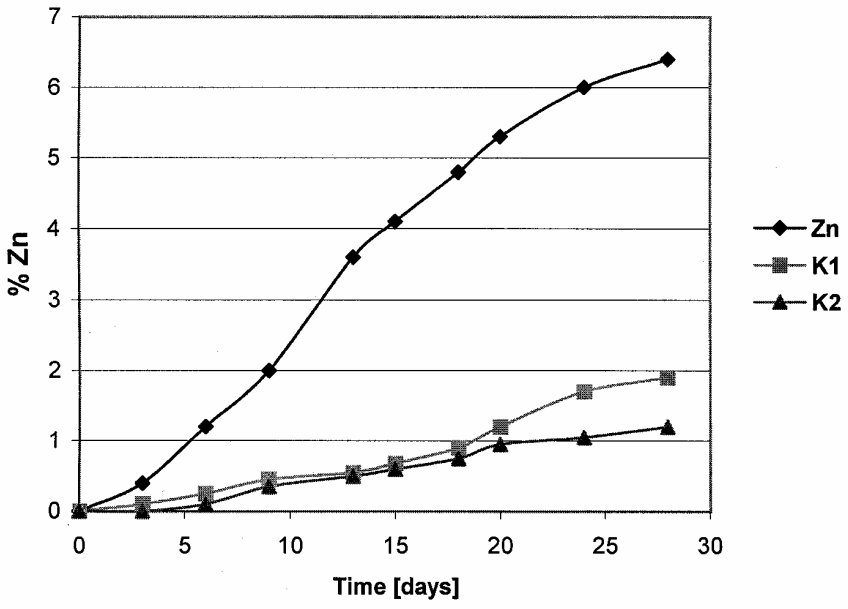

Fig. 3. Percent of zinc leached with *A.ferrooxidans* F7-01 and *A.thiooxidans* T1-01

Results, shown in Figure 3, reveal poor efficiency of zinc bioleaching process. In this manner, zinc minerals contained in black shale ore can be classified as slightly bioleachable. These results were consistent with those reported in literature (Muszer 2002).

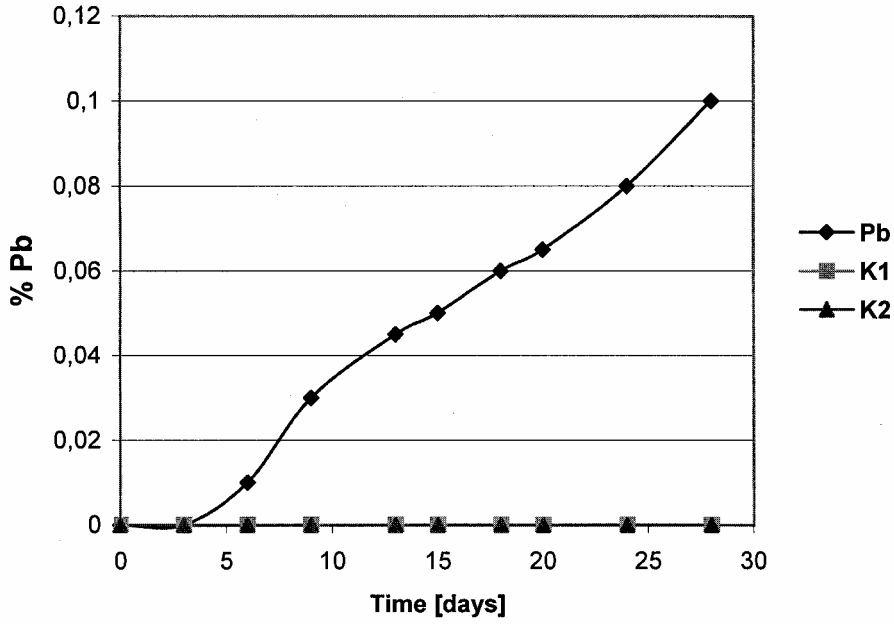

Fig. 4. Percent of lead leached with *A.ferrooxidans* F7-01 and *A.thiooxidans* T1-01

As shown in Figure 4 shape of curves proves that the lead sulfide, contained in black shale ore is biologically unleached and the results obtained agree with previous studies (Karavaiko et al. 1989).

CONCLUSIONS

The results of investigations confirm our assumptions that Polish back shale ore could be a source of many metals by bioleaching in acid medium. The initial stage of the process was bioleaching of copper sulphide. When 50% of this compound was extracted, a process of nickel bioleaching started. Considering our results, we can suggest that 50% of copper contained in shale is a chalcocite because bioleaching of them was the most effective (Karavaiko et al. 1989, Muszer 2002).

The effect of bioleaching sphalerite contained in black shale ore was very low. We have failed to bioleach galena. The following conclusion can be drown: batch strains used in our study convert PbS into $PbSO_4$, which is sparingly soluble and forms precipitate.

REFERENCES

FARBISZEWSKA T., FARBISZEWSKA-KICZMA J. (2002), *Bioługowanie polskich surowców miedzionośnych w: Biometalurgia metali nieżelaznych podstawy i zastosowanie,* Cuprum, Wrocław, s. 81-101.

KARAVAIKO G.I., ROSSI D., AGATE A., GROUDEV S., AVAKIAN Z.A. (1989), *Biogeotechnologija metalov*, Moskva, s.338.

KELLY D.P., WOOD A.P. (2000), *Reclassification of some species of Thiobacillus to the newly designated genera Acidithiobacillus gen. Nov., Halothiobacillus gen. nov. and Thermithiobacillus gen. nov*., Internacional Journal of Systematic and Evolutionary Microbiology, Vol.50, s. 511-516.

KUCHA H., MAYER W. (1996), *Geochemia skał zmineralizowanych* w: Monografia KGHM Polska Miedź S.A., Lubin, s. 237-247.

MUSZER A. (2002), *Mikroskopowa charakterystyka mineralogiczna koncentratów bornitowo chalkozynowych po procesie bioługowania* w: Biometalurgia metali nieżelaznych podstawy i zastosowanie, Cuprum, Wrocław, s. 81-101.

SAWŁOWICZ Z., SPECZIK S. (1996), *Substancja organiczna i jej rola w procesach złożotwórczych* w: Monografia KGHM Polska Miedź S.A., Lubin, s. 252-258.

Farbiszewska T., Farbiszewska-Kiczma J., Bąk M., *Bioługowanie metali z polskich łupków bitumicznych*, Physicochemical Problems of Mineral Processing, 37 (2003) 51-56 (w jęz. ang.).

Lubińskie złoża rud miedzi zbudowane są z trzech odmian litologicznych: węglanowej, piaskowcowej i łupkowej. Najbogatsza w miedź i wiele innych metali jest warstwa łupkowa. Charakteryzuje się ona zmienną zawartością metali i zawiera średnio 5,5% Cu, a także między innymi około 0,01% Ag, czy 0,03% V. Tworzą ją przede wszystkim łupki bitumiczne, które składają się głównie z minerałów ilastych, węglanów, substancji organicznej i detrytycznego kwarcu. W łupkach bitumicznych metale występują w formie siarczków i tzw. związków „sandwiczowych", w których metale tworzą połączenia organometaliczne z węglowodorami, np. porfiryny niklowe. Właściwości rudy łupkowej czynią ją niewzbogacalną metodą flotacji, stosowaną z pozytywnym skutkiem do wzbogacania rud piaskowcowych i węglanowych. W istniejących technologiach wzbogacania ruda łupkowa jest w znacznym stopniu niewykorzystana i przechodzi do odpadów. Od wielu lat wiadomo, że ruda ta winna być wzbogacana osobno, właściwymi dla niej metodami, ale dopiero od niedawna nowe technologie eksploatacyjne umożliwiają oddzielne pozyskiwanie łupka. W tej sytuacji wydaje się zasadne prowadzenie badań nad biohydrometalurgiczną przeróbką rudy łupkowej.

W pracy przedstawiono wyniki bioekstrakcji polimetalicznego, smolistego łupka miedzionośnego, pochodzącego z rejonu lubińsko-głogowskiego. Po wstępnej obróbce zawierał on: 5,6% Cu, 0,017% Ni, 0,67% Pb, 0,2% Zn, 0.014% Co, 0,014% Ag, 0,014% Mo, 0,035% V, 0,03% As. Materiał biologiczny stanowiły, wcześniej wyizolowane i zaadaptowane do jonów Cu, Ni, As i Ag, autochtoniczne szczepy bakterii rodzaju *Acidithiobacillus*. Były to szczepy *A.ferrooxidans* F7-01 i *A.thiooxidans* T1-01, przechowywane w muzeum szczepów Katedry Biologii Stosowanej i Eksperymentalnej Uniwersytetu Opolskiego. Proces prowadzono w dużej skali laboratoryjnej w bioreaktorze. Oceniając przebieg bioługowania porównano wyrażoną w procentach ilość wyługowanej miedzi, niklu, cynku i ołowiu w kolejnych dniach trwania procesu. Stwierdzono, że polski łupek miedzionośny bardzo łatwo ulega procesowi bioługowania w środowisku kwaśnym. Najpierw bioługują siarczki miedzi, a dopiero po ich połowicznym wyługowaniu rozpoczyna się bioługowanie niklu. Należy przypuszczać, że 50% miedzi zawartej w łupku to miedź chalkozynowa, gdyż minerał ten bioługuje się najłatwiej. Po wyługowaniu chalkozynu (Cu_2S) rozpoczyna się bioługowanie niklu. Zawarty w łupku sfaleryt (ZnS) bioługuje bardzo słabo, a bioługowania galeny PbS nie stwierdzono.

Physicochemical Problems of Mineral Processing, 37 (2003) 57-68
Fizykochemiczne Problemy Mineralurgii, 37 (2003) 57-68

Małgorzata PACHOLEWSKA*

MICROBIAL LEACHING OF BLENDE FLOTATION CONCENTRATE USING *ACIDITHIOBACILLUS FERROOXIDANS* AND *ACIDITHIOBACILLUS THIOOXIDANS*

Received March 2003, reviewed, and accepted May 15, 2003

Bacterial leaching of blende flotation concentrate from Zakłady Górniczo-Hutnicze „Bolesław" was carried out using single cultures and mixed cultures of acidophilic sulphur- and iron- oxidizing bacteria *Acidithiobacillus thiooxidans and Acidithiobacillus ferrooxidans*. The accelerating effect of mixed cultures of bacteria on the metal leaching was amplified by correcting pH leaching medium to low values. The overall conversion of zinc exceeded 35-40%. The leaching rates of ZnS depended on redox potential, concentration of Fe(III)/Fe(II) and pH. X-ray analysis and electron scanning microscopy showed that in inoculated solution new solid phases: jarosite, elemental sulphur and anglesite were formed.

Key words: blende flotation concentrate, microbial leaching, Acidithiobacillus thiooxidans, Acidithiobacillus ferrooxidans

INTRODUCTION

Extraction of zinc fom sulphide minerals using iron- and sulphur oxidizing bacteria has been studied by many investigators (Konishi et al. 1992, Pistorio et al. 1994, Cwalina et al. 1994, Sanmugasunderam et al. 1988, Ahonen et al.1995, Fowler et al.1998, Boon et al. 1998) but the reported efficiency of bioleaching process was varying. It was found that semiindustrial tank leaching of zinc sulphide concentrates by *Acidithiobacillus ferrooxidans* resulted in zinc concentration in pregnant solution as high as 120 g/dm^3 and rates of release of zinc into the solution as fast as 1300 mg/dm^{3}h (Torma 1988). A previous study (Gormely et al. 1975) showed that, while continous mikrobiological leaching of Zn from ZnS concentrate was technically feasible, extraction levels tended to be rather low (range 11-72 %, average 45%). To

* Politechnika Śląska, Katedra Metalurgii, 40-019 Katowice, ul. Krasińskiego 8, Poland, malg@polsl.katowice.pl

improve the recovery of metal, addition of the second reactor stage or separation of the unleached residue and recycling it back to the reactor were proposed. Lochmann and Pedlik (1995) stated, that during the chemical leaching of sphalerite concentrates in acidic ferric sulphate solution, the dissolution rate of zinc decreased with time and overall conversion has not exceeded 30%. They found, that the growing elemental sulphur layer on the surface of each particle was found to be the cause of this passivation. The microorganisms *Acidithiobacillus ferrooxidans* are able to oxidize ferrous ions and the reduced sulphur compounds (Orłowska and Gołąb 1990) and *Acidithiobacillus thiooxidans* are able to oxidize only reduced sulphur compounds, summarized by the global reaction (Skłodowska 1990, Cwalina 1994):

$$2Fe^{2+} + 2H^{+} + 0.5O_2 + \text{bacteria} = 2Fe^{3+} + H_2O \quad (1)$$

$$S^{2-} \rightarrow S^{o} \rightarrow S_2O_3^{\ 2-} \rightarrow S_4O_6^{\ 2-} \rightarrow SO_3^{\ 2-} \rightarrow SO_4^{\ 2-} \quad (2)$$

The product of oxidation of ferrous ions, ferric ions, is a strong oxidant that is capable of oxidizing sulfide materials. The overall leaching process occurs by bacterial oxidation referred to as indirect mechanism (Hansford and Vargas 2001) is:

$$ZnS + 2Fe^{3+} = Zn^{2+} + S + 2Fe^{2+} \quad (3)$$

or as direct interact with the mineral:

$$ZnS + 2H^{+} + 0.5O_2 + \text{bacteria} = Zn^{2+} + H_2O + S \quad (4)$$

The new integral model described by (Sand et al. 2001) stated that the mechanism and biodegradation of sulphide minerals is determined by theirs structure. Sphalerite is degradable by iron (III) and proton attack. The dissolution proceeds via H_2S^{**} radical and polysulfides to elemental sulphur. The kinetics is mainly dependent on the concentration of Fe(III) and on the solubility product.

The objective of this study was to determine the efficiency of zinc extraction during bacterial leaching of blende-sphalerite flotation concentrate obtained from ZGH "Boleslaw" using a) single bacterial culture and b) mixed bacterial cultures of strains *Acidithiobacillus ferrooxidans* and *Acidithiobacillus thiooxidans*.

EXPERIMENTAL METHODS

BLENDE-FLOTATION CONCENTRATE

Blende flotation concentrate was supplied by ZGH "Boleslaw". The Zn-Pb ores from local deposits are concentrated in flotation plant "Olkusz-Pomorzany" with prior concentration in heavy liquids. Analysis of the concentrate and the particle size distribution of the concentrate were shown in Table 1. The major minerals present in

those samples were sphalerite (78%), galena (3%), with small amounts of pyrite (8%) marcasite (4%), dolomite and calcite (5%), hydrocerrusite (1%) and quarzite (1%). Concentrate samples containing different particle sizes were used in the experiments.

BACTERIA

The bacteria used were a strain of *Acidithiobacillus ferrooxidans* (F3-02) and a strain of *Acidithiobacillus thiooxidans* (T5-02), isolated from the source of mineral water coming from Głębokie and Łomnica (Nowy Sącz county), (Pacholewski and Pacholewska 2001). *Acidithiobacillus ferrooxidans* were harvested in a medium Silverman - Lundgren 9K (Silverman and Lundgren 1959) consisting of: $(NH_4)_2SO_4$ - 3.0; KCl - 0.1; K_2HPO_4 - 0.5; $MgSO_4 \cdot 7H_2O$ - 0.5; $Ca(NO_3)_2$ - 0.01; $FeSO_4 \cdot 7H_2O$ - 44.2 g/dm^3. To adapt the original strain to the ZnS concentrate as a solid substrate, the strain was subcultured in the modified 2K (2.0 g/dm^3 Fe(II)) liquid medium supplemented with 5% w/v ZnS concentrate. The bacteria *A. thiooxidans* were harvested in a Waksman-Joffe medium consisting of: $(NH_4)_2SO_4$ - 0.2; KH_2PO_4 - 3.0; $MgSO_4$ $7H_2O$- 0.5; $CaCl_2$ $6H_2O$ - 0.25; S^o element. 10.0 g/dm^3. All cultures for leaching experiments were treated with 10 cm^3 of inocula in 300 cm^3 Erlenmeyer flasks containing 100 cm^3 of leaching medium (2K) with 5.0 g sphalerite concentrate. The volume of inoculum of single bacterial cultures was 10 cm^3 and the mixed culture was 5 cm^3 of *A. thiooxidans* and 5 cm^3 *A. ferrooxidans*. Experiments were started under exactly the same solution conditions of pH and redox potential of leaching medium in bacterial and control leaching. $NH_4Fe(SO_4)_2$ (ferric ammonium sulphate) was added to initial control samples as a source of Fe(III). The pH of the medium was adjusted to 2.0 by adding H_2SO_4. The samples were placed in laboratory water bath-shaker with shaking 1at 30 oscillation/min and amplitude 5. The temperature during leaching was maintained at 22-23^{o}C. All the experiments were done three times.

ANALYSIS

To quantify the amount of zinc and iron dissolved in the leaching media, a 1 cm^3 sample was filtered and the filtrate was analyzed by an atomic absorption spectrophotometer (SOLAAR M6-UNICAM Atomic Absorption). 1 cm^3 solution was taken also to determine the concentration of ferrous ion by manganometric method using 0.002 M $KMnO_4$ reagent. The precipitates after leaching were washed with etanol to fix the bacteria on the surfaces of the mineral particles, after that they were dried and preserved for subsequent analysis. Total sulphur in solid residues and S-sulphate were analyzed by classical weight method. X-ray diffraction patterns for the precipitates were generated by expossing the dried samples to Cu -$K\alpha_1$ radiation at 40 kV, 35 mA. Scanning electron microscope HITACHI-4200 has been used to image the microscopic structural properties of probes.

RESULTS AND DISCUSSION

LEACHING BY SINGLE CULTURES

Figure 1 shows the results of the experiment in which the dissolved zinc concentration from sulphide flotation concentrates was determined in the 2K medium in the presence of different bacteria cultures. The results indicated that the zinc concentration in solution was higher in the presence of *Acidithiobacillus ferrooxidans* as compared to *Acidithiobacillus thiooxidans* and the control experiment. The maximum concentration of zinc leached in this way amounted to about 5.35 g/dm^3. After reaching maximum concentration, zinc tended to reprecipitate in further leaching. The results of the control leaching experiments were similar to the results of bacterial leaching experiments but the dependency of the released zinc from the mineral in time did not come up to maximum. The total amount of zinc leached in 312 h (15 days) amounted to about 32.36 % with bacteria *A. ferrooxidans* and 21.82 % with *A. thiooxidans*, without 22.69% - Table 2.

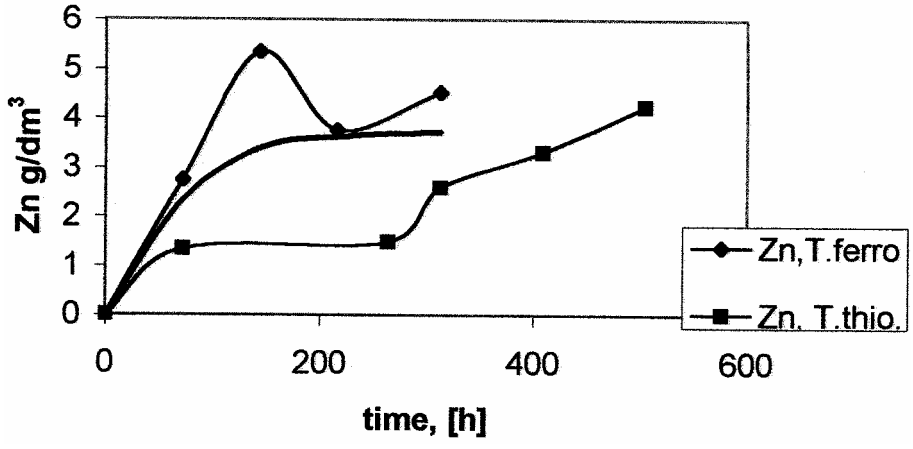

Fig.1. Effect of *Acidithiobacillus ferrooxidans* and *Acidithiobacillus tiooxidans* on leaching rate of sphalerite concentrate

LEACHING BY MIXED CULTURES

Mixed cultures of *A. ferrooxidans* and *A. thiooxidans* generally showed increased leaching rates of zinc compared with single cultures (Fig. 2). Two-stage course of zinc dissolution reaction can be observed. Initially there was a constant growth of zinc concentration until it has reached the point where there was rapid change of reaction rate. The maximum concentration of zinc leached in this way was 10.28 g/dm^3 in 408 h (17 days). It was observed that after obtaining maximum, the zinc was repricipitated and the concentration of Zn remined constant at the level of about 7.5g/dm^3 for further 768 h of leaching, showing passivation tendency, as stated by (Lochmann and Pedlik

1995). The observed tendencies reveal that zinc sulphide is most likely initially disolved by the activity of the sulphur-oxidizing bacteria and then by iron- and sulphur-oxidizing bacteria. *A. thiooxidans* which was expected to produce sulphuric acid from sulphides, did not reduce strongly enough the acid requirement. It was necessary to add acid to the system. A solution of sulphuric acid was added in order to bring the pH to 2.0. The results of the second experiment showed in Fig.2, in which continous control of pH leaching solution was applied, gave the similar level of dissolved zinc in 504 h of leaching - 8.28 g/dm^3. However, in this case the rate of dissolution of zinc from sulphide concentrate increased continously with time. It was observed that after start of leaching process (about 144 h) H_2S gas was generated. The total amount of zinc leached in 768 h with mixed culture was 40.28% and 37.53% during 504 h in solution with correcting pH (Table 2).

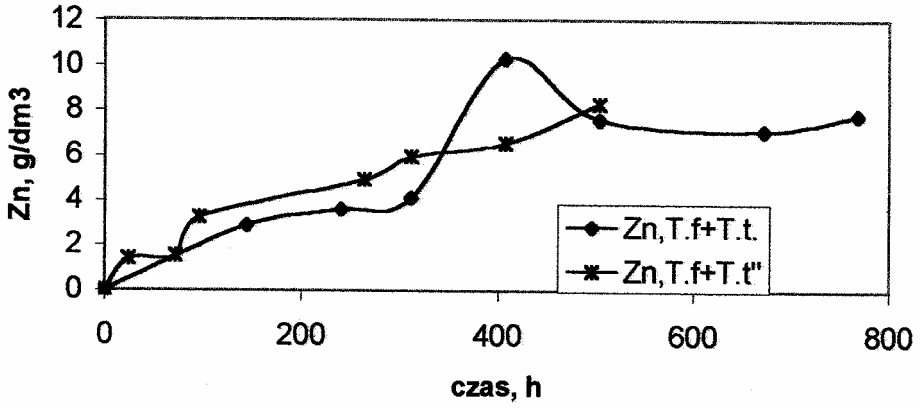

Fig.2 Effect of a mixed cultures of *Acidithiobacillus ferrooxidans* and *Acidithiobacillus thiooxidans* on leaching rate of sphalerite concentrate

Table 1. Compositions of blende (sphalerite) concentrate from Zakłady Górniczo-Hutnicze "Bolesław"

Compounds	[%]	Mean particle diameter [mm]	Weight fraction [%]
Zn	53.55	0.16	7.76
Pb	1.50	0.125	12.72
Cd	0.29	0.100	16.12
Stotal	31.3	0.063	23.16
S SO_4	0.29	<0.063	40.22
S S	31.0		
MgO	0.98		
CaO	2.78		
SiO_2	0.40		

Table 2. Composition of solid residues after bioleaching and control leaching

Sample	Zn [%]	Pb [%]	Fe [%]	CaO [%]	Cd [%]	S total [%]	S so4 [%]	Weight of residue [g]	Extract. of Zn [%]
ZnS1 *A. ferroox.*	48.31	1.64	6.33	0.97	0.27	31.84	1.73	3.7543	32.36
ZnS11 *A. thioox.*	53.93	1.49	4.40	1.47	0.29	30.91	1.24	3.8815	21.82
ZnS5 Mixed culture	50.46	1.52	4.98	1.38	0.29	30.91	1.48	3.1686	40.28
ZnS8 Mixed culture pH 2.0	49.70	1.57	6.05	1.28	0.27	32.23	1.85	3.3654	37.53
ZnS13 Control	56.00	1.52	4.39	0.78	0.30	31.06	0.81	3.6963	22.69

pH EFFECT

Figure 3 presents summary results of pH changes of the solutions at leaching time of zinc sulphide concentrate in the environment of different bacteria cultures and in the control leaching. The lowest pH was observed (as it has been expected) in the solution with *A. thiooxidans* whereas the highest pH was observed in the solutions with *A. ferrooxidans*. In Fig. 3 the changes of pH before adjustment to constant value have been presented.

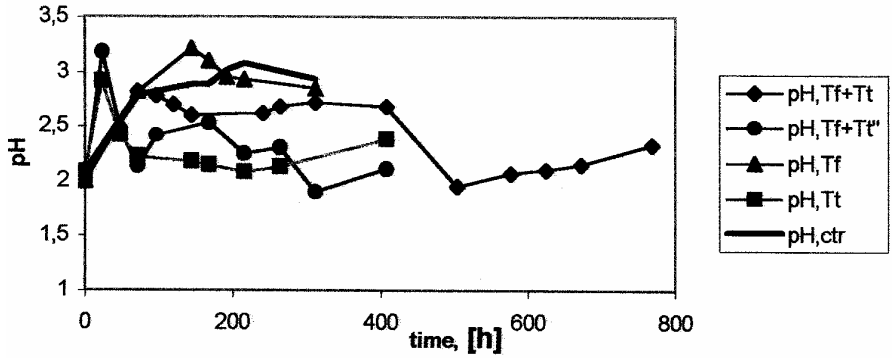

Fig. 3. pH evolution during leaching of blende concentrate in the presence of: *Acidithiobacillus ferrooxidans* and *Acidithiobacillus tiooxidans* and mixed cultures .*(")* -adjusting solution to pH 2.0

EFFECT OF Eh - REDOX POTENTIAL

The changes of redox potential in the course of time have been presented in Fig.4. It can be clearly seen that the most rapid growth of oxidizing properties can be noticed when the mixed culture has been used (*A. ferrooxidans and A. thiooxidans*) in the solution with constant pH control up to 2.0. The growth of oxidizing properties is also due to the presence of Fe(III) ions in the solution. The highest output of zinc dissolved from sulphide concentrates can be obtained in such conditions where low pH guarantees the stability of Fe(III) ions in the solution. At the same time there is no possibility to precipitate Fe(III) ions into the sediments. This has been confirmed by the previously presented data (Fowler et al. 1998).

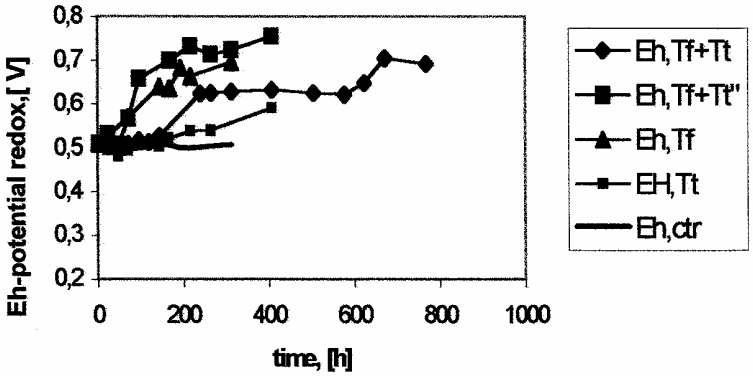

Fig. 4. Eh - redox potential during leaching of the blende concentrate in the presence of : *Acidithiobacillus ferrooxidans* and *Acidithiobacillus tiooxidans* and mixed cultures. (")-adjusting to pH 2.0

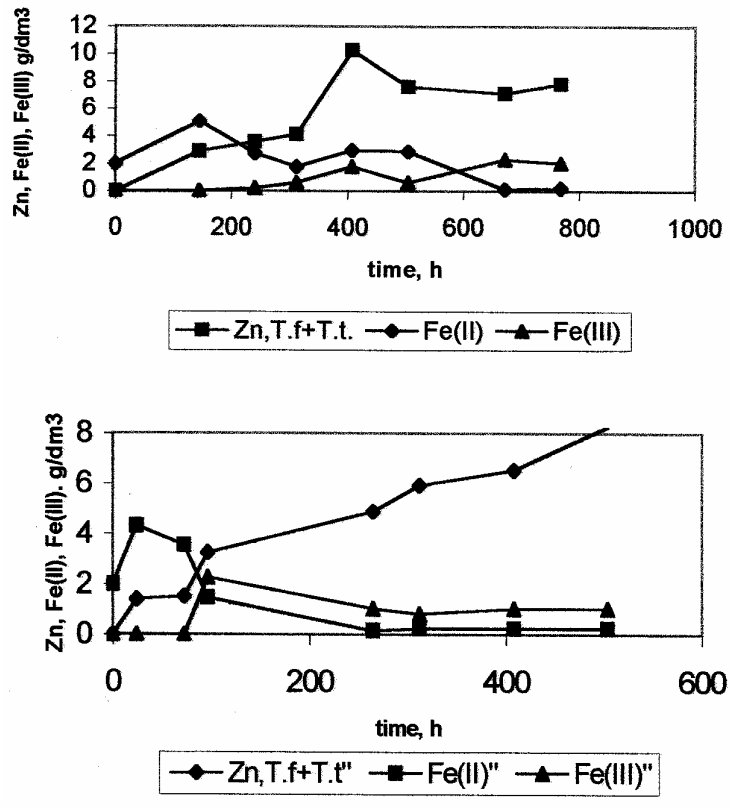

Fig.5. Changes in Zn, Fe(II) and Fe(III) concentration during bioleaching of blende flotation concentrate using mixed culture of *A. ferrooxidans and A..thiooxidans*, and (") with adjusting pH

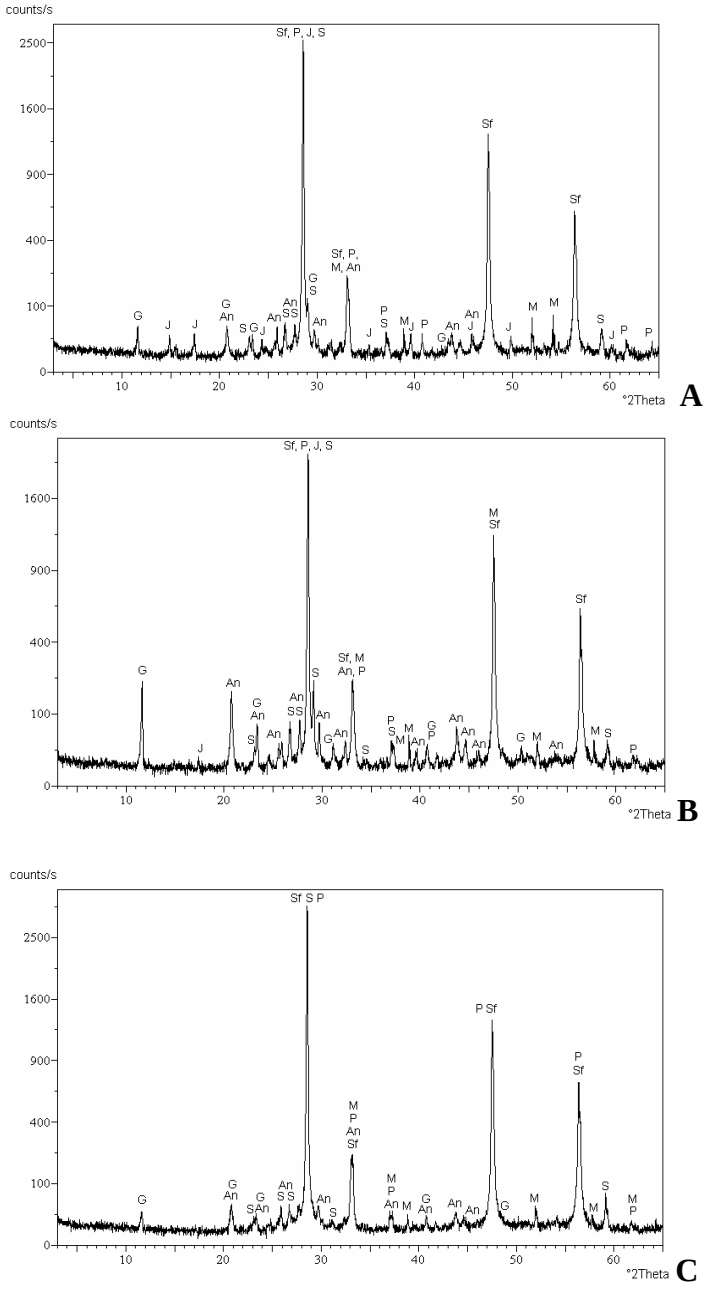

Fig. 6. X-ray diffraction patterns recorded for the products after A- bioleaching using *A. ferrooxidans*, B- bioleaching using the mixed cultures of *A .ferrooxidans and A. thiooxidans*. and C-control leaching of blende concentrate in 2K solutions: J-hydronium and potassium jarosite, Sf-sphalerite, S-sulphur, An-anglesite, G-gypsum, M-markasite, P-pyrite

EFFECT OF Fe(II) AND Fe(III) CONCENTRATION

The changes of Fe(II) and Fe(III) concentration in leaching medium using mixed cultures of *A. ferrooxidans and A. thiooxdans* have been presented in Fig.5. It is demonstrated that a rapid rate of dissolution of sphalerite from blende concentrate depends on a sufficient concentration of iron (III) ions in solution. Iron (III) ions are importance for cell attachment and degradation of metal sulphides, as described by (Sand et al. 2001). Correcting pH to low value provided a constant concentration of Fe(III) ions in solution (Fig. 5).

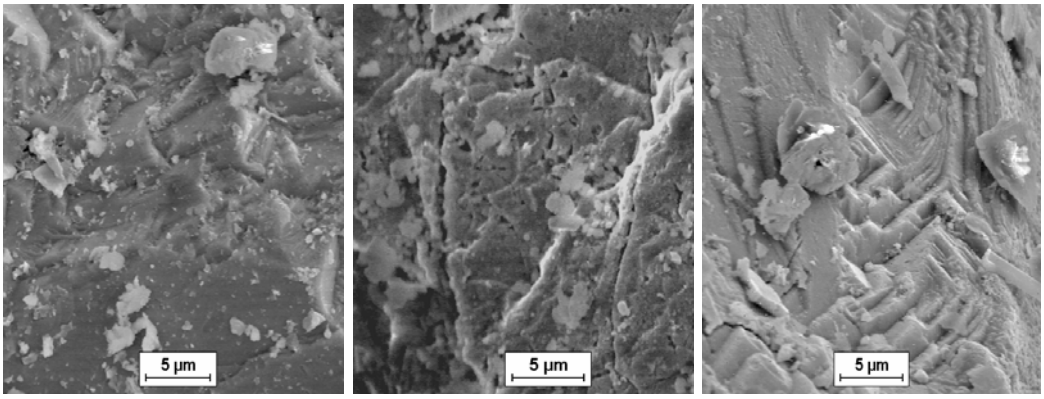

Fig. 7. Scanning electron microscopy of samples: A-blende (sphalerite) flotation concentrate, B-blende after bioleaching using *A. ferrooxidans*, C- sfterile control leaching

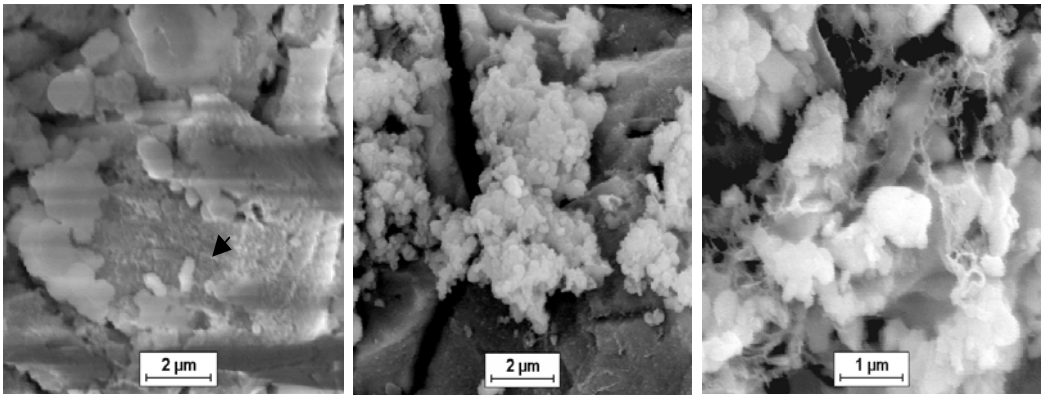

Fig. 8. Scanning electron microscopy image of blende (sphalerite) surface with cells (on image A indicated by arrow). B-complex of cells, C- extracellular polymeric substances (?) produced by *A. ferrooxidans*

X-RAY DIFFRACTION STUDIES

The X-ray diffraction patterns of the residues were examined for crystalline phases and it was observed that the new identifiable phases were jarosite, sulphur, anglesite and gypsum. It was stated that samples obtained after leaching using *A. ferrooxidans* consist of two new phases: the crystalline jarosite (hydronian jarosite) - about 8 % and sulphur-about 3 % - Fig.6A. In the samples after leaching using mixed cultures of *A. thiooxidans and A. ferrooxidans* there was a higher amonunt of elemental sulphur-about 4% (Fig. 6B). In some cases, samples without bacteria, no jarosite phase was identified , amount of elemental sulphur was about 2% (Fig. 6C)

SCANNING ELECTRON MICROSCOPY ANALYSIS

In order to determine the presence of minor components and bacteria in solid residues electron microscopy techniques were used. SEM revealed several important differences between solids precipitated from different solutions. Observations of the residue of concentrate by SEM showed it had undergone important changes compared with the biologically untreated concentrate. The angular forms of the particles had been rounded and smoothed (Fig. 7). The bacteria were present on the surface as the microcolonies or the single microorganism (Fig. 8). Possibly, there are extracellular polymeric substances excreted by bacteria *Acidithiobacillus ferrooxidans.*

CONCLUSIONS

The results obtained in this research work show that higher yields of extraction of zinc from blende (sphalerite) flotation concentrate can be obtained using a mixed culture of *Acidithiobacillus ferrooxidans and Acidithiobacillus thiooxidans* in comparison to a single culture of bacteria. One of the reason of the low leaching capacity is the lack of oxidizing agent in leaching medium i.e. Fe(III) ions. The main cause of it is that the experimental conditions favoured jarosite compounds generation and precipitation. The layer of jarosites and sulphur, which were generated during the course of leaching time hindered bacterial action. It was observed that in the presence of different microorganism in the leaching medium there has been a succesion in the treatment of components of sulphide minerals from flotation concentrate. At first reduced sulphur compounds appeared to be oxidized, and then ferous ions. It was observed that the cultures of microorganisms from mineral water sources used in this study have been active in the experimental conditions and the increase of zinc and other metal leached from blende flotation concentrate were non toxic for them.

ACKNOWLEDGEMENTS

The work was supported by the State Committee for Scientific Research in Poland, Project No.7 T09D 00221

REFERENCES

AHONEN L., TUOVINEN O. (1995), *Bacterial leaching of complex sulfide ore samples in bench-scale column reactors*, Hydrometallurgy Vol. 37, 1-21.

BOON M., SNIJDER M., HANSFORD G.S., HEIJNEN J.J. (1998), *The oxidation of zinc sulphide with Thiobacillus ferrooxidans,* Hydrometallurgy Vol. 48, 171-186.

CHENG-HSIEN HSU, HARRISON ROGER G. (1995), *Bacterial leaching of zinc and copper from mining wastes.* Hydrometallurgy Vol. 37, 169-179.

CWALINA B. (1994), *Metabolizm siarki u Thiobacillus ferroxidans w procesie ługowania metali z minerałów siarczkowych*. Wyd. UŚ, Katowice.

CWALINA B., DZIERŻEWICZ Z., FARBISZEWSKA T., MIKLUSZKA K. (1994), *Zdolność biotransformacji nieorganicznych związków siarki przez wybrane szczepy autotroficznych i miksotroficznych bakterii siarkowych i żelazowych*, Biotechnologia, 2 (25), 67-74.

DAS R. P., ANAND S. (1996), *Thermogravimetric and XRD studies on iron compounds precipitated from Fe(II)-SO4-NH3-O2 system*. Int. J. Miner. Process. Vol. 48, 159-168.

FOWLER T.A., CRUNDWELL F.K. (1998), *Leaching of Zinc Sulfide by Thiobacillus ferrooxidans: Experiments with a Controlled Redox Potential Indicate No direct Bacterial Mechanism*. Applied and Environmental Microbiology, Vol.64, No 10, 3570-3575.

FOWLER T.A., CRUNDWELL F.K. (1999), *Leaching of Zinc Sulfide by Thiobacillus ferrooxidans : Bacterial Oxidation of the Sulfur Product Layer Increases the Rate of Zinc Sulfide Dissolution at High Concentration of Ferrous Ions,* Applied and Environmental Microbiology, Vol.65, No 12, 5285-5292.

GORMELY L.S., DUNCAN D.W., BRANION R.M.R., PINDER K.L. (1975), Biotechnology and Bioengineering, Vol.17, 31.

HANSFORD G.S., VARGAS T. (2001), *Chemical and electrochemical basis of bioleaching process,* Hydrometallurgy, Vol. 59, 135-145.

KARAVAIKO G.I. (1985), *Microbiological Processes for Leaching of Metals from Ores*, ed.Torma A.E., Moscow.

KONISHI Y., KUBO H., ASAI S. (1992), *Bioleaching of zinc sulfide concentrate by Thiobacillus ferrooxidans,* Biotechnology and Bioengineering, Vol.39, No1, 66-74.

LAZAROFF N., SIGAL W., WASSERMAN A. (1982), *Iron Oxidation and Precipitation of Ferric Hydroxysulfates by Resting Thiobacillus ferrooxidans Cells,* Applied and Environmental Microbiology, Vol. 43, No 4., 924-938.

LIZAMA H. M., SUZUKI I. (1989), *Bacterial leaching of a sulfide Ore by Thiobacillus ferroxidans and Thiobacillus thiooxidans. Part II. Column Leaching studies.* Hydrometallurgy Vol.. 22, 301-310

LOCHMANN, PEDLIK M.(1995), *Kinetic anomalies of dissolution of sphalerite in ferric sulfate solution.* Hydrometallurgy, Vol. 37, 89-96.

LOPEZ -DELGADO A., ALGUACIL F.J., LOPEZ F.A. (1997), *Recovery of iron from bio-oxidized sulphuric pickling waste water by precipitation as basic sulphates,* Hydrometallurgy Vol. 45, 97-112.

ORŁOWSKA B., GOŁĄB Z.(1990), *Thiobacillus ferrooxidans - jako czynnik biologicznego ługowania metali*, Post. Mikrobiol., XXIX, No 3-4, 185-203.

PACHOLEWSKI A., PACHOLEWSKA M. (2001), *Naturalne zdolności do utleniania związków żelaza (II) przez bakterie żelazowe ze źródła wody mineralnej Łomniczanka.* Współczesne Problemy Hydrogeologii, t.X, 389-396.

PISTORIO M., CURUTCHET G., DONATI E., TEDESCO P. (1994), *Direct zinc sulphide bioleaching by Thiobacillus ferroxidans and Thiobacillus thiooxidans,* Biotechnology Letters Vol. 16, No4, 419-424.

SAND W., GEHRKE T., JOZSA P-G., SCHIPPERS A. (2001), *(Bio)chemistry of bacterial leaching - direct vs. indirect bioleaching.* Hydrometallurgy, 59, 159-175.
SILVERMAN M.P., LUNDGREN D.G. (1959), J. Bacteriol., vol.77, , 642-647.
SKŁODOWSKA A. (1990), *Utlenianie mineralnych związków siarki przez bakterie z rodzaju Thiobacillus,* Post. Microbiol., XXIX, No 1-2, 29-41.
TORMA A.(1998), *Leaching of Metals*, Chapter 12 [in:] *Biotechnology - A Comprehensive Treatise in 8 Volumes*, ed. H.-J. Rehm, G.Reed, Vol.6 b, Weinheim.

Pacholewska M., Mikrobiologiczne ługowanie koncentratów blendy flotacyjnej przy użyciu A*cidithiobacillus ferrooxidans* oraz *Acidithiobacillus thiooxidans,* Physicochemical Problems of Mineral Processing, 37 (2003) 57-68 (w jęz. ang.).

W pracy przedstawiono wyniki badań nad mikrobiologicznym ługowaniem krajowych siarczkowych koncentratów blendy flotacyjnej pochodzących z ZGH"Bolesław" przy użyciu szczepów bakterii *Acidithiobacillus ferrooxidans* oraz *Acidithiobacillus thiooxidans* w roztworach 2K stosowanych jako pożywki dla wzrostu bakterii żelazowych. Stopień roztworzenia cynku z koncentratu blendowego do roztworu wyniósł 40,28 % dla prób biologicznych z udziałem mieszanych kultur bakteryjnych oraz 22,69 % dla prób prowadzonych w warunkach sterylnych. Stwierdzono, że reakcja roztwarzania cynku ulega zahamowaniu przez powstające stałe produkty reakcji jarosyty i siarkę elementarną. Prowadzenie ługowania koncentratu blendowego przy stałej korekcie pH2,0 roztworu umożliwia częściowe zachowanie związków żelaza w roztworze, przeciwdziałając w ten sposób osadzaniu się stałych produktów reakcji. W toku badań zaobserwowano, że stosowane mieszane kultury bakteryjne wykazują sukcesję w odniesieniu do procesu roztwarzania minerałów siarczkowych utleniając początkowo jony siarczkowe a następnie jony żelaza (II) a ponadto są odporne na obecność jonów cynku w roztworze.

Physicochemical Problems of Mineral Processing, 37 (2003) 69-76
Fizykochemiczne Problemy Mineralurgii, 37 (2003) 69-76

Ewa JAŻDŻYK, Zygmunt SADOWSKI*

EFFECT OF ARTIFICIAL POLYMER FILM ON BIOOXIDATION OF ARSENOPIRYTE WASTES

Received March 2003, reviewed, and accepted May 15, 2003

The effect of polymer film on the biooxidation of arsenopyrite tailings was examined. Adsorption of a typical sugar polymer, dextrin, on the mineral particles was studied. The effect of pH on the adsorption at the biooxidation range was determined. The microelectrodes were used to measure the dissolved oxygen concentration in the polymer film. Based on these results, the oxygen diffusion coefficient has been calculated to be 1.6 10^{-5} cm^2/s. The biooxidation results show that polymer film plays a key role in both the immobilization of microbial cells and oxygen diffusion. For effective biooxidation of arsenopyrite tailings the presence of polymer film onto the solid surface is indispensable.

Kay wards: biooxidation, biofilm, dextrin, Acidothiobacillus ferrooxidans, diffusion coefficient

INTRODUCTION

Gold in the refractory ores is encapsulated as fines in the crystal structure of the arsenopyrite matrix. To effectively extract gold from these ores an oxidative pretreatment is necessary to break down the arsenopyrite matrix. Biological pretreatment of the refractory gold ores is the most popular method for the gold recovery (Karas, Sadowski, 2002).

The concept of the microbial cells immobilization was checked by (Karamanev et al. 2001). Immobilization of microbial cells prevent them from moving freely. The oxygen mass-transport rate in the immobilized system (biofilm) is very high. Formally, molecular diffusion is considered the predominant mechanism for the oxygen transport in the biofilm (De Beer at al., 1997).

The term biofilm encompasses a variety of extracellular polymer substances (EPS), which microbial cells colonized. The diffusion through these biofilms controls the microbial oxidation reaction. Microbial activity in biofilms is controlled by transport

* Technical University of Wroclaw, Institute Chemical Engineering and Heating Equipment, Wybrzeze Wyspiańsiego 27, 50-370 Wrocław, Poland, sadowski@iic.pwr.wroc.pl

process (Lewandowski et al., 1998, Rasmussen et al., 1998 a). The biopolymer film is capable of transportation of trace organic and inorganic compounds. The oxygen diffusion through the biofilm controls the microbial oxidation of minerals. The diffusion coefficient of dissolved oxygen through a biofilm formed by filtering nitrifiers through a membrane filter was found between 80 and 100% of its value in water (Lewandowski et al., 1991).

The studies of the migration of oxygen within structurally heterogeneous biofilm demonstrated the importance of biofilm architecture to the oxygen transport (Rasmussen et al., 1998 b, Stoodley et al., 1998).

The goal of this paper was to calculate the diffusion coefficient of the polymer film created onto the mineral surface.

MATERIALS AND METHOD

MINERAL SAMPLES

The material used in this study was obtained from the out-of-operation arsenic mine at Zloty Stok (Lover Silesia, Poland) The sample tailing was collected from the "Jan" heap and it contained gold-bearing minerals such as loellingite and arsenopyrite. The samples were ground and wet-screened to obtained -0.5 +0.125 mm size fraction. The results of chemical analysis of this size fraction is presented in Table 1.

Table 1. Chemical composition of arsenic sample

Elements	Composition [%]
Fe	24.65
As	3.22
Si	13.02
S	7.42
Al	2.41

The specific surface area of the mineral samples was determined by the BET method using FlowSorb II 2300 and was equal to 1.63 m^2/g.

BACTERIA

Acidithiobacillus ferrooxidans was used in this work. This strain was isolated from mine water from the Zloty Stok mine. A part of culture was adapted to grow in the high As ion concentration solutions. *A.ferrooxidans* was grown in 300 ml Erlenmeyer flasks at 30°C while shaking at 150 rpm using 130 ml 9K medium of composition presented at Table 2. The pH of this medium was adjusted to 2.0. A 10% (v/v) inoculum of the 4 days old culture was used for bacterial iron oxidation studies.

The microorganism cells concentration correlates to the protein concentration. Protein concentration was determined by reacting the proteins with copper ions to form a purple copper-protein complex. The complex concentration was determined by using a spectrometer.

REAGENTS

The polymer film was created by a polysaccharide (DEXTRIN) adsorption on the solid surface. Dextrin was purchased from Sigma Chemical Co. and used without further purification.

OXIDATION PROCEDURE

The packed-bed reactor was used for the bioxidation experiments. We utilized a glass column with 210 mm-high and 47 mm-inside diameter. The perforated glass plate supported the mineral material at the bottom. The column works in a flooded way with recycling the medium using a peristaltic pump. Air was supplied to the supernatant at the rate of 960 ml/min. The experiments were run at 25^{o}C. The biooxidation process was monitored by measurements of the following parameters: pH, Eh, Fe^{3+}, Fe^{2+}, total As and proteins concentrations.

POLYMER ADSORPTION

Adsorption experiments were conducted in plastic 100 ml bottles. Solid samples of 1.0g were mixed with 100 ml of polymer solution. The suspensions were equilibrated for 10 hours. The solid particles were centrifugated for 15 minutes at 4500 rpm and about 10 ml of supernatants was pipetted out for analysis. Dextrine concentration after adsorption was determined by colorimetric method (Dubois et al., 1956). The adsorbed amount of polymer was calculated by depletion.

DETERMINATION OF OXYGEN PROFILE

Oxygen profiles were measured by a microelectrode connected with a micromanipulator. The electrodes were mounted on a micromanipulator (Model MM33) World Precision Instruments. The electrodes were moved from the bulk solution down through the polymer film.

EXPERIMENTALS AND DISCUSSION

Figure 1a shows the adsorption behaviour for pH of the suspension between 1.85 and 4.09. This narrow pH range corresponds with the biooxidation conditions. It is evident that the adsorption density is almost independent of pH in the investigated pH range. The results of dextrin adsorption are presented in Fig. 1b. It shows that the isotherm exhibits Langmuirian behaviour. It is apparent that the equilibrium adsorption density was about 0.9 mg/m^2.

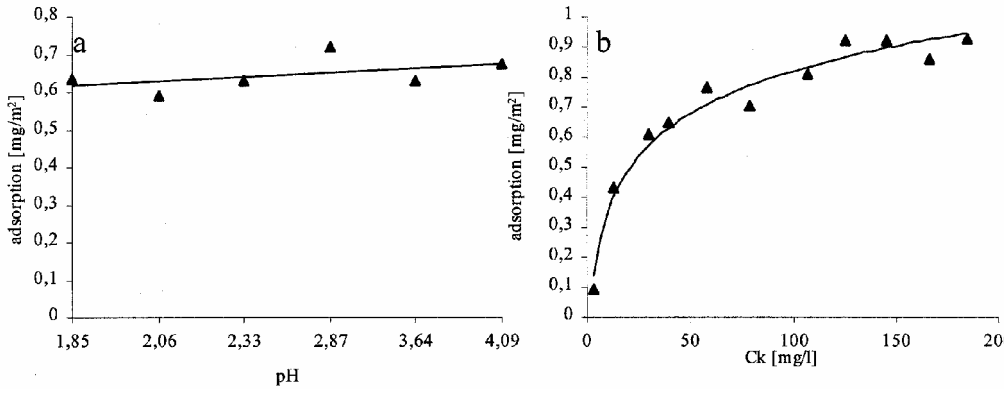

Fig. 1. Isotherms of dextrin adsorption onto the +0.125 –0.5 mm fraction of arsenic waste: a) effect of different values of pH, b) effect of different dextrin concentrations (C_k)

Dissolve oxygen profiles were also measured. Figure 2 shows the oxygen concentration profiles at various locations inside the polymer film. The numbers from 1 to 5 show different places of microelectrode.

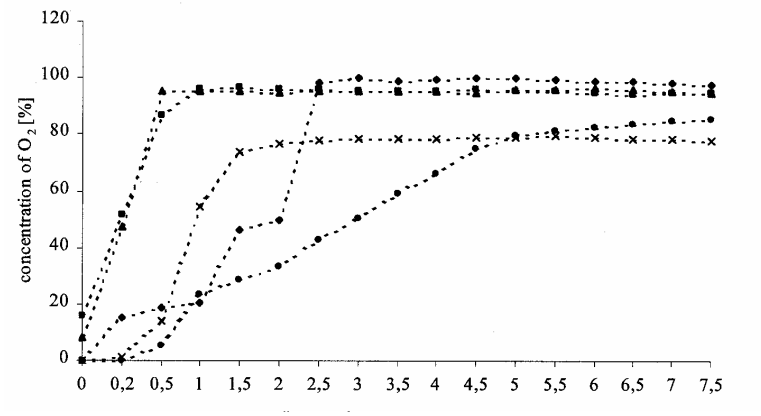

Fig.2. Oxygen concentration profiles

The rate of change of oxygen concentration inside the polymer film can be described by the equation resulting from differential mass balance (Lewandowski et al., 1991).

$$\frac{\partial c}{\partial t} = D_f\left(\frac{\partial^2 c}{\partial x^2} - \frac{V_{MAX}c}{K_S + c}\right), \tag{1}$$

where: D_f is the diffusion coefficient for the dissolved oxygen [cm^2/s]; c is the oxygen concentration at the point x (x = 1,2,3,4,5); V_{MAX} is the rate of oxygen consumption [mg/dm^3 s] and c is the oxygen saturation concentration [mg/dm^3].

If the polymer film is partially penetrated, the above equation can be transformed to the form:

$$\frac{\partial c}{\partial x} = \sqrt{2\frac{V_{MAX}}{D_f}\left(c - K_f\, ln\frac{K_S + c}{K_S}\right)}. \tag{2}$$

The fist derivative $\frac{\partial c}{\partial x}$ should be linearly related to $\sqrt{c - K_f\, ln\frac{K_S + c}{K_S}}$.

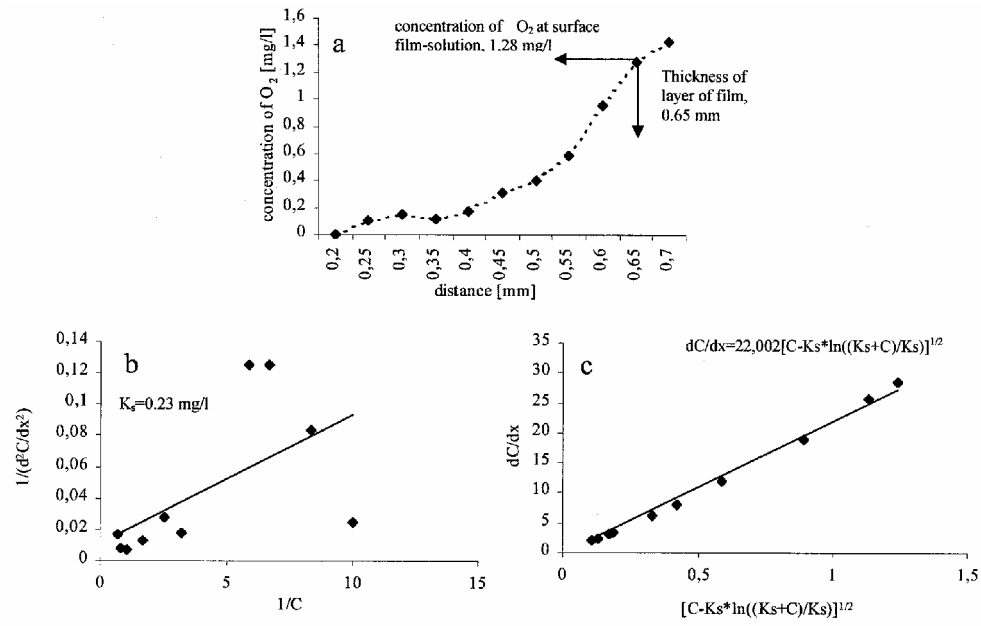

Fig. 3a. The dissolved oxygen profile within the distance of 0.2 to 0.7 mm; 3b. Determination of the half saturation coefficient (K_S); 3c. Determination of diffusion coefficient for oxygen

The slope of the line from Fig. 3b divided by the intercept gives K_S. For dissolved oxygen concentration K_s is 0.23 mg/l. The regression line is shown in Fig 3b and Equation 3.

$$\frac{\partial c}{\partial x} = 22.002\left[c - K_S\, ln\frac{K_S + c}{K_S}\right]^{\frac{1}{2}}. \tag{3}$$

The flux of oxygen must be preserved at the polymer film - solution interface. The oxygen diffusion coefficient can be calculated from the equation:

$$D_f\left(\frac{dC}{dx}\right)_f = D_w\left(\frac{dC}{dx}\right)_w . \tag{4}$$

The mass transfer coefficients for the biofilm obtained by Lewandowski (Yaung et al., 1995) were 0.0003 and 0.00034 m. s^{-1} and the diffusion coefficient for oxygen in the biofilm was 1.75 10^{-5} cm^2s^{-1}. The diffusion coefficient of dissolved oxygen in water is $D_w = 2.0\ 10^{-5}$ $cm^2\ s^{-1}$. In our experiments the diffusion coefficient for oxygen is 1.6 10^{-5} cm^2s^{-1}.

The arsenopyrite oxidation data for both cases, that is in the presence and absence of polymer film are presented in Fig.4. The data indicate that in the presence of polymer the kinetics of biooxidation of arsenopyrite was enhanced. The total arsenic concentration obtained, when the polymer film was presented, was around 30 mg/l. The measurements of the protein concentration showed an increasing trend for both cases. However, we found that the protein concentration in the solution was lower in the presence of the biofilm. It can explain by the low diffusion of the protein through the polymer film. In contrast to arsenic, iron(III) ions the extraction from the tailing was low. It results from the $FeAsO_4$ precipitation (Sadowski et al., 2001).

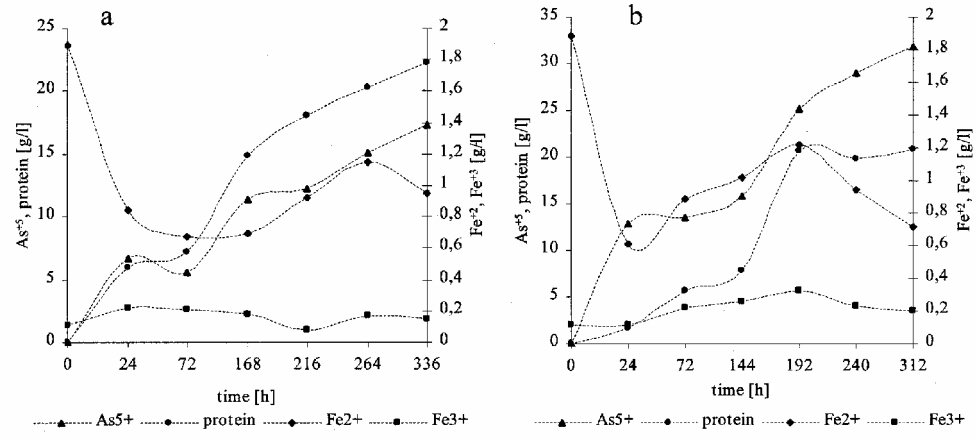

Fig. 4. Variation of Fe^{+2}, Fe^{+3}, As^{+5} ions and protein concentration in bioleaching of arsenic refractory ores in percolator: a) without polymer film, b) with polymer film

Table 2 shows the surface areas of the mineral powder used for biooxidation. It is evident that the presence of polymer film causes an increase of the surface area. An increase in the surface area from 1.63 to 42.68 m^2/g in the presence of polymer film was observed.

Table 2. The surface area of fine fraction after biooxidation of arsenic refractory wastes

Following samples	Surface area [m^2/g]	Increase of surface area after biooxidation
Initial sample	1.63	
After biooxidation without polymer film	30.87	18.94
After biooxidation with polymer film	42.68	26.18

CONCLUSION

In conclusion, we can say that:

- The adsorption of dextrin onto the mineral surface creates a special polymer film which improves oxygen diffusion
- According to the differential mass balance model the diffusion coefficient of oxygen in the polymer film is $D_f = 1.6\ 10^{-5}$ cm^2/s. It is comparable with the literature data
- An application of the polymer film provides a strong improvement of the biooxidation of arsenopyrite waste
- After the biooxidation process, the surface area of aresenopyrite increases from 1.63 to 42.68 m^2/g. It is 7.24 – fold greater than the biooxidation process without the polymer film

REFERENCES

RASMUSSEN K., LEWANDOWSKI Z., (1998), *The accuracy of oxygen flux measurements using microelectrodes,* Wat. Res.,32 (12), 3747-3755.

RASMUSSEN K., LEWANDOWSKI Z., (1998), *Microelectrode measurements of local mass transport rates in heterogeneous biofilms,* Biotechnol. Bioeng., 59 (3), 302-309.

De BEER D., STOODLEY P., LEWANDOWSKI Z., (1997), *Measurement of local diffusion coefficients in biofilms by microinjection and confocal microscopy,* Biotechnol. Bioeng., 53 (2), 151-158.

STOODLEY P., LEWANDOWSKI Z., BOYLE D.J., LAPPIN-SCOTT M.H., (1998), *Oscillation characteristics of biofilm streamers in turbulent flowing water as related to drag pressure drop,* Biotechnol. Bioeng., 57 (5), 536-544.

LEWANDOWSKI Z., CUNNINGHAM B.A., (1998), *Biofilm process fundamentals*, in Bioremendiation: Principles and Practice, volume 1, S.K.Sikdar, R.L. Irvine (Eds.), Technomic Publishing, Co., Inc., Lancaster, Basel, 511-546.

KARAS H., SADOWSKI Z., (2002), *Biometalurgia metali nieżelaznych, podstawy i zastosowanie,* W.Charewicz (Ed.),Wrocław, CBPM Cuprum, Uniwersytet Wrocławski, 40-50.

KARAMANEV D., MARGARITIS A., CHONG N., (2001), *The application of immobilization to the bioleaching of refractory gold concentrate,* Int. J. Miner. Process., 62, 231-241.

YAUNG S., LEWANDOWSKI Z., (1995), *Measurement of local mass transfer coefficient in biofilm,* Biotechnol. Bioeng., 48, 737-744.

LEWANDOWSKI Z., WALSE G., CHARACKLIS W.G., (1991), *Reaction kinetics in biofilms,* Biotechnol. Bioeng., 38. 877-882.

DUBOIS M., GILLES K.A., HAMILTON J.K., REBERS P.A., SMITH F., (1956), *Colorimetric method for determination of sugars and related substances*. Anal. Chem., 28 30, 350-356.

SADOWSKI Z., JAZDZYK E., FARBISZEWSKA T. FARBISZEWSKA-BAJER J. (2001), *Biooxidation of arsenic refractory ores in the presence of polymer film*, Biohydrometallurgy: Fundamentals, Technology and Sustainable Development, V.S.T.Ciminelli, O.Garcia Jr. Eds., Elsevier, 217-223.

Jażdżyk E., Sadowski Z., *Wpływ sztucznego filmu utworzonego z polimeru na proces bioutleniania odpadów arsenopirytowych,* Physicochemical Problems of Mineral Processing, 37 (2003) 69-76 (w jęz. ang.).

Określono wpływ filmu utworzonego z dekstryny na proces bioutleniania odpadów arsenopirytowych. Zbadano proces adsorpcji typowego polimeru cukrowego, dekstryny, na powierzchni materiału mineralnego. Określono wartości odczynu pH dla procesu bioutleniania odpadów arsenopirytowych. Stosując mikroelektrodę tlenowa określono profile stężeń tlenu w filmie z polimeru. Korzystając z uzyskanych wyników obliczono współczynnik dyfuzji tlenu w warstwie utworzonego filmu. Współczynnik ten wyniósł 1.6 10^{-5} cm^2/s. Wyniki uzyskane dla procesu bioutleniania wskazują na to, że film utworzony z polimeru odgrywa kluczową rolę zarówno w procesie unieruchomienia komórek bakteryjnych jak i w dyfuzji tlenu. W celu zintensyfikowania procesu bioutleniania odpadów arsenopirytowych niezbędna wydaje się być obecność filmu z polimeru na powierzchni ciała stałego.

Physicochemical Problems of Mineral Processing, 37 (2003) 77-86
Fizykochemiczne Problemy Mineralurgii, 37 (2003) 77-86

Małgorzata ULEWICZ[*], Władysław WALKOWIAK[**]

SEPARATION OF ZINC AND CADMIUM IONS FROM SULFATE SOLUTIONS BY ION FLOTATION AND TRANSPORT THROUGH LIQUID MEMBRANES

Received March 2003, reviewed, and accepted May 15, 2003

An experimental investigation is presented on zinc(II) and cadmium(II) ions separation from aqueous sulfate solutions, containing equimolar mixture on both metal ions, by ion flotation (IF) and transport through polymer inclusion membrane (PIM) processes. The IF experiments from dilute aqueous solutions ($c_{Me} = 1 \cdot 10^{-5}$ M) with an anionic surfactant (sodium dodecylbenzene sulfonate) and a cationic surfactant (hexadecylpyridinium chloride) are shown. With a cationic surfactant, the flotation separation of Cd/Zn grows with SO_4^{2-} concentration increase. In addition, the selective transport of Zn(II) and Cd(II) from aqueous sulfates source phase ($c_{Me} = 1 \cdot 10^{-2}$ M) through PIM containing cellulose triacetate (support), o-nitrophenyl pentyl ether (plasticizer) and di(2-ethylheksyl)phosphoric acid D2EHPA (ion carrier) is shown. The transport selectivity of Zn/Cd decreases with Na_2SO_4 concentration increase in source phase. Results obtained are discussed in terms of the stability constants of sulfate complex species for zinc(II) and cadmium(II).

Keywords: ion flotation, polymer inclusion membrane, zinc, cadmium, sulfates

INTRODUCTION

Selective separation of heavy metal ions from industrial and waste aqueous solutions is frequently required in hydrometallurgical processing (Davies 1987). The ion flotation and transport through liquid membrane are methods used for separation of metal ions from aqueous solutions. Ion flotation process has special position for the removal of ions from very dilute solutions, i.e. at the concentration below $1.0 \cdot 10^{-4}$M. Ion flotation involves the removal of surface inactive ions from aqueous solutions by the introduction of a surfactant and the subsequent passage of gas bubble through the aqueous solution (Lemlich 1972). The transport through liquid membrane is used for

[*] Department of Chemistry, Technical University of Częstochowa, 42-200 Częstochowa, Armii Krajowej 19 Street, Poland, e-mail: ulewicz@mim.pcz.czest.pl
[**] Institute of Inorganic Chemistry and Metallurgy of Rare Elements, University of Technology, 50-370 Wrocław, Wybrzeże Wyspiańskiego 27, walkowiak@ichn.ch.pwr.wroc.pl

selective separation and concentration of metal ions from source aqueous phase, in which the concentration of metal ionic species is above $1 \cdot 10^{-4}$ M.

The selectivity of cationic surfactants foward anions has been established in several ion flotation experiments including chloride and cyanide metal complexes of Zn(II), Cd(II), Hg(II), and Au(III) (Walkowiak and Grieves 1976, Walkowiak et al. 1976 and 1992). Jurkiewicz (1984-85) investigated foam separation of Cd(II) ions by dodecyl sulfate from aqueous solutions in the presence of electrolytes and found a negative influence of these electrolytes on Cd^{2+} foam separation. Also Jurkiewicz (1985) investigated separation of thiocyanate and iodide complexes of cadmium(II) from acidic aqueous solutions with hexadecyltrimethylamonium bromide. The influence of chloride, bromide, iodide and thiocyanate ions on the separation of Zn(II) and Cd(II) ions was also studied by Jurkiewicz (1990). On the other hand, Skrylev el al. (1997) investigated the removal of Zn(II) and Cd(II) in the presence of inorganic ligands from sulfate solutions using fatty acid containing $10 \div 14$ carbon atoms. The influence of zinc and cadmium concentrations on the effectiveness of flotation removal with potassium oleate was studied by Sinkova (1998); Zn(II) and Cd(II) ions were removed effectively from aqueous solution. Also Scorcelli et al. (Scorcelli et al 1999) studied the removal of Cd(II) using sodium dodecylsulfate as an anionic collector. The best removal (99 %) was obtained for metal cations to collector ratio equal to 1:3. Study of Cd(II) over Zn(II) ions separation in the presence of inorganic ligands by anionic and cationic collectors was conducted by Ulewicz et al. (2001) and Walkowiak (2002).

There are different types of liquid membranes, i.e. bulk (BLM), emulsion (ELM), supported (SLM), as well as polymer inclusion membranes (PIM). PIM provides metal ion transport with high selectivity, as well as easy setup and operation (Sugiura et al. 1987). The casting solution contains cellulose triacetate (support), a membrane plasticizer and an ion-exchange carrier. There are few papers, which deal with Cd(II) removal and Cd(II) over Zn(II) separation by supported liquid membranes. Breembroek et. al. (1998) has reported on cadmium extraction through a flat sheet and hollow fiber supported liquid membranes using tertiary amines as ion carriers. Also Urtiga and Ortiz (1999) studied cadmium removal from aqueous phosphoric acid by SLM. The separation of Cd(II) over Zn(II) from chloride media by a supported liquid membrane using quaternary ammonium salts as ion carriers was reported by Danesi et al. (1983) and Hoh et al. (1990). Li et al. (1997, 1998) studied transport of Cd(II) ions through liquid membrane with tri-n-octylamine, triisooctylamine and sorbitan monooleate. They investigated the effect of KI, KBr and KSCN concentration in the feed solutions on Cd(II) removal. The removal studies of Cd(II) from chloride aqueous solutions by PIMs were published by Hayashita (1996) and Hayashita et al. (1994). Preliminary research of Cd(II) over Znc(II) ions separation by PIM from chloride aqueous solutions was conducted by Kozłowski et al. (2000 and 2002).

The present work deals with the separation of zinc(II) and cadmium(II) metal ionic species from sulfate aqueous solutions containing equimolar mixture of both metals by ion flotation ($c_{Me} = 1 \cdot 10^{-5}$ M) and transport across polymer inclusion membranes ($c_{Me} = 1 \cdot 10^{-2}$ M).

EXPERIMENTAL

ION FLOTATION

The ion flotation experiments were carried out in a glass column 45.7 cm in high and 2.4 cm in diameter. The flow rate was maintained at 12 cm^3/min through a sintered sparger of 20–30 μm nominal porosity. The volume of each initial aqueous solution was 100 cm^3, and the temperature was maintained at 22 ± 2 ^{0}C.

The initial aqueous solutions were prepared with double distilled water and the compounds of $ZnSO_4$, $CdSO_4$, Na_2SO_4, H_2SO_4 all from POCh, Gliwice (reagents of analytical grade). The surfactants concentration, i.e. sodium dodecylbenzene sulfonate (DBSNa) and hexadecylpyridinium chloride (CPCl), in the initial solutions were kept constant at $2.0 \cdot 10^{-4}$ M throughout this investigation. The gamma radioactive isotopes, i.e. Zn-65 and Cd-115m were of sufficiently low specific activity to neglect the effect of carrier concentration (Zn-65: 9.2 GBq/g, Cd-115m: 2.2 GBq/g). These isotopes were from the Atomic Energy Institute (Świerk).

The time dependence of zinc(II) and cadmium(II) concentrations in the bulk solution (c) was recorded continuously during each ion flotation run by means of radioactive analytical tracer, and gamma radiation spectrometry, following a procedure described previously (Walkowiak and Ulewicz 1999). A single channel, gamma radiation spectrometer was applied as the detector of radioactive intensity of specific energy. The c versus time curves enabled the calculation of the percent removal (M):

$$M = [1 - (c_r/c_i)] \cdot 100\% \tag{1}$$

where c_i is the initial metal concentration, c_r is the metal concentration in residual solution after foam ceased. Also selectivity coefficients (S) of ion metal *Me1* over *Me2* were calculated:

$$S_{Me1/Me2} = M_{Me1}/M_{Me2}\,. \tag{2}$$

POLYME R INCLUSION MEBRANE

A solution of cellulose triacetate (as the support), di(2-ethylheksyl)phosphoric acid D2EHPA (as the ion carrier), and *o*-nitrophenyl pentyl ether (as the plasticizer) in dichloromethane was prepared. A portion of this organic solution was poured into a membrane mold comprised of a 9.0 cm glass ring attached to a plate glass with cellulose triacetate-dichloromethane glue. Dichloromethane, as the organic solvent,

was allowed to evaporate overnight and the resultant polymer inclusion membrane was separated from the glass plate by immersion in water. The membrane was stored in water. The concentration of D2EHPA was 1.50 M based on plasticizer.

Transport experiments were conducted in a permeation cell in which the membrane film (at surface area of 4.9 cm^3) was tightly clamped between two cell compartments. Both, i.e. source and receiving aqueous phases (45 cm^3 each), were mechanically stirred at 600 rpm. The receiving phase was 1.0 M aqueous solution of sulfuric acid. The PIM transport experiments were carried out at the same temperature as IF runs. Small samples (0.1 cm^3 each) of the aqueous receiving phase were removed periodically via a sampling port with a syringe and analyzed to determine zinc and cadmium concentrations by atomic absorption spectroscopy method (AAS Spectrometer, Solaar 939, Unicam).

The inorganic chemicals, their purity, and producer were the same as in ion flotation experiments. The organic chemicals, i.e. cellulose triacetate (Fluka), di(2-ethylheksyl)phosphoric acid (Fluka), *o*-nitrophenyl pentyl ether (Fluka), and dichloromethane (POCh) were of analytical reagent grade. The percent removal and selectivity coefficients were calculated according to equations (1) and (2) in which c_i and c_r are the initial and residual metal concentrations in the aqueous source phase.

RESULTS AND DISCUSSION

First, the competitive ion flotations were studied to determine the sulfates influence on flotation kinetics of Zn(II) and Cd(II) ions with an anionic and a cationic surfactant (Fig. 1).

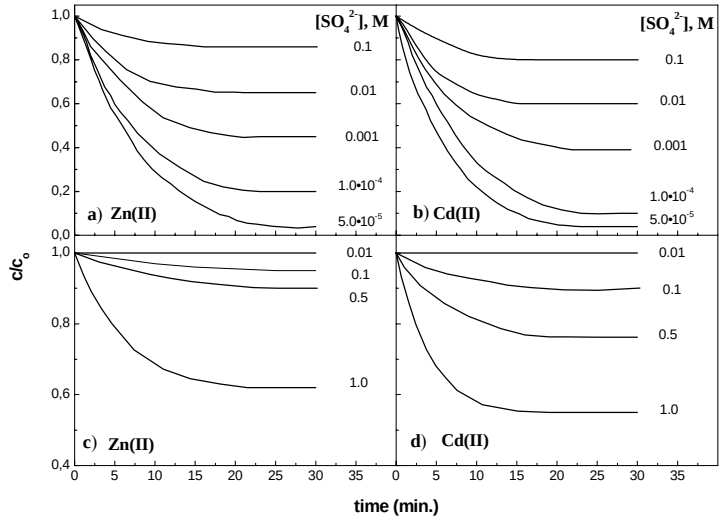

Fig. 1. Rate curves of zinc(II) and cadmium(II) concentration vs. time from aqueous solution containing equimolar mixture of both metals ($c_{Me} = 1.0 \cdot 10^{-5}$ M) in presence of sulfates with DBSNa (a, b) and with CPCl (c, b), $c_{surf.} = 2.0 \cdot 10^{-4}$ M

According to Figs 1a and 1b, with the increase of sulfates concentration the rate and removal of both floated ions, i.e. zinc(II) and cadmium(II), with DBSNa decreases. At concentration of sulfates equal to $5 \cdot 10^{-5}$ M, percent removal of zinc and cadmium reaches 97 %, and 99 %, respectively, whereas at concentration of sulfates equal to 0.10 M, percent removal of zinc and cadmium decreasses to 12 %, and 19 %, respectively. Separation of Cd/Zn does not occurred because percent removal of both metal ions is comparable. Contrary influence of sulfates concentration on competitive ion flotation of zinc and cadmium is observed using a cationic surfactant, i.e. CPCl (Figs 1c and 1d). In this case both flotation rate and percent removal of Zn(II) and Cd(II) increase with SO_4^{2-} concentration increase but the separation of cadmium over zinc is low (Fig. 2). With sulfates concentration increase the percent removal of cadmium(II) grows faster than zinc(II).

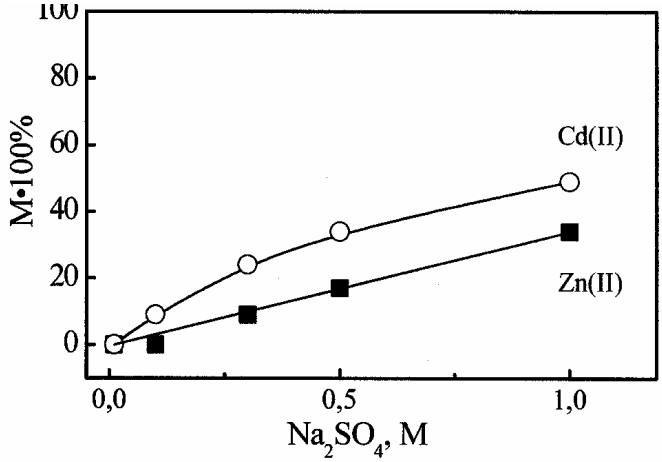

Fig. 2**.** Percent removal of zinc(II) and cadmium(II) in competitive ion flotation with CPCl from aqueous solutions containing equimolar mixture of both metals vs. sulfates concentration. Experimental conditions as in Fig.1

Next, the competitive transport of zinc(II) and cadmium(II) ions from aqueous source phase ($c_{Me} = 1.0 \cdot 10^{-2}$ M) containing sulfates through polymer inclusion membranes with D2EHPA into receiving aqueous phase was investigated. The kinetics of zinc(II) and cadmium(II) ions transport through PIM from aqueous source phase containing equimolar mixture of both metals is shown in Fig. 3.

Comparison of both processes kinetics, i.e. IF and transport across PIM (Figs 1 and 3) shows that transport through polymer inclusion membranes is much slower than ion flotation of adequate metals, and it takes 24 hours to remove more than 86 % of zinc from source aqueous phase. In contrast to IF, the PIM transport of zinc(II) is faster than cadmium(II). The dependence of percent removal of Zn(II) and Cd(II) ions from a source aqueous phase as a function of Na_2SO_4 concentration is presented in Fig. 4.

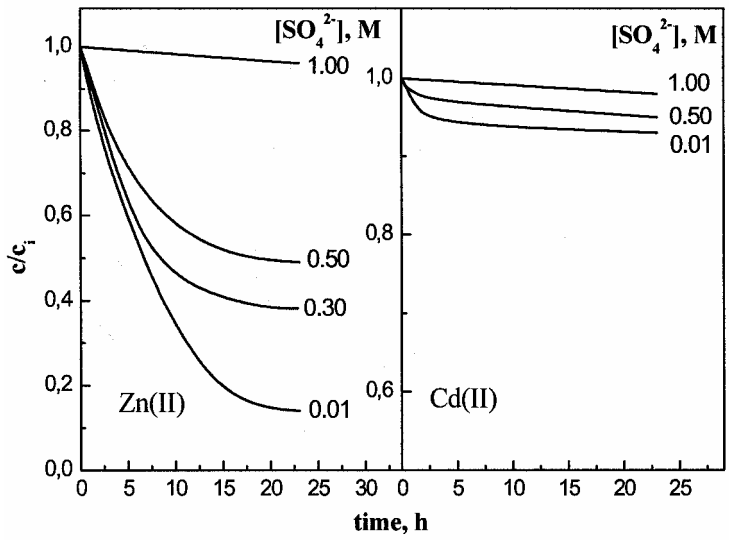

Fig. 3. Kinetics of zinc(II) and cadmium(II) transport through PIM with D2EHPA from source aqueous phase vs. Na_2SO_4 concentrations, ($c_{Me} = 1.0 \cdot 10^{-2}$ M), pH =4.0. Membrane: 2.6 cm^3 ONPOE / 1g CTA, 1.5 M D2EHPA

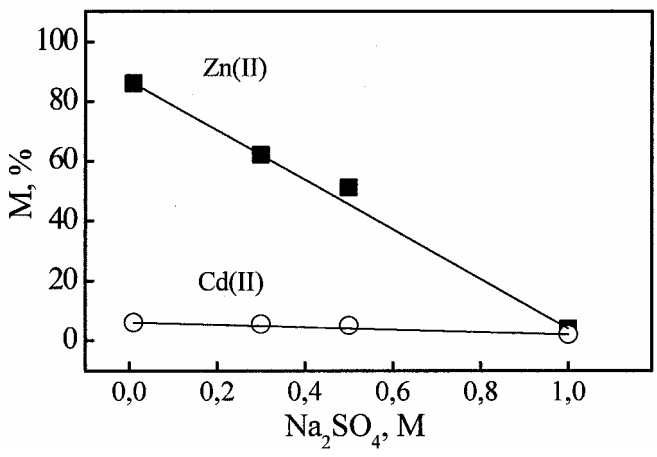

Fig. 4. Percent removal of zinc(II) and cadmium(II) ions through PIM from source aqueous phase containing equimolar mixture of both metals ($c_{Me} = 1{,}0 \cdot 10^{-2}$ M) vs. Na_2SO_4 concentration in source phase. Experimental conditions as in Fig.3

Fig. 4 shows that the percent removal of zinc ions decreases with Na_2SO_4 concentration increase and at SO_4^{2-} concentration equal to 1.0 M transport through PIM does not occur. This causes that separation coefficient of Zn/Cd is the highest for low concentrations of sulfates, i.e. 0.010 M. The separation coefficients of zinc(II) over cadmium(II) in polymer inclusion membrane processes at 0.01, 0.3, 0.5 and

1.0 M concentrations of sulfates, reache 14.3; 11.7; 10.2 and 2.0, respectively. Wherease the separation coefficients of cadmium(II) over zinc(II) in ion flotation were between 1.2 ÷ 1.6. The dependence of separation coefficients of metal ions versus SO_4^{2-} concentration for both processes is different. For ion flotation, $S_{Cd/Zn}$ values are insignificantly growing with SO_4^{2-} concentration increase while coefficients values of $S_{Zn/Cd}$ for polymer inclusion membranes are decreasing with Na_2SO_4 concentration increase. To explain IF and PIM experimental results, the contributions of formed complex species of zinc(II) and cadmium(II) in aqueous sulfates solution were calculated. The percent molar contributions of sulfates complex species for those metals versus SO_4^{2-} concentration are presented in Fig. 5. α_0 is the percent molar contribution of uncomplexed cations (i.e. Zn^{2+} and Cd^{2+}); α_1, α_2, α_3 and α_4 are percent molar contributions of complexed ions with 1, 2, 3, and 4 ligands, respectively. Values of stability constants for Zn(II) + SO_4^{2-} and Cd(II) + SO_4^{2-} systems were taken from Stability Constants of Metal-Ion Complexes (1982).

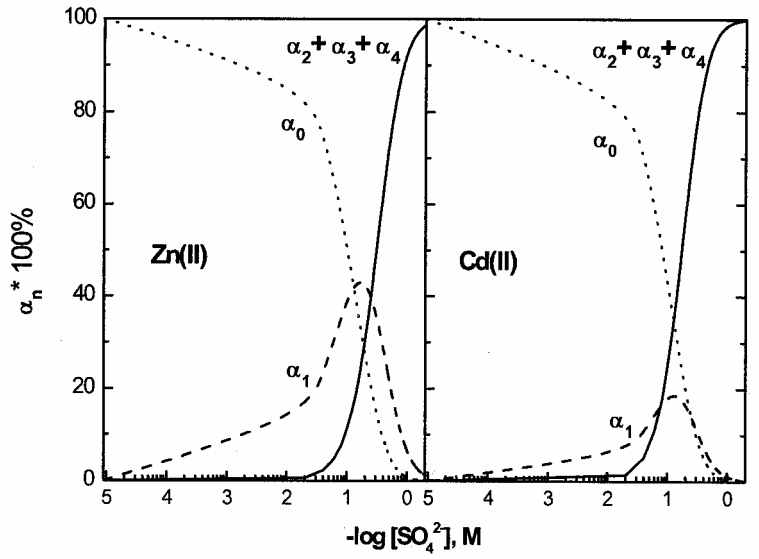

Fig. 5. Percent molar contributions ($\alpha_n \cdot 100\%$) of sulfate complex species for zinc(II) and cadmium(II) vs. sulfates concentration

In the presence of sulfates at concentration range from $5 \cdot 10^{-5}$ to 0.10 M zinc(II) and cadmium(II) exist as cations in 100 - 50 % and 100 - 43 %, respectively. But percent removal of both metals in ion flotation process with an anionic surfactant is much lower than values of α_0 molar contributions (Fig. 1). This is caused by interfering influence of sodium cations on ion flotation process. Percent removal of zinc(II) in IF process with a cationic surfactant increases in smaller part than cadmium(II) with sulfates concentration increase (Fig. 2). This correlates with low percent molar

contribution of Zn(II) anionic forms (i.e. $\alpha_2 + \alpha_3 + \alpha_4$) which reaches 89.6 % and 96.7 % for Zn(II) and Cd(II), respectively (Fig. 6). On the other hand, Cd(II) and Zn(II) percent removal is much lower than values of $\alpha_2 + \alpha_3 + \alpha_4$ molar contributions and reaches 55 % and 38 % for 1.0 M Na_2SO_4, respectively (Fig. 2).

In case of polymer inclusion membrane transport, which is significantly slower process (in comparison with IF), the main factor influencing on the Zn/Cd separation is different affinity of D2EHPA to Zn(II) and Cd(II) in experimental conditions (Binghua et al. 1996). The separation of Zn/Cd ratio decreases with Na_2SO_4 concentration increase.

CONCLUSION

Zinc(II) and cadmium(II) can be effectively removed from aqueous sulfate solutions in hydrometallurgical processes of ion flotation and transport across polymer inclusion membrane. The removal of zinc(II) and cadmium(II) ions by ion flotation with an anionic surfactant (DBSNa) decreases with SO_4^{2-} concentration increase. Separation of Cd/Zn does not occurr because percent removal of both metal ions is comparable The ion flotation with a cationic surfactant (CPCl) allow to partial separation of both metal ions, i.e. cadmium(II) over zinc(II), from dilute aqueous solutions ($c_{Me} = 1 \cdot 10^{-5}$ M). The removal of zinc(II) and cadmium(II) ions by ion flotation with CPCl increases with SO_4^{2-} concentration increase. Competitive transport of zinc(II) and cadmium(II) from an aqueous sulfate source phase ($c_{Me} = 1 \cdot 10^{-2}$ M) through polymer inclusion membranes containing di(2-ethylheksyl) phosphoric acid (D2EHPA) as ion carrier into aqueous sulfuric acid solution enables separation of zinc(II) over cadmium(II). The selectivity coefficients of Zn/Cd for PIM decreases with Na_2SO_4 concentration increase in source phase. In both studied separation methods, i.e. IF with DBSNa and transport across PIM, zinc(II) and cadmium(II) are removed from an aqueous sulfuric solutions in the form of Zn^{2+} and Cd^{2+}, respectively. On the other hand, in IF with CPCl zinc(II) and cadmium(II) are removed from solutions in the of forms anionic complexes. Results are discussed in terms of the sulfate complex species stability for zinc(II) and cadmium(II).

ACKNOWLEDGMENT

Financial support of this work was provided by Polish Science Foundation Grants No. 4 T09B 107 22 .

REFERENCES

BINGHUA Y., NAGAOSA Y., SATAKE M., NOMURA A., HORITA K., (1996), *Solvent extraction of metal ions and separation of nicke(II) from other metal ions by organophosphorus acids,* Solvent extraction and Ion Exchange, 14 , 849-870.

BREEBROEK G. R. M., WITKAMP G. J., VAN ROSMALEN G. M., (1998), *Extraction of cadmium with trilaurylamine-kerosine through a flat-sheet-supported liquid membrane*. J. Membr. Sci., 147, 195-206.

BREEMBROEK G. R. M, VAN STRAALEN, A., WITKAMP G. J., VAN ROSMALEN G.M., (1998), *Extraction of cadmium and copper using hollow fiber supported liquid membranes*. J. Membr. Sci., 146, 185-195.

DANESI P. R., CHIARIZIA R., CASTAGNOLA A., (1983), *Transfer rate and separation of Cd(II) and Zn(II) chloride species by a trilaurylammonium chloride-triethyl-benzene supported liquid membrane*, J. Membr. Sci., 14, 161-174.

HAYASHITA T., (1996), *Heavy metal ion separation by functional polymeric membranes*. ACS Symposium series 642, Chemical separation with liquid membranes. R. A. Rartsch, J. D. Way, Eds., Washihgton DC, 303-318.

HAYASHITA T., KUMAZAWA M., YAMAMOTO M., (1994), *Selective permeartion of cadmium(II) chloride complex through cellulose triacetate plasticizer membrane containing trioctylmethylammonium chloride carrier*, Chemistry Letters, 37-39.

HOH Y.C., LIN C.Y., HUANG T.M., CHIU T.M., (1990), *Separation of cadmium from zinc in a chloride media by a supported liquid membrane,* Proc. of the International Solvent Extraction Conference. Solvent Extraction, Part B, 1543-1548, Ed. by A. Sekine, S. Kusakabe, Elsevier, Amsterdam 1992.

JURKIEWICZ K., (1984-85), *Study on the separation of Cd from solutions by foam separation. I. Foam separation of cadmium cations, Sep. Sci. Technol.,* 19, 1039 - 1050.

JURKIEWICZ K., (1985), *Studies on the separation of Cd from solutions by foam separation. III. Foam separation of complex cadmium anions, Sep. Sci. Technol.,* 20, 179 - 192.

JURKIEWICZ K., (1990), *The removal of zinc solutions by foam separation. I. Foam separation of complex zinc anions*, Intern. J. Min. Process, 28, 173-188.

KOZŁOWSKI C., ULEWICZ M., WALKOWIAK W., (2000), Separation of zinc and cadmium ions from aqueous chloride solutions by ion flotation and liquid membranes, Physicochemical Problems of Mineral Processing, 34, 141-151.

KOZŁOWSKI C., WALKOWIAK W., PELLOWSKI W., KOZIOL J., (2002), Competitive transport of toxic metal ions by polymer inclusion membranes, J. Radioanalytical Nuclear Chem., 253, 389-394.

LEMLICH R. Ed., (1972), *Adsorptive bubble separation techniques*, Academic Press, New York.

LI Q., LIU Q., LI K. TONG S., (1997), Separation study of cadmium through an emulsion liquid membrane, Talanta, 44, 657-662.

LI Q., LIU Q., LI K. ZHANG Q.F., WEI X.J., GUO J.Z., (1998), Separation study of cadmium through an emulsion liquid membrane using triisooctylamine as mobile carrier, Talanta, 46, 927-932.

SINKOVA L. A. (1998), Influence of zinc and cadmium ions concentration on effectiveness of flotation removal from aqueous solutions with potassium oleate, Ukr. Kim. Zhrn. 64 , 94-99.

SCORZELLI I. B., FRAGOMENI A. L., TOREM M. L., (1999), *Removal of cadmium from a liquid effluent by ion flotation*, Minerals Engineering, Vol. 12, 905-917.

SKRYLEV L. D., SKRYLEVA T. L., SAZANOVA V. F., (1997), *Pyrometallurgical processing of a froth product during flotation of polyvalent metal ions by fatty acid collectors,* Izv. Vyssh. Uchebn. Zaved., Tsvetn. Metall., 1, 7 - 10.

SUGIURA M., KIKKAWA M., URITA S. (1987), *Effect of plasticizer in carrier-mediated transport of zinc ion through cellulose triacetate membranes,*. Sep. Sci. Technol., 22, 2263-2271.

Stability Constants of Metal-Ion Complexes, Part A: Inorganic Ligands, Pergamon Press, New York, 1982.

URTIAGA M., ORTIZ I., (1999), *Comparison of liquid membrane processes for the removal of cadmium from wet phosphoric acid,* J. Membr. Sci., 164, 229-240.

ULEWICZ M, WALKOWIAK W (2002), *Flotation of zinc(II) and cadmium(II) ions from dilute aqueous solutions in the presences of inorganic ligands*, Physicochemical Problems of Mineral Processing, 36, 225-232.

ULEWICZ M, WALKOWIAK W., KOZŁOWSKI C., (2001), Selective flotation of zinc(II) and cadmium(II) ions from aqueous solutions in the presence of halides, Physicochemical Problems of Mineral Processing, 35, 21-29.

WALKOWIAK W., (1992), *Mechanism of selective ion flotation technology, In: Innovation in flotation technology,* Edited by P. Mavros, K. A. Matis, *NATO ASI Series, Kluwer Academic Publishers, London,* 455-473.

WALKOWIAK W., BHATTACHARYYA D., GRIEVES R. B., (1976), *Selective foam fractionation of chloride complex of Zn(II), Cd(II), Hg(II), and Au(III),* Anal. Chem., 48, 975-473.

WALKOWIAK W., GRIEVES R. B., (1976), *Foam fractionation of cyanide complex of zinc(II), cadmium(II), mercury(II), and gold(III),* J. Inorg. Nucl. Chem., 38, 1351-1356.

WALKOWIAK W., ULEWICZ M., (1999), *Kinetics studies of ion flotation*, Physicochemical Problems of Mineral Procesing, 33, 201-214.

Ulewicz M., Walkowiak W., *Separacja jonów cynku i kadmu z roztworów siarczanowych w hydrometalurgicznych procesach flotacji jonowej i ciekłych membran,* Physicochemical Problems of Mineral Processing, 37 (2003) 77-86 (w jęz. ang.).

Zbadano selektywność procesów wydzielania jonów cynku(II) i kadmu(II) z wodnych roztworów siarczanowych zawierających równomolową mieszaninę obu metali za pomocą flotacji jonowej (IF) i transportu przez polimerowe membrany inkluzyjne (PIM). Pokazano wyniki IF z rozcieńczonych roztworów wodnych (c_{Me}=1,0·10^{-5} M) za pomocą kolektora anionowego (dodecylobenzenosulfonian sodu) i kationowego (chlorek hexadecylopirydyniowy). Wykazano, że dla kolektora anionowego ze wzrostem stężenia siarczanów wydzielanie jonów cynku i kadmu maleje, a separacja obu metali nie jest możliwa ponieważ jony obu metali wydzielane są w porównywalnym stopniu. Natomiast w przypadku kolektora kationowego ze wzrostem stężenia siarczanów w roztworze wydzielanie jonów cynku i kadmu wzrasta ale wzrost selektywności flotacji Cd/Zn nie jest duży. W pracy prezentowane są również wyniki transportu Zn(II) i Cd(II) z wodnej fazy zasilającej (c_{Me}=1,0·10^{-2} M) przez PIM zbudowaną z trójoctanu celulozy (nośnik), eteru o-nitrofenylopentylowego (pastyfikator) i kwasu di(2-ethyloheksylo) fosforowego (przenośnik jonów). Selektywność transportu Zn/Cd przez PIM malała wraz ze wzrostem stężenia Na_2SO_4 w fazie zasilającej. Wyniki przedyskutowano w świetle zakresów trwałości poszczególnych form jonów kompleksowych Zn(II) i Cd(II) z siarczanami. W procesie IF z CPCl wydzielano jony cynku i kadmu w formie anionów, natomiast w procesie IF z DBSNa i PIM wydzielano kationowe formy obu metali.

Physicochemical Problems of Mineral Processing, 37 (2003) 87-96
Fizykochemiczne Problemy Mineralurgii, 37 (2003) 87-96

Joanna NIEMCZEWSKA[*], Ryszard CIERPISZEWSKI[**], Jan SZYMANOWSKI[*]

EXTRACTION OF ZINC(II) FROM MODEL HYDROCHLORIC ACID SOLUTIONS IN LEWIS CELL

Received March 2003, reviewed, and accepted May 15, 2003

Extraction of zinc(II) from model hydrochloric acid solutions was studied in Lewis cell mixing the bulks of both phases and keeping a stable interfacial surface. It was found that Lewis cell experiments, although dynamic in nature, support the extracting of $ZnCl_2 \cdot 2$ TBP chlorocomplex from model solutions containing 5 M Cl^- and 0,55 M H^+. The initial fluxes of zinc(II), HCl, Cl^-, chloride present in the zinc(II) complex and water depend upon the concentration of tributyl phosphate and the mixing rates. The diffusion step in the organic phase gives a higher resistance to the mass transfer than the diffusion step in the aqueous phase. The physical transfer of small water molecules is less sensitive upon the mixing rates than the transfer of bulky zinc(II) chlorocomplex.

Key words: extraction, zinc(II), hot-dip galvanising, Lewis cell

INTRODUCTION

Hot-dip zinc galvanising is the most common method of protecting steel from corrosion. The method generates spent pickling solutions containing iron(II), iron(III) and zinc(II) in hydrochloric acid. Hydropyrolysis is the most often used method to process such solutions. However, the method can not be used when the content of zinc(II) exceeds 0.5 g/dm^3. Such solutions are obtained when the spent pickling liquor is used for depleting the bad quality zinc protective layers.

Solvent extraction is one of different techniques which can be used to recover zinc(II) from such solutions [Schügerl et al., 1996; Bart, 2000]. Tributyl phosphate (TBP) is the most suitable reagent and enables both the effective extraction of zinc(II) from HCl solutions and subsequent stripping with water [Regel et al., 2001,Tórz et al., 2002]. However, iron(III) is strongly co-extracted and must be reduced to iron(II)

[*] Institute of Chemical Technology and Engineering, Poznan University of Technology, pl. M. Sklodowskiej-Curie 2, 60-956 Poznan, Poland, jan.szymanowski@pnt.poznan.pl
[**] Poznan Univesity of Economics, Faculty of Comodity Science, al. Niepodleglosci 10, 60-967 Poznan, Poland

prior the extraction of zinc(II). Up to now, the kinetics of zinc(II) extraction from HCl solutions with TBP was not studied, and the scope of the published works was limited only to equilibrium studies [Navratil, 1987].

The aim of the work was to study the kinetics of zinc(II) extraction from model HCl solutions with TBP. A Lewis cell was used as a contractor. The intensive mixing of both phases enabled to decrease substantially the effects of diffusion steps upon the transfer of zinc(II) to the TBP phase. The fluxes and mass transfer coefficient could be easily estimated when experiments were performed with a stable interfacial surface.

EXPERIMENTAL

The composition of model aqueous solutions was as follows: [Zn(II)]=0.31 M; $[H^+]$=0.55 M; $[Cl^-]$=5 M (adjusted with NaCl). All reagents ($ZnCl_2$, NaCl and HCl from P.O.Ch. Gliwice) were pure grade. Deionised water from reverse osmosis was used. Pure tributyl phosphate (Fluka) was diluted with aliphatic kerosene Exxsol D 220/230 (Deutsche Exxon Chemical GmbH).

Extraction was carried out in a home-made Lewis cell (Fig. 1) elaborated by Plucinski and Nitsch [1992]. The volumes of each phase were equal to 95 cm^3. The interfacial surface area was 16.56 cm^2. The phases were mixed by independent stirrers. The mixing rate (MR) of one phase was constant (120 rpm), while the mixing rate of the second phase was changed from 80 to 200 rpm.

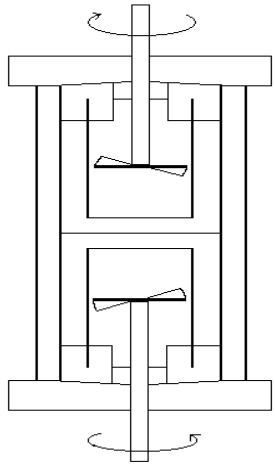

Fig. 1. Scheme of Lewis cell

One cm^3 samples of the organic phase were taken at appropriate periods of time and stripped with 10 cm^3 water. Samples of fresh TBP solution (1 cm^3) were added to keep the constant volume of the organic phase. The content of zinc(II) in the stripping

solution was determined by atomic absorption Spectr AA 800, Varian, Australia. The contents of HCl and chloride ions were determined by potentiometric titration with 0.05 M NaOH and 0.05 M $AgNO_3$, respectively, using Titrino 702 SM, Metrohm, Switzerland. In titration with NaOH the second equivalent point was observed at about pH 9 reflecting the presence of zinc chlorocomplexes considered as weak acid. The content of complexed chloride ions was determined in this way. The content of water in the organic phase was determined by Karl Fisher titration with Hydronal Composite 5 (Riedel de Haen).

Equilibrium extraction data were obtained in a classical way described in previous work [Cierpieszewski et al., 2002, Kirschling et al., 2001]. All experiments were carried out at room temperature.

Medusa program [Puigdomenech] was used to estimate the distribution of zinc(II) chlorocomplexes in the aqueous feed.

RESULTS AND DISCUSSION

In the aqueous feed zinc(II) is mainly in the form of $ZnCl_4^{2-}$ (92 mole %). The contents of $ZnCl_3^-$ and $ZnCl_2$ are estimated as equal to 8 and 0 mole %, respectively. The composition of the aqueous phase does not change significantly in the Lewis cell experiments. However, the effect must be taken into account in classical counter-current extraction.

The precision of considered species determination is good. The confidence limits at significance level of 0.05 calculated from 10 independent measurements are equal to ±0.026 mg/dm^3, ±0.003 M; ±0.003 M, ±0.004 M, ±0.053% for zinc(II), HCl, Cl^-, chloride present in the complex and water, respectively.

In equilibrium TBP extracts better Zn(II) than HCl (Table 1). However, at least 80% TBP must be used to obtain an effective extraction of zinc(II).

Table 1. Distribution coefficients for the extraction of Zn(II), HCl and Cl^- and the conten t of water in TBP phase in equilibrium

TBP concentration	Zn(II)	HCl	Cl^-	H_2O [%]
% vol	-	-	-	-
50	0.56	0.17	0.07	1.88
60	0.95	0.21	0.09	2.43
70	1.08	0.26	0.10	3.09
80	1.74	0.40	0.12	3.88
90	2.33	0.48	0.13	5.03
100	3.33	0.58	0.15	5.29

Low values of the distribution coefficients obtained for chloride ions are the result of great Cl^- excess in the aqueous feed (5 M). The equilibrium transfer of water increases with an increased concentration of TBP, i.e. from 0.92 M for 50% TBP to 2.86 M for 100% TBP. The mole ratio of transferred water to TBP also increases in the same order and amounts 0.56, 0.60, 0.65, 0.72, 0.83, 0.78 for 50, 60, 70, 80, 90 and 100% TBP, respectively.

The concentration of zinc(II) in the TBP phase increases with time and with an increased mixing rate (Fig. 2). A strong blocking of the interface connected with the stop of zinc(II) transfer is not observed in the Lewis cell, even when in some cases the system is near equilibrium after 2 hours of experiments (Table 2). As a result, the period of 20 minutes was arbitrary chosen to determine the "initial fluxes" j defined as

$$j = \left(\frac{V}{A}\right) * \left(\frac{\Delta c}{\Delta t}\right), \tag{1}$$

where V denotes the volume of the organic phase, A stands for the interfacial surface area and Δc denotes the change of concentration in the organic phase for Δt = 20 minutes (c=0 for t=0). After 20 minutes of the process the transfer of zinc(II) is in the range usually below 20% of the equilibrium value, for low mixing rates (80 rpm). However, the process of zinc(II) extraction increases with MR increase even up to 50% for 200 rpm. The conclusion is also valid for the transfer of HCl and water to the TBP phase (Table 2). The transfer was decreased below 30% for Δt= 10 minutes.

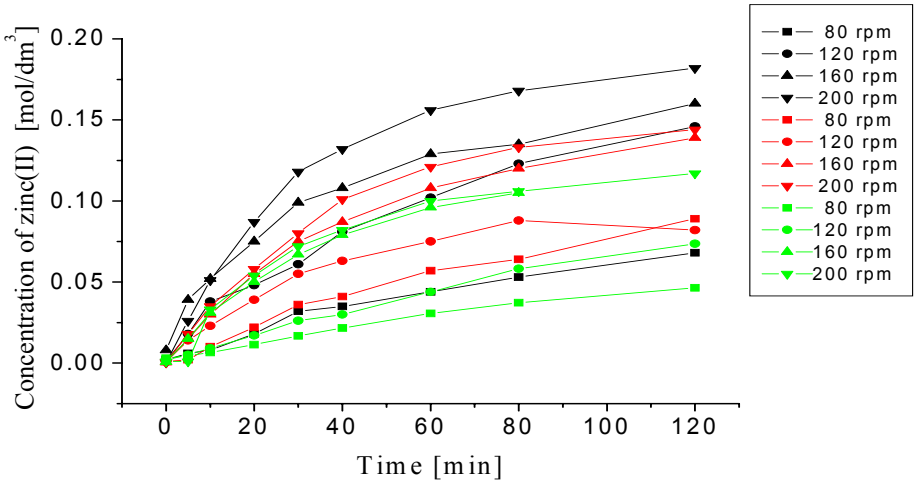

Fig. 2. Change of zinc(II) concentration in the organic phase for the constant rate mixing in the aqueous phase (MR_w=120 rpm) and different mixing rates in the organic phase (■ 80 rpm, ● 120 rpm, ▲ 160 rpm,▼ 200 rpm) and various contents of TBP (– – – 60 %, – – – 80 %, ——— 100%)

Table 2. Progress of zinc(II) extraction in the Lewis cell after 10, 20 and 120 minutes in respect with equilibrium (EP_{10}, EP_{20} and EP_{120}, respectively)

TBP concentration	Constant rate mixing (120 rpm) in							
	Aqueous phase				TBP phase			
	MR_O	EP_{10}	EP_{20}	EP_{120}	MR_W	EP_{10}	EP_{20}	EP_{120}
% vol	rpm	%	%	%	rpm	%	%	%
60	80	4.49	7.81	29.83	80	12.04	13.41	68.81
	120	6.26	20.93	63.54	120	6.26	20.93	63.54
	160	21.50	32.60	69.94	160	21.59	40.98	79.27
	200	22.89	38.12	79.49	200	28.07	45.05	71.59
80	80	5.01	12.00	47.40	80	8.69	16.76	71.78
	120	12.07	20.94	43.77	120	12.07	20.94	43.77
	160	15.87	29.37	74.46	160	23.94	41.67	93.34
	200	18.78	30.75	77.01	200	23.15	39.79	85.64
100	80	3.47	7.86	31.98	80	6.26	21.78	68.69
	120	16.64	11.78	50.74	120	16.64	11.78	50.74
	160	22.78	34.40	-	160	17.42	35.82	76.06
	200	22.18	36.99	80.78	200	22.53	48.91	78.93

Subscript ''o'' and ''w'' denote the organic and aqueous phase, respectively.

The effect of the mixing rate upon the "initial" fluxes of zinc(II), HCl, chloride present in the complex and water are shown in Figs 3-6. The results indicate that the transfer of considered components increases generally with an increase of TBP concentration. An atypical change of flux is only observed for zinc(II) and for low mixing rate. It can be caused by an experimental error but it can also reflect some blocking of the interface by the bulky chlorocomplex $ZnCl_2 \cdot 2TBP$, which is probably formed at the aqueous side of the interface or near its venicity

$$ZnCl_4^{2-} + 2TBP = ZnCl_2 \cdot 2TBP + 2Cl^- \quad (2)$$

and then slowly transferred to the organic phase. By analogy to the formation of $ZnCl_2 \cdot 2TBP$ complex given by Morris and Short [1962] and interfacial reactions of Cu(II) with hydroxyoximes [Szymanowski, 1993] the reaction can be described according to the scheme given in Fig. 7. The alternative version should take into account the protonation of TBP with HCl, i. e. the formation of intermediate $(BuO)_3P{=}O \bullet\bullet\bullet HCl$.

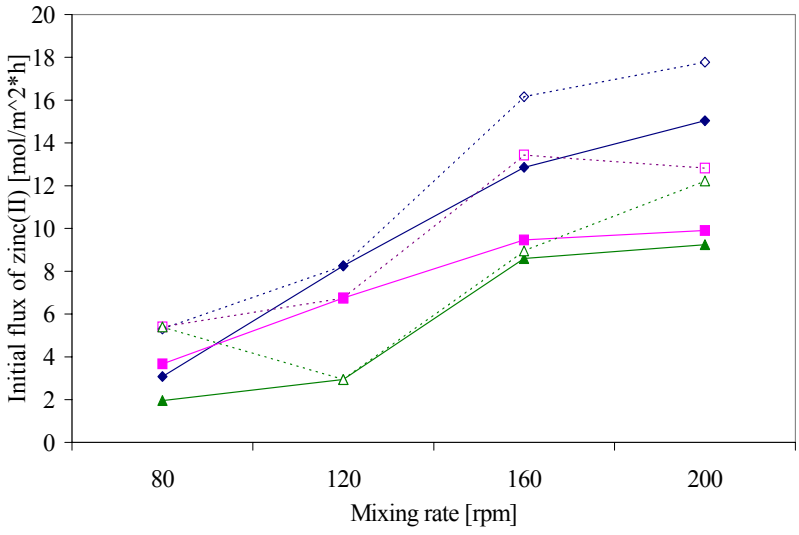

Fig. 3. Effect of mixing rate and TBP concentration upon the "initial flux" of zinc(II) (▲,△, 60% TBP; ■,❑, 80% TBP; ♦,◇, 100% TBP; full points, RM_w = 120 rpm; empty points RM_o= 120 rpm)

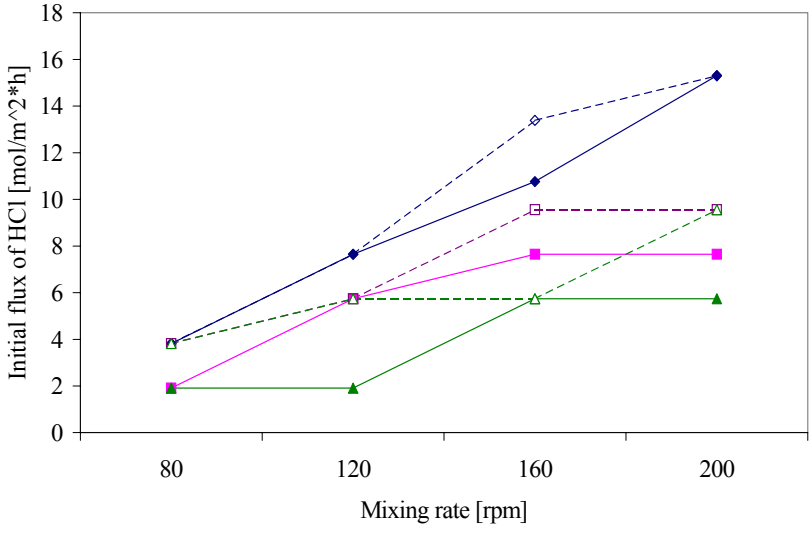

Fig. 4. Effect of mixing rate and TBP concentration upon the "initial flux" of HCl (▲,Δ, 60% TBP; ■,□, 80% TBP; ♦,◇, 100% TBP; full points, RM_w = 120 rpm; empty points, RM_o= 120 rpm)

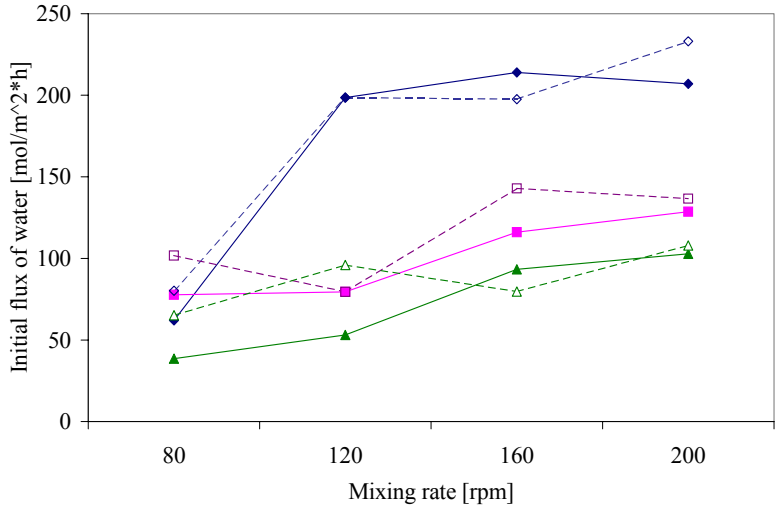

Fig. 5. Effect of mixing rate and TBP concentration upon the "initial flux" of water (▲,Δ, 60% TBP; ■,□, 80% TBP; ♦,◊, 100% TBP; full points, RM_w = 120 rpm; empty points, RM_o= 120 rpm)

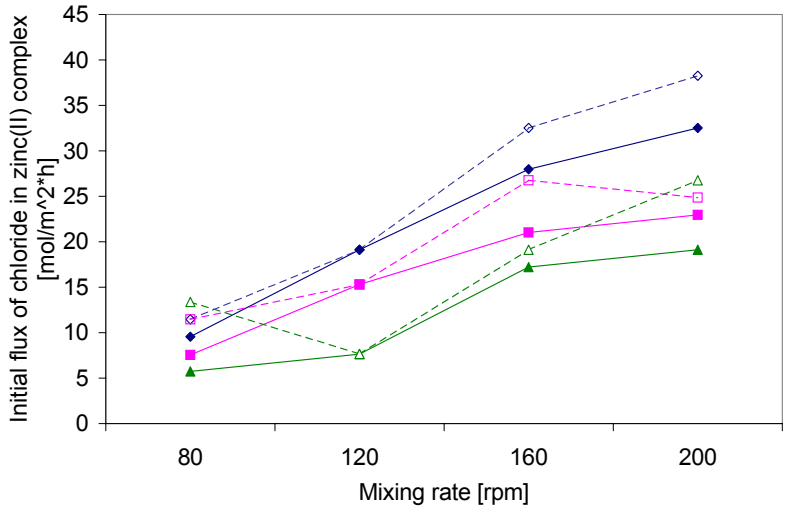

Fig. 6. Effect of mixing rate and TBP concentration upon the initial flux of chloride present in zinc(II) complex (▲,Δ, 60% TBP; ■,□, 80% TBP; ♦,◊, 100% TBP; full points, RM_w = 120 rpm; empty points, RM_o = 120 rpm)

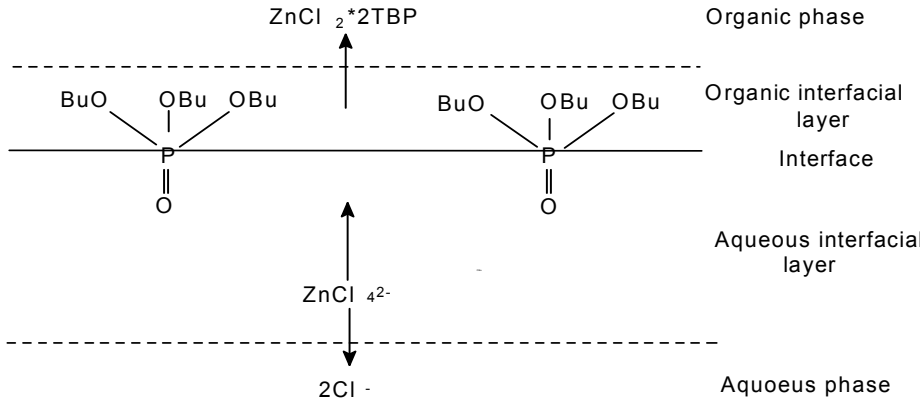

Fig. 7. Complexation of zinc(II) in the interfacial region

The extraction of $ZnCl_2 \cdot 2TBP$ complex is supported by the ratio of initial fluxes R_{20} determined for the transport of zinc(II) and chlorides present in zinc(II) complex considered as a weak acid and characterised by the equivalent point in potentiometric titration at pH about 9 (Table 3). The ratio is near to the theoretical value (0.5 mol/mol) for $ZnCl_2 \cdot 2TBP$ complex, having the values of confidence limits equal to 0.43±0.03 and 0.46±0.02 for the constant mixing rates (120 rpm) in the aqueous and organic phase, respectively. A similar ratio (0.45 mol/mol) was obtained from equilibrium extraction data. Thus, the Lewis cell kinetic experiments give additional support for the extraction of the complex $ZnCl_2 \cdot 2TBP$, although zinc(II) is almost qualitatively present in the aqueous phase in the form of anion chlorocomplexes.

Generally, an increase of the mixing rate causes an increase of the fluxes. However, the character of this relationship is different for considered components and TBP concentrations.

Approximately constant fluxes for zinc(II), HCl and chloride ions present in extracted chlorocomplexes are obtained for high mixing rates, i.e. 170-200 rpm, suggesting the elimination of the diffusion resistance in the mixed phase upon the mass transfer of the total process. The plateau region increases for the transport of water and approximately constant fluxes are obtained for the mixing rates changed from 110 to 200 rpm. In the used Lewis cell it is impossible to increase the rate of mixing above 200 rpm because the interface becomes unstable and/or vertex is formed. As a result, a sharp increase of the flux calculated with assumption of the constant interfacial surface area is observed.

Table 3. Ratios of initial fluxes (R_{20}) of zinc(II) determined by atomic absorption and chlorides complexed with zinc(II) determined by potentiometric titration

TBP concentration	MR_W = 120 rpm		MR_O = 120 rpm	
	MR_O	R_{20}	MR_W	R_{20}
% vol	rpm	mole Zn(II)/mole Cl^-	rpm	mole Zn(II)/mole Cl^-
60	80	0.34	80	0.40
	120	0.39	120	0.39
	160	0.50	160	0.47
	200	0.48	200	0.46
80	80	0.51	80	0.47
	120	0.44	120	0.43
	160	0.45	160	0.50
	200	0.43	200	0.52
100	80	0.32	80	0.46
	120	0.43	120	0.43
	160	0.46	160	0.50
	200	0.46	200	0.46
Confidence limits (α=0,05)		0.43±0.03		0.46±0.02
		0.46±0.02*		

* - after rejection of ratios below 0.40

The observed effects are in a good agreement with the discussed extraction mechanism. The transfer of the zinc(II) complex can depend not only upon the both diffusion steps but also upon the chemical reaction giving an addition interfacial resistance. Contrary, the transfer of water can be considered as physical extraction. Moreover, the water transfer should be rather limited by the diffusion step in the organic phase. One can also expect a higher diffusion resistance in the organic phase in comparison to the aqueous phase for the transfer of bulky zinc(II) chlorocomplex. The hypothesis finds support in experimental data presented in Table 4. An increase of the mixing rate in the organic phase has always a stronger positive effect than MR increase in the aqueous phase.

Table 4. Effect of mixing rate from 80 to 200 rpm upon initial fluxes' ratios j_{200}/j_{80} at constant mixing rate in the second phase for Zn(II), complexed Cl^-, HCl and water

TBP concentration	MR_w or MR_w	Zn(II)	Cl^- in complex	HCl	H_2O
% vol	rpm	-	-	-	-
60	MR_w =120	4.71	3.33	3.00	2.67
	MR_o =120	2.25	1.99	2.45	1.65
80	MR_w =120	2.56	3.03	4.00	1.66
	MR_o =120	2.37	2.17	2.50	1.34
100	MR_w =120	4.88	3.40	4.00	3.34
	MR_o =120	3.35	3.33	4.00	2.91

REFERENCES

BART H. J. (2000), *Reactive Extraction*, Springer, Berlin.

CIERPISZEWSKI R., MIESIĄC I., REGEL-ROSOCKA M., SASTRE A. M., SZYMANOWSKI J. (2002), *Removal of Zinc(II) from Spent Hydrochloric Acid Solutions from Zinc Hot Galvanazing Plants,* Ind. Chem. Eng. Res., Vol. 41, pp 598-603.

KIRSCHLING P., NOWAK K.,MIESIĄC I., NITSH W., SZYMANOWSKI J. (2001), *Membrane Extraction-Stripping Process for Zinc(II) Recovery from HCl Solution,* Solvent Extr. Res. Dev.., Jpn, Vol. 8, pp. 135-143.

MORRIS D. C. F., SHORT E. L. (1962), *Zinc Chloride and Zinc Bromide Complexes. Part II. Solvent-Extraction Studies with Zinc – 65 as Tracer,* J. Chem. Soc., pp 2662-2671.

NAVRATIL J. M., Handbook *Science and Technology of Tributyl Phosphate,* CRC Press. Inc. Boca Raton, Florida 1987.

PLUCINSKI P., NITSCH W. (1992), *Two Phases Kinetics of the Solubilization in Reversed Micelles,* Solvent Extraction, pp. 847-852, Elsevier Science Publishers BV.

PUIGDOMENECH I., *Medusa,* Royal Institute of Technology, Sweden.

REGEL M., SASTRE A. M., SZYMANOWSKI J.(2001), *Recovery of Zinc(II) from HCl Spent Pickling Solutions by Solvent Extraction,* Environ. Sci. Technol., Vol. 35, pp. 630-635.

SCHÜGERL K., LARM A., GUDORF M. (1996), *Recovery of Zinc from Zinc Mordant Solutions of Dovetail Plants,* ISEC Melboune Australia, pp. 1543-1547.

SZYMANOWSKI J. (1993), *Hydroxyoximes and Copper Hydrometallurgy*, CRC Press, Boca Raton, USA.

TÓRZ M., ALEJSKI K., SZYMANOWSKI J.(2002), *Recovery of zinc(II) from model hydrochloric acid solutions in hollow fibre modules,* Phycochem. Prob. Mineral. Process., Vol. 36, pp 101-113.

ACKNOWLEDGEMENT

The work was supported by the NATO grant Science for Peace No. 972398 and Polish KBN grant No. 7 T09B 054 21.

Niemczewska J., Cierpiszewski R., Szymanowski J., *Ekstrakcja cynku(II) z modelowych roztworów HCl w komórce Lewisa,* Physicochemical Problems of Mineral Processing 37 (2003) 87-96 (w jęz. ang.).

W pracy badano ekstrakcję cynku(II) fosforanem tributylu (TBP) z modelowych roztworów HCl. Stosowano komórkę Lewisa z mieszaniem obu faz przy stabilnej granicy międzyfazowej. Stwierdzono, że eksperymenty w komórce Lewisa, chociaż dynamiczne w naturze, potwierdzają ekstrakcję chlorokompleksu $ZnCl_2 \cdot 2TBP$ z roztworów modelowych zawierających 5 M Cl^- i 0,55 M H^+. Początkowe strumienie Zn(II), HCl, Cl^-, chlorków zawartych w kompleksie cynku oraz wody zależą od stężenia TBP oraz szybkości mieszania faz. Etap dyfuzji w fazie organicznej daje większy opór od etapu dyfuzji w fazie wodnej. Fizyczne przeniesienie małych cząsteczek wody jest mniej wrażliwe na szybkość mieszania od przeniesienia przestrzennego dużego chlorokompleksu cynku(II).

Physicochemical Problems of Mineral Processing, 37 (2003) 97-105
Fizykochemiczne Problemy Mineralurgii, 37 (2003) 97-105

Maciej TORZ*, Krzysztof ALEJSKI*, Jan SZYMANOWSKI*

MODELLING OF ZINC(II) EXTRACTION FROM MODEL HYDROCHLORIC ACID SOLUTIONS IN HOLLOW FIBER MODULES

Received March 2003, reviewed, and accepted May 15, 2003

The recovery of zinc(II) from model hydrochloric acid solutions in hollow fiber modules was studied. It was found that zinc(II) could be removed from these model solutions by 80% and 40% tributyl phosphate in kerosene. A steady-state and an unsteady-state models of zinc(II) extraction in hollow fiber modules were formulated and experimentally verified. The proposed advanced mathematical model describes the system with high accuracy. The presented models of mass transfer in hollow fibre modules much better described the process of zinc(II) extraction than the model showed previously (Torz et al., 2002). The analysis of the experimental data and theoretical calculations showed that the kinetics of the mass transfer process was limited by the diffusion of species in the membrane's pores.

Key words: hollow fiber module, extraction, hot-dip galvanizing, modelling

INTRODUCTION

The problem of recovery of metal ions from waste waters has been increasingly important in recent years. Traditional technologies of solute recovery like ion-exchange, adsorption, precipitation or solvent extraction are usually low-efficient or generate secondary pollution problems. Among new methods proposed for removing of toxic ions liquid membranes have been particularly promising (De Gyves and de San Miguel, 1999). The methods comprise the advantages of solvent extraction (high selectivity and distribution coefficient) at the same time enabling to overcome typical extraction's drawbacks (loss of extractant due to dispersion, emulsification).

* Institute of Chemical Technology and Engineering, Poznan University of Technology, pl. M. Sklodowskiej-Curie 2, 60-956 Poznan, Poland, jan.szymanowski@put.poznan.pl

Solvent extraction as well as membrane techniques have been proposed for the recovery of zinc(II) from spent hydrochloric acid solutions (Regel et al., 2001, Kirschling et al., 2001). Such solutions, produced in hot-dip zinc galvanizing plants, generate a serious environmental and technological problems due to high toxicity of zinc and the presence of large amounts of iron in the waste stream. Recent studies has led to the selection of tributyl phosphate as a selective extractant enabling to remove zinc(II) ions. However, TBP is a weak extractant and therefore has to be used as a concentrated solution. Its using in high concentrations produces many potential problems like extractant's loss due to solubility in aqueous phase, formation of a second organic phase, emulsification. The problems could be avoided if the extractant was immobilised in a membrane. Since flat-sheet membranes offer low mass transfer area, recent interests have focused on hollow fiber modules. The modules usually operate in a two-phase mode with one phase passing through the lumen side and the other through the shell side. The interface is located in the membrane's pores. The efficiency of the extraction in the module depends on the distribution coefficient of solute and hydrodynamics. Several mathematical models of the batch process have been presented in literature (Escalante et al., 1998). In this paper a steady-state and an unsteady-state models of zinc(II) extraction in hollow fiber modules were formulated and verified.

EXPERIMENTAL

The composition of model aqueous phase was chosen to resemble spent pickling solutions from galvanizing plants (Kirschling et al., 2001): $[Zn^{2+}]$ = 20 g/dm^3, $[H^+]$ = 0.54 mol/dm^3, $[Cl^-]$ = 5 mol/dm^3. The model solution did not contain iron since the selected extractant, which was tributyl phosphate diluted with kerosene (40% and 80%), did not exhibit affinity towards Fe(II) ions extraction. All used inorganic chemicals (P.O.Ch. Gliwice) were of pure for analysis grade; TBP (Fluka or Sigma Aldrich) had the original purity of 97%.

Prior to membrane experiments zinc(II) distribution coefficient for different TBP concentrations (0-100%) was found in a dispersive system. Equal volumes of both phases were shaken in separatory funnels for two hours and equilibrium zinc(II) concentrations were determined.

Membrane extraction experiments were carried out in an one-module system (Fig. 1). The system was comprised of a hollow fibre module (Liqui-Cel 2.5×8″ X30 and X50 for 80% and 40% TBP, respectively), two tanks with ideal mixing (a magnetic stirrer was used when the flowrates were small), flowrate and pressure regulatory valves. A 0.5-bar overpressure was kept at the aqueous phase side to avoid the forming of dispersion. Geometrical parameters for the modules and tanks were collected in Table 1.

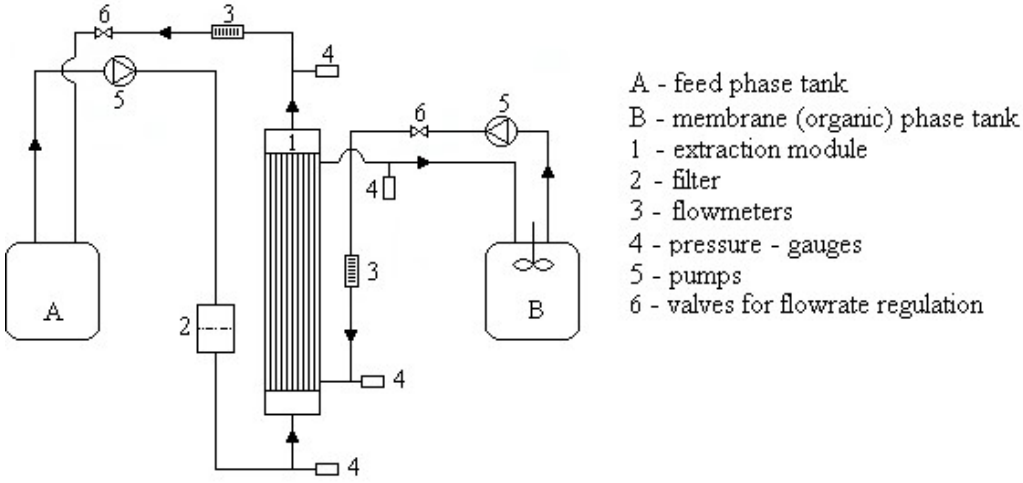

Fig. 1. Experimental extraction set-up

Table 1. Geometrical parameters for the Liqui-Cel Extra-Flow 2.5×8″ X30 and X50 modules and tanks

Parameter	80% TBP system with X30 modules	40% TBP system with X50 modules
Fibre internal diameter	240 μm	220 μm
Fibre wall thickness	30 μm	40 μm
Effective pores size	0.03 μm	0.04 μm
Porosity	40%	40%
Effective fibre length	15 cm	15 cm
Effective surface area	1.4 m^2	1.4 m^2
Tubeside volume	145 ml	145 ml
Shellside volume	195 ml	400 ml
O-rings material	Viton	Karlez
Feed phase tank volume	400 ml	1315 ml
Organic phase tank volume	200 ml	1200 ml

RESULTS

Preliminary equilibrium experiments showed that zinc(II) distribution coefficient for the fixed zinc(II) concentration (20 g/dm^3) and the volumetric ratio of phases 1:1 depended highly on the TBP concentration when TBP content was higher than 50% (Fig. 2). Below this value the extractant was practically saturated with zinc(II). Two

concentrations of tributyl phosphate were selected for membrane experiments: 40% ($m_{Zn} < 0.5$) and 80% ($m_{Zn} \approx 2$).

Typical zinc(II) concentration profile for membrane experiments was presented in Fig. 3. The solute concentration variation was strong in the first period of experiments since the driving force of the process was high. When the zinc(II) concentration approached its equilibrium value the curves reached plateau. Similar profiles were observed for HCl concentration in the 80% TBP system; the extraction of 1 mole of zinc(II) was accompanied by the transfer of ca. 1.2 mole of HCl. However, when the concentration of extractant was 40%, only negligible amount of HCl was transferred from the aqueous phase.

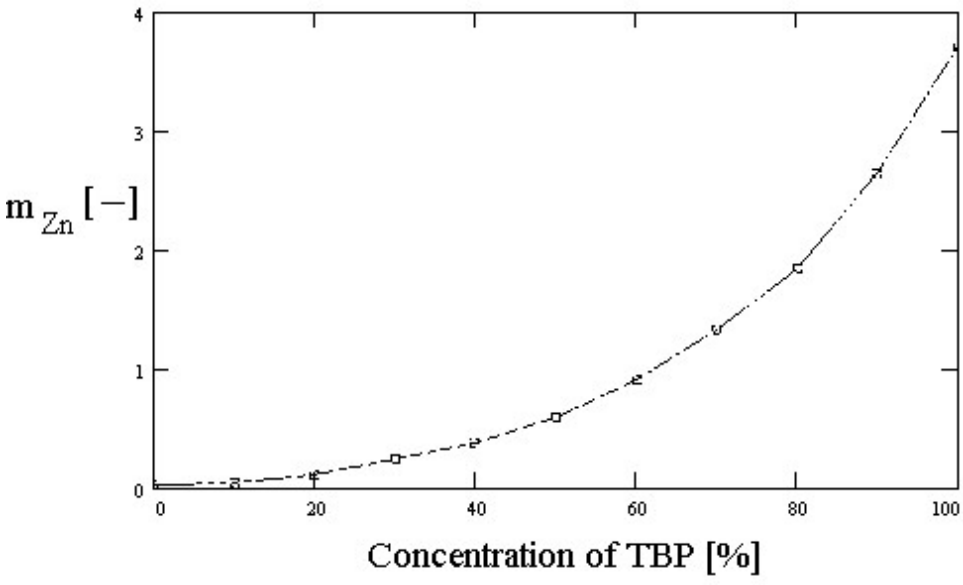

Fig. 2. The dependence of zinc(II) distribution coefficient on the volumetric concentration of TBP

MODELLING OF MASS TRANSFER

In our previous paper (Torz et al., 2002) a simplified mass transfer model based on a driving force defined as the difference between actual and final zinc(II) concentrations was presented. Despite satisfactory results of fitting to experimental data the model could be regarded as artificial because the definition of real driving force of the mass transfer process should take into account the difference between actual activities (usually approximated as concentrations) of the solute in both phases.

If at a fixed time the solute concentration could be considered constant in a given phase, which is true when the residence time in any part of the installation is short, then a general model equation could be expressed as:

$$-V_w \cdot \frac{dC_{Zn}}{dt} = K_1 \cdot \frac{A_m}{Q_w} \cdot \left(C_{Zn} - C_{Zn}^*\right) \tag{1}$$

where: A_m - mass transfer area, C_{zn} - actual zinc(II) concentration in the feed phase, K_1 - average mass transfer coefficient, Q_w - aqueous phase volumetric flowrate, V_w - volume of the aqueous phase, t - time.

Here, the driving force of mass transfer was defined as the difference of actual zinc(II) concentrations, because:

$$C_{Zn}^* = \frac{C_{Zn(o)}}{m_{Zn}} \tag{2}$$

where: $C_{zn(o)}$ - actual zinc(II) concentration in the organic phase, m_{Zn} - zinc(II) distribution coefficient.

To integrate the model equation an additional mass balance equation was introduced:

$$C_{Zn(o)} = \left(C_{Zn,i} - C_{Zn}\right) \cdot \frac{V_w}{V_o} \tag{3}$$

For the initial condition t = 0, $C_{zn} = C_{zn,i}$ the solution was:

$$C_{Zn}(t) = \frac{V \cdot C_{Zn,i}}{1+V} + \frac{C_{Zn,i}}{1+V} \cdot \exp\left[-K_1 \cdot \frac{A_m}{V_w} \cdot (1+V) \cdot t\right] \tag{4}$$

where $V = \dfrac{V_w}{V_o \cdot m_{Zn}}$.

Table 2. Mass transfer coefficients K_1 and K_2 in 40% TBP extraction system

$Q_w \times 10^3$ [m^3/min]	$Q_o \times 10^3$ [m^3/min]	$K_1 \times 10^7$ [m/s]	$K_2 \times 10^7$ [m/s]
1.7	2.0	1.0	1.0
1.9	2.0	1.0	1.0
3.3	2.0	1.1	1.1
4.5	2.0	1.1	1.0
4.8	2.0	1.1	1.1
5.6	2.0	1.1	1.1
3.8	0.7	0.9	0.9
3.8	0.3	0.9	0.9

The only parameter to be fitted was the average mass transfer coefficient K_1. Its values, calculated using the least square method, were collected in Tables 2 and 3. As shown in Fig. 3, the fitting of the model equation (4) to experimental data was satisfactory; no significant discrepancies were observed in the whole experimental region.

Table 3. Mass transfer coefficients K_1 in 80% TBP extraction system

$Q_w \times 10^3$ [m^3/min]	$Q_o \times 10^3$ [m^3/min]	$K_1 \times 10^7$ [m/s]
1.6	0.5	2.9
2.4	0.5	3.0
4.0	0.5	3.9
2.4	0.6	3.9
2.4	1.0	5.5
2.4	1.6	6.1

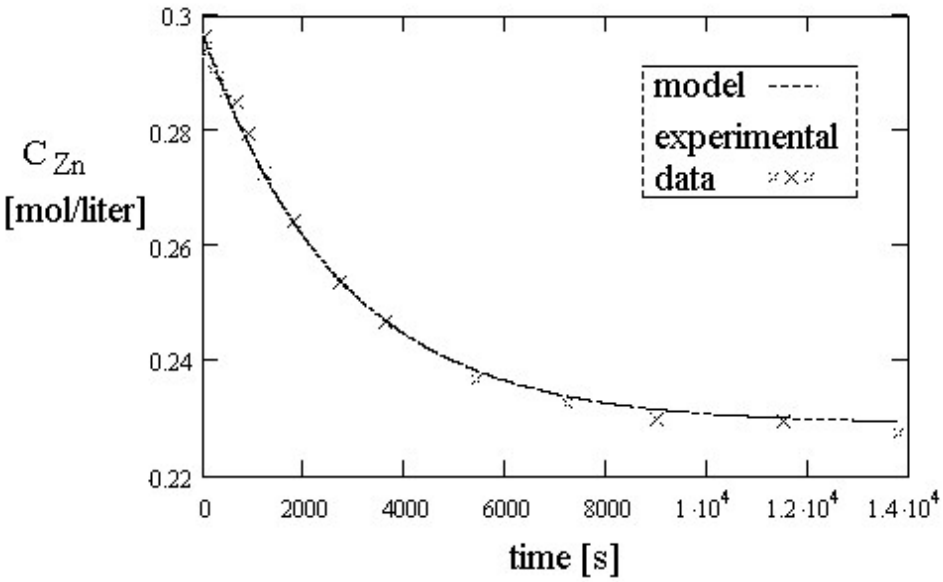

Fig. 3. Experimental concentration profile of zinc(II) in the feed phase and theoretical results from the fitting of model equation (4) (40% TBP, $Q_w = 1.9 \times 10^{-3}$ m^3/min, $Q_o = 2 \times 10^{-3}$ m^3/min)

As mentioned before, the model equation (1) was built on the presumption of negligible variations of zinc(II) concentration at a fixed time in a given phase. In such an approach no differentiation between module and tanks was introduced and thus the

mathematical description was simplified. To improve the precision of modelling, the solute concentration changes in tanks and modules were described by separate equations. The concentration of zinc(II) in the module varied both with time and with axial position. A mass balance resulted in the following equations for lumen side and shell side, respectively:

$$-\frac{V_w^m}{Q_w \cdot L}\cdot\frac{\partial C_{Zn}}{\partial t}-\frac{\partial C_{Zn}}{\partial t}=\frac{A_m}{Q_w \cdot L}\cdot K_2\cdot\left(C_{Zn}-C_{Zn}^*\right) \tag{5}$$

$$\frac{V_o^m}{Q_o \cdot L}\cdot\frac{\partial C_{Zn(o)}}{\partial t}-\frac{\partial C_{Zn(o)}}{\partial t}=\frac{A_m}{Q_o \cdot L}\cdot K_2\cdot\left(C_{Zn}-C_{Zn}^*\right) \tag{6}$$

where: L - effective length of the fibres, V^m - volume of the lumen side (subscript w) or shell side (subscript o).

If the assumption of an ideal mixing in the tanks was valid, then the concentration changes of zinc(II) in both reservoirs with time could be expressed by two differential equations:

$$\frac{dC_{Zn}}{dt}=\frac{Q_w}{V_w^t}\cdot\left[C_{Zn}(L)-C_{Zn}\right] \tag{7}$$

$$\frac{dC_{Zn(o)}}{dt}=\frac{Q_o}{V_o^t}\cdot\left[C_{Zn(o)}(L)-C_{Zn(o)}\right] \tag{8}$$

where: V^t - volumes of tanks.

A set of initial and boundary conditions was introduced:

$$t=0\, C_{Zn}=C_{Zn,i}\, C_{Zn(o)}=0$$

$$z=L\, C_{Zn}=C_{Zn}(L)\, C_{Zn(o)}=C_{Zn(o)}(L)$$

The model given by equations (5) - (8) constituted a set of differential and partial differential equations over two domains. To solve it, the implementation of a numerical method was necessary. The model was solved by means of gPROMS software. A special procedure made it possible to introduce discontinuities caused by the volume depletion due to sampling. The average mass transfer coefficients K_2 were calculated by the least square method. Their values for 40% TBP system were collected in table 2.

Exemplary results of fitting to experimental data were shown in Fig. 4. The fitting was better than the one obtained from the simplified model, and proved a superior precision of modelling. However, the comparison of average mass transfer coefficients K_1 and K_2 for 40% TBP system (Table 2) showed that the respective values were almost identical. Therefore, the complicated and time-consuming model was not solved for 80% TBP system. The simplified model proved to be sufficient for evaluating kinetics of the process.

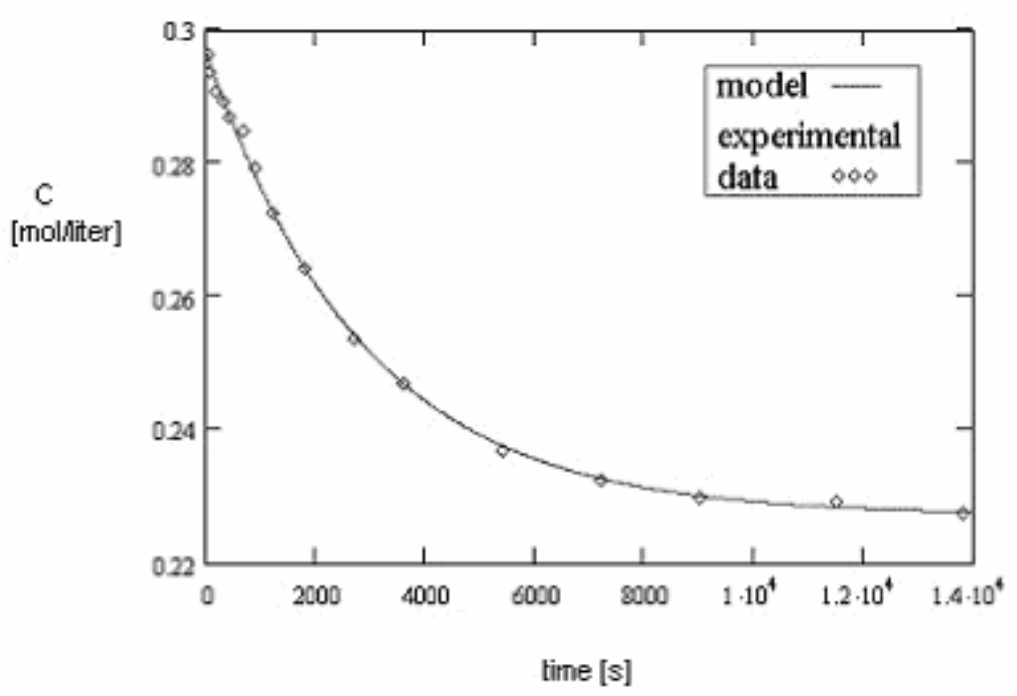

Fig. 4. Experimental concentration profile of zinc(II) in the feed phase and theoretical results from the fitting of model equations (5) - (8) (40% TBP, $Q_w = 1.9 \times 10^{-3}$ m^3/min, $Q_o = 2 \times 10^{-3}$ m^3/min)

DISCUSSION AND CONCLUSIONS

The presented models of mass transfer in hollow fibre modules much better described the process of zinc(II) extraction than the model showed previously (Torz et al., 2002) based on an artificial driving force. The model curves covered the experimental data well, although the only parameter to be fitted was mass transfer coefficient.

Although the precision of modelling was improved when the process was considered as an unsteady-state, with zinc(II) concentration varying both with time and axial position in the module, the mass transfer coefficients were almost identical to those obtained from the simplified model.

The variation of mass transfer coefficients with flowrates for 80% TBP system (Table 3) suggested that the concentration of extractant was high enough to enable an increase of zinc(II) flux with the increase of flowrates. The kinetics of the process was improved when either aqueous phase or organic phase flowrate was increased. However, the hydrodynamics on the shell side (organic) phase exerted stronger influence on the process kinetics within the investigated flowrates' range.

While the zinc(II) flux could be increased in the 80% TBP system, such phenomenon was not observed in the 40% TBP system. As shown in table 2, practically no variation of mass transfer coefficients with either flowrates occurred. The obtained flux of zinc(II) was maximal within the investigated range of flowrates. Therefore, it might be concluded that the kinetics of the mass transfer process was limited by the diffusion of species in the membrane's pores.

ACKNOWLEDGEMENT

The work was supported by the NATO grant Science for Peace No. 972398 and Polish KBN grant No. 7T09B05421.

REFERENCES

ESCALANTE H., ALLONSO A. I., ORTIZ I., IRABIEN A., 1998, *Modelling of Liquid-Liquid Non-dispersive Extraction Processes in Hollow Fiber Modules*, Liquid-Liquid Two Phase Flow and Transport Phenomena, Marn D. M. (Ed.), Begell House Inc., New York, pp. 155-164.

DE GYVES J., DE SAN MIGUEL E. R., 1999, *Metal Ions Separations by Supported Liquid Membranes*, Ind. Eng. Chem. Res., Vol. 38, pp. 2182-2202.

KIRSCHLING P., NOWAK K., MIESIAC I., NITSCH W., SZYMANOWSKI J., 2001, *Membrane Extraction-Stripping Process for Zinc(II) Recovery from HCl Solutions*, Solvent Extr. Dev., Jpn, Vol. 8, pp. 135-143.

REGEL M., SASTRE A. M., SZYMANOWSKI J., 2001, *Recovery of Zinc(II) from HCl Spent Pickling Solutions by Solvent Extraction*, Environ. Sci. Technol., Vol. 35, pp. 630-635.

TORZ M., ALEJSKI K., SZYMANOWSKI J., 2002, *Recovery of Zinc(II) from Model Hydrochloric Acid Solutions in Hollow Fiber Modules*, Physicochemical Problems of Mineral Processing, Vol. 36, pp. 101-113.

Torz M., Alejski K., Szymanowski **J.**, *Modelowanie ekstrakcji cynku(II) z modelowych roztworów kwasu solnego w modułach z włóknami kapilarnymi,* Physicochemical Problems of Mineral Processing, 37 (2003) 97-105 (w jęz. ang.).

W pracy przedstawiono wyniki badań ekstrakcji cynku(II) z modelowych roztworów kwasu solnego w modułach z włóknami kapilarnymi. Stwierdzono, że cynk(II) może być usuwany z badanych, modelowych roztworów przy pomocy zarówno 40%, jak i 80% roztworów fosforanu tributylu w nafcie. Sformułowano i eksperymentalnie zweryfikowano model matematyczny procesu uwzględniający pracę w stanie ustalonym, jak i nieustalonym. Zaproponowany złożony model matematyczny opisuje pracę modułu z dużą dokładnością. Rozpatrywany model transportu masy w modułach z włóknami kapilarnymi opisuje proces znacznie dokładniej niż model opracowany wcześniej (Tórz et al., 2002). Analiza wyników eksperymentalnych oraz obliczeń teoretycznych pokazuje, że kinetyka transportu masy jest limitowana dyfuzją w porach membrany.

Physicochemical Problems of Mineral Processing, 37 (2003) 107-114
Fizykochemiczne Problemy Mineralurgii, 37 (2003) 107-114

Željko KAMBEROVIĆ*, Miroslav SOKIĆ**, Marija KORAĆ*

ON THE PHYSICOCHEMICAL PROBLEMS OF AQUEOUS OXIDATION OF POLYMETALIC GOLD BEARING SULPHIDE ORE IN AN AUTOCLAVE

Received March 2003, reviewed, and accepted May 15, 2003

The paper presents a study on the physical and chemical changes of iron, copper and zinc sulphide minerals in process of pressure oxidation. Oxidation in autoclave is a pre-treatment unit operation for refractory sulphide ores and concentrates in order to valorisat gold, which is encapsuled mainly in pyrite matrix. Raw materials and solid residues are charasterisated. Basing on the results of chemical reactions and on shape of solids residue, we came to a conclusion concerning the mechanism of oxidation in autoclave. The results show that modelling of the process parameters of oxidation in autoclave can be used to predict efficiency of pre-treatment of sulphide refractory ores for valorisation of gold.*

Key words: polymetallic ore, gold, oxidation, oxygen, hydrometallurgy

INTRODUCTION

Today high-grade gold ores are almost entirely exploited, so that low grade ores and ores from which gold could not be easily extracted became the only source of precious metals (Maslenickii 1987, Zelikman 1983, Habaschi 1998, Maslenickii 1969, Sinadinovic 1998).

Gold could not be extracted from low-grade ores with satisfactory degree of extraction, therefor it is known as refractory gold. The term “refractory” applies to ores, which do not yield a sufficient gold and silver recovery if processed through conventional cyanidation. Sulphide ores where gold is encapsuled in a sulphide matrix

*Faculty of Technology & Metallurgy, Karnegijeva 4, 11120 Belgrade, P. O. Box 3505, Serbia and Montenegro, tel: +381 11 3370475, fax:+381 11 3370387, E-mail: kamber@elab.tmf.bg.ac.yu
**Institute for Technology of Nuclear and Other Mineral Raw Materials, Belgrade, Serbia and Montenegro

as of submicron size particles [Maslenickii 1969, Sinadinovic 1998, Schweigart 1986, Jha 1987, Hausen 1989,Kontopoulos 1988, Vracar 2001) have turned out to be the hardest to process. Gold cannot be liberated by fine grinding, so that the efficiency of cyanide leaching process is low (Jha 1987, Hausen 1989,Kontopoulos 1988, Vracar 2001).

The main task of extractive metallurgy of gold is to find a suitable pre-treatment for refractory ores, which could provide high extraction of gold.

There are several pre-treatment procesdures, which could be used to process the refractory gold ores. But from economic, metallurgical and ecological point of view the prospectus pre-treatment of refractory gold ores its pressure of oxidation in autoclaves (Kontopoulos 1988, Vracar 2001, Papangelakis 1990, Kontopoulos 1990, Mason 1985).

All processes, which involve hydrometallurgical treatment of raw materials are suitable for processing of not just oxides, but also sulphide ores and concentrates.

Table 1. The major reaction of oxidation of Fe, Cu and Zn sulphides and Gibbs energies at 298 and 473 K under pressure 101.325 kPa.

	Reaction	$-\Delta G^{\theta}$ (298 K)	$-\Delta G^{\theta}$ (473 K)
Fe 1	$FeS_{2(s)} + H_2O_{(l)} + 7/2\ O_{2(g)} = FeSO_{4(aq)} + H_2SO_{4(aq)}$	1117.6	1019.6
Fe 2	$FeS_{2(s)} + 2\ O_{2(g)} = FeSO_{4(aq)} + S^{o}_{(s)}$	664.77	611.44
Fe 3	$2\ S^{o}_{(s)} + 3\ O_{2(g)} + 2\ H_2O_{(l)} = 2\ H_2SO_{4(aq)}$	905.66	816.42
Fe 4	$2\ FeSO_{4(aq)} + H_2SO_{4(aq)} + 1/2\ O_{2(g)} = Fe_2(SO_4)_{3(aq)} + H_2O_{(l)}$	160.19	137.83
Fe 5	$FeS_{(s)} + 2\ O_{2(g)} = FeSO_{4(aq)}$	724.98	663.08
Fe 6	$Fe_2(SO_4)_{3(aq)} + 3\ H_2O_{(l)} = Fe_2O_{3(s)} + 3\ H_2SO_{4(aq)}$	-160.8	-152.10
Fe 7	$3Fe_2(SO_4)_{3(aq)} + 12\ H_2O_{(l)} = 2Fe_3(SO_4)_2(OH)_5 \times 2H_2O_{(s)} + 5H_2SO_{4(aq)}$	1214.6	1302.1
Fe 8	$2\ FeSO_{4(aq)} + 1/2\ O_{2(g)} + 5\ H_2O_{(l)} = 2\ Fe(OH)_{3(s)} + 2\ H_2SO_{4(aq)}$	-44.69	-78.87
Fe 9	$Fe_2(SO_4)_{3(aq)} + n\ (H_2O)_{(l)} = Fe_2O_3 \times (n-3)\ H_2O_{(s)} + 3\ H_2SO_{4(aq)}$, n=4	-165.7	-164.29
Fe 10	$FeS_{2(s)} + CuSO_{4(aq)} = CuS_{(s)} + FeSO_{4(aq)} + S^{o}_{(s)}$	52.91	63.85
Cu 1	$CuFeS_{2(s)} + H_2SO_{4(aq)} + 1¼O_{2(g)} + ½H_2O_{(l)} = CuSO_{4(aq)} + Fe(OH)_{3(s)} + 2S^{o}_{(s)}$	367.16	314.14
Cu 2	$CuFeS_{2(s)} + H_2SO_{4(aq)} + 1/2\ O_{2(g)} = CuS_{(s)} + FeSO_{4(aq)} + S^{o}_{(s)} + H_2O_{(l)}$	214.19	230.49
Cu 3	$Cu_5FeS_{4(s)} + 2\ H_2SO_{4(aq)} + O_{2(g)} = 4\ CuS_{(s)} + CuSO_{4(aq)} + FeSO_{4(aq)} + 2H_2O_{(l)}$	383.25	339.67
Cu 4	$Cu_5FeS_{4(s)} + H_2SO_{4(aq)} + 1/2\ O_{2(g)} = Cu_2S_{(s)} + 3\ CuS_{(s)} + FeSO_{4(aq)} + H_2O_{(l)}$	212.54	194.19
Cu 5	$CuS_{(s)} + H_2SO_{4(aq)} + 1/2\ O_{2(g)} = CuSO_{4(aq)} + H_2O_{(l)} + S^{o}_{(s)}$	159.02	139.38
Cu 6	$Cu_2S_{(s)} + 5/2\ O_{2(g)} + H_2SO_{4(aq)} = 2\ CuSO_{4(aq)} + H_2O_{(l)}$	782.56	693.07
Cu 7	$Cu_2S_{(s)} + O_{2(g)} + 2\ H_2SO_{4(aq)} = 2\ CuSO_{4(aq)} + S^{o}_{(s)} + 2H_2O_{(l)}$	329.73	284.86
Cu 8	$Cu_2S_{(s)} + 1/2\ O_{2(g)} + H_2SO_{4(aq)} = CuSO_{4(aq)} + CuS_{(s)} + H_2O_{(l)}$	170.71	145.48
Cu 9	$CuS_{(s)} + 2O_{2(g)} = CuSO_{4(aq)}$	611.85	547.59
Cu 10	$Cu_2S_{(s)} + 2\ Fe_2(SO_4)_{3(aq)} = 2\ CuSO_{4(aq)} + 4\ FeSO_{4(aq)} + S^{o}_{(s)}$	9.35	9.19
Zn 1	$ZnS_{(s)} + H_2SO_{4(aq)} = ZnSO_{4(aq)} + H_2S_{(g)}$	16.49	31.76
Zn 2	$ZnS_{(s)} + H_2SO_{4(aq)} + ½\ O_{2(g)} = ZnSO_{4(aq)} + S^{o}_{(s)} + H_2O_{(l)}$	220.27	202.20
Zn 3	$ZnS_{(s)} + 2\ O_{2(g)} + H^{+}_{(aq)} = Zn^{2+}_{(aq)} + HSO^{-}_{4\ (aq)}$	705.96	629.69
Zn 4	$H_2S_{(g)} + ½\ O_{2(g)} = S^{o}_{(s)} + H_2O_{(l)}$	203.78	170.44
Pb 1	$PbS_{(s)} + H_2SO_{4(aq)} + ½\ O_{2(g)} = PbSO_{4(s)} + S^{o}_{(s)} + H_2O_{(l)}$	263.67	246.43
Pb 2	$PbS_{(s)} + H_2SO_{4(aq)} = PbSO_{4(s)} + H_2S_{(g)}$	59.88	75.99

The major reactions of the oxidation of relevant sulphides, are shown in Table 1. (Maslenickii 1987, Zelikman 1983, Habaschi 1998, Maslenickii 1969, Vracar 2001, Vracar 1975, Vracar 1977, Vracar 1987, Vracar 1997, Long 1999) and Gibbs energies at 298 and 473 K. Gibbs energies were calculated using the HSC Chemistry software.

The values of $\Delta_r G^{\theta}$ indicate that there is a thermodynamic possibility of oxidation of the above sulphides into elementary sulphur and sulphates within temperature range 298–473K.

HYDROMETALLURGICAL OXIDATION OF SULPHIDE RAW MATERIALS IN AUTOCLAVES

Application of hydrometallurgical processes in extractive metallurgy dates from middle of last century. In the beginning these processes were used for extraction of Ni, Co and Cu from sulphide ores. From then there's been numerous investigations in this field.

Pioneer in using of autoclave technology in extractive metallurgy of sulphide ores is Canadian company Sherritt Inc. (Habaschi 1998, Maslenickii 1969), which started to use this technology for extraction of nickel. Since then this proces was developed to process of Zn concentrates and complex gold ores. Presently, the whole group of autoclave technologies is available in Canadian company Dynatec Corporation, Fort Saskatchewan, Alberta.

Raw materials used in our experiments are domestic sulphide concentrates:

- Pyrite concentrate, carrier of precious metals, which is product of flotation of polymineral raw materials (K1),
- FeS_2-Cu-Zn-Pb polymetallic collective flotation concentrate, with refractory precious metals (K2),
- Pb-Zn-Cu-FeS_2 polymetallic collective flotation concentrate (K3).

Different analytical and instrumental methods were used to characterizate these concentrates: volumetric and gravimetric analysis, atomic adsorption spectroscopy (AAS), SEM and EDS analysis with quantitive analysis of size and shape of particles, RDA analysis, AES-ICP, differential thermal analysis (DTA), and thermo gravimetric analysis (DTA).

Analysis show that all three concentrates are mostly made of iron and sulphur. They also contain small amounts of copper, zinc, lead and arsenic. Contents of other elements are not significant. (Table 2). First two concentrates contain small amounts of gold and silver, while in concentrate K3 their content is considerable.

Table 2. Chemical analysis of input concentrates (% w/w)

	Fe	S	Cu	Zn	Pb	As	Au, g/t	Ag, g/t
K1	45.96	48.00	0.60	-	-	0.70	49.5	27.5
K2	19.46	30.55	6.50	6.375	1.8	0.91	24.2	182.7
K3	23.18	31.29	2.00	9.16	10.40	0.32	598.7	485.8

Granulometric analysis of concentrates gives Gauss type distribution curve with maximum at particle size of 20-30 μm and frequency of appearance of 60%.

From polished surfaces of concentrates samples one can see that basies of them is made of pyrite. In first two concentrates visible gold is not detected, therefore that one can conclude that gold is completely associated in pyrite, so that it's accessibility to common leaching solutions does not exist. In concentrate K2 gold and copper, zinc and lead minerals are captured in pyrite, therefore a secondary refractoriness appears. From all of above it comes that pre-treatment is necessary to extract precious metals from this kind of ores. On the other hand, in concentrate K3 visible gold particles (10-15μm) are detected, so that the K3 concentrate has little refractoriness comparing to the first two concentrates and gold could be extracted from it with common leaching solutions without any pre-treatment.

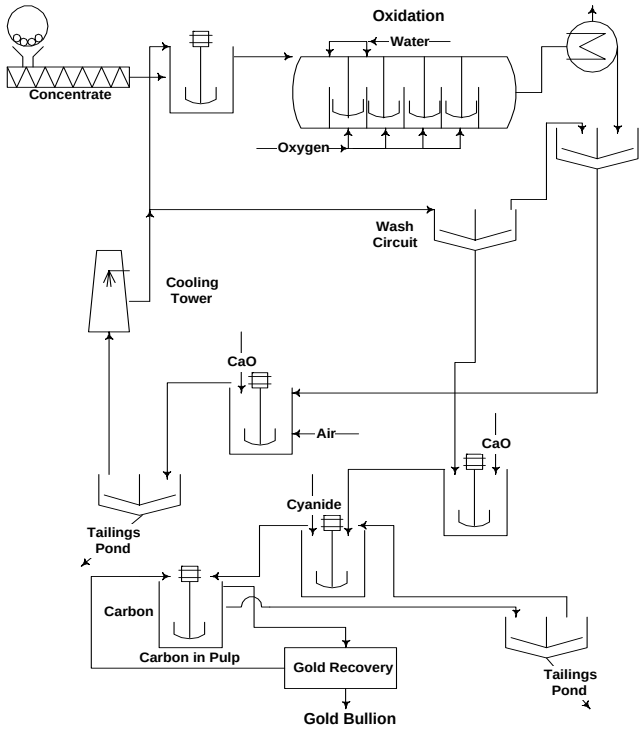

Fig. 1. Diagram of autoclave oxidation with operation stream

Process of autoclave oxidation is shown in Figure 1. with all process parameters. Pressure oxidation is conducted at 200°C at oxygen pressure of 2MPa, and with constant stirring with propeller mixer (200 rpm). Experimental research (Vracar 2001) has shown that the oxidation is predominantly influenced by temperature and time, so that high degree of transfer of most metals (except lead) into solutions can be achieved

by applying the partial oxygen pressure of 2 MPa, S/L ratio of 80 g/dm^3 with technically and technologically justified particle size as well as adequate choice of temperature and time. The residue after the oxidation can be successfully processed by pyrometallurgicall or hydrometallurgical methods in order to obtain precious metals. After completing of pressure oxidation the final solution contains Fe^{2+} and Fe^{3+} and copper and zinc (Cu^{2+}, Zn^{2+}). This solution can be used as a feed for extraction of copper and zinc, but valorisation of iron is not economicly justifiable. Solid residue consist of iron, lead, gang materials and precious metals, as well.

Solid residues contens gold and gangue materials, lead transfers to solid as insoluble $PbSO_4$. Silver partially reacts making sulphates, goes into solid. Solid residue of autoclave oxidation contains precious metals and lead, which are released from pyrite matrix and become accessible to leaching solutions.

A microphotographs (figure 2.) of solid residues of concentrate K1 reveals irregularly shaped particles of several μm. There is also spekularite- iron oxide in sulphate basis. The needle shaped phase could be associated with gangue minerals, aluminosilicate contender of size of several μm. Spekularite is randomly disturbed throughout structure.

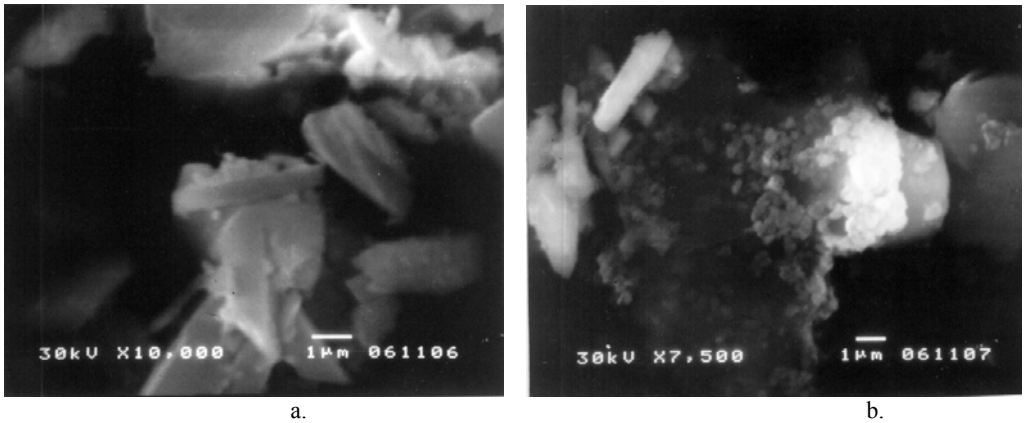

a. b.

Fig. 2. SEM microphotographs solid residues of concentrate K1, a. spekularit in sulphide-iron basis, 10000×, b. spekularit with gangue minerals magnified 7500×

Solid residue of concentrate K2 is characterized with highly developed surface of sulphur compounds of iron and lead. Besides particles, gangue minerals (SiO_2) could be detected in this microphotographs (figure 3.). Sulphur compounds of barium and iron are in feather shaped particles ~μm. This shape of particles have tendency to agglomerate. Feather shaped particles can capture gold, so this shape is not suitable.

In solids residue of concentrate K3 particles are usually like so finely grained agglomerated crystals. There are noticeable needle shaped crystals of spekularit, same as in residue of concentrate K1.

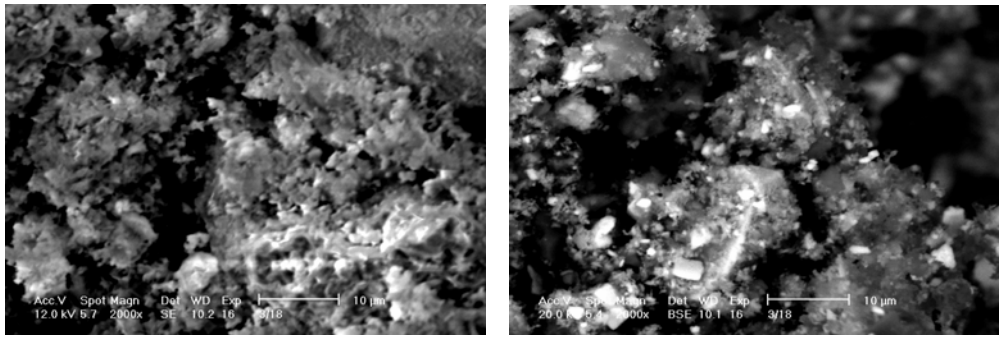

Fig. 3. SEM microphotographs solid residues of concentrate K2 III/18, a. magnified 200×, b. sulphur-salts with SiO_2, magnified 500×

a. b.

Fig. 4. SEM microphotographs solid residues of concentrate K3, a. sulphur-salts of iron and lead with SiO_2 in center, magnified 2000×, b. sulphur-salts of iron, magnified 3500×

Structural and morphological characteristic of solid residues for autoclave oxidation of studied concentrates are suitable for leaching with tiourea. All residues have a fine-grained structure. Effect is predominant of particle shape on the rate of solid-liquid separation velocity.

DISCUSSION

Pressure oxidation of sulphide ores and concentrates leads to new method of determination of level of refractoriness, and to applicability of this processes to different ores and economic feasibility of processes.

The dependence of recovery of refractory gold on oxidation of sulphide sulphur is shown at figure 5, (Berezowski 1991). This diagram represent dependences for some famous pyrite and arsenic-pyrite concentrates like as Porgera, Olympius, Campbell etc, together with concentrates used in this study K1, K2 and K3. For concentrates,

which have, even layout of gold in their structure the dependence is a straight line. This concentrates, like Porgera request high grade of oxidation of sulphide sulphur. On the other hand in Olympius concentrate gold is mostly associated in arsenic-pyrite, which can explain high rate of reaction and better reactibility.

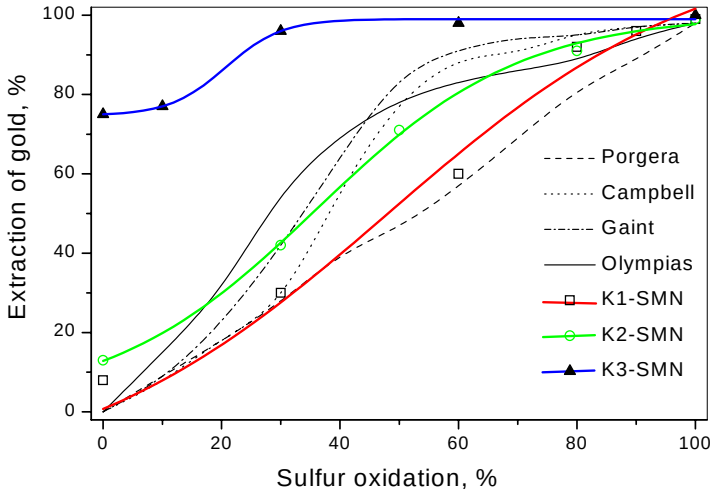

Figure 5. Extraction of gold in dependence of oxidation of sulphide sulphur

CONCLUSION

From charasteristics of concentrates, processes, chemical reactions and structual-morfological changes of raw materials during pressure oxidation the mechanism of oxidation can be identified. Experimental results on chemical reactions and shape of solid grains remained after oxidation, modelling of the process parameters can be used to design efficient process of pre-treatment of sulphide refractory ores for valorisation of gold. By treating domestic polymetallic ores (gold is associated with sulphides of iron and copper), we can suggest the technology with great significant importance in both economic and ecological sense. Pressure oxidation and treatment of leaching by extraction of copper and zinc, as well as extraction of lead and precious metals from solid residue represents complex way of exploitation of useful components from concentrates and also reducing of global environment pollution.

REFERENCES

BEREZOWSKY, R.M.G.S., COLINS, M.J., KERFOOT, D.G.E., TORRES, N., JOM, 2 (1991): 9.

HABASHI F., *Pressure hydrometallurgy: Past, present and future*, Proceedings of the 3rd international conference oh hydrometallurgy at Kunming, China, November 1998, 27-34.

HAUSEN, D.M., JOM, (4) (1989): 45.

HENDRIKS, L.P., *The recovery of gold from refractory materials at Consolidated Murchison using low alkalinity pressure cyanidation*, Proc. Randol Gold Forum 88, Randol Inter., Golden, (1988): pp. 227-232.

JHA, M.C., *Refractoriness of certain gold ores to cyanidation: probable causes and possible solutions*, Mineral Processing and Extractive Metallurgy Review, (2) (1987): 331.

KONTOPOULOS, A., STEFANAKIS, M., *Process Options for Refractory Sulfide Gold Ores: Technical, Environmental and Economic Aspects*., Proc. EPD Congress '90., TMS, ed. D.R.Gaskell., (1990): pp. 393-412.

KONTOPOULOS, A., STEFANAKIS, M., *Process selection for the Olympias refractory gold concentrate*., Proc. Precious Metals 89*,* ed. M.C.Jha, S.D.Hill. TMS, Warrendale, PA (1988): pp. 179-209.

LONG, H., DIXON D.G., *A kinetic study on pressure oxidation of pyrite at high temperature*, Proc.128th Annual TMS Meeting, Proceedings, San Diego, California, (1999): p. 66.

MASLENICKII, I.N., CHUGAEV, L.V., BORBAT, V.B., NIKITIN, M.B., STRIZKO, L.S., *Precious Metals Metallurgy*, Metallurgii, Moscow (1987): pp 25-161.

MASLENICKII, I.N., DOLIVO-DOBROVOLSKII, V.V., DOBROHOTOV, G.N., SOBOLJ, S.I., CHUGAEV, L.V., BELIKOV, V.V., *Autoklavnii processi v cvetnoj metallurgii*, Metallurgii, Moscow (1969): pp 1-150.

MASON, P.G., O'KANE, P.T., *Refractory gold-process options*., Proc. at the 24th Ann. Conf. of Metall., Vancouver, B.C., (1985): (from ref.11)

PAPANGELAKIS, V.G., DEMOPOULOS, G.P., *Gold extraction from refractory concentrates by autogenous pressure oxidation*., Proc. of the 14th Inter. Prec. Metals Conf. and Exhi. San Diego, California, ed. D.A.Corrigan, (1990): pp. 61-73.

PIETSCH, H.B., TÜRKE, W.M., RATHJE, G.H., Ertzmetall, 36 (1983): 261.

SCHWEIGART, H., LIEBENBERG, W.R., *Mineralogy and chemical behaviour of some refractory gold ores from the Barberton Mountain land*., NIM Report No 8 (1986): pp. 426-431.

SINADINOVIC, D., KAMBEROVIC, Z., *Oxidative autoclaving of refractory gold ore Coka Marin*., Proc. 1st International Conference of the Chem. Soc. of the South-East Eur. Countries, Greece, Vol 1, (1998): OR42.

VRAČAR R., SINADINOVIĆ D., KAMBEROVIĆ Ž., *On the aqueous oxidation of polymetallic Cu-Zn-Pb gold-bearing sulphide ore in an autoclave*, Bulletin, vol 94, june 2001, 123-128

VRACAR, R., CEROVIC, K., Hydrometallurgy, 44 (1997): 113.

VRACAR, R., Erzmetall, 28 (6) (1975): 271.

VRACAR, R., J. Prikladnii Himii, 7 (1987): 1458.

VRACAR, R., J. Ser. Chem. Soc., 8 (1977): 613.

ZELIKMAN, A.N., VOLDMAN, G.M., BELYEVSKA, L.V., *Theory of Hydrometallurgical Process*., Metallurgii, Moscow (1983): pp 120-261.

Kamberović Ž., Sokić M., Korać M., *Fizykochemiczne problemy utleniania polimetalicznej rudy złotonośnej w autoklawie,* Physicochemical Problems of Mineral Processing, 37 (2003) 107-114 (w jęz. ang.)

W pracy zostały przedstawione fizyczne i chemiczne zmiany jakim ulegają minerały siarczkowe żelaza, miedzi i cynku w trakcie ciśnieniowego utleniania. Utlenianie w autoklawie jest operacją przygotowawczą w przerobie trudnych do ługowania siarczkowych rud metali oraz koncentratów. Operacja ta jest konieczna dla „uwolnienia" złota, które zamknięte jest w matrycy z pirytu. Surowa ruda oraz półprodukty końcowe zostały scharakteryzowane. Na podstawie wyników reakcji chemicznych oraz kształtu otrzymanych produktów, można było wyciągnąć wnioski dotyczące mechanizmu procesu utleniania siarczków w autoklawie. Otrzymane wyniki pokazują, że modelowe parametry procesu utleniania w autoklawie, mogą zostać wykorzystane do przewidzenia korzyści uzyskiwanych z procesu przygotowania rud siarczkowych pod kątem ekstrakcji złota.

Physicochemical Problems of Mineral Processing, 37 (2003) 115-122
Fizykochemiczne Problemy Mineralurgii, 37 (2003) 115-122

Gulhan ÖZBAYOĞLU*, Kejhanak Rowshan TABARI*

BRIQUETTING OF IRAN-ANGOURAN SMITHSONITE FINES

Received March 2003, reviewed, and accepted May 15, 2003

In conventional zinc carbonate ore processing, crushed ore is charged to Waelz furnace for the recovery of zinc through volatilization. When the feed size is fine which does not meet the requirements, briquetting is employed to convert the fines and dusts into chargable lumps.

The aim of this research was to determine the possibility of briquetting of Iran-Angouran zinc carbonate fines produced in Dandi concentration plant.

During the briquetting test, the effects of pressure, type and amount of binder, moisture, temperature, and fineness of the feed were determined. The quality of briquette was controlled in terms of the compressive strength, abrasion index and resistance to weathering.

The optimum briquetting result was obtained when the zinc carbonate fines was mixed with 6% water, 5% molasses and 1.5% lime at a briquetting pressure of 200 kg/cm^2 and drying at 105°C for 2 hours.

Keywords:Waelz furnace, zinc carbonate, briquetting, molasse

INTRODUCTION

Agglomeration which can be defined as any method of size enlargement of particle consolidation has become of fundamental importance in the utilization of fine material originated by the mineral industry due to their difficulty in handling, transportation and direct utilization. Iron oxide, magnesium oxide, lime, bauxite and alumina fines, phosphate and fluorspar concentrates are agglomerated and returned to the process. Recovery of dust materials increases the efficiency of the pyrometallurgical process and decreases environmental and disposal problems.

There are three methods of agglomeration of powder materials: pelletizing, briquetting and sintering. It can also be classified as agitation, compaction and heat treatment on the basis of agglomeration forces.

* Middle East Technical University, Dept. of Mining Engineering, 06531Ankara-Turkey, gulhano@metu.ed.tr

All types of balling devices (e.g. pelletizers) are agglomerators by agitation. Briquetting, compacting, tableting and extrusion are examples of agglomeration by compaction. Agglomeration by heat treatment includes sintering and nodulizing.

Briquetting is one of the most widely used methods of agglomeration over many decades. It is defined as the formation of pillow, almond, cylindrical or other shaped pieces from finely divided solids by the application of external pressure. Roll type presses are most frequently employed. A number of physical and chemical mechanisms serve to bind solid particles together when they are compacted into a briquette. This is accomplished by matching moulds in the surface of the rollers whereby each essentially represents one half of the briquette volume. During this process the bulk density of the feed is increased. Suitable binders may assist in the formation of briquette and the development of their strength. Water often acts as a binder as well as providing lubrication. Mixing the fine solids with a higher content of a tacky viscous fluid provides a matrix which cements the particles when they are pressed together. Pitches, spent sulfite liquor, mixtures of molasses and lime, and other sticky fluids act as matrix binders.

Extensive research was conducted for the agglomeration of iron, coal, chromite etc, but research performed on the agglomeration of zinc oxide and zinc carbonate was limited (Planka, 1971, Göksel, 1980, Chaptykov, 1987, Lugscheider, 1989, Özbayoğlu, 1993).

The aim of this research was to determine the possibility of briquetting of Iran-Angouran zinc carbonate fines for the preparation of feed to Waelz furnace.

MATERIAL AND METHOD

To conduct briquetting tests, Angouran (İran) zinc carbonate fines were tested. The chemical analysis and particle size distribution of the representative sample are shown in Table 1 and 2.

Table 1. Chemical analysis of smithsonite fines

Element	%	Element or Comp.	%
Zn	27.72	Cl	0.070
Pb	5.06	Co	0.026
Cd	0.24	Mn	0.044
Fe	3.20	Bi	<0.0005
Cu	0.014	Ag	<0.0053
Ni	0.078	Al_2O_3	1.55
As	0.77	SiO_2	26.0
Sb	0.50	MgO	0.38

Table 2. Screen analysis of the sample

Screen Aperture (microns)	Wt, %	Cum.Wt.% Retained	Cum.Wt,% Passing
+417	2.30	2.30	97.70
+295	2.65	4.95	95.05
+208	2.76	7.71	92.29
+147	13.14	20.85	79.15
+104	15.35	36.20	63.80
+74	12.69	48.89	51.11
+53	12.54	61.43	38.57
+45	5.55	66.98	33.02
-45	33.02	-	-

In briquetting tests, a cylindrical shape, 39 mm in diameter and 39 mm in length steel mold was used. The test sample was premixed with predetermined amount of water and binder. The pressure was applied by a Tinius Olsen Standart Super L type hydraulic press with 200 tons capacity. The briquettes were dried in an oven at 105°C. The quality of the briquets was controlled by means of compressive strength test, tumbling test and weathering test on oven dried briquettes.

The compressive strength test which assess the ability to withstand the pressure of the burden in the storage is performed by compressing the briquette between two movable steel plates from the oblique surface. The crushing load in radial direction is used to express the tensile strength of a cyclindrical briquet according to the equation: $\sigma = \frac{2P}{DL}$ where σ=tensile strength, kg/cm^2, P=crushing load, (kg), D:diameter of specimen (mm), L=length of specimen (mm). Since D and L are constant, the crushing load may be used instead of tensile strength.

Tumbling (abrasion) test was performed to find out the resistance of briquettes to abrasion action during transportation and loading. A drum, with 20 cm in diameter and 30 cm in length, containing four lifters in 2 cm width was used for the determination of abrasion index. A 500 g sample was placed into the drum and rotated for 2 min at 30 rpm. The weight percentage of the dust finer than 850 μm was expressed as abrasion index.

The durability of the agglomerate at the outdoor stockpile was determined by weathering test. When the briquette was put into water, if it kept its original form at least for two hours, it was accepted as water resistant.

EXPERIMENTAL RESULTS AND DISCUSSIONS

In briquetting tests, the effects of pressure, type and amount of binder, moisture content, drying temperature and fineness of the sample on briquette quality were investigated.

THE CHOICE OF BINDER

The preliminary tests showed that the briquettes produced by the addition only water had no compressive strength. In order to improve the strength of the briquettes, various binders have been added into the briquet charge; their results are shown in Table 3.

Table 3. Effect of different binders on briquetting

Binder %	Crushing load(kg/briquet)
-	144
Molasses	434
Dextrin	561
Starch	209
Bentonite	143
Lime	141
Black cement	245
Na_2CO_3	193
NaCl	218
Na_2SiO_3	140
Polyvinyl acetate	297
Peridur XC3	266
CMC	141

Briquetting conditions: Binder: 5%, Moisture: 6%, Pressure: 200 kg/cm^2, Drying temp.: 105°C, Particle size: original sample

As seen in Table 3, the briquets produced by the addition of dextrin and molasses showed higher compressive strength than the others; molasses was chosen as the binder, as it is much cheaper.

EFFECT OF AMOUNT OF BINDERS

Molasses has been added in various amounts into the briquette charges. The addition of molasses above 1,5 % was sufficient for the production of briquettes with compressive strengths above 100 kg. It was found that the increase in the binder amount increased the strength of the briquette.

Although, the briquette produced by the addition of molasses alone were sufficiently strong, their resistance to water was nil when they were brought in contact with it. In order to improve the resistance of briquettes to weathering, hydrated lime was added besides molasses. Table 4 shows the results of hydrated lime addition.

Table 4. Effect of amount of hydrated lime with molasses

Amount of Lime (%)	Crushing Load (kg/briquette)	Water Resistance
-	460	20 % disintegration in water
0,5	396	20 % disintegration in water
1,0	376	15 % disintegration in water
1,5	388	Water resistant
2,0	384	Water resistant

Briquetting conditions: Binder: 5% molasses, Moisture: 6 %,
Pressure: 200 kg/cm^2, Drying temp.: 105°C,
Particle size: original sample, briquettes were kept in water for 2 hours

As seen, hydrated lime addition improved the water resistant property of the briquettes when it was added above 1.5 % by wt. However, the compressive strength of the briquettes decreased by the hydrated lime addition.

There are two different proposals about the hardening mechanism of the briquets. One is that the hydrated lime added as binder react with carbon dioxide in air, producing calcium carbonate and water. Here, the molasses act as a catalyst and the calcium carbonate gives the briquette the required strength. Another theory is becoming more popular that the molasses taking part in the reaction to form calcium sucrates.

In order to find out the amount of molasses used in combination with hydrated lime, a series of tests have been performed by the use of molasses between 1 to 6 % by wt. As shown in Table 5, increasing the amount of molasses increased the crushing strength. By taking into consideration the water resistant properties of the briquettes, 5 % molasses addition was found sufficient for the production of water resistant briquettes.

Table 5. Effect of amount of the molasses used in briquetting

Amount of Lime (%)	Crushing Load (kg/brique tte)	Water Resistance
1.0	127	No resistance to water
2.0	163	No resistance to water
3.0	237	No resistance to water
4.0	287	15 % disintegration in water
5.0	366	Water resistant
6.0	514	Water resistant

EFFECT OF PRESSURE

At optimum molasses+hydrated lime addition, the briquettes were produced by applying different pressures whose results are shown in Table 6.

Table 6. Effect of pressure on briquette

Briquetting Pressure, kg/cm^2	Crushing Load (kg/briquette)	Water Resistance
100	184	20 % disintegrated in water
150	294	15 % disintegrated in water
200	386	water resistant
300	418	water resistant
400	486	water resistant
500	470	water resistant
600	294	water resistant

Briquetting conditions: Binder: 5% molasses+1,5% lime,
Moisture: 6%, Drying temp.: 105°C, Particle size: original sample,
briquettes were kept in water for 2 hours

As the pressure decreases the void spaces and increases the contacts between the particles,the crushing strength of the briquettes and their resistance to water improved. 200 kg/cm^2 pressure was found sufficient to achieve strong and water resistant briquettes.

EFFECT OF MOISTURE

The water was added between 1% to 8% to moist the briquette charge. The briquettes produced with the addition of more than 6% water, their water resistant properties were improved.

EFFECT OF FINENESS OF THE SAMPLE

In order to investigate the effect of fineness of sample on the strength of the briquets, various amount of minus 44 microns fraction was added to the original sample. As shown in Table 7, the effect of increasing fines in the briquette mixture was insignificant. In other words, the fines had no appreciable positive or negative effect on the quality of the briquette.

Table 7. Effect of fines on briquetting

-44 microns Fraction(%)	Crushing Load (kg/briquette)	Water Resistance
10	373	water resistant
20	362	water resistant
30	371	water resistant
40	375	water resistant
50	379	water resistant

Briquetting conditions: binder: 5% molasses+1,5% lime,
Moisture: 6%, Pressure: 200kg/cm^2, Drying temp.: 105°C,
briquettes were kept in water for 2 hours

CONTROL OF CALCINATION PROPERTY OF THE BRIQUETTE

In order to control the suitability of briquette size in calcination, it was calcined in the Gebr Rushtrat laboratory muffle furnace at 1100ºC for 2 hours. The calcinated briquette was analysed by XRD method, which is shown in Figure 1.

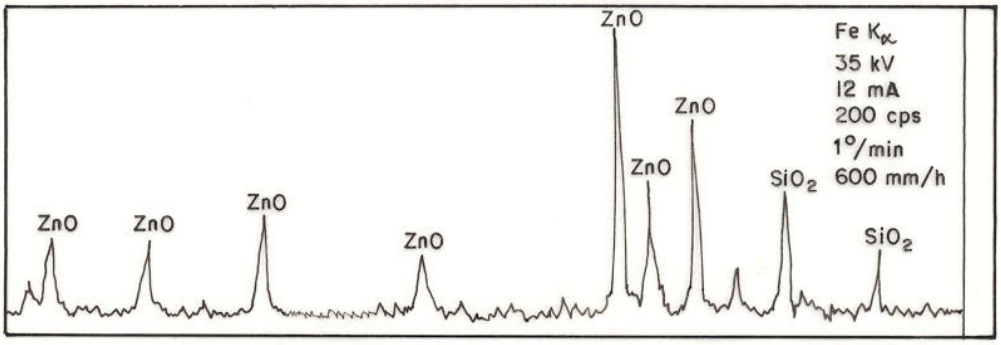

Fig. 1. XRD of zinc concentrate of iran after calcination

The chart of XRD test showed that no smithsonite was present in calcined sample due transformation of smithsonite to ZnO. It showed the suitability of the briquet size to calcination.

TUMBLING TEST ON BRIQUETS PRODUCED AT OPTIMUM CONDITIONS

Briquettes produced with 5% molasses and 1.5 % hydrated lime and with a briquetting pressure of 200 kg/cm^2, were fed to the tumbling drum, to determine the abrasion resistance. The tumbling test showed that the dust percentage was around 1%. It proves that the briquettes are very resistant to abrasion.

CONCLUSIONS

1. On the basis of briquetting tests, it was concluded that Angouran smithsonite sample could be successfully agglomerated by briquetting method.
2. During briquetting, binder addition was found essential. Among twelve organic and inorganic based binders, molasses was found suitable.
3. Although, the briquettes produced by the addition of molasses alone were sufficiently strong, they did not show any resistance to water. This was overcome by the use of hydrated lime with molasses.
4. The briquetting pressure had a significant effect on the strength and water resistant property of the briquettes.
5. The fineness of the sample had no appreciable effect on the quality of the briquettes.

6. Optimum briquets were produced by the addition of 5% molasses, 1.5 % hydrated lime, 6% water. The pressure and drying temperature were 200 kg/cm^2 and 105ºC, respectively. These briquettes showed above 300 kg crushing strength and around 1% abrasion index with no disintegration in water.

REFERENCES

CHAPTYKOV, P.G., MAISKII, O.V., LOGINOV, N.V., SHNAIDER, I.G., RUDKO, N.A. (1987), *Charge of Sintering Zinc-Containing Materials*, Otkrytiya Izabret, 127.

GÖKSEl, M.A., (1980), Proc. Bienn. Conf. Inst., Briquet Agglom, 57.

LUO SCHEIDER, W., POSHMARSKI, L. (1989), *Recovery of zinc from smelter dust and sludges by ore briquetting,* Eur. Pat. Appl., 1.

PLANKA, J. MOROWSKI, J. (1971), *Sintering of sulfide-oxide zinc-lead concentrates with additions of coke breeze,* Pr.Inst.Hutn, 145.

ÖZBAYOĞLU, G., HIÇYILMAZ, C., AKDEMIR, Ü. (1993), *Briquetting of zinc oxide fines*, Powder Technology, 77, 153-158.

Özbayoğlu G., Tabari K.R., *Brykietowanie drobnych ziarn smitsonitu z Angouran w Iranie,* Physicochemical Problems of Mineral Processing, 37 (2003) 115-122 (w jęz. ang.).

Rudę zawierającą węglan cynku przerabia się w sposób tradycyjny w piecu Waelza, w celu odzysku cynku w wyniku procesu rozkładu termicznego. W przypadku, gdy nadawę do procesu stanowią drobne ziarna, musi być zastosowany proces brykietowania drobnych ziarn. Celem pracy było określenie warunków fizykochemicznych brykietowania drobnych ziarn węglanu cynku ze złoża Angouran w Iranie, które przerabiane są w zakładzie wzbogacania Dandi. W trakcie prowadzonych doświadczeń, badano wpływ ciśnienia, ilości cieczy mostkującej, wilgoci, temperatury i wielkości ziaren na proces brykietowania. Optymalne warunki brykietowania otrzymano, gdy drobne ziarna węglanu cynku były mieszane z 6% wody, 5% melasy oraz 1.5% wapna. Ciśnienie zastosowane do brykietowania wynosiło 200kg/cm^2, a temperatura suszenia 105^{0}C przez okres 2 godzin.

Physicochemical Problems of Mineral Processing, 37 (2003) 123-130
Fizykochemiczne Problemy Mineralurgii, 37 (2003) 123-130

Janina GRODZKA*, Andrzej KRYSZTAFKIEWICZ*, Teofil JESIONOWSKI*, Dominik PAUKSZTA*

CARBONATE-SILICATE FILLERS PRECIPITATED FROM SOLUTIONS OF ALKALINE SILICATES AND CALCIUM HYDROXIDE USING CARBON DIOXIDE

Received March 2003, reviewed, and accepted May 15, 2003

A procedure was worked out to precipitate highly dispersed carbonate-silicate fillers using solutions of sodium metasilicate, calcium hydroxide and gaseous carbon dioxide. In course of fillers precipitation effects of changes of Na_2SiO_3:$Ca(OH)_2$ solutions v/v ratios and temperature were examined. The precipitated fillers were subjected to a comprehensive physicochemical analysis (bulk density, capacities to absorb water, dibutyl phthalate and paraffin oil, flow-off point were estimated). Also particle size and particle size distribution, homogeneity of particles, their tendency to form agglomerates and particle surface morphology were examined using SEM and DLS techniques. Carbonate-silicate fillers were evaluated also in respect to their structure by means of WAXS method. Carbonate-silicate filler precipitated at the Na_2SiO_3:$Ca(OH)_2$ v/v ratio=4:1 characterized high particles homogeneity, high values of paraffin oil absorbing capacity and flow off point, as well as low bulk density.

Key words: carbonate-silicate fillers, precipitation, SEM, DLS, calcite structure

INTRODUCTION

The non-toxic character of both the chalk and of the silicate fillers argues for their increasingly comprehensive application, particularly in polymer processing (Niedermeier, 2002; Hasse, 2002). Common carbon black fillers, which are produced in laborious processes, loose their popularity (for example, in rubber industry) (Donnet, 1993). In this regard, carbonate-silicate filler, composed of two non-toxic components, may provide a very attractive alternative. In addition, it is of significance that such a filler is obtained in the process of precipitation and, therefore, it forms a uniform composition, representing a nanofiller of calcium carbonate and calcium

* Poznan University of Technology, Institute of Chemical Technology and Engineering, Pl. M. Sklodowskiej-Curie 2, 60-965 Poznan, Poland, e-mail: Teofil.Jesionowski@put.poznan.pl

silicate (Krysztafkiewicz, 1990). Moreover, the precipitation process can be controlled in such a way that the co-precipitated calcium carbonate may exist in two crystalline forms, calcite and aragonite (Domka, 1996).

Presence of the co-precipitated calcium carbonate favours augmented activity of the carbonate-silicate filler. In this case, of particular importance is the presence of silanol groups, directly linked to the silicate portion of the filler (Daniels, 1998). Silanol groups at the surface of the carbonate-silicate filler may form active centres, so significant in processes of modification of the surface (Chu, 1998; Trens, 1996). For example, silane coupling agents could react with hydroxyl surface groups of fillers (Plueddemann, 1982; Mittal, 1992). Precipitated calcium carbonates are not suitable to chemical modification due to the absence at their surface of hydroxyl groups (Pizzi, 1994). Therefore, the hybrid calcium carbonate/calcium silicate system can be subjected to physical interaction with modifiers which are popular for chalks, e.g., with fatty acids and their salts and with silane coupling agents which chemically react with silicate silanol groups.

Carbonate-silicate fillers can be applied not only in the rubber industry and in processing of plastics but also in shoe industry, production of paints and varnishes, in pharmaceutical industry, cosmetics, food and paper industry.

EXPERIMENTAL

MATERIALS

Substrates for production of a carbonate-silicate filler included: solution of calcium hydroxide, solution of sodium metasilicate of silicate modulus - 3.3, gaseous carbon dioxide. The process was conducted as specified by the following scheme (Fig.1).

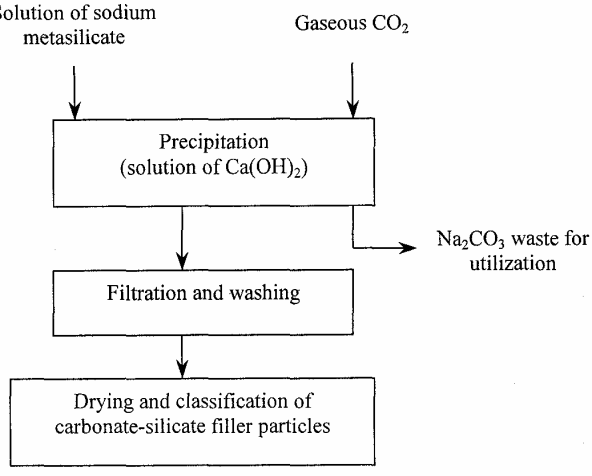

Fig. 1. Block diagram of precipitation of carbonate-silicate fillers

METHODS

Following precipitation, the carbonate-silicate fillers were subjected to physicochemical tests, their bulk density as well as, water, dibutyl phthalate and paraffin oil absorbing capacities were estimated (Krysztafkiewicz, 1987). Their flow-off point was also estimated, the typical parameter of chalk (carbonate) fillers (Katz, 1978). In order to obtain data on dispersion, particle size, surface morphology, structure of individual particles and agglomeration of carbonate-silicate fillers, their samples were studied by scanning electron microscopy (SEM) to obtain reliable images of the filler surface (using Philips SEM 515 equipment).

The identification analysis involved studies using WAXS technique. The results were analysed employing XRAYAN software (Marciniak, 1998). The diffraction patterns were executed employing the horizontal diffractometer TUR-M62. Nickel-filtered CuKα radiation (λ=1.5418 Å) was used in the measurements. The following measuring conditions were employed: anode voltage - 30 kV, anode current - 25 mA the measurement range of 2θ: 3-60^o, measuring step - 0.04^o.

Particle size and their size distribution, also representing principal property of carbonate-silicate fillers, were measured taking advantage of the dynamic light scattering (DLS) technique (Żurawska, 2002), using optoelectronic systems of ZetaPlus apparatus. Aqueous suspension of the filler was stabilised, placed in a cuvette and particle size distribution of the sample was measured using equipment of Brookhaven Instruments, USA.

RESULTS AND DISCUSSION

Principal physicochemical properties of precipitated carbonate-silicate fillers for various v/v ratios of calcium hydroxide and sodium metasilicate solutions are listed in Table 1.

As demonstrated by data in Table 1, samples of fillers precipitated at v/v ratio of Na_2SiO_3:$Ca(OH)_2$=1:2, independently of temperature, exhibited relatively high bulk densities (above 260 g/dm^3) and low values of flow-off point (as low as 13-18 cm^3/10g). Capacities to absorb dibutyl phthalate and paraffin oil were also low. Fillers precipitated at Na_2SiO_3:$Ca(OH)_2$ ratio equal to 1:1 exhibited slightly lower bulk densities (of the order of 210-225 g/dm^3) and higher values of flow-off point (17-18.5 cm^3/10g). The capacities to absorb dibutyl phthalate and paraffin oil were comparable.

Very interesting results were obtained following precipitation of carbonate-silicate fillers at the v/v ratio of Na_2SiO_3:$Ca(OH)_2$=2:1 (particularly at 60^{o}C). The sample manifested low bulk density (170 g/dm^3), a high flow-off point (26.5 cm^3/10g) and high capacities to absorb dibutyl phthalate (300 cm^3/100g) and paraffin oil (450 cm^3/100g). Even higher physicochemical parameters were demonstrated by sample 10, precipitated at Na_2SiO_3:$Ca(OH)_2$ v/v ratio = 4:1 at 60^{o}C. The sample manifested low

bulk density, 165g/dm^3 and a high flow-off point, 27.0 cm^3/10g. Capacities to absorb dibutyl phthalate and paraffin oil amounted to 310 cm^3/100g and 470 cm^3/100g, respectively.

Table 1. Physicochemical properties of obtained carbonate-silicate fillers

Sample No.	Temp. (°C)	Bulk density (g/dm^3)	Flow-off point (cm^3/10g)	Water absorbing capacity (cm^3/100g)	Dibutyl phthalate absorbing capacity (cm^3/100g)	Paraffin oil absorbing capacity (cm^3/100g)
Na_2SiO_3 : $Ca(OH)_2$ = 1:2						
1	40	275	13.0	200	250	300
2	60	260	13.0	250	250	350
3	80	270	18.0	200	220	300
Na_2SiO_3 : $Ca(OH)_2$ = 1:1						
4	40	220	18.0	200	250	250
5	60	210	18.5	250	250	350
6	80	225	17.0	250	220	250
Na_2SiO_3 : $Ca(OH)_2$ = 2:1						
7	40	170	25.5	250	300	400
8	60	170	26.5	305	300	450
9	80	180	23.0	200	250	300
Na_2SiO_3 : $Ca(OH)_2$ = 4 :1						
10	60	166	27.0	310	300	470

Particle size distribution of the carbonate-silicate filler precipitated at the Na_2SiO_3:$Ca(OH)_2$ v/v ratio = 1:1 at 60°C is presented in Fig. 2.

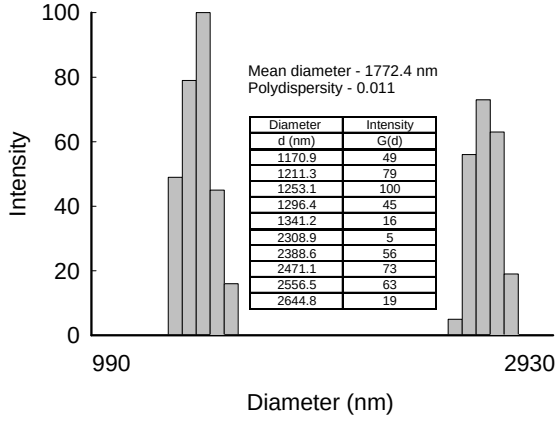

Fig. 2. Multimodal particle size distribution of carbonate-silicate filler (sample 5)

As demonstrated by the particle size distribution for the carbonate-silicate filler (sample 5), the specimen demonstrated relatively low homogeneity. In the particle size distribution presence of two bands of distinct intensity could be noted, which represented particles of smaller and larger diameters, respectively, frequently linked into agglomerate structures. The band of higher intensity could be ascribed to primary particles and primary agglomerates (aggregates) and it fitted the range of 1170.9 – 1341.2 nm (maximum intensity of 100 corresponded to aggregates of 1253.1 nm in diameter). The less intense band corresponded to larger secondary agglomerate structures and was positioned in the diameter range of 2,308.9-2,644.8 nm (maximum intensity of 73 corresponded to agglomerates of 2,471.1 nm in diameter). Mean diameter of particles was 1,772.4 nm, and polydispersity was 0.011.

Particle size distribution of the carbonate-silicate filler precipitated at the Na_2SiO_3 :$Ca(OH)_2$ v/v ratio = 4:1, at 60^{o}C (sample 10) is presented in Fig.3.

As demonstrated by the size distribution, only one particle band was present, pointing to highly increased homogeneity of the filler particles. Moreover, as compared to sample 5, particles of sample 10 formed band with particles of much lower diameters, present within the range of 316.2 – 1,333.5 nm (maximum intensity of 100 corresponded to particles and primary agglomerates of 562.3 nm in diameter). The mean particle diameter was 668.0 nm, and polydispersity was 0.005.

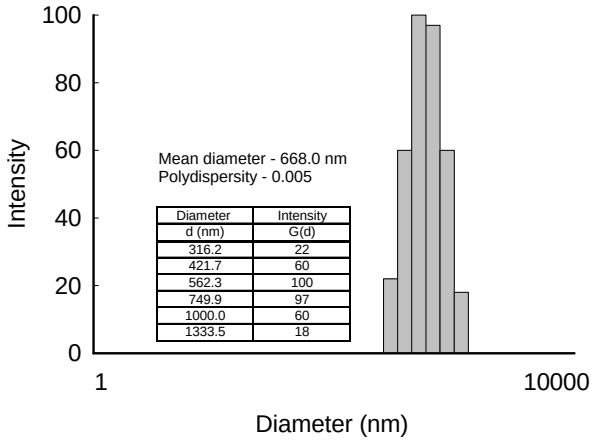

Fig. 3. Multimodal particle size distribution of carbonate-silicate filler (sample 10)

SEM microphotograph of the carbonate-silicate filler (sample 10) is presented in Fig. 4. The photograph confirmed extensive homogeneity of the sample precipitated in such conditions.

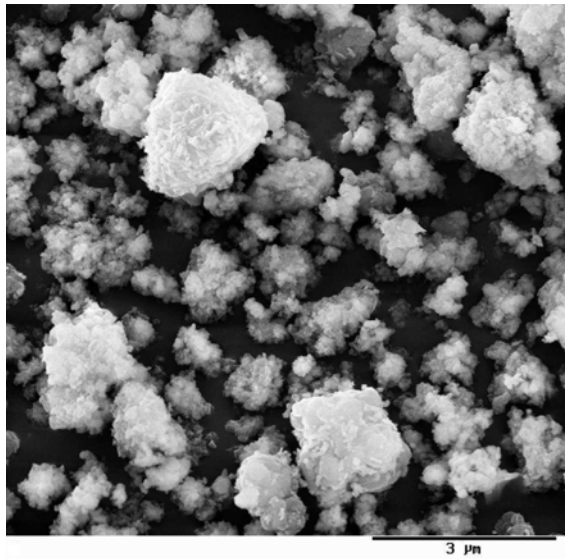

Fig. 4. SEM micrograph of carbonate-silicate filler (sample 10)

X-ray patterns of carbonate-silicate filler samples precipitated at 60°C at various Na_2SiO_3:$Ca(OH)_2$ v/v ratios (samples 8 and 10) are shown in Figs. 5 and 6 (the diffraction maxima, originating from calcite, were analyzed).

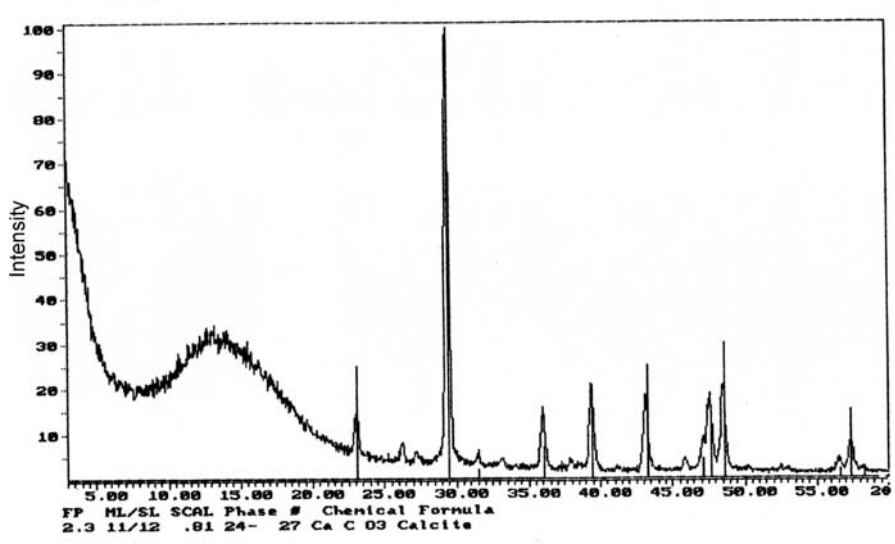

Fig. 5. WAXS pattern of carbonate-silicate filler (sample 8)

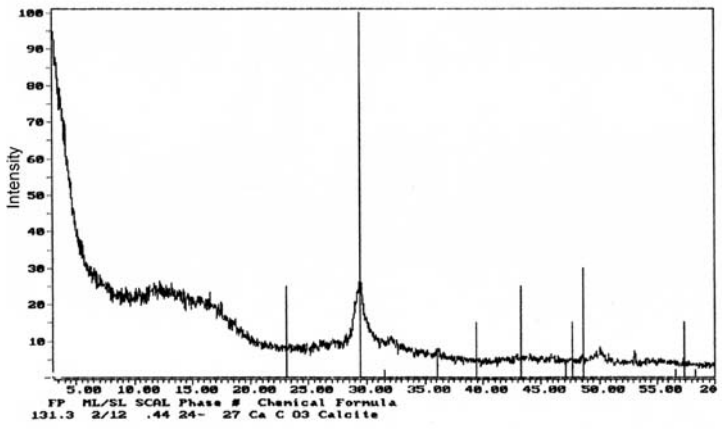

Fig. 6. WAXS pattern of carbonate-silicate filler (sample 10)

Diffraction pattern of sample 8 (Fig. 5) unequivocally demonstrated that the carbonate-silicate filler obtained from solutions of calcium hydroxide and sodium metasilicate (Na_2SiO_3:$Ca(OH)_2$ v/v ratio = 2:1) contained exclusively calcite. No traces of other polymorphic forms, as well as, aragonite and waterite, were detected.
Carbonate-silicate filler precipitated at larger volumes of sodium metasilicate (Na_2SiO_3:$Ca(OH)_2$ v/v ratio = 4:1) exhibited a significantly amorphic character, as proven by the respective diffraction pattern (Fig. 6). However, presence of the crystalline form of calcite could be noted although maxima typical for the structure were much less intense than those noted for the sample 8. Also in this case not even minimum amounts of aragonite and waterite forms could be noted.

The amorphic phase was accompanied by higher amounts of co-precipitated calcium silicate. Such a filler manifested more advantageous physicochemical parameters as well as the presence of fine particles with a decreased tendency to form agglomerates. The data were confirmed by SEM and DLS studies.

CONCLUSIONS

- Carbonate-silicate filler precipitated at the Na_2SiO_3:$Ca(OH)_2$ v/v ratio = 2:1, at 60^{o}C exhibits relatively good physicochemical parameters, an average homogeneity and a tendency to form large complexes of agglomerates.
- Sample of carbonate-silicate filler precipitated in the presence of increased amounts of sodium metasilicate (Na_2SiO_3:$Ca(OH)_2$ solution v/v ratio = 4:1) manifests higher homogeneity and markedly improved physicochemical parameters (high values of flow-off point).
- Carbonate-silicate filler precipitated in the presence of augmented amounts of sodium metasilicate shows an amorphic character while the filler precipitated at Na_2SiO_3:$Ca(OH)_2$ v/v ratio = 2:1 is crystalline (in the polymorphic form as a calcite).

REFERENCES

CHU L., DANIELS M.W. and FRANCIS L.F. (1998), *Use of (glycidoxypropyl)-trimethoxysilane as a binder in colloidal silica coatings,* Chem. Mater. 9, 2577-2582.

DANIELS M.W. and FRANCIS L.F. (1998), *Silane adsorption behaviour, microstructure and properties of glycidoxypropyltrimethoxysilane-modified colloidal silica coatings*, J. Colloid Interf. Sci. 205, 191-200.

DOMKA L. (1996), *Otrzymywanie syntetycznego węglanu wapnia z kredy kalcynowanej ze złoża Kornica,* Fizykochemiczne Problemy Mineralurgii 30, 119-126.

DONNET J.-B., BANSAL R.C. and WANG M.-J. (1993), *Carbon black science and technology,* 2nd edition, Marcel Dekker, New York.

HASSE A., KLOCKMANN O., WEHMEIER A. and LUGINSLAND H.-D. (2002), *Influence of the amount of di- and polysulfane silanes on the crosslinking density of silica-filled rubber compounds,* Kautschuk Gummi Kunststoffe 55, 236-243.

KATZ H. and MILEWSKI J. (1978), *Handbook of fillers and reinforcements for plastics,* Van Nostad Reinhold Company, New York.

KRYSZTAFKIEWICZ A. (1987), *Metody oceny mineralnych napełniaczy elastomerów,* Chemia Stosowana 31, 443-461.

KRYSZTAFKIEWICZ A. (1990), *Use of highly dispersed precipitated carbonate-silicate powders as fillers for elastomers,* Powder Technol. 63, 1-11.

MARCINIAK H. and DIDUSZKO R. (1998), *XRAYAN – the programme for the identification purposes,* PWN, Warsaw.

NIEDERMEIER W., FROEHLICH J and LUGINSLAND H.-D. (2002), *Reinforcement mechanism in the rubber matrix by active fillers,* Kautschuk Gummi Kunststoffe 55, 356-366.

MITTAL K.L. (1992), *Silane and other coupling agents,* VSP, Utrecht.

PIZZI A. and MITTAL K.L. (1994), *Handbook of adhesive technology,* MDI, New York.

PLUEDDEMANN E.P. (1982), *Silane coupling agents,* Plenum Press, New York.

TRENS P. and DENOYEL R. (1996), *Adsorption of (γ-aminopropyl)triethoxysilane and related molecules at the silica/heptane interface,* Langmuir 12, 2781-2784.

ŻURAWSKA J., JESIONOWSKI T. and KRYSZTAFKIEWICZ A. (2002), *Studies on precipitation of highly dispersed silica from sodium metasilicate – sodium hydrogen carbonate system,* J. Chem. Technol. Biotechnol. 77, 917-924.

ACKNOWLEDGEMENTS

This work was supported by the PUT Research Grant DS No. 32/115/2003.

Grodzka J., Krysztafkiewicz A., Jesionowski T., Paukszta D., *Napełniacze węglanowo-krzemianowe strącanie z roztworów krzemianów alkalicznych i wodorotlenku wapnia za pomocą dwutlenku węgla,* Physicochemical Problems of Mineral Processing, 37 (2003) 123-130 (w jęz. ang.).

Opracowano metodykę strącania wysoko zdyspergowanych napełniaczy węglanowo-krzemianowych, stosując roztwory metakrzemianu sodu i wodorotlenku wapnia oraz gazowy dwutlenek węgla. W trakcie strącania tych napełniaczy zmieniano między innymi stosunek objętościowy Na_2SiO_3:$Ca(OH)_2$ oraz temperaturę. Strącone napełniacze poddawano wszechstronnej analizie fizykochemicznej (oznaczono gęstość nasypową, chłonności wody, ftalanu dibutyu i oleju parafinowego oraz punkt spływania). Analizowano również wielkość cząstek oraz rozkład wielkości cząstek, jednorodność, tendencję do tworzenia aglomeratów, jak również morfologię powierzchni cząstek przy pomocy technik SEM i DLS. Napełniacze węglanowo-krzemianowe oceniano również pod względem krystaliczności metodą dyfraktometrii rentgenowskiej. Napełniacz węglanowo-krzemianowy strącony przy stosunku objętościowym Na_2SiO_3:$Ca(OH)_2$=4:1 odznacza się dużą jednorodnością cząstek, dużymi wartościami chłonności oleju parafinowego i punktu spływania oraz małą gęstością nasypową.

Physicochemical Problems of Mineral Processing, 37 (2003) 131-140
Fizykochemiczne Problemy Mineralurgii, 37 (2003) 131-140

Michał WIECZOREK*, Teofil JESIONOWSKI*, Andrzej KRYSZTAFKIEWICZ*

INFLUENCE OF ORGANIC POLYMER MODIFICATION ON PHYSICOCHEMICAL PROPERTIES OF BENTONITES

Received March 2003, reviewed, and accepted May 15, 2003

In the studies we used bentonites hydrophobically transformed through surface modification with organic polymers. They were compared with commercially available bentonites modified with polymers of the Teq gel HD, Swell gel as well as with the pure Fluka bentonite and local bentonites, originating from Zakłady Metalowo-Górnicze Zębiec. Alterations in physicochemical properties were demonstrated using scanning electron microscopy, dynamic light scattering, elemental analysis and X-ray techniques. Elemental analysis confirmed bentonite processing with polymers in cases of Teq gel and Swell gel samples. Morphological and particle size studies demonstrated a destructive effect of polymer modification on bentonite structure including evidently decreased diameter of particles and agglomerates.

Key words: bentonite, polymer intercalation, nanocomposites

INTRODUCTION

Many scientific centres around the world have recently aimed their studies at the potential for production and application of stratified silicate – polymer nanocomposites (Gemeay, 2002; Kacperski, 2002; Park, 2002). The bentonite exhibits a hydrophilic character and, therefore, its application in hydrophobic systems requires that its surface is modified to increase its affinity to organic radicals (Breakwell, 1995). Offered by us schematic mechanism of the modification is shown in Fig. 1. At the first stage, delamination of bentonite should be followed by ionic exchange.

Ions contained in interpacket spaces (sodium ions are most favourable but also calcium and magnesium ions) are exchanged to monomer particles. Subsequently, the monomer particles in bentonite matrix is subjected to polymerisation. In this way the

* Poznan University of Technology, Institute of Chemical Technology and Engineering, Pl. M. Sklodowskiej-Curie 2, 60-965 Poznan, Poland, e-mail: Teofil.Jesionowski@put.poznan.pl

intercalate structure nanocomposite is obtained of an unordered array or in an intermediate form. Bentonite is a mineral of extremely variable composition which varies significantly depending upon the source of origin (Breen, 1988; Benito, 1998, Christidis, 1998; Cara, 2000; Wieczorek, 2001). Principal physicochemical properties of bentonites are shown in Table 1 (Wypych, 1999; Murray, 2000).

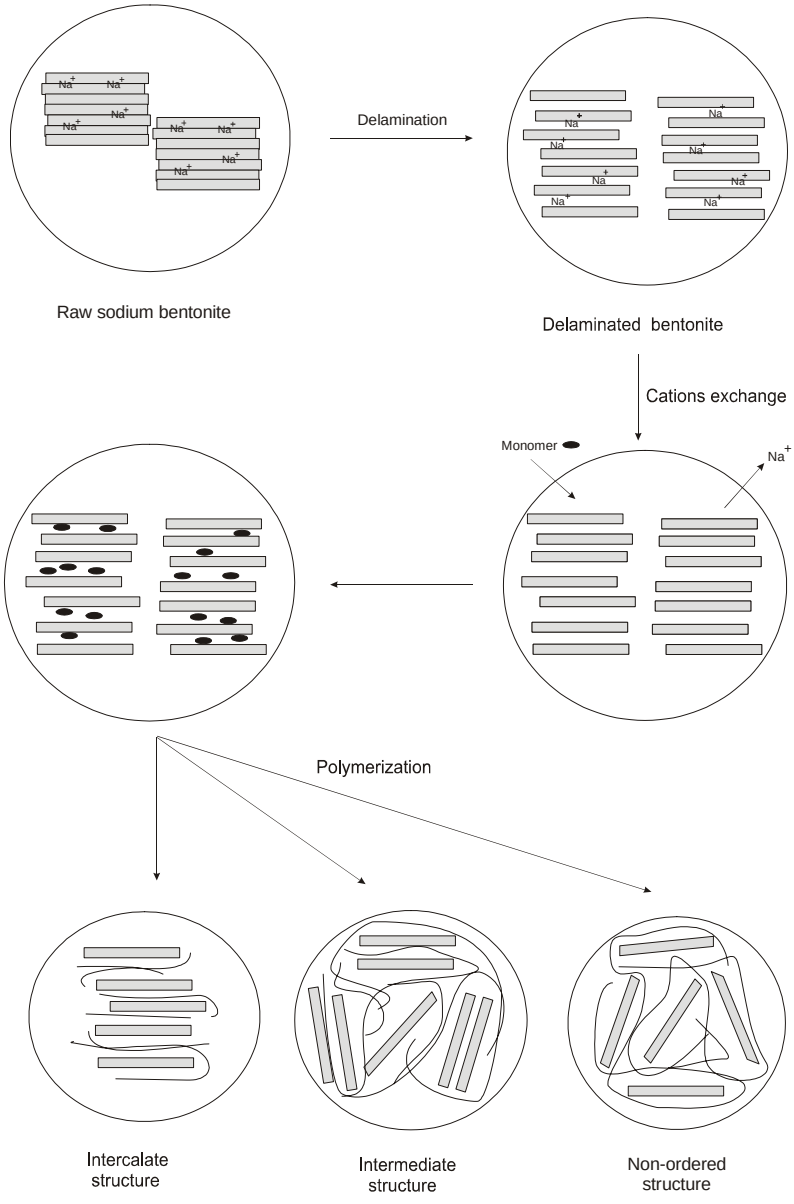

Fig. 1. Schematic of bentonite-nanocomposite generation.

In this paper, the following question was consider: How does intercalation of bentonite with polymer influence its basic properties? The influence of intercalation was examined on shape and size of bentonite molecules, capacity to absorb of water, exo- and endothermic transformations in a temperature gradient. Various analytic techniques were used, traditionally applied in studies on nanocomposites.

Table 1. Physicochemical properties of bentonites

Chemical formula	$(Na, Ca)(Al, Mg)_6(Si_4O_{10})_3(OH)_6 \cdot nH_2O$
Chemical composition, (%)	SiO_2 – 56-72; Al_2O_3 – 13-21; Fe_2O_3 – 0.9-5.0 MgO – 1.7-2.4; CaO – 0.7-2.2; Na_2O – 0.3-2.7; K_2O – 0.2-0.3
Trace elements	As, Ba, Cd, Pb, Se, Hg
Density, (g/cm^3)	1.6-3.0
Mohs hardness	1-2
Loss on ignition, (%)	8.4-11.9
Moisture content, (%)	2-14
pH of water suspension	7-10.6
Water solubility, (%)	3
Color	white; cream; grey, tan, light green
Particle size, (μm)	0.18-1
Oil absorption, (g/100g)	36-52
Swelling	high
Specific surafce area, (m^2/g)	50-300
Applications	drillnig muds, foundry boundands, paints, coatings, paper, sealans, adhesives, polymer fillers, pharmaceuticals

EXPERIMENTAL

MATERIALS

The following materials were used for comparative studies: pure montmorillonite MMT (Fluka), Izol and Specjal Extra U activated local bentonites made in Zakłady Metalowo-Górnicze "Zębiec" and bentonites modified with polymer compounds, Teqgel HD (Heads) and Swell gel (Phrikolat).

METHODS

The identification analysis involved studies using WAXS technique. The results were analysed employing XRAYAN software (Marciniak, 1998). The diffraction patterns were executed employing the horizontal diffractometer TUR-M62. Nickel-filtered CuKα radiation (λ=1.5418 Å) was used in the measurements. The following measuring conditions were employed: anode voltage - 30 kV, anode current - 25 mA the measurement range of 2θ: 3-60°, measuring step - 0.04°.

Particle size and particle size distribution, also representing principal properties of bentonites, were measured taking advantage of the dynamic light scattering (DLS)

technique, using optoelectronic systems of ZetaPlus apparatus. Aqueous suspension of the filler was stabilised, placed in a cuvette and particle size distribution of the sample was measured using equipment of Brookhaven Instruments, USA.

Moreover, the zeta potential results were estimated using electrophoretic light scattering (ELS) also on ZetaPlus equipment.

Examinations of particle shape and morphology were conducted using scanning electron microscopy (SEM). The observations were performed with the Phillips SEM 515 microscope.

The bentonite material and functionalised silica samples were characterised by quantitative elemental analysis (C, H and N analysis) using the automatic type EA 1108 instrument (Carlo-Erba). The studies of water wettability of selected bentonites were carried out using K-100 tensiometer (Krüss).

RESULTS AND DISCUSSION

Physicochemical properties of examined bentonites are listed in Table 2. In Teqgel HD bentonite, elemental analysis showed the carbon content of 1.4%. Unmodified bentonites contained, approximately, 0.4% of carbon. The increased amount of carbon in Teqgel HD bentonite was a consequence of bentonite modification process using the polymer.

Table 2. Examined properties of bentonites

Bentonite	Teqgel HD	Swell gel	MMT	Izol	Special extra U
Moisture content, (%)	14.76	12.14	7.00	8.41	8.69
Loss on ignition at 600^{o}C, (%)	5.86	1.24	4.44	3.49	4.65
Mean particle diameter, (nm)	716.1	637.8	773.8	565.0	615.4
Polydispersity	0.218	0.102	0.211	0.005	0.228
Zeta potential*, (mV)	-38.35	-37.19	-21.81	-41.44	-41.35

*at pH=6.5

Studies on electrokinetic (zeta) potential provided evidence for high stability of dispersion of tested minerals. The montmorillonite, which is the active component of bentonite, without additional salt contamination, demonstrated the lowest absolute zeta potential value (-21.81 mV). The impurities markedly affected adsorptive character of the studied mineral in a water solution. The occurrence of primary particles in the form of larger clumps, i.e. aggregates or agglomerates was characteristic for all samples of studied bentonites (Fig. 2a-6a). The diameters of bentonite particles were within the range of 560 – 770 nm. Teqgel HD and Swell gel bentonites manifested three ranges of particles size. Monmorillonite, which represent pure chemical form of bentonite also demonstrated three ranges of particles size. In

this case, a relatively vast "fraction" of primary particles and of aggregates was present. An almost monodisperse character was shown by particles of Izol bentonite (not activated with polymers) (Fig. 5a). Its range of particle diameters was 561-574 nm. Polydispersity of the bentonite showed the lowest value, 0.005 (Table 2). Particle size distribution of Specjal extra U bentonite, not modified with polymers, is shown in Fig. 6a. An intense band of primary agglomerates was present in the range of 189 – 874 nm. As predicted, MMT, Izol Specjal Extra U bentonites demonstrated a primary packet structure and their particles manifested the form of more or less deformed flakes (Figs. 4b-6b). On the other hand, samples of Teqgel HD and Swell gel bentonites had the shape of irregular blocks. This was probably caused by mechanical processing of the material, mainly during activation by the polymers.

Studies on wettability in water of selected bentonites (Fig.7) showed that, in comparison with bentonites activated by polymers, the sample of Izol had a significantly higher affinity to water. The extent of hydrophobic transformation was the highest in the case of Teqgel HD bentonite.

X-ray curves of the Teqgel HD and Swell gel bentonites (Figs. 8 and 9) demonstrated maximum intensities within the ranges typical for smectite group minerals. Analysis of inter-pack distances, determined using Bragg's equation, proved that no polymer intercalation took place to inter-pack spaces of the clay. The bentonite-polymer interaction was exclusively of the physical adsorption nature.

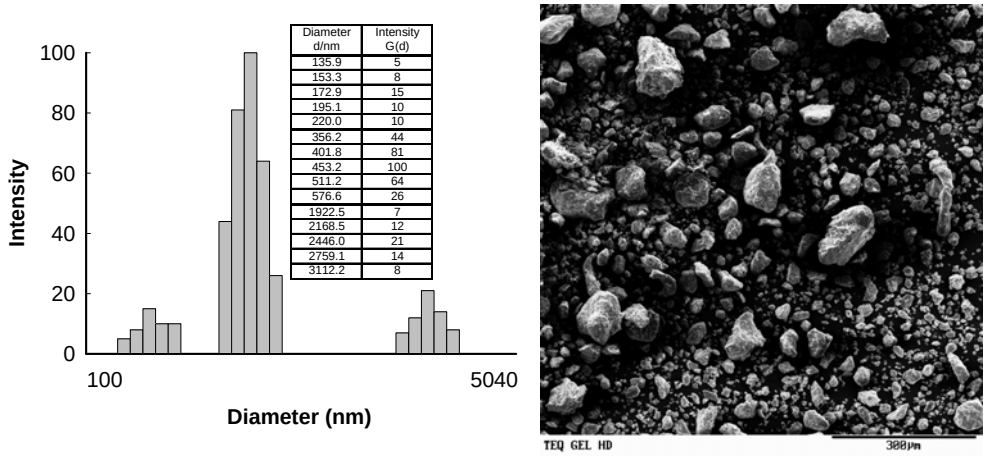

(a) (b)

Fig. 2. Teqgel HD bentonite (a) multimodal particle size distribution (b) SEM micrograph.

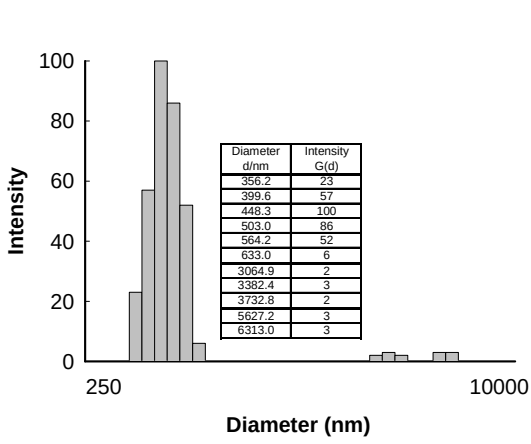

(a) (b)

Fig. 3. Swell gel bentonite (a) multimodal particle size distribution (b) SEM micrograph

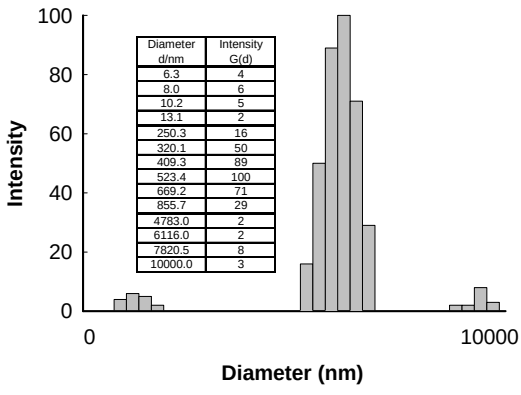

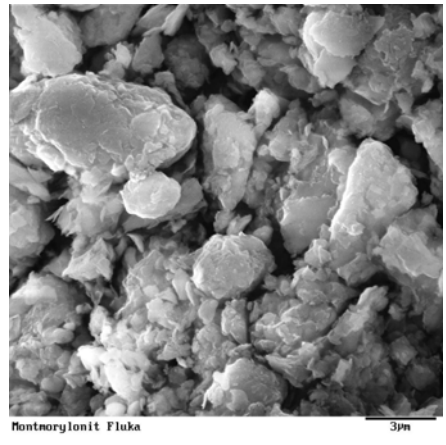

(a) (b)

Fig. 4. Bentonite MMT (a) multimodal particle size distribution (b) SEM micrograph

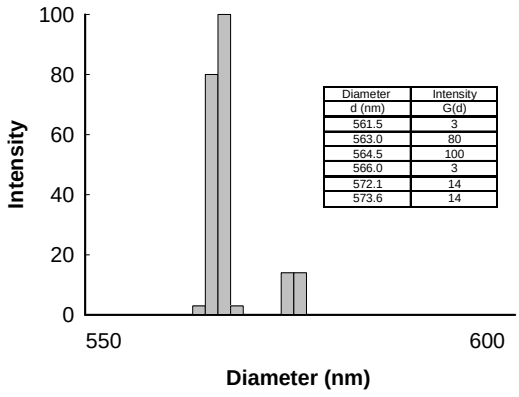

Diameter d (nm)	Intensity G(d)
561.5	3
563.0	80
564.5	100
566.0	3
572.1	14
573.6	14

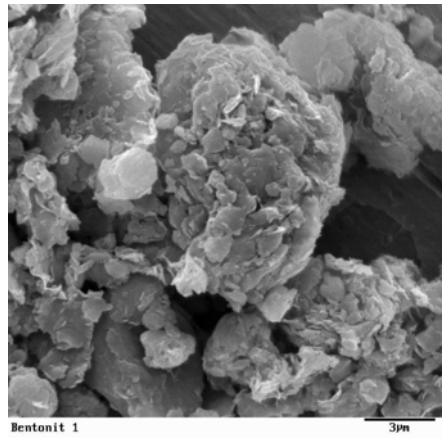

(a) (b)

Fig. 5. Izol bentonite (a) multimodal particle size distribution (b) SEM micrograph

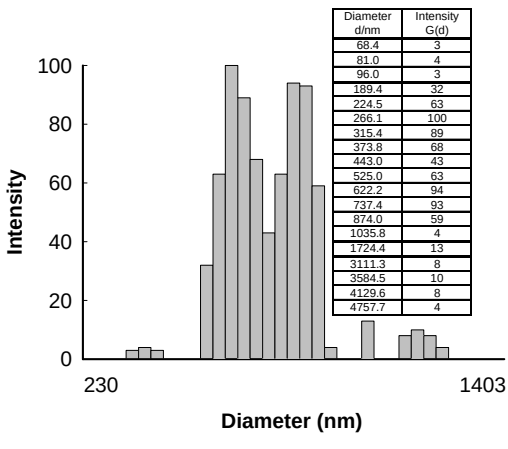

Diameter d/nm	Intensity G(d)
68.4	3
81.0	4
96.0	3
189.4	32
224.5	63
266.1	100
315.4	89
373.8	68
443.0	43
525.0	63
622.2	94
737.4	93
874.0	59
1035.8	4
1724.4	13
3111.3	8
3584.5	10
4129.6	8
4757.7	4

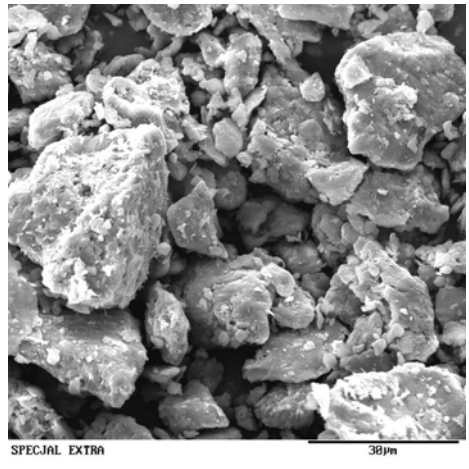

(a) (b)

Fig. 6. Specjal Extra U bentonite (a) multimodal particle size distribution (b) SEM micrograph

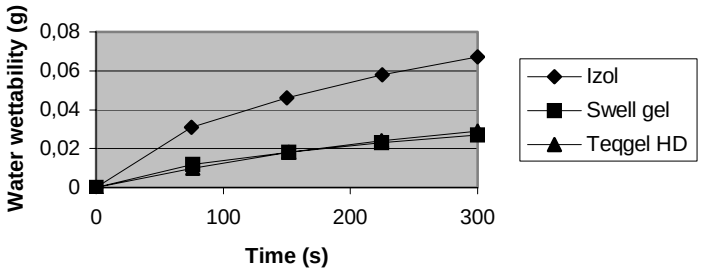

Fig. 7. Dependence of water wettability of bentonites in time

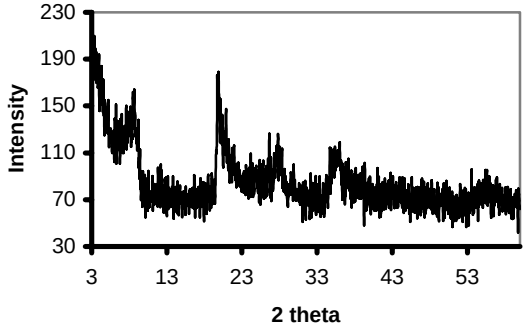

Fig. 8. WAXS pattern of Teqgel HD bentonite.

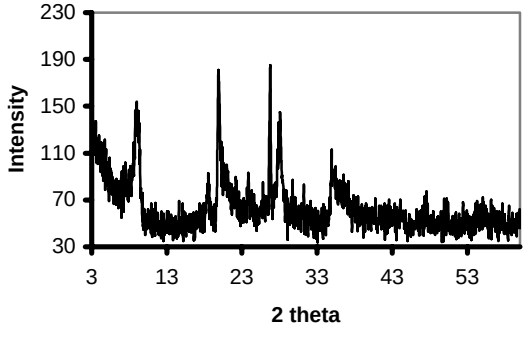

Fig. 9. WAXS pattern of Swell gel bentonite

CONCLUSIONS

The Teqgel HD bentonite contains around 2% of organic modifiers, whereas Swell gel contains approximately 0.5% of organic compounds. The bentonite modifiers contain no nitrogen atoms, thus exclusing application of amines and quaternary ammonium salts. The studied bentonites exhibit a surface structure typical for modified bentonites, in which destruction of primary structure takes place. Nevertheless, they partially preserve their stratified microstructural morphology. Activation with organic compounds fails to significantly affect size of particles (aggregates) of studied bentonites (mean particle diameter approximates 700 nm). Also zeta potential acquires almost identical values for unactivated and polymer-activated bentonites (the exception involves MMT). The enclosed X-ray patterns of studied minerals illustrate their crystalline structure, typical for the smectite group. No polymer intercalation takes place to the inter-packet spaces.

REFERENCES

BENITO R., GARCIA-GUINEA J., VALLE-FUENTES F.J. and RECIO P. (1998), *Mineralogy, geochemistry and uses of the mordenite-bentonite ash-tuff beds of Los Escullos, Almeria, Spain*, J. Geochemical Exploration 62, 229-240.

BREAKWELL I.K., HOMER J. and LAWRENCE M.A.M., McWHINNIE W.R. (1995), *Studies of organophilic clays: The distribution of Quaternary ammonium compounds on clay surfaces and the role of impurities*, Polyhedron 14, 2511-2518.

BREEN C. (1998), *The characterisation and use of polycation-exchanged bentonites*, Appl. Clay Sci. 15, 187-219.

CARA S., CARCANGIU G., PADALINO G., PALOMBA M. and TAMANINI M. (2000), *The bentonites in pelotherapy: chemical, mineralogical and technological properties of materials from Sardinia deposits (Italy)*, Appl. Clay Sci. 16, 117-124.

CHRISTIDIS G.E., (1998), *Physical and chemical properties of some bentonite deposits of Kimolos Island, Greece*, Appl. Clay Sci. 13, 79-98.

GEMEAY A.H., EL-SHERBINY A.S. and ZAKI A.B., (2002) *Adsorption and Kinetic Studies of the intercalation of Some Organic Compounds onto Na^+-Montmorillonite,* J. Colloid Interf. Sci. 245, 116-125.

KACPERSKI M. (2002) *Nanokompozyty polimerowe. Cz. 1. Charakterystyka ogólna, napełniacze oraz nanokompozyty na podstawie polimerów utwardzalnych,* Polimery 47, 801-807.

MURRAY H.H., (2000), *Traditional and new applications for kaolin, smectite and palygorskite: a general overview*, Appl. Clay Sci. 17, 207-221.

PARK S.-J., SEO D.-I. and LEE J-R. (2002) *Surface Modification on Surface Acid-Base Characteristics of Clay and Thermal Stability Of Epoxy/Clay Nanocomposites,* J. Colloid Interf. Sci. 251, 160-165.

WIECZOREK M. and KRYSZTAFKIEWICZ A. (2001), *Characteristics of domestic bentonites and application,* Prace Naukowe Instytutu Górnictwa Politechniki Wrocławskiej 31, 66-74.

WYPYCH G. (1999), *Handbook of fillers,* ChemTec Publishing, Toronto - New York, pp.43-44.

YALÇIN H. and GŰMŰŞER G. (2000), *Mineralogical and geochemical characteristics of late Cretaceous bentonite deposits of the Kelkit Valley Region, Northern Turkey*, Clay Minerals 35, 807-825.

ACKNOWLEDGEMENTS

This work was supported by the PUT Research Grant DS No. 32/115/2003.

Wieczorek M., Jesionowski T., Krysztafkiewicz A., *Wpływ modyfikacji polimerami organicznymi na właściwości fizykochemiczne bentonitów,* Physicochemical Problems of Mineral Processing, 37 (2003) 131-140 (w jęz. ang.).

W badaniach wykorzystano bentonity hydrofobizowane przez powierzchniową modyfikację polimerami organicznymi. Porównywano komercyjne bentonity modyfikowane polimerami o symbolach Teq gel HD, Swell gel oraz czysty bentonit z Fluki i bentonity krajowe pochodzące z Zakładów Metalowo-Górniczych Zębiec. Zmiany w właściwościach fizykochemicznych wykazano wykorzystując następujące techniki: skaningową mikroskopię elektronową, dynamiczne rozpraszanie światła, analizę elementarną oraz technikę rentgenowską. Analiza elementarna potwierdza obróbkę bentonitu polimerami w przypadku próbek Teq gel i Swell gel. Badania morfologiczne i wielkości cząstek wykazały wpływ destrukcyjny modyfikacji polimerami na strukturę bentonitu oraz spowodowały wyraźne zmniejszenie średnic cząstek i aglomeratów.

Physicochemical Problems of Mineral Processing, 37 (2003) 141-147
Fizykochemiczne Problemy Mineralurgii, 37 (2003) 141-147

Ludwik DOMKA[*], Andrzej WĄSICKI[**], Maciej KOZAK[***]

THE MICROSTRUCTURE AND MECHANICAL PROPERTIES OF NEW HDPE-CHALK COMPOSITES

Received March 2003, reviewed, and accepted May 15, 2003

Increasing demands on the quality and specific properties of polymers imply increasing demands on the mineral fillers used in composite materials. They are expected not only to reduce the cost of production but also improve the mechanical properties of the composites or endow them with new features, e.g. thermostability. The paper presents a method for obtaining polyethylene composites with chalk modified by two new 1-alcoxymethyl-3-hydroxypyridinium chlorides: 3-hydroxy-1-octyloxymethylpyridinium chloride (salt 1) and 3-hydroxy-1-octadecyloxymethylpyridinium chloride (salt 2) and gives a characterisation of the composites obtained. Introduction of chalk modified with ammonium salts results in an increased values of MFI of the composites. The MFI changes are the most pronounced for the PE composites containing the filler in concentrations from 0.05 to 2.0% wt. Addition of the chalk modified with the ammonia salts causes greater changes in some mechanical properties of the composites (Young modulus) than addition of unmodified chalk, while changes in some other properties (stress at break) was practically the same.

Key words: chalk, surface modification, quaternary ammonium salts, polyethylene

INTRODUCTION

Mineral fillers used in polymer industry should be chemically inert towards the polymer matrix and components. They should show thermostability and ability to easy and fast dispersion in a polymer medium (Plueddemmann, 1974). The problem is that commonly used mineral fillers have hydrophilous surface while that of polymers is usually hydrophobic. Therefore, to improve the interphase interactions in a composite

[*] Technological Centre, A. Mickiewicz University, Grunwaldzka 6, 60-780 Poznań, Poland.
[**] Department of Polymer Technology, Technical and Agricultural Academy of Bydgoszcz, Seminaryjna 3 85-326 Bydgoszcz, Poland.
[***] Department of Macromolecular Physics, A. Mickiewicz University, Umultowska 85, 61-614 Poznań, Poland, mkozak@amu.edu.pl.

a hydrophobisation of the filler surface is necessary (Domka, 1994). It is achieved with the use of proadhesive compounds such as organic acids and their derivatives, polyoxyethylene glycols, silane coupling agents or some surfactants like quaternary ammonium salts (Mittal, 1992; Domka et al., 2002a, 2002b). The later are particularly valuable because of bacterio- and fungistatic properties. The modified calcium carbonates are particularly suitable as fillers of the PE-LD and PE-LLD foils, containing up to 40% of carbonates. The foils have been commonly used in packaging thanks to their high mechanical strength and easy acceptance of print. The paper presents results of analysis of microstructure and mechanical properties of polyethylene composites filled with chalk modified with the two 1-alcoxymethyl-3-hydroxypyridinium chlorides substituted with C_8H_{17} or $C_{18}H_{37}$: 3-hydroxy-1-octyloxymethylpyridinium chloride (salt 1) and 3-hydroxy-1-octadecyloxymethyl-pyridinium chloride (salt 2).

MATERIALS AND METHODS

Chalk used in the study originated from the Sobków deposit. Chemical composition of the chalk included $CaCO_3$ (96.8%), Fe (0.033%), Mn (0.020%), H_2O (0.15%), Cu (traces) and insoluble residue (0.70%). The chalk manifested density of 2.59 g/cm^3, specific surface area of 8.6 m^2/g, bulk density of 336 g/dm^3, crystallographic structure of calcite. For modification of chalk, two newly synthesized quaternary 1-alcoxymethyl-3-hydroxypyridinium chlorides were used. The modification process was described in our previous work (Domka et al, 1983, 2002b)

The composites were made with high density polyethylene (HDPE) Stavrolen 276-73, made in Russia. The samples to be studied were mixtures of the polyethylene with the chalk modified with quaternary ammonium salts with aliphatic substituents C_8H_{17} and $C_{18}H_{37}$. The modifies chalk was introduced into HDPE in the amounts of 10, 5, 2, 1, 0.5, 0.1 and 0.05% wt. The mixtures containing from 1 to 10% wt of chalk were obtained by introducing appropriately weighted portions of chalk into molten polymer. The mixtures containing 0.05 to 0.5% of chalk were obtained by diluting earlier prepared concentrations containing a proper weight percent of chalk with polyethylene. The mixtures were homogenised in a Brabender plastograph with a measuring head of 50 g in capacity. The head was heated to about 150 ^{o}C and the plasticised polyethylene chalk powder or concentration were added in small portions. After addition of each portion the mixtures were stirred for 20 minutes. After homogenisation the hot samples were removed from the head chamber and divided into three portions. The portions were pressed by a hydraulic press PHM-63 between two steel plates and anti- adhesive layers made of enforced teflon foil. The pressing was performed at 220 ^{o}C under pressure increased to 15 MPa for 30 minutes. To obtain the foils, during the first 5 minutes the samples were heated between the plates not fully closed, for the next 5 minutes with the plates closed but under normal pressure, then for 15 minutes under pressure gradually increasing to 15 MPa. After

removal of the steel plates the pressed foils between the Teflon foil layers were cooled to ambient temperature. Then the Teflon foil was removed, the polyethylene foil samples in the form of oars were cut out, the shape B according to the standard ISO 3167-1996. The oar-shaped samples were used for the measurements estimating the strength of the foils, flow rate, and morphology of the hypermolecular aggregations.

SCANNING ELECTRON MICROSCOPY

The surface and cross sections of the composites were observed under SEM. To be able to do this the samples were sputtered with gold in an ionising sputtering chamber. Observations were made under a SEM -515 (Philips) at the exciting voltage of 20 kV.

STRENGTH MEASUREMENTS

The oar-shaped samples were subjected to strength determinations with a TIRA Test 2200. For determinations of the Young modulus the samples were stretched at the rate 1 mm/ min, for determinations of the bulk modulus of elasticity - at the rate of 20 mm/min (ISO 1133-1991).

RESULTS AND DISCUSSION

SEM photographs of the composites filled with the unmodified and appropriately modified chalk are presented in Figs 1 and 2. The influence of the modification on the tendency to agglomeration and aggregation of the fillers in the polymer matrix is apparent.

After the modification the fillers are capable of uniform dispersion in the matrix. This effect is definitely more pronounced for the chalk modified with salt 1. As a result of both types of modification the filler grains do not agglomerate. The mean size of the filler particles after the two modifications is similar.

For the samples containing 10% wt. of chalk with salts 1 and 2 the results were similar, Fig. 3. For these samples MFI was close to 1g/10 min, at the pressure on the piston of 35 N. With decreasing content of the chalk in PE the value of MFI increases, especially for the chalk concentrations of 0.1 and 0.05%. However, this increase is much lower than for unmodified chalk. The presence of chalk considerably decreases the MFI value (Fig. 4), and the presence of salt 2 containing a greater aliphatic substituent decreases it to a greater degree.

The Young modulus: its value depends on the type of chalk used. The smallest modulus have the samples with unmodified chalk (Fig. 5). The value of the modulus also depends on the concentration of chalk reaching the highest values for the chalk concentrations of 10 and 0.1% wt.

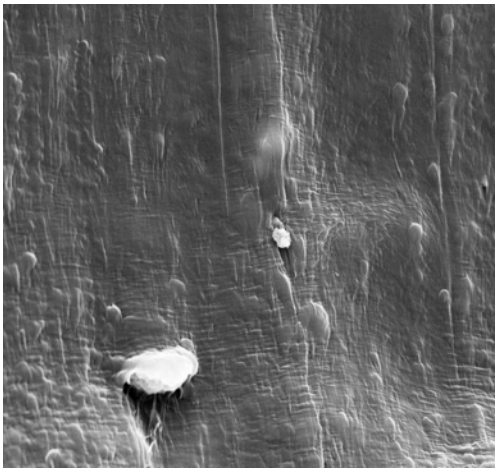

Fig. 1. SEM micrograph of HDPE filled with 20% unmodified chalk

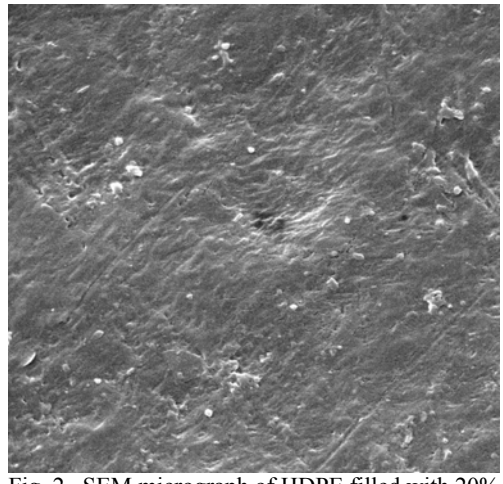

Fig. 2. SEM micrograph of HDPE filled with 20% chalk modified with salt 1

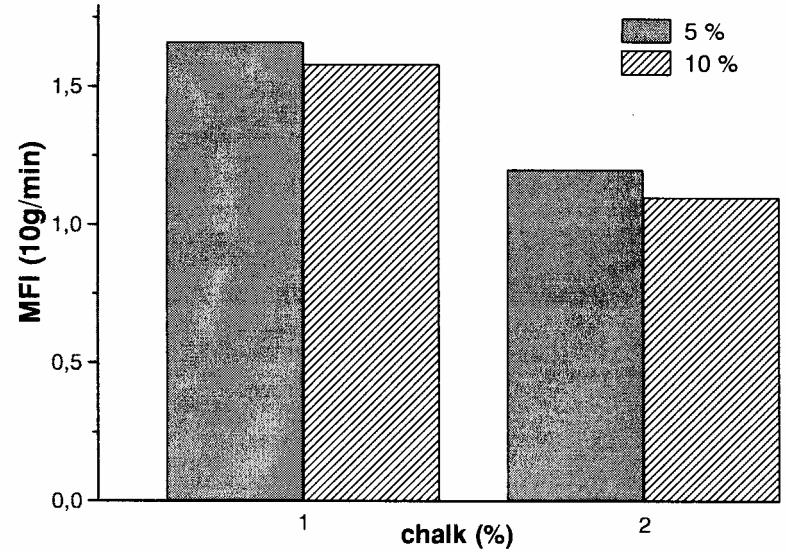

Fig. 3. Changes in MFI (melt flow index) of the PE samples with 5 and 10% wt of: chalk modified with ammonium salt 1 (1),chalk modified with ammonium salt 2 (2). Results obtained under the piston pressure of 35N

The increased value of the modulus for the sample with 0.1%wt chalk can be related to changes in PE crystallisation, although it has not been confirmed by other methods. The samples of PE modified with chalk and salt 1 with a shorter hydrocarbon substituent are characterised by higher modulus than those modified with chalk and salt 2, which means that the use of a properly selected substituent can have stabilising effect on the modified polymer.

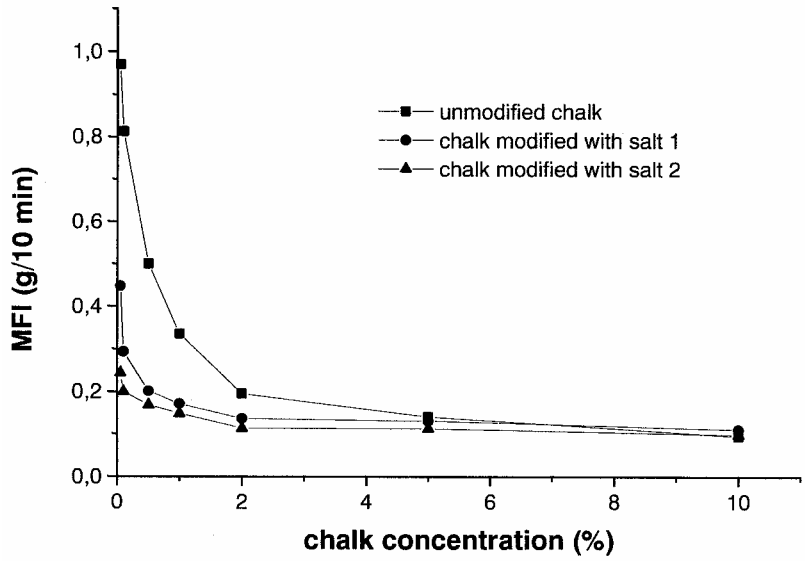

Fig. 4. Changes in MFI (melt flow index) of the PE samples with 0.05 - 10% wt of unmodified chalk or chalk modified with salt 1 and chalk modified with salt 2. Results obtained under the piston pressure of 35 N

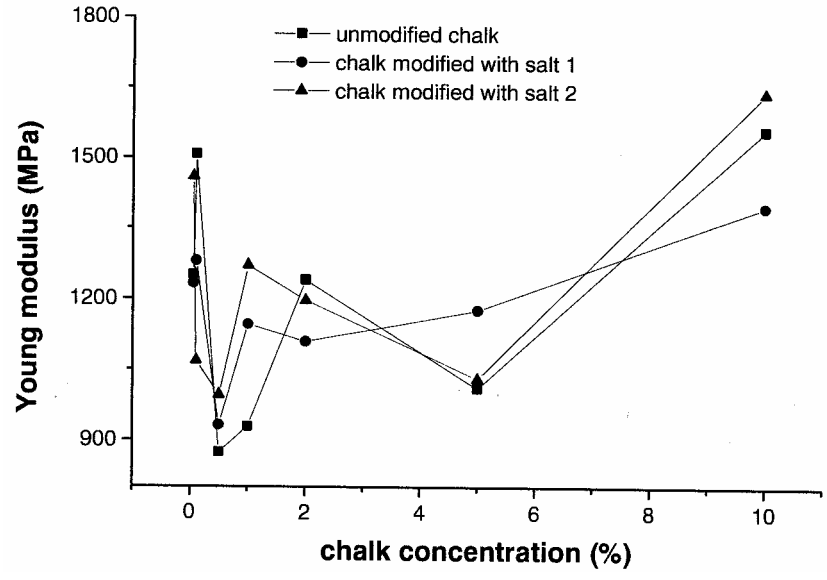

Fig. 5. The effect of the chalk additions on the Young modulus of HDPE composites with unmodified chalk, chalk modified with salt 1 and chalk modified with salt 2

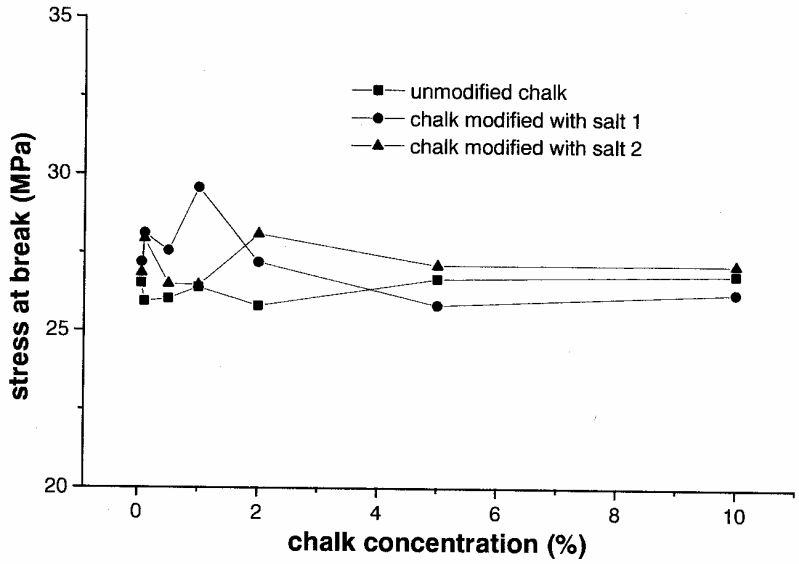

Fig. 6. The effect of chalk addition on the stress at break of HDPE composites with unmodified chalk, chalk modified with salt 1 and chalk modified with salt 2

The values of stress at break (Fig. 6) were practically the same for all samples, which means that the effect of the modifier on this parameter is negligible.

Similar influence of the chalk and coupling agents on the mechanical properties of composites has been recently observed. For titanates used as a coupling agents in PP/HDPE/$CaCO_3$ composites (Gonazales et al, 2002) an increase was verified in Young's modulus at 0.7 wt.% and in elongation at break (up to 0.7 wt.%). The vales of the tensile stress and the complex melt viscosity of polyethylene composites filled with calcite (modified with stearic acid) were higher than those of unfilled ones, implying the reinforcing effect of calcium carbonate (Kwon et al., 2002).

CONCLUSIONS

1. Introduction of chalks modified with ammonium salts to HDPE causes a greater increase in MFI than the addition of unmodified chalks. The greatest increase in MFI has been noted for the samples containing chalks in concentrations between 0.05 and 2.0% wt. The presence of chalk modified with the salt containing a greater aliphatic substituent causes a greater decrease in MFI than the presence of chalk modified with the salt containing a smaller substituent.
2. The presence of chalk in HDPE does not affect the course of the polymer crystallisation taking place on foil production. After etching, the SEM of the surface of the foil containing chalk shows the crystalline aggregations identical to those in PE foil without chalk.

3. The addition of chalks modified with ammonium salts causes greater changes in the elasticity modulus than the addition of unmodified chalk. The Young modulus of the former samples is greater. The greatest changes in the Young modulus are observed for PE with chalk modified with the salt containing a greater aliphatic substituent.
4. If the addition of modified chalk changes some properties of HDPE, these changes are always more pronounced for the samples containing chalk modified with the salt with a greater aliphatic substituent.

ACKNOWLEDGEMENTS

This work was supported by a Scientific Grant 2P03B 09919 from the Polish Committee for Scientific Research.

REFERENCES

DOMKA L., JESIONOWSKI T., MORAWSKA A., KOZAK M. (2002a). *Influence of pyridinium chlorides on physicochemical character, morphology and particle size distribution of natural chalk.* Tenside Surfactants Detergents 39, 33-39.

DOMKA L., KRYSZTAFKIEWICZ A, KOZAK M. (2002b) *Silane modified fillers for reinforcing of polymers.* Polymers & Polymer Composites 10, 541-552.

DOMKA L., 1994, *Modification estimate of kaolin, chalk and precipitated calcium carbonate as plastomer and elastomer fillers,* Colloid Polym. Sci. 272, 1190.

DOMKA L., MARCINIEC B., KRYSZTAFKIEWICZ A., 1983, *Sposób modyfikacji powierzchniowej materiałów proszkowych*, Pat. PRL 115671.

GONZALEZ J., ALBANO C., ICHAZO M., DIAZ B. (2002). *Effects of coupling agents on mechanical and morphological behaviour of PP/HDPE blend with two different $CaCO_3$.* European Polymer Journal 38, 2465-2475.

KWON S., KIM K.J., KIM H., KUNDU P.P., KIM T.J., LEE Y.K., LEE B.H., CHOE S. (2002). *Tensile property and interfacial dewetting in the calcite filled HDPE, LDPE, and LLDPE composites.* Polymer 43, 6901-6909.

MITTAL K.L., 1992, *Silane and Other Coupling Agents*, Utrecht, VSP.

PLUEDDEMMANN E.P., 1974, *Interfaces in Polymer Composites*, New York, Academic Press.

Domka L., Wąsicki A., Kozak M., *Mikrostruktura i własności mechaniczne nowych kompozytów HDPE-kreda,* Physicochemical Problems of Mineral Processing, 37 (2003) 141-147 (w jęz. ang.).

Nowoczesne przetwórstwo polimerów stawia coraz wyższe wymagania napełniaczom mineralnym stosowanym w kompozytach. Powinny one poza obniżeniem kosztów produkcji kompozytów polimerowych także poprawiać ich własności mechaniczne czy nadawać im nowe jak termostabilność. W pracy przedstawiono metodę otrzymywania kompozytów polietylenu z kredą modyfikowaną dwoma nowymi chlorkami 1-alkoksymetylo-3-hydroksypirydyniowymi: 3-hydroksy-1-oktyloksy-metylopirydyniowym i 3-hydroksy-1-oktadecyloksymetylopirydyniowym oraz scharakteryzowano mikrostrukturę oraz wybrane własności mechaniczne uzyskanych kompozytów. Wprowadzenie do HDPE kred modyfikowanych solami amoniowymi spowodowało większy wzrost MFI stopów niż dodatek kredy nie modyfikowanej. Zmiany MFI widoczne są najwyraźniej dla kompozytów PE zawierających pomiędzy 0,05 i 2,0% wag napełniacza. Dodatek kred modyfikowanych solami amoniowymi powoduje większe zmiany niektórych właściwości wytrzymałościowych (np. moduł sprężystości wzdłużnej) niż kreda nie modyfikowana. Natomiast naprężenie przy zerwaniu mało różniło się w próbkach napełnianych modyfikowanymi i niemodyfikowanymi kredami.

Physicochemical Problems of Mineral Processing, 37 (2003) 149-158
Fizykochemiczne Problemy Mineralurgii, 37 (2003) 149-158

Piotr STASZCZUK, Janina PĘKALSKA*

METHODS OF PREPARATION OF MAGNESIUM ORGANIC COMPOUNDS FROM NATURAL DOLOMITE

Received March 2003, reviewed, and accepted May 15, 2003

A simple method of preparation of organic magnesium compounds (citrate, acetate and aspartate) from natural dolomite with simple apparatus was worked out. In the first stage dolomite was converted into magnesium sulfate and then into basic magnesium carbonate by combination with citric and acetic acids. However, magnesium aspartate was prepared by converting magnesium sulfate into hydroxide and then combining it with aspartic acid. The contents of trace element were determined in the final preparations with ASA. Thermal decompositions of the obtained compounds was studied by means of the thermal analysis. Results could be useful in elaborating method of production of these magnesium compounds from domestic dolomite.

Key words: dolomite, magnesium citrate, acetate and aspartate, ASA, thermal analysis

INTRODUCTION

Dolomite $MgCa(CO_3)_2$, a mineral commonly occurring in nature, finds applications in many fields of industry. For example, it is a fluxing agent in metallurgical, glass and ceramic industry, filling material in paper, rubber and plastic production, a sorbent in desulfurization of exhaust gases as well as a filter for water treatment. Large amounts of dolomite are also used in building industry and agriculture (dolomite fertilizers). In chemical industry dolomite is first of all a source of magnesium compounds - oxide, hydroxide, basic calcium, and magnesium carbonates, which are used as ecological anti-oxide frost agent. It is the subject of many interests and research (Bobolewski, 1982; Łukwiński et al., 1994; Biskupski et al., 1996). Lately, there has been worked out a method for preparing *dolomite sorbent* which exhibits very good adsorbing properties towards dangerous poisons like nitrogen and sulfur

* Department of Physicochemistry of Solid Surface, Faculty of Chemistry, Maria Curie-Sklodowska University, M. Curie-Sklodowska Sq.3, 20-031 Lublin, Poland,piotr@hermes.umcs.lublin.pl

oxides as well as chromium(VI) ions (Staszczuk et al., 1996; Staszczuk et al., 2000). The presence of magnesium (so-called *life metal*) in dolomite (*life rock*) promoted exploitation of its beds in order to counterbalance the loss of this precious but deficient element in nature. Therefore, we now have dolomite fertilizers, fodder addition and pharmaceutical preparations. Magnesium deficit in the environment and in human organism becomes such serious so that it makes a social problem. This is caused mainly by the environment pollution, diet, stresses, incorporation of lead from exhaust gases. An improvement may come from consumption of full value food or taking special magnesium preparations. A suitable amount of magnesium in human organism protects it against the effects of different pollutions, such as: lead, cadmium, chlorides. Dolomite provides a cheap source of magnesium can be used as a raw material for production of readily available magnesium compounds. The magnesium oxide, hydroxide, chloride, sulfate, carbonate, accetate, citrate, levulinian, ascorbinian, asparginian are widely used in medicine to compensate for magnesium deficit in the organism and to treat many diseases. Basic magnesium carbonate is used for preparation of mixtures and tablets used in deacidification treatment like the hydroxide. Magnesium sulfate (i.e. bitter salt) has been known for a long time as the purgation medication. However, magnesium aceatte is a component of the preparations used for parent injections in treatment with magnesium. Magnesium sulfate is used for skin and mucous membrane treatment as well as the antiphlogistic preparation as well as in treatment of keratitis. Magnesium salts are used as transplant preservatives. The above examples of application of magnesium salt indicate great demand for this element. It is believed that the orally administered organic magnesium salts dissolved in water are more readily available and tolerable than insoluble ones. Moreover, it is assumed that organic magnesium salts are more active than inorganic ones (Durlach, 1991; Gumińska Ed., 1990; Staszczuk et al., 1994).

Therefore, an effort has been made to use the domestic dolomite as a raw material for production of readily available organic magnesium compounds. Simple method of preparation of these salts from the domestic natural dolomite has been elaborated.

MATERIALS AND REAGENTS

The domestic dolomite from Ołdrzychowice-Romanowo (Kłodzko Valley) 0-0.3 mm grain diameter calcinated for 4 hours at 1000º C in laboratory furnace was used. The mineral composition was determined using AAS-3 spectrophotometer (Carl Zeiss, Jena, Germany) (Tables 1 and 2). Thermal decomposition of final compounds was studied using Q-1500 D deriwatograph (MOM Budapest, Hungary) (Staszczuk et al., 1992). Analytically pure reagents from POCH, Gliwice were used.

Table 1. Quantitative composition of dolomite
(Staszczuk et al., 1992; Staszczuk et al., 1994)

Component	Content,%
CaO	29.54
MgO	19.36
Fe_2O_3	0.30
SiO_2	3.10
MnO	0.22
Na_2O	0.01

Table 2. Contents of trace elements in dolomite
(Staszczuk et al., 1994; Stefaniak et al., 2000)

Element	Content, ppm
Mn	286.74 ± 0.99
Zn	50.33 ± 0.10
Pb	24.00 ± 0.36
Cd	3.86 ± 0.30
Al.	< 10
Ni	< 0.5

RESULTS AND DISCUSSION

EXPERIMENTAL

Organic magnesium salts were prepared in three stages. The first included formation of magnesium sulfate (separation of Ca and Mg and removal of impurities contained in the raw material). The second one was the synthesis of basic magnesium carbonate and hydroxide from magnesium sulfate. The last stage consisted of combination of basic magnesium carbonate will acetic or citric acid as weel as combination of magnesium hydroxide with aspartic acid.

Preparation of monohydrate magnesium sulfate $MgSO_4 \cdot H_2O$

The water magnesium sulfate $MgSO_4.H_2O$ was prepared as follows (Supniewski, 1958; Staszczuk et al., 1994). The 50 g calcinated natural dolomite after heating in laboratory furnace (0-0.3 mm grain size) were dissolved in 180 cm^3 of 10% HCl (the amount needed to dissolve half of sample) and then stirred for 7 hours. The resultant mixture was filtrated. The sediment containing mainly magnesium carbonate was washed with a small amount of water and dried at 90º C for two hours. Then, its mass was 26.5 g. Thereafter, it was stirred with 133 cm^3 of 20% sulfuric acid at 90^o C for 3.5 h. The final mixture was filtered to separate the solid impurities. Then, 2g MgO was added into the clear, heated filtrate for neutralization and adsorption of precipitated impurities (mainly iron) on undissolved magnesium sulfate. Purified filtrate was acidified with sulfuric acid and concentrated until crystallization. Crystals

of $MgSO_4 \cdot 7H_2O$ were separated and the filtrate was concentrated until crystallization. The resultant crystals of $MgSO_4 \cdot 7H_2O$ were dried for two hours at 150° C. 26.6 g of $MgSO_4 \cdot H_2O$ was obtained (Staszczuk et al., 1994).

Preparation of basic magnesium carbonate $MgCO_3 \cdot Mg(OH)_2 \cdot 2H_2O$

The Na_2CO_3 solution (26.5 g, 65 cm^3 H_2O) was added dropwise into stirred magnesium sulfate solution (26.6 g, 70 cm^3 H_2O). The reaction mixture was heated slowly at 60° C for one hour. The white precipitate of basic magnesium carbonate was filtered, washed with distilled water till the complete removal of SO_4^{-2} ions was achieved, and dried at room temperature. The 18.7 g of basic magnesium carbonate was obtained (Biskupski et al., 1996).

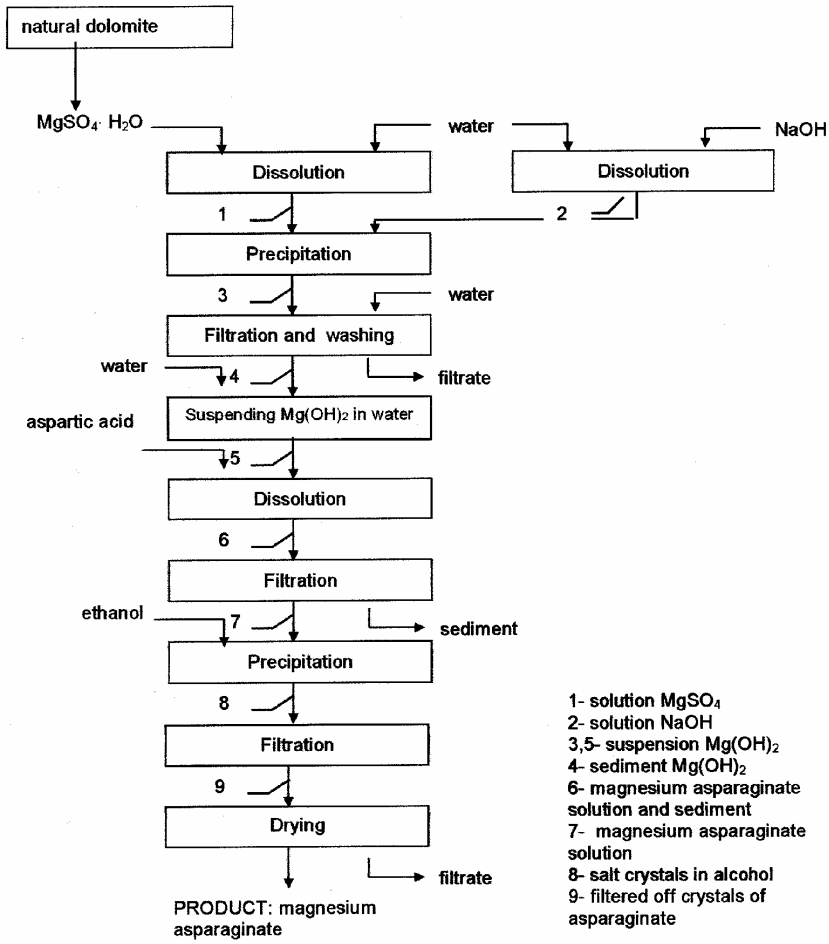

Fig. 1. Scheme of preparation of magnesium acetate

Preparation of magnesium acetate $(CH_3COO)_2Mg{\cdot}4H_2O$

Basic magnesium carbonate (5.5 g) suspended in a small amount of distilled water was added batchwise into 32 cm^3 of stirred 20% acetic acid solution to obtain a slightly alkaline solution. The mixture was filtered, concentrated to a thick syrup consistency and dried in the dryer at 70º C for 6 h. The product was refined and dried at 100º C for 1 h. 10.5 g magnesium acetate was obtained at the reaction yield 95% (Fig. 1).

Preparation of magnesium citrate $Mg_3(C_6H_5O_7)_2{\cdot}9H_2O$

4.5 g of basic carbonate were added batchwise into 6 g of citric acid dissolved in 20 cm^3 distilled water and stirred to give a slightly alkaline solution. Solution was filtered, then magnesium citrate was precipitated by dropping 80 cm^3 of 96% ethanol and stirring. Magnesium citrate precipitates as a resin. The precipitate was filtered, washed with ethanol and dried at room temperature. 10.5 g of magnesium citrate was obtained at the yield 70% (Fig. 2).

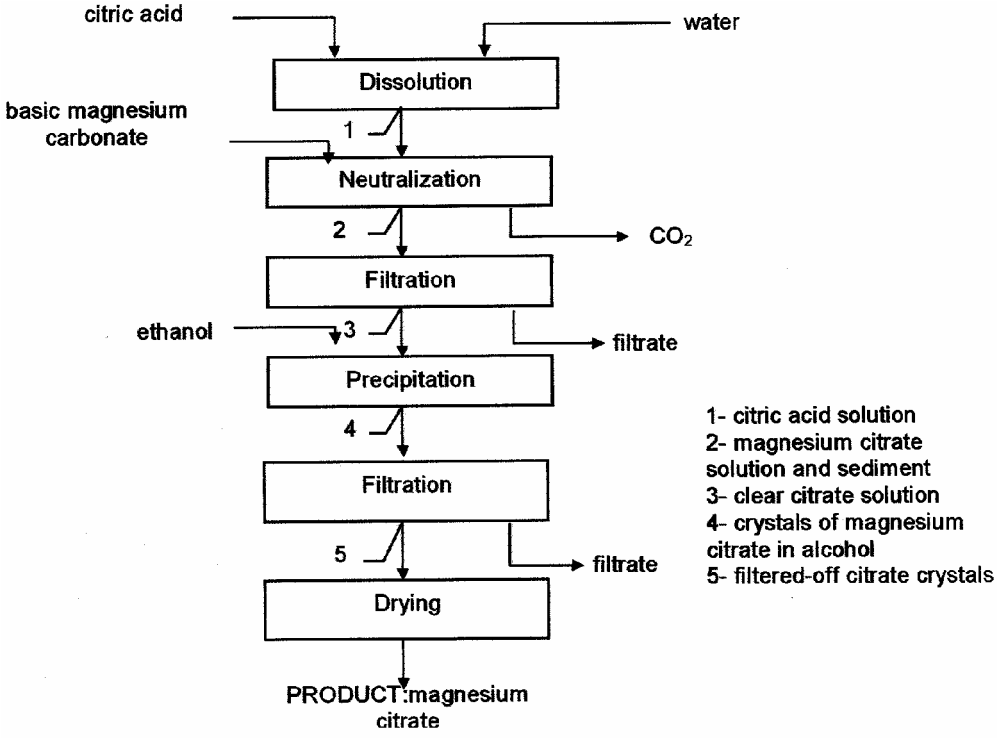

Fig. 1. Scheme of preparation of magnesium citrate

Preparation of magnesium aspartate $[HOOCH(NH_2)CH_2COO]_2Mg \cdot 4H_2O$

Sodium hydroxide solution (1.2g, 10 cm^3 H_2O) was dropped into stirred magnesium sulfate solution (2g $MgSO_4 \cdot H_2O$, 15 cm^3 H_2O). The precipitate of magnesium hydroxide was filtrated and washed with destilled water in order to remove $SO_4^=$ ions. Solution of aspartic acid solution (1.2g, 10 cm^3 H_2O) was added to moist sediment $Mg(OH)_2$ suspended into 20 cm^3 of distilled water. The final solution was treated with 96% ethanol (70 cm^3) dropped in slowly at continuous stirring. Magnesium aspartate precipitates as a resin was ground with a glass rod. The obtained precipitate was filtered, washed with ethanol and dried at room temperature. 2.5 g of magnesium aspartate was obtained at the reaction yield 75.8% (Fig. 3).

THE ASA AND THERMOGRAVIMETRIC ANALYSES

Quality and composition of preparations

The quantitative composition (mainly a number of crystalization water molecules) of the final preparations was determined from the thermal analysis while the contents of trace elements were determined with AAS-3 spectrophotometer. Content of Ca, Fe, Zn, Mn, Pb, Cu, Ni, Cd, Cr and Sr are shown in Table 3 (Stefaniak et al., 2000).

Table 3. Results of AAS analysis of produced compounds

Content, ppm

Compound	Ca	Fe	Zn	Mn	Pb	Cu	Ni	Cd	Cr	Sr
Magnesium sulfate	277	6.68	0.86	17.5	<0.10	<0.03	<0.05	<0.02	<0.05	<0.10
Basic magnesium carbonate	2044	24.6	10.5	97.0	<0.10	<0.03	<0.05	<0.02	<0.05	<0.10
Magnesium acetate	1396	7.6	2.45	1.47	<0.10	<0.03	<0.05	<0.02	<0.05	<0.10
Magnesium asparaginate	112	17.8	15.6	16.8	<0.10	<0.03	<0.05	<0.02	<0.05	<0.10
Magnesium citrate	1289	22.0	23.7	84.0	<0.10	<0.03	<0.05	<0.02	<0.05	<0.10

From Table 3 it follows that there a very low content of Pb, Cu, Ni, Cd, Cr and Sr were found. Their concentrations were below the detection limit, so that our preparations might be called *spectral purity* compounds.

Decomposition of magnesium compounds

Studies of mechanism and kinetics of decomposition of the magnesium compounds were carried out with derivatograph Q-1500 D. A conventional method was applied (platinum measuring crucibles) at the rate of heating 10 °/min. Temperature T, mass loss TG, differential DTG as well as DTA curves were registered. Figures 4-7 present thermal analysis curves for magnesium acetate, citrate and aspartate, respectively. On the DTG and DTA curves one can observe peaks or inflexions resulting from the stage decomposition of the compounds due to the sample heating. The. peaks on the DTG curves are very distinct and of good resolving power. They a 3-stage decomposition processes of studied compounds result from:

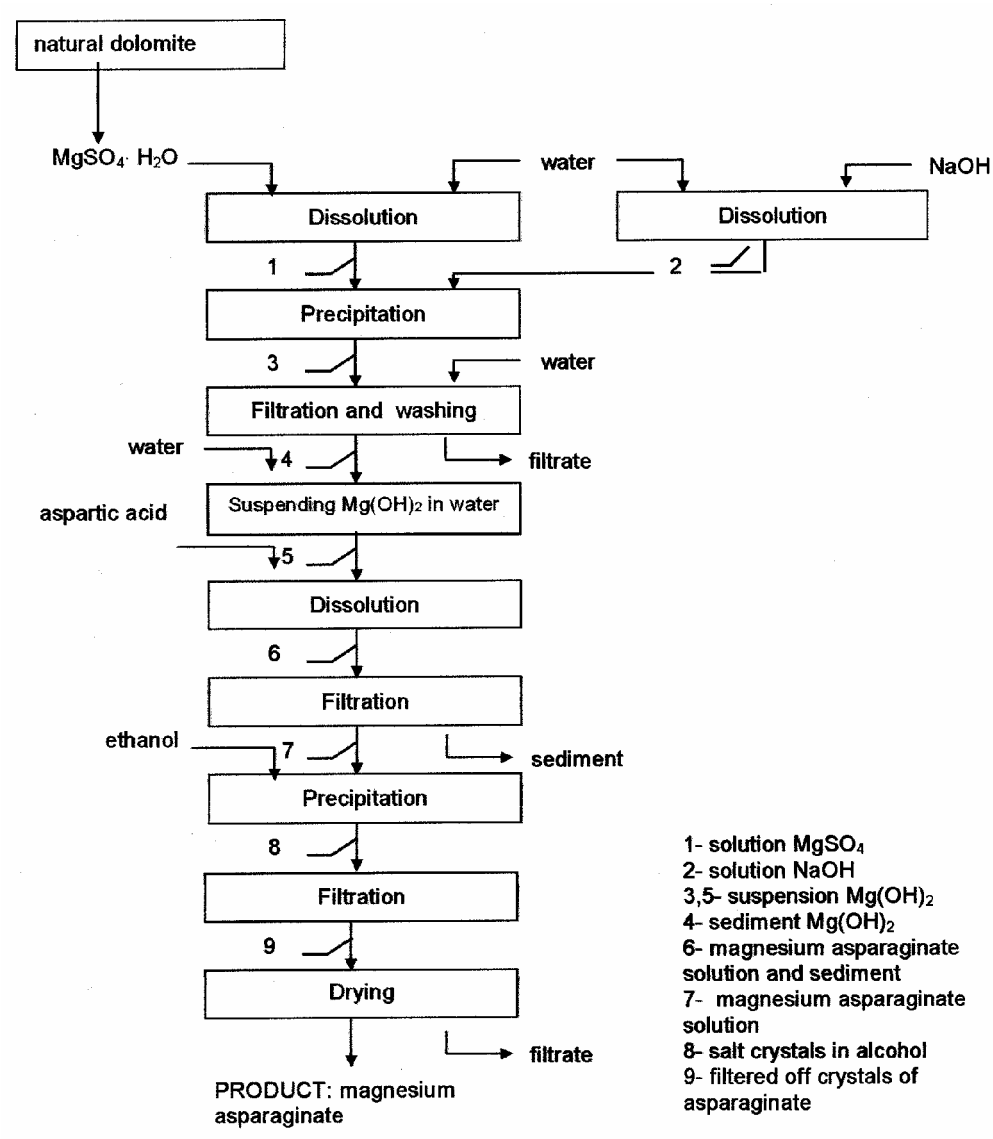

Fig. 3. Scheme of preparation of magnesium asparaginate

a) decoposition of magnesium acetate (Fig. 4):

$$(CH_3COO)_2Mg \cdot 4H_2O \xrightarrow{185^oC} (CH_3COO)_2Mg + 4H_2O$$

$$(CH_3COO)_2Mg + H_2O \xrightarrow{260^oC} MgCO_3 + CO_2 + 3H_2O$$

$$MgCO_3 \xrightarrow{513^oC} MgO + CO_2$$

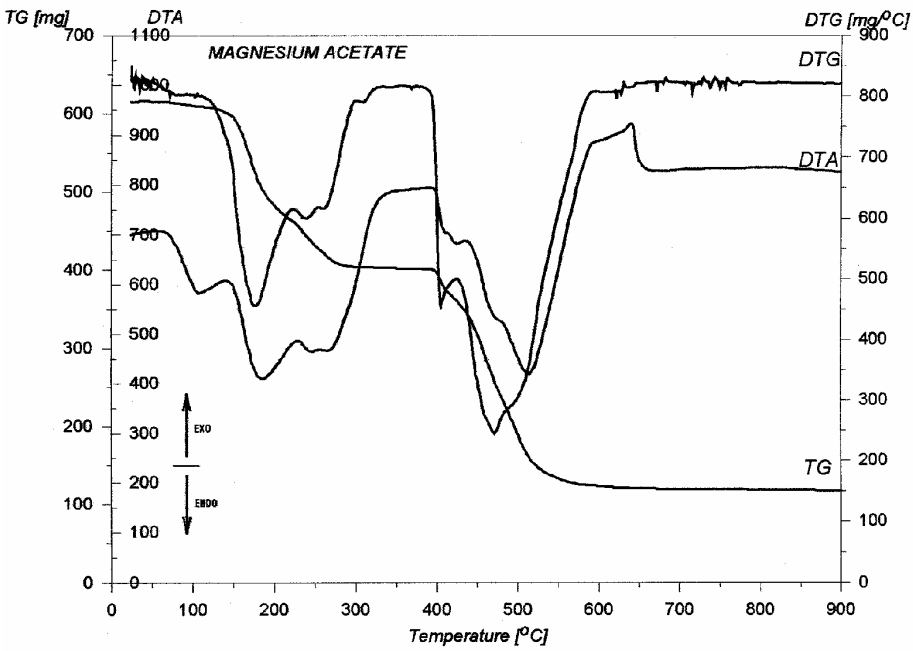

Fig. 4. Thermal decomposition of magnesium acetate

b) decomposition of magnesium citrate (Fig. 5):

$$Mg_3(C_6H_5O_7)_2 \cdot 9H_2O \xrightarrow{175^oC} Mg_3(C_6H_5O_7)_2 + 9H_2O$$

$$3MgCO_3 \xrightarrow{568^oC} 3MgO + 3CO_2$$

$$Mg_3(C_6H_5O_7)_2 \cdot 9O_2 \xrightarrow{420^oC} MgCO_3 + 9CO_2 + 5H_2O$$

c) decomposition of magnesium asparate (Fig. 6):

$$MgC_8H_{12}N_2O_8 \cdot 4H_2O \xrightarrow{281^oC} MgC_8H_{12}H_2O_8 + 4H_2O$$

$$MgC_8H_{12}N_2O_8 + \frac{19}{2}O_2 \xrightarrow{408-652^oC} MgCO_3 + 7CO_2 + 6H_2O + 2NO_2$$

$$MgCO_3 \xrightarrow{836^oC} MgO + CO_2$$

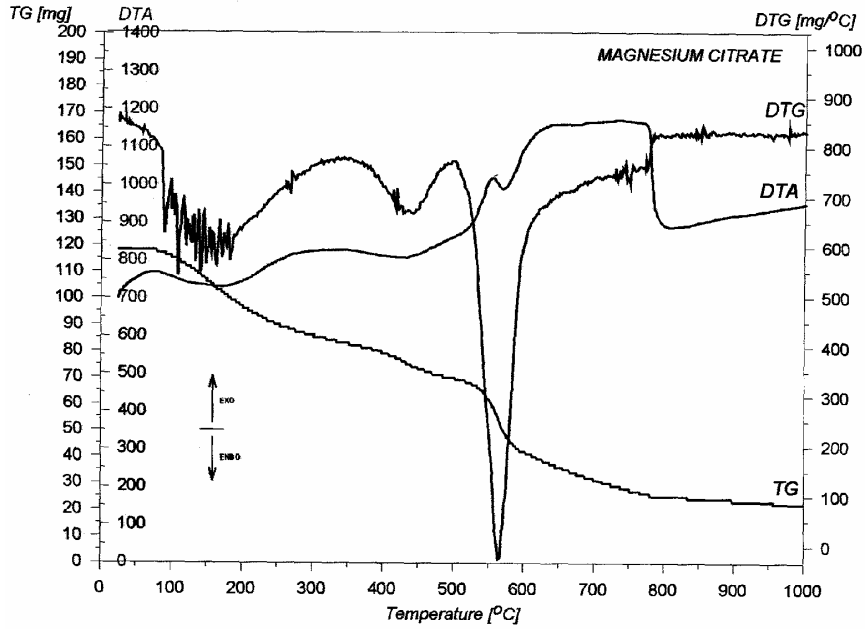

Fig. 5. Thermal decomposition of magnesium citrate

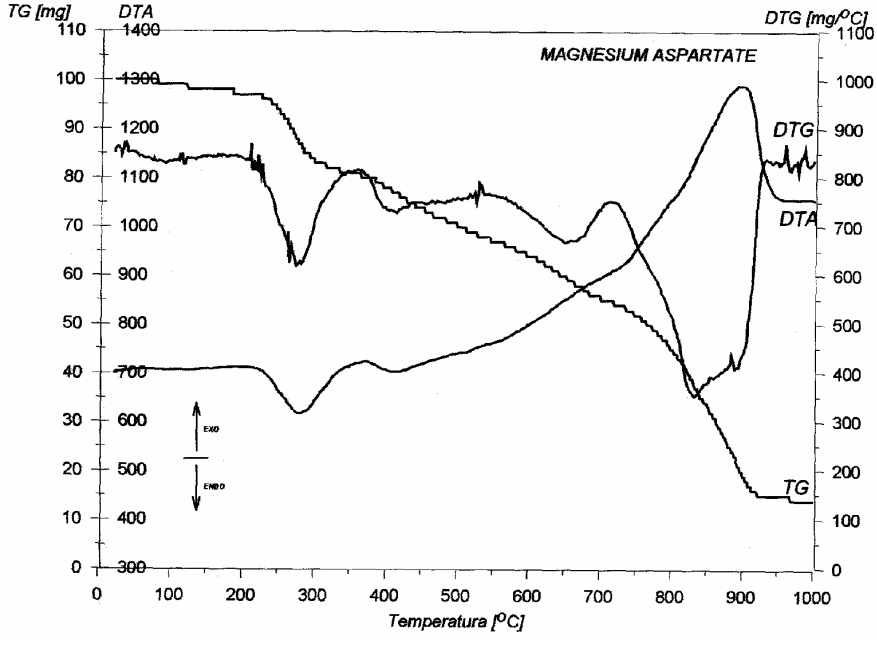

Fig. 6. Thermal decomposition of magnesium asparate

It is worth to note that the second stage of decomposition of anhydrous aspartate proceeds in two steps within a wide temperature range (408-652 ºC). Mechanism of this decomposition is very similar to that of thermal decomposition of hydrated calcium oxalate (a standard reagent used for calibration of derivatographs (MOM Instruction, 1980), which also proceeds in two stages in the temperature range from 425 to 533 ^{o}C. This may result from a similar chemical structure of both compounds (presence of carboxyl groups in a molecule).

CONCLUSIONS

As it comes from the above studies, simple method of synthesis of magnesium compounds synthesis from natural dolomite can be successfully applied to produce cheap preparations. Owing to their spectral purity, these organic magnesium compounds can be used as preparations counteracting magnesium incorporation of dangerous poisons by organisms.

REREFENCES

BISKUPSKI A., BOROWIK M. (1996), *Badania procesu otrzymywania z dolomitu zasadowego węglanu magnezu metodą wodorowęglanową z zastosowaniem obiegu związków sodu*, Przem. Chem., Vol**.** 75, 59-62.

BOLEWSKI A. (1982), *Mineralogia szczegółowa,* PWN, Warszawa.

DURLACH J. (1991), *Magnez w profilaktyce klinicznej,* Państw. Zakład Wyd. Lekarskich, Warszawa.

GUMIŃSKA M. Ed. (1990), *Chemiczne substancje toksyczne w środowisku i ich wpływ na zdrowie człowieka,* Komisja Nauk Medycznych, Oddział PAN, Kraków.

MOM Instruction, Derivatograph Q-1500 (MOM Budapest, Hungary), 1980.

STASZCZUK P., BILIŃSKI B., STEFANIAK E., SZYMAŃSKI E. (1992), *A investigations of Physicochemical Properties of Polish Dolomites*, Adv. Composite Mater*.,* Vol. 2**,** 251-259.

STASZCZUK P., BILIŃSKI B., STEFANIAK E., SZYMAŃSKI E. (2000)*, Sposób otrzymywania adsorbentu i adsorbent,* Patent RP*,* No. 177 841.

STASZCZUK P., STEFANIAK E., SZYMAŃSKI E. (1996)*, Badania adsorpcji tlenków siarki i azotu na materiałach dolomitowych,* Przem. Chem., Vol. 75, 224-226.

STASZCZUK P., Radkiewicz S., Stefaniak E., Szymański E. (1994), *Preparation of Magnesium Compounds from Dolomite,* Polish J. Appl. Chem*.,* Vol. 38, 625-629.

STEFANIAK E., Dobrowolski R., Staszczuk P. (2000), *On the Adsorption of Chromium (VI) Ions on Dolomite and 'Dolomitic Sorbents',* Adsorption Sci. & Technol., Vol. 18, 107-115.

SUPNIEWSKI J. (1958), *Preparatyka nieorganiczna,* PWN, Warszawa.

Staszczuk P., Pękalska J., *Metoda otrzymywania organicznych związków magnezu z dolomitu naturalnego,* Physicochemical Problems of Mineral Processing, 37 (2003) 149-158 (w jęz. ang.)

W pracy opisano prostą metodę otrzymywania cytrynianu, octanu i asparaginianu magnezu z dolomitu naturalnego, która nie wymaga skomplikowanej aparatury. W pierwszym etapie dolomit został przekształcony w siarczan magnezu, a następnie w zasadowy węglan magnezu, który poddano reakcji z kwasem cytrynowym lub octowym. Asparaginian magnezu otrzymano po przeprowadzeniu siarczanu magnezu w wodorotlenek i po reakcji z kwasem asparaginowym. Śladowe zawartości metali ciężkich w otrzymanych preparatach określono metodą ASA. Ponadto, wykonano analizy rozkładu termicznego preparatów za pomocą derywatografu. Otrzymane wyniki badań mogą być użyteczne w opracowaniu metody produkcji magnezowych związków organicznych z krajowego dolomitu.

Physicochemical Problems of Mineral Processing, 37 (2003) 159-168
Fizykochemiczne Problemy Mineralurgii, 37 (2003) 159-168

Ashraf M. AMER[*] , Kadry. N. SEDIEK[**]

COMPOSITIONAL AND TECHNOLOGICAL CHARACTERISTICS OF SELECTED GLUACONY DEPOSITS OF NORTH AFRICA

Received March 2003, reviewed, and accepted May 15, 2003

The studied gluacony deposits were collected from the Egyptian and Libyan outcrops. The Egyptian gluacony deposits are widely recorded in the Upper Cretaceous, while Libyan gluacony lies within the Oligocene succession. The collected gluacony rocks were subjected to petrographic and infrastructure investigation. Also chemical investigations using microprobe analysis were carried out on some pellet-like gluacony grains. The results of chemical analysis showed that the studied gluacony grains in both areas did not have identical K_2O content. Egyptian gluacony had from 5.30 to 10.07% K_2O while the Libyan type had relatively higher content of K_2O, which vary from 8.9 to 12.67%. The studied gluacony samples had similar contents of Fe, Al, Cu, and Zn with different contents of Ca, Mg and V oxides. Direct acid leaching laboratory studies were conducted as an alternative route of the roast-leach treatment for the extraction of potassium from studied gluacony. The effects of leaching temperature, acid concentration, leaching time, and particle size were investigated.

Key word: gluacony deposits, petrography, extraction, potassium, leaching

INTRODUCTION

Gluacony deposits are known and represented in many sedimentary formations, especially those of Cretaceous, Eocene and Oligocene ages. Green Sand, Green Marl and Green Earth were the names given to the sediments rich in the yellowish, bluish to greenish black minerals which contain gluaconite. The term gluacony has been used after such eminent workers as Odin and Matter (1981) as well as Van Hauten and Purucker (1984). In spite of numerous works on gluacony all over the world, a few studies have been carried out on the Egyptian gluacony rocks (El Sharkawi and Khalil, 1977; Glenn and Arther, 1990; Ahmed, 1995; and Sediek, 1999). Previously the gluacony deposits were used as fertilizers (Tedrow, 1957).

[*] Alexandria University, Faculty of Science, Environmental Science Department, Alexandria, Egypt
[**] Alexandria University, Faculty of Science, Geology Department, Alexandria, Egypt

Many crops improve with the use of gluacony, especially the forage type. On the other hand some crops are poisoned or burned with the use of gluacony due to the presence of sulfur and sulfides. There is a great need in Egypt for the development of a new process for extraction of potassium from secondary sources to meet the demand of the potassium fertilizer industry (Choudhurry et al., 1973; Soni, 1990; Yedav and Sharma, 1992 and Mazumder and Sharma, 1993). Roast-leach method is considered as a traditional technique used for potassium extraction from the glauconitic sandstone. This investigation aim is to gather data on the mineralogical, petrographic and chemical composition of studied gluacony, kinetic of direct acid leaching of gluacony samples as well as the reaction mechanism.

GEOLOGIC SETTING

The studied gluacony samples were collected from the Libyan and Egyptian outcrops. The Libyan gluacony deposits were taken from the area located in the Northeastern side of Al Jabal al Akhdar, which lies in the northeastern part of Libya about 65 km from Benghazi City. Geologically the Libyan gluacony deposits were created during the late middle Oligocene of Abraque Formation, which occur in the Northwestern side of the Jabal Akhdar anticlinorium, Northern Cyrenaica platform, NE Libya (EL Hawat and Shelmani, 1993). The thickness of these deposits is about 4 meters that is underlain by calcarenitic limestone and overlain by marl limestone. The Egyptian gluacony samples were collected from three main localities, two of them lie in the Western Desert (Abu Tartur Plateau and Gebel Teneda). The third locality lies in the Eastern Desert (Abu Syndyk) close to Wadi Qasseib. The stratigraphic position of the studied gluacony deposits in the Western Desert lies within the upper member of the Phosphatic Formation of Campanian-Maastrichtian (Youssef, 1957; Awad and Ghobrial, 1965), while gluacony of the Eastern Desert lies in the Raha Formation of Cenomanian Age. The Abu Tarture and Teneda gluacony deposits occur in an alternating position with black and gray claystone, siltstone and sandstone beds. On the other hand the Abu Syndyk gluacony alternates with pale yellow to gray skale, marl and limestone bands.

MATERIALS AND METHODS

Thirty gluacony samples were taken from the gluacony beds of the described localities. Thin sections of the collected samples have been examined petrographically under polarized microscope. The gluacony grains or pellets were picked and concentrated after treatment with diluted acetic acid to remove the carbonate material. The picked gluacony grains were examined under binocular microscope to investigate the morphology of the particles. Some of the separated grains were mineralogically investigated by X-ray diffraction (XRD). Others were chemically analyzed with X-ray fluorescence (XRF) and/or microprobe analyses at the Technical University of Berlin (Germany) or Central Laboratory of the Faculty of Science of Alexandria University.

The grains and pellets of six different selected samples have been examined by scanning electron microscopy (SEM) also in the Central Laboratory to define their characteristic nano-structure.

The pressure leaching experiments were carried out in 2 dm^3 capacity vertical autoclave. The experimental procedures and leaching system were similar to that described before (Sharma and Roy, 1979). Before leaching a representative sample of gluacony deposits was ground in a ball mill and sieved into the following fractions (300-180 μm), (180-150 μm), (150-106 μm), (106-75 μm), and (-75 μm). The following parameters regarding potassium extraction were studied: temperature (125-225 °C), hydrochloric acid concentration (20 wt.%), grain size (300-75 μm), leaching time (15-90 minutes).

PETROGRAPHIC INVESTIGATION

LIBYAN GLUACONY DEPOSITS (LG)

The Libyan gluacony rocks are of granular faces. The rock groundmass consists of sand-sized green pellet-like grains. Their sizes vary from coarse sand to coarse silt. The morphological forms of gluacony pelletal grains vary from ovoid, globular, oblate, sphenoid to capsule and are given in order of their decreasing in abundance. These pellet-shaped grains occur as admixture with the carbonate constituents, which are commonly expressed by foraminiferal tests and detritus of nummulites. The components of the admixture here are cemented by micro-sparry calcite. The rock ground mass is free from any detrital quartz grains.

EGYPTIAN WESTERN DESERT GLUACONY ROCKS (WDG)

Sediek (1999) has studied the petrography of the gluacony rock. Two main types have been described. The first was the Abu Tarture dark green structure-less glauconic sandstone, and the second was Teneda light green laminated glauconic sandstone. For both types the pellet-type grain forms dominate and vary from 59 to 68% for the first type and from 58 to 63% for the second one.

EGYPTIAN EASTERN DESERT GLUACONY ROCKS (EDG)

This type of gluacony deposits differs from the above mentioned types, where the rock framework is composed of two main types of grains. The less common grains (about 15%) are represented by quartz and feldspar detritus grains, which show a wide degree of roundness and vary from sub-rounded to angular and display normal to wavy extinction under the crossed nicol. The more common grains (about 60%) are represented by the grass green gluacony grains, their sizes vary from silt to medium sand size and display various forms, which vary from well rounded to irregular elongate grains. Both types of grains are cemented by argillaceous material of brownish staining.

SCANNING ELECTRON MICROSCOPY (SEM)

Gluacony minerals are easily interpreted with the aid of scanning electron microscopy based on the shape and position of the mineral laminae. In the case of Libyan gluacony the SEM microphotograph shows predominantly, closely packed platy and lamellar structure, which commonly characterizes illitic gluacony, interfered with laminae of a swollen lamina creating a box work-like structure of smectite, forming about 20% of the lamellar structure (Fig. 1).

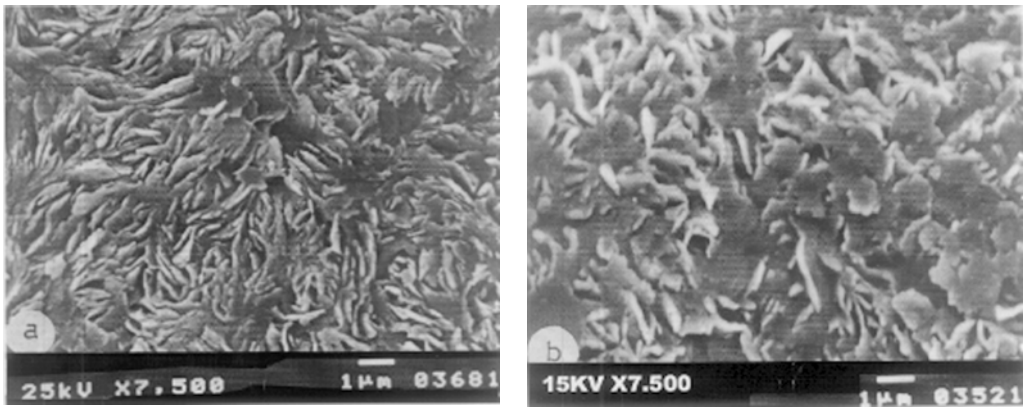

Fig.1 SEM microphotographs of a North Africa gluacony samples (a) Libyan gluacony, (b) Egyptian gluacony

In the Egyptian gluacony (EDG), the SEM microphotograph shows a relatively larger, less closely platy structure, in comparison to the Libyan type. These plates include a swollen lamellar structure of gluacony smectite, forming < 15% of the lamellar structure (Fig.1). The infra-structure of the WDG shows similar characters to the Libyian type (Sediek, 1999).

CHEMICAL COMPOSITION

In order to discuss the chemistry of the gluacony minerals, study the relationship between cation contents one must take in consideration the genesis of these gluacony materials. The results of the microprobe analysis of the representative samples are given in Table l. The obtained data show that the SiO_2 content remains fairly constant at certain level and lies between 49.66 and 54.25%. There is no a great difference of silica contents in different gluacony samples. The silica content resembles the data of Smulikowski (1954) and Odin and Matter (1981). The contents of Al_2O, lie between 5.09 and 13.22%. The highest value is observed for gluacony of the Eastern Desert while the lowest for the Libyan gluacony. Generally, the EDG shows high contents

relatively to the other studied areas either on local or wide scale as in the works ofFoster (1969) and Odin and Matter (1981). The content is high but does not reach the alumina content of Paleozoic gluacony. It means that the alumina content in gluacony deposits more or less depends on the geologic age or at least on the degree of post depositional evolution.

The results of the chemical analysis show more or less wide variation of MgO content, which is between 1.31 and 5.28%, with a relatively higher values for the Libyan type than for the Egyptian one (Table 1). Generally, the obtained results of MgO correspond well with the data given by Odin and Morton (1988). The Fe_2O_3 contents of the studied samples lie between 16.21 and 28.78%. The lowest values were detected in the WDG samples, while the highest content of Fe_2O_3 was recorded in the LG type. The obtained data for Fe_2O_3 agree well with the results of Foster (1969) and Odin (1975). Potassium is a common element in the studied gluacony sediments, and is considered as the main indicator of the behavior and evolution of gluacony. The Libyan gluacony shows high content of potassium (8.90-13.74%) while the Egyptian gluacony contains 5.06-7.40%. The presence of potassium is related to the marine origin.

Table 1. Chemical analysis of some gluacony deposits of North Africa

Sample	SiO_2	Al_2O_3	MgO	K_2O	CaO	TiO_2	V_2O_3	Fe_2O_3	CuO	ZnO
Libyan gluacony										
L.G.1	51.01	5.09	3.49	8.90	0.00	0.00	0.00	28.78	1.35	1.39
L.G.3	49.66	5.48	4.58	13.74	0.00	0.00	0.00	24.45	1.02	1.08
L.G.5	52.00	6.36	4.99	12.00	0.00	0.00	0.00	25.24	1.04	1.04
L.G.7	52.16	6.44	5.28	12.76	0.00	0.00	0.00	20.62	1.04	1.04
Western Desert Egyptian gluacony										
Ab.1	50.04	5.18	2.03	6.24	2.13	0.09	0.00	22.39	0.00	0.00
Ab.4	44.00	6.02	3.08	5.71	2.54	0.18	0.00	25.43	0.00	0.00
T.4	54.25	6.08	2.17	5.55	1.58	0.19	0.00	16.21	0.00	0.00
T.7	51.84	5.67	2.24	5.06	1.53	0.17	0.00	18.33	0.00	0.00
Eastern Desert Egyptian gluacony										
As.1	53.02	7.97	2.51	7.40	0.71	0.09	0.02	22.34	1.13	1.78
As.2	51.63	13.22	1.31	6.78	0.66	0.19	0.00	19.85	2.16	2.00

The results of microprobe analysis shows that the CaO content varies from zero, as in Libyan gluacony to about 2.54 %, as in WDG (Table 1). There is a relationship between the CaO and K_2O content, which occur in the interlayer structure. There is an increasing content of K_2O on the expense of CaO as in Libyan gluacony and vice versa in the Egyptian one (Table 1). Other oxide such as TiO_2,V_2O_3, CuO and ZnO are invariably present in the studied gluacony. The first two oxides are present in trace content (EDG and WDG samples) or are completely absent, as in LG (Table.l). The second two oxides are also invariably present, but in a minor amounts as in LG and EDG, or are completely absent, as in WDG.

TECHNOLOGICAL STUDY

The gluacony deposits were leached for 2 hours at 125-225°C with 20 wt. % HCl and the results are plotted in Figure 2, where the potassium extraction increases with the increasing temperature and acid stoichiometry. More than 90% is extracted within 2 hours at > 150°C. Potassium extraction was 60 and 65% at 175°C and 225°C, respectively. Increasing the acid concentration to 100% of the theoretical acid requirement extracted only 70% of the potassium at 150°C. Increasing the acid available to 120% of the theoretical amount increased the extraction to 85%. Leaching time was investigated to define the minimum retention time for maximum extraction of potassium at a minimum effective temperature.

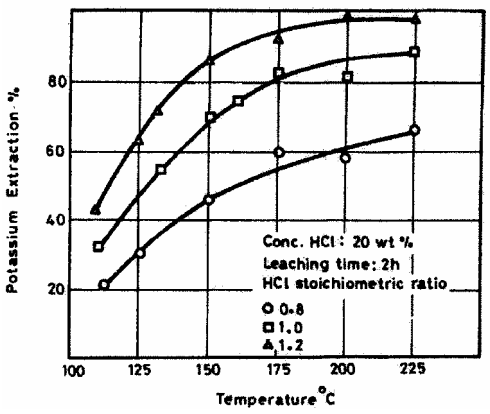

Fig. 2 Effect of temperature on potassium extraction

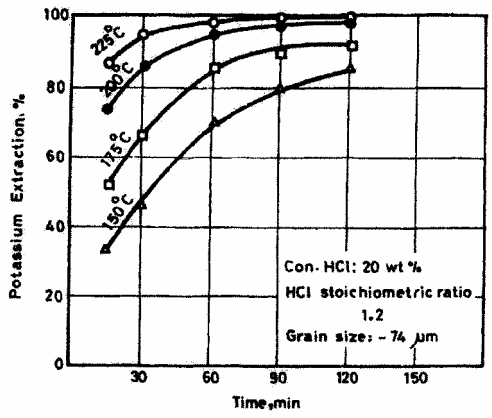

Fig. 3 Effect of leaching time on potassium extraction

The studied gluacony deposits were leached with 20% HCI at 175°C and 200°C for periods of 15 min to 2h. Experimental data are plotted in Figure 3, where more than 90% of potassium was extracted in most experiments that have leaching times of 90 min at temperature 175 to 225°C and all curves showed an increase in potassium extraction with increase in time of leaching. In experiments, which have a stoichiometric ratio equal to 1.2 or greater, about 98 to 99% of potassium was extracted within 60 min for experiments conducted with a stoichiometric ratio of 1:2. Analysis of the experimental data indicates that increasing of HCI stoichiometry from 1.00 to 1.20 is more effective in improving potassium extraction than increasing leaching temperature from 150°C to 200°C, or leaching time from 30 to 90 min (Fig. 3).

Most of the hydrochloric leaching research reported by many authors (Surana and Warren, 1969; Amer, 1994) were made with a 20 wt. % excess of 27% HCl solution. This choice was based on calculations to provide the maximum concentration of potassium chloride. Higher HCl concentrations would cause the precipitation of

$KCl \cdot 6H_2O$ in the leaching slurry, which would lead to blinding the filter. Lower acid concentrations, which would require evaporation using a double extraction, did not improve the filtration characteristics of the residue. From Figure 4, it can observed that the percent of potassium extraction increases with decreasing particle size of glauconitic particles. This may be due to a better liberation of potassium in the finer sizes of gluacony as indicated in Table 2. The behavior of aluminum, silicon and iron during the hydrochloric acid leaching of gluaconite is given in Table 3.

Table 2. Size –wise chemical analysis of gluacony samples

Size (μm)	Weight %	K_2O %
+ 180	9.66	1.99
- 180 + 150	31.37	5.31
-150 + 106	7.80	5.42
-106 + 75	15.16	5.66
-75	6.01	5.71

Table 3. Behavior of alumina, iron and silicon during HCl pressure leaching of the gluacony samples

Experiment No.	Stoichio-metry	Temp. C°	Analyses						
			Pregnant liquor				Residue		
			Al_2O_3	Fe_2O_3	HCl	Density	Al_2O_3	Fe_2O_3	SiO_2
1	0.8	125	5.0	0.11	4.88	1.139	24.4	0.63	59.0
2	0.8	150	7.3	0.15	N.d	1.164	13.5	0.45	66.6
3	0.8	175	7.5	0.16	N.d	1.162	11.2	0.35	70.8
4	0.8	200	7.1	0.15	N.d	1.170	10.9	0.62	75.2
5	0.8	225	5.8	0.15	0.09	1.154	9.91	0.57	76.4
6	1.0	125	7.5	0.16	N.d	1.195	8.55	o.31	69.5
7	1.0	125	8.2	0.17	N.d	1.212	6.80	0.28	81.8
8	1.0	125	8.5	0.19	0.46	1.217	3.28	0.19	83.5
9	1.0	125	8.6	0.19	N.d	1.217	1.65	0.15	85.5
10	1.2	125	3.4	0.07	N.d.	N.d.	27.2	0.68	55.0
11	1.2	135	6.1	0.13	N.d.	1.177	13.5	0.49	73.4
12	1.2	150	6.5	0.14	3.93	1.193	2.92	0.17	77.8
13	1.2	175	7.3	0.16	N.d.	1.197	0.86	0.14	85.3
14	1.2	200	7.3	0.16	3.38	1.197	0.81	0.12	85.3
15	1.2	225	6.5	0.14	N.d.	1.190	0.61	0.12	87.4

N.d = Not determined

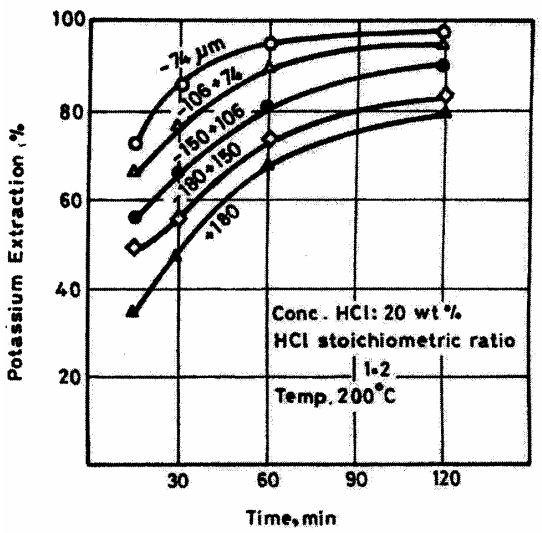

Fig. 4. Effect of particle size on potassium extraction

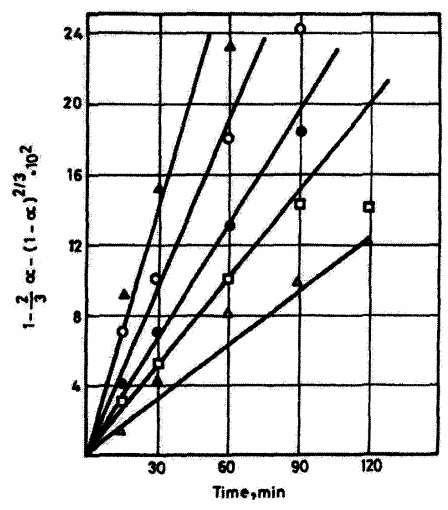

Fig. 5. Relation between 1- 2/3 α-(1-α)²/³ and t

KINETIC ASPECTS

The identification of the reaction mechanism constitutes an important step in the analysis of the high temperature kinetic data. For this purpose the Ginstling-Brunshtein equation has been used:

$$1 - 2/3\ \alpha - (1 - \alpha)^{2/3} = Kt$$

where α is the fraction of potassium converted to potassium chloride, K the rate constant and t is the leaching time. The values of $1 - 2/3\ \alpha - (1 - \alpha)^{2/3}$ have been plotted against time t as shown in Figure 5. For further confirmation of the rate-controlling step, the data presented in Figure 3 are represented using the Ginstling-Burnshtein equation, the plots are shown in Figure 5. As these plots also yielded straight lines, it is conformed that the present process is diffusion controlled. For determination of the apparent activation lines, as shown in Figure 6, K values were plotted against 1/t as shown in the Arrhenius plot (Fig. 7), where the value of the calculated activation energy equals to 16.6 kJ/mol. This value agrees with the diffusion controlled mechanisms of Levenspiel (1972).

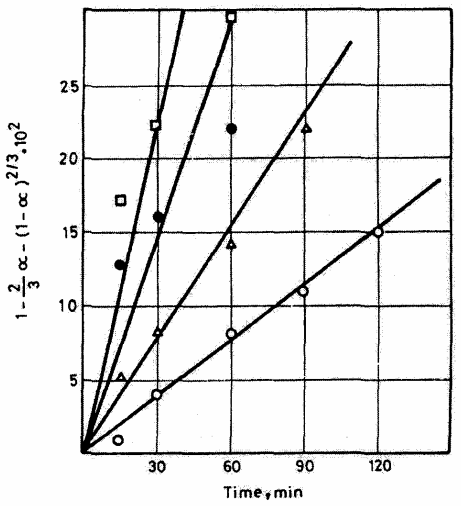

Fig.6. Ginstling- Brunshtein plot for different particle size

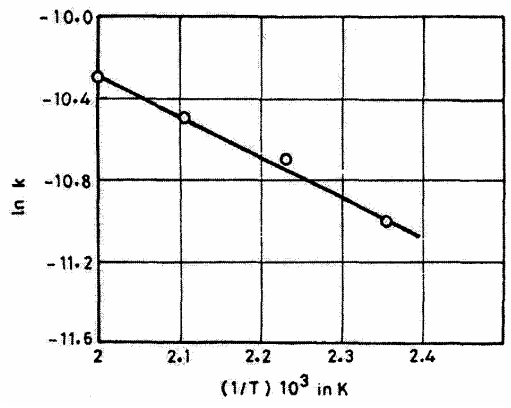

Fig.7. Arrhenius plot for determination of apparent activation energy

CONCLUSION

The studied gluacony rocks contain grains with granular faces. They form a considerable percent of the rock framework and vary from 60 to 68%. The remaining percent is represented either by detrital quartz or by carbonate grains. The results of chemical analysis proves that the gluacony pellets have high silicon, aluminum, iron oxides and considerable percent of potassium, while low percent of calcium and magnesium oxides. Other oxides as TiO_2, V_2O_3, CuO and ZnO are also present but in trace amounts. A direct hydrochloric acid processing of the Egyptian and Libyan gluacony deposits was carried out to produce chlorides of potassium and aluminum by a autoclave leaching as an alternative route to the roast-leach processing technique. The most favorable conditions for extraction of 95% of the potassium present in the gluacony deposits of both Egyptian and Libyan types are: temperature 200°C, acid concentration 20% by weight, gain size -75 μm, and leaching time 90 min. Calculation of the temperature dependence of the rate constant gives the activation energy of 16.6 kJ/mol, which is consistent with the values of the activation energies reported for diffusion controlled reactions.

REFERENCES

AMER, A.M. (1994), *Hydrometallurgical processing of Egyptian black shale of the Qusseir-Safaga region,* Hydrometallurgy, 36, 95-107.

AHMED, E.A. (1995), *Mineralogical and geochemical characteristics of some Upper Cretaceous gluaconites of Abu Tartur and Red Sea areas*, Egypt. Bull., Fac. Sci., Assuit University, 24, 23-52.

AWAD, G.H. and GHOBRIAL, M.G. (1965), *Zonal stratigraphy of the Kharga Oasis*. Geol. Surv. Egypt, Paper No. 34, 77.

CHOUDHURRY, R.,BALAGOPAL, A.T., and BANERJEE, K.C. (1973), *Availability of potash from non-traditional sources,* Technology 10, 128-131.
EL SHARKAWI, M.A. and KHALIL, M.A. (1977), *Gluaconite, a possible source of iron for El Gedida iron ore deposits,* Bahariya Oasis, Egypt. Egyptian J. Geo., 21, 109-117.
GLENN, R. G. and ARTHER, M. A. (1990), *Anatomy and origin of a Cretaceous phosphorite - green sand giant*, Egypt. Sedimentology, 37, 123-154.
EL- HAWAT, A.S. and SHELMANI, M.A. (1993), "*Short notes and guidebook on the geology of A1 Jabal A1 Akhdar Cyrenaica, NE Libya"*. 70p., Benghazi Libya. LEVENSPIEL, O. (1972), *Chemical Reaction Engineering*, Wiley, New York , 2"d. Ed. P. 3 57-3 77.
FOSTER, M.D. (1969), *Studies of celadonite and gluaconite,* U. S. Geol. Surv., Professional Pap. 614F: 17.
ODIN, G.S. (1975), *De gluaconiarium costitione, origine acetateque*, Ph.D. Dis., Univ. Pierre Et Marie Curie, Paris: 280.
ODIN, G.S. and MATTER, A. (1981), *De gluaconiarum origine,* Sedimentology, 28, 611-641.
ODIN, G.S. and MORTON, A.C. (1988), *Authigenic green particles from marine environment,* In: Development in Sedimentology, 43, Diagenesis, II, (Chiligarian, G. V., and Wolf, K.H. editors) Elsevier : 213-268.
SEDIEK, K.N. (1999) *Contribution to the sedimentation of some gluacony deposits of the Kharga-Dakhla stretch, Western Desert*. Egyptian Miner. J. Egypt. 11, 211-230. SMULIKOWSKI, K. (1954), *The problem ofgluaconite*, Pol. Akad. Nauk. Komitet. Geol., Arc. Min. Warsaw, 18, 21-21.
SONI, M.K. (1990), *On the possibility of using gluaconite sandstone as a source of raw material for potash fertilizer*, Ind. Min. Eng. Tour. Nov. 3-10.
SURANA , V. S. and WARREN, H.I. (1969), *The leaching of goethite,* Trans. Inst. Min. Metall. 78, 133-149.
TEDROW, C.F. (1957), *"Greensand Soils subject of study by Station Scientists",* New Jersey Agriculture, Nov.-Dec., 3.
YEDAV, V.P. and SHARMA, T. (1992), *Leaching ofgluaconite sandstone in acid lixiviants,* Min. Eng., 5, 715-720.
MAZUMDER, A.K., SHARMA, T. and RAO, T.C. (1993), *Extraction ofpotassium from gluaconite sandstone by the roast-leach method,* Int. Jour. Min. Processing. 38, 111-123.
VAN HAUTEN, F.B. and PURUCKER, M.E. (1984), *Gluaconitic pelloids and chamositic ooids favorable factors, constraints and problems*, Earth Sci. Rev., 20, 211-243.
YOUSSEF, F. I. (1957), *Upper Cretaceous rocks in Kosseir area*, Bull. Inst. Desert, Egypt. 7, 3 5-54.

Amer A.M., Sediek K.N., *Skład i charakter technologiczny glaukonitu ze złóż w północnej Afryki,* Physicochemical Problems of Mineral Processing, 37 (2003) 159-168 (w jęz. ang.)

Badaniom poddano złoża glaukonitu znajdujące się w Egipcie i Libanie. Złoże egipskie pochodzi z okresu Dolnej Kredy, podczas gdy złoże libańskie pochodzi z Oligocenu. Skały glaukonitowe badano petrograficznie oraz analizowano ich strukturę wewnętrzną. Dodatkowo przeprowadzono badania za pomocą mikrosondy wybranych próbek glaukonitu z dwóch złóż, nie mają identycznych zawartości K_2O. Glaukonit pochodzący z Egiptu zawierał od 3,9 do 12,6% K_2O. Badane próbki glaukonitu z Libanu zawierały od 3,9 do 12,6%. Badane próbki glaukonitu zawierały taką samą ilość Fe, Al, Cu i Zn. Różnice wystąpiły w przypadku tlenków Ca, Mg i V. Bezpośrednie kwasne ługowanie było przeprowadzone w warunkach laboratoryjnych. Badania nad ługowaniem zostały przeprowadzone jako alternatywna metoda ekstrakcji potasu. Badano wpływ temperatury, stężenia kwasu, czas ługowania oraz wielkość ziaren na parametry procesu.

Physicochemical Problems of Mineral Processing, 37 (2003), 169-181
Fizykochemiczne Problemy Mineralurgii, 37 (2003) 169-181

Antoni CIEŚLA*

PRACTICAL ASPECTS OF HIGH GRADIENT MAGNETIC SEPARATION USING SUPERCONDUCTING MAGNETS

Received March 2003, reviewed, and accepted May 15, 2003

Since the 1970s, magnetic separation has been increasingly used for purification of liquid, such as heavy-metal ion removal from laboratory waste-water, purification of kaolin clay in the paper-coating industry, waste water recycling in the steel industry, and recycling of glass grinding sludge in cathode-ray tube polishing factories. In the 1980s, large superconducting magnets were adopted for the field coils of high-gradient magnetic separation system used for kaolin clay purification.

In this paper some practical aspects of the construction of a matrix high-gradient separator equipped with the DC superconducting electromagnet as well as the problems of working conditions of the separator are presented.

Key words: magnetic separation, DC superconducting electromagnet, high – gradient magnetic separation, matrix separator

INTRODUCTION

The phenomena of magnetism and magnetic behaviour of materials have allowed the process of magnetic separation to be successfully employed in industrial processing. A wide variety of magnetic separation systems exist that have been used for industrial beneficiation processes for many years. Whether by a lifting, trapping or deflection technique, a magnetic field is generated that will selectively act upon one material in preference to another by virtue of their different magnetic response. Several forms of magnetic behaviour exist but perhaps the most important, with regard to high field superconducting magnets, is the group defined as paramagnetic. Many ele-

* AGH - University of Science and Technology, Department of Electrical Engineering, al. Mickiewicza 30, PL 30 - 059 Kraków, Poland, e-mail: aciesla@uci.agh.edu.pl

ments and inorganic compounds exhibit a low level positive response to the applied magnetic field, but to act upon particles by a magnetic field a high magnetic force is required. One of the most successful industrial applications of magnetic separation is the High Gradient Magnetic Separation (HGMS) removal of colour influencing contaminants from kaolin. For several decades large magnet systems have been employed to increase the brightness and remove contamination from this slurried material in order to improve its whiteness and so increase its commercial value. Initially, large power hungry resistive based magnet systems were used, but as the science and technology associated with superconductivity improved, these resistive systems have been replaced with superconducting magnet based systems. The introduction of superconductivity to this industry was significantly accelerated as a result of resistive coil burnouts. Rather than return a power hungry coil to operation, a superconducting coil replacement has been used instead. Many such "retrofits" have been carried out to reducing the power consumption from 300 to 400 kW, down to something in the in the order of 80 kW with the first system. Due to physical geometry of these systems and the requirement for a massive iron casing to focus the magnetic field, they were required to operate in switch on / switch off mode in order for the magnetic materials trapped on the gradient enhancing stainless steel matrix to be removed.

In this paper some practical aspects of the construction of a matrix high-gradient separator equipped with the DC superconducting electromagnet as well as the problems of working conditions of the separator are presented.

PRINCIPLE OF USE

When fine particles are dispersed in air, water, sea water, oil, organic solvents, etc., their separation or filtration by using a magnetic force is called magnetic separation. To increase the separation efficiency of these systems we must increase the magnetic force acting on particles by increasing the particle volume, relative magnetization between the particles (dispersoid) and the dispersion medium, the magnitude of the magnetic gradients (Ohara, 2001).

To understand the principles of magnetic separation for this, let us consider the magnetic forces (Ohara, 2001). By calculating the gradient of magneto-static energy difference between magnetized particles of volume, V_p and the dispersion medium of the same volume, ΔU_p, the magnetic force acting on a particle, $\vec{F}_m$, is:

$$\vec{F}_m = -\nabla\left(\Delta U_p\right) = -\nabla\left\{\frac{V_p\left(\mu_0 \vec{M}_p \cdot \vec{H}\right)}{2} - \frac{V_p\left(\mu_0 \vec{M}_f \cdot \vec{H}\right)}{2}\right\} \tag{1}$$

where:

$\vec{M}_p$ - particle magnetization, [A · m^{-1}]

$\vec{M}_f$ - magnetization of dispersion medium, [A · m^{-1}]

$\vec{H}$ - magnetic field. [A · m^{-1}]

By assuming a spherical particle with volume magnetic susceptibility, χ_p , and uniform magnetization $\vec{M}_p$, we obtain:

$$F_{m\xi} = V_p \cdot \mu_0 \cdot M^* \cdot \nabla_\xi H, \qquad \xi = x,y,z, \tag{2}$$

where:

$$M^* = H_0 \frac{9(\chi_p - \chi_f)}{(3+\chi_p)(3+\chi_f)} \tag{3}$$

χ_f - volume magnetic susceptibility of the dispersion medium, [-]

M^* - relative magnetization between the dispersoid and the dispersion medium, [A ·m^{-1}]

H_0 - applied magnetic field. [A ·m^{-1}]

Equation (2) indicates that the magnetic force on particles depends on three key parameters: V_p , M^*, and $\nabla_\xi H$. For $F_{m\xi} \neq 0$, V_p , M^*, and $\nabla_\xi H$ are all non-zero. Therefore, Eqs. (2) and (3) indicate that to generate a magnetic force ($F_{m\xi} \neq 0$), a dispersoid with susceptibility different from that of the dispersion medium (i.e., $\chi_p \neq \chi_f$) must be placed in nonhomogeneous magnetic field (i.e., $\nabla_\xi H \neq 0$).

When the dispersed particle is weakly magnetized, $M^* = (\chi_p - \chi_f)H_0$, and $F_{m\xi}$ is proportional to the susceptibility difference between the dispersoid and the dispersion medium; to H_0 ; and to $\nabla_\xi H$. When the dispersoid is a ferromagnetic particle, M_p becomes saturated at a relatively low magnetic field strength. The enhancement of $F_{m\xi}$ through the use of strong magnetic field is therefore limited. M_p also becomes saturated at relatively small susceptibilities of $\chi_p \sim 10$ because M_p is proportional to $\chi_p/(1+N\chi_p)$, where N is a demagnetizing factor.

Effective ways of enhancing the magnetic force include: (a) increasing M_p by "magnetic seeding" of the dispersoid, (b) increasing $\nabla_\xi H$, (c) using high intensity magnetic fields, and (d) selecting a dispersion medium with a large value of $(\chi_p - \chi_f)$.

Various devices have been used to generate strong magnetic forces, which are described in detail elsewhere (Ohara, 2001). Methods for increasing the magnetic field gradient include superconducting coils in a drum-type separator, multi-pole supercon-

ducting coil in separators or HGMS systems. In High Gradient Magnetic Separators, a field gradient $|(\nabla H)|$, as high as $1.6 \cdot 10^{10}$ A/m^2 ($|\nabla(\mu_0 H)|$ = 20,000 T/m) is reached, and the magnetic force is enhanced by a factor of 1000 – 10,000 (Ohara, 2001).

Before the development of HGMS, magnetic separation was only performed on large diameter ferromagnetic particles, while using HGMS, weakly magnetized particles down to tens of microns can be magnetically separated in practical systems. High-gradient magnetic fields are generated near a ferromagnetic wire with several hundred microns in diameter placed under an applied uniform magnetic field. If the magnetic field is strong enough, in principle, all the particles with either positive or negative magnetic susceptibility dispersed in the medium are captured onto the wire. Weakly magnetized particles and typical dispersion media have magnetic susceptibilities much smaller than 1. Substituting this condition into Eq. (3) yields $M^* = (\chi_p - \chi_f)H_0$ and $F_m \propto (\chi_p - \chi_f)H_0(\nabla H)$ (Eq. (2)). Thus, use of high intensity, high gradient magnetic fields is necessary to increase the magnetic force on magnetic particles. In conventional magnetic separators this force is less than 0.01 % of the magnetic force acting on ferromagnetic particles, and is usually disregarded. However, because the magnetic field gradient of HGMS systems is much higher than that used in conventional magnetic separators, separation of weakly magnetized particle is now possible. It is confirmed by Fig. l. where various types of magnetic separators, used for separation of particles with different magnetic properties and granulations, are presented (Svoboda, 1987).

TYPES OF THE HIGH GRADIENT MAGNETIC SEPARATORS

The discussion presented in above section reveals that the HGMS separators have numerous applications. Thus, that type of the separators will be the subject of the following considerations.

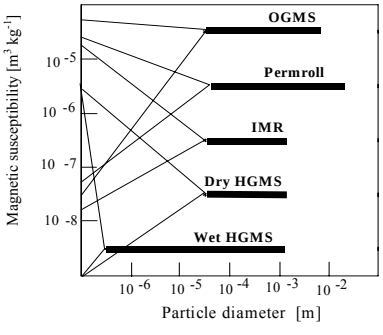

Fig. 1. Particle size ranges of high-intensity magnetic separators (Svoboda, 1987)

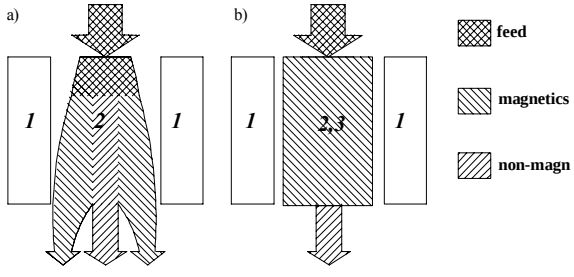

Fig. 2. High Gradient Magnetic Separators: a) deflecting separator, b) matrix separator 1 – source of magnetic field, 2 – separation zone, 3 – matrix of the separator (Cieśla, 1996)

There are two kinds of separators for separation of mixtures with HGMS using superconducting magnets: deflecting and capturing (matrix) separators (Fig. 2).

The deflecting separators are continuous devices in which the magnetic field deflects the magnetic fraction from a vertical stream of a slurry. The separation takes place in the region of strong nonhomogenity. The most common constructions of the source of the magnetic field in deflecting separators are solenoids of various configurations, e.g. dipoles, multipoles, quadrupoles etc. Selection of the proper configuration depends on the value of magnetic induction, as well as on physical properties of the material to be separated. The systems mentioned above are of complicated construction and of considerable cost, particularly for auxiliary equipment (nontypical forms, of a cryostat, for instance).

In matrix separators a solenoid coil of a simple design generates the field. The field nonhomogeneity does not result from the form of the coil but is generated by ferromagnetic elements (e.g. steel wool fibres). This ferromagnetic material is placed in a canister introduced into the magnetic field. The magnetic fractions of the feed pass through the matrix (a canister with steel wool) and are attached to the ferromagnetic elements. The non-magnetic particles are collected outside the matrix. This type of a device is treated as a magnetic filter.

High gradient matrix separator often operates in a cyclic mode. After the matrix is loaded with captured particles (after effective time t_e), a cleaning stage must follow (dead time t_d). In order to increase the effectiveness - the time t_e must be increased and t_d reduced. Cleaning of the matrix takes place in absence of magnetic field. The field on the matrix can be removed by three methods: by ramping the current in the magnet down, by using a continuously moving matrix, e.g. carousel, and by using a reciprocating canister.

A comparison of the separators characteristics is presented in Table 1 (Cieśla, 2000)

Table 1. Comparison of deflecting and matrix magnetic separator (Cieśla, 2000)

Type of Separator	Deflecting	Matrix
Principle of Operation	Continuous	Cyclic
Winding Design	Complex (dipole, multipole and quadrupole)	Simple (solenoid)
Cryostat Design	Complex (the separation channel must be near the winding)	Simple
Separator Design	Simple	Complex (matrix replacement is necessary)
Size of material to be separated [μm]	≤ 20	≤ 1
Throughput [t/h]	up to 100	up to 20

The comparison of both high-gradient separators presented in Table 1 leads to a conclusion that separation of μm granulation is carried out with matrix separator (magnetic filters).

KINETIC MODEL OF THE SEPARATION IN MATRIX HGMS

A comfortable tool to consider the kinetics of extraction of particles from a slurry by magnetic force in the matrix separator is the so-called macroscopic model (Cieśla, 1996). It can be assumed that the physical properties of the slurry flowing through the matrix separator (see Fig. 3) does not change.

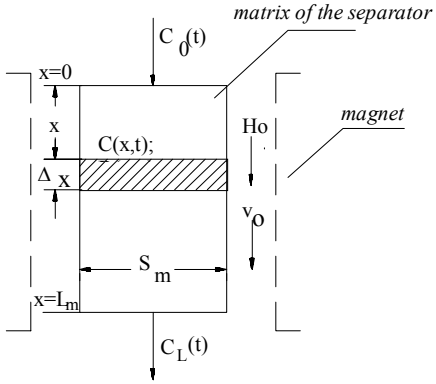

Fig. 3. Slurry of concentration $C_0(t)$ is flowing across the matrix separator (Cieśla, 1996)

The extraction of particles during the separation process can be characterised by the following equations (Cieśla, 1996):

$$\frac{\partial P(x,t)}{\partial t} = \beta C(x,t)\left[1 - \frac{P(x,t)}{A}\right] \tag{4}$$

$$\frac{\partial C(\mathrm{x,t})}{\partial t} + v_0 \frac{\partial C(\mathrm{x,t})}{\partial x} + \frac{\partial P(\mathrm{x,t})}{\partial t} = 0 \tag{5}$$

where:

$P(x,t)$ - concentration of particles captured in the separator, [kg ·m^{-3}]
$C(x,t)$ - concentration of particles in the slurry that flows through the separator, [kg ·m^{-3}]
A - maximum value of the concentration of particles that were captured by the matrix , [kg ·m^{-3}]
β - activity factor of the deposition process, which takes into account all aspects of the particle extraction by the magnetic field, [s^{-1}]
t - time of the extraction, [s]
x - position of the particles in the matrix, [m]
v_0 - velocity of slurry flow across the matrix, [m ·s^{-1}]

Solution of equation (4) and (5) by taking into account the initial and boundary conditions:

$$P(x,t)=\begin{cases} A\dfrac{e^{-\frac{C_0\beta}{v_0}(x-v_0)}-1}{e^{-\frac{C_0\beta}{v_0}(x-v_0)}+e^{-\frac{A\beta}{v_0}x}-1} & for\ \ x-v_0t\le 0 \\ 0 & for\ \ x-v_0t>0 \end{cases} \tag{6}$$

$$C(x,t)=\begin{cases} C_0\dfrac{e^{-\frac{C_0\beta}{v_0}(x-v_0)}}{e^{-\frac{C_0\beta}{v_0}(x-v_0)}+e^{-\frac{A\beta}{v_0}x}-1} & for\ \ x-v_0t\le 0 \\ 0 & for\ \ x-v_0t>0 \end{cases} \tag{7}$$

where:

$$\beta=\frac{2R_k\lambda_0 v_0}{S_k\varepsilon_0} \tag{8}$$

$$A=\frac{\varepsilon_0}{4}\rho_c\left(a^2-1\right) \tag{9}$$

$$2R_k\lambda_0=D\left(\frac{4d^2\chi_c H_0 H_p S_c}{9\pi\eta v_0}\right)^{1/3} \tag{10}$$

$$a=\frac{r_{msr}}{R_k}$$

Full description of the mathematical model and its interpretation of the symbols are given elsewhere (Cieśla, 1996).

To consider the influence of the parameters on the separation effectiveness, the author proposes to transform formula (7) (for x = L_m) as follows:

$$\frac{C(x,t)}{C_0}\Big|x=L_m=\frac{C_{out}(t)}{C_0}=N=\frac{1}{1+e^U\left(e^T-1\right)} \tag{11}$$

where:

$$U=\frac{C_0\beta}{A}\left(\frac{x}{v_0}-t\right),\qquad T=\frac{\beta x}{v_0}$$

Formula (11) show the parameters which make the separation possible. The values are as: velocity of slurry flow across the matrix v_0, packing factor of porous medium with ferromagnetic elements ε_0, diameter of the gradient-creating element R_k. How-

ever, the most essential parameter, influencing not only the quality of the process but also the time of the effective working time of the separator is a magnetic induction.

Subsequent steps of a grain movement in the vicinity of the ferromagnetic element of the matrix – collecting grains of particular magnetic properties – are presented in Fig. 4. The analysis of the grains movement allows to find the width of the collector "pick up" zone in the matrix, which is $2R_k\lambda_0$ (see Eq. (10)).

One can learn from Fig. 5 that the magnetic induction determines the width of the catching zone. The rise of the zone width causes also prolongation of the effective working time of the separator. It results from the increase of ability of the matrix to accumulate greater number of particles.

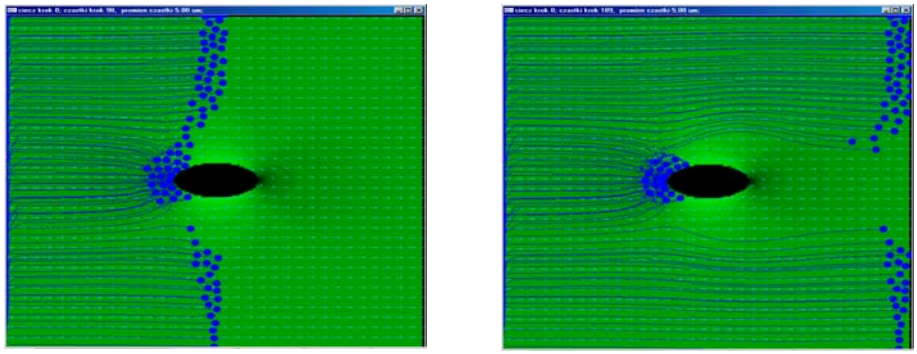

Fig.4. Steps of particles movement in the vicinity of the collector in the matrix separator (Cieśla, 2003)

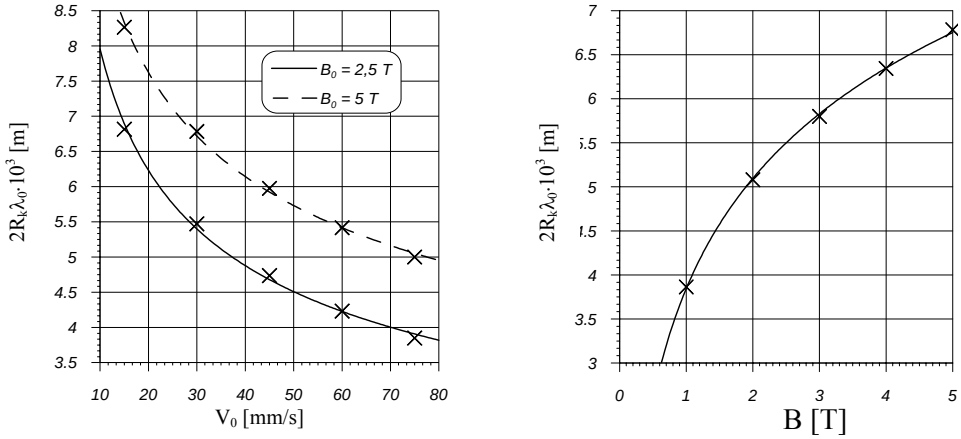

Fig.5. "Pick up" zone width ($2R_k\lambda_0$) vs. velocity of slurry flow through the matrix separator for induction B_0 = 2,5 T and B_0 = 5 T (a) and magnetic field induction in separator matrix for v_0 = 0.03 ms^{-1} (b) (Cieśla, 2000)

A confirmation of this argument is Fig. 6 presenting the dependency $N = f(t)$ (Eq.11) for three magnetic inductions and two slurry flow velocities across the matrix. The particles concentration at the separator outlet versus the inlet concentration C_0 changes considerably with the time of the separation. When a defined concentration of slurry in the filter outlet is requires, then the filtration process must be stopped after the time called the effective working time of the filter, t_e. After time t_e, the factor N exceeds the assumed value.

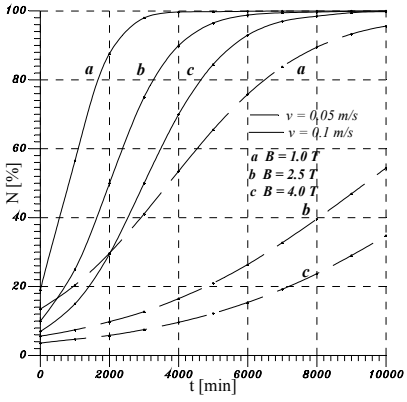

Fig. 6. Factor N vs. the separation time t (Cieśla, 2000)

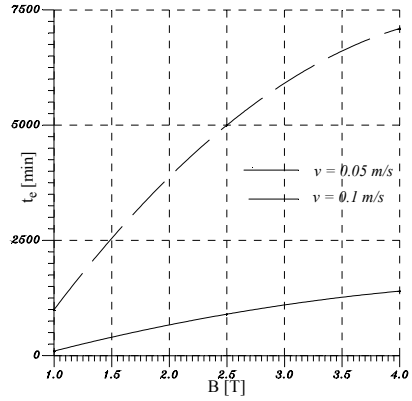

Fig. 7. Effective filtration time t_e vs. magnetic induction B (Cieśla, 2000)

For example, it has been assumed that the N value should not exceed 20% and, on the basis of data from Fig. 6, the dependency of the time t_e vs. magnetic induction has been plotted (Fig. 7). One can notice essential increasing of the effective working time of the separator following the induction growth. So, the effectiveness of the separation process also increases. The presented data univocally confirm that application of strong magnetic field in the separation process is beneficial. So, the best devices to generate the fields are the superconducting electromagnets.

CONSTRUCTIONS OF SUPERCONDUCTING MAGNETIC SEPARATORS ON A COMMERCIAL SCALE

In some references (Brevis 1996, Richards 1997, among others), one can find informations on practical applications of HGMS devices (also with superconducting magnets): e.g. for concentration of iron ores (ilmenite, hematite, goethite, limonite), concentration of paramagnetic minerals (wolframite, chromonite, ilmenite), rejection of paramagnetic minerals (siderite or ilmenite from cassiterite). There are 2 versions of magnetic separators – based on the way of matrix cleaning. In the first one, proposed by ERIEZ Magnetics, accumulation ability renewal (cleaning) of the matrix

takes place when the magnetic fields is turned off. Proper position of feed check valves allows to get considerable pressure of cleaning water that rinses out magnetic particles from the steel wool fibres. After the matrix cleaning, re-set of the valves begins next cycle of the separation. The commercial scale construction of ERIEZ Magnetics is given in Fig. 8 (Watson, 1994).

Fig. 8. View of the superconducting HGMS built by Eriez Magnetics, Erie, PA, USA and installed at the plant of J.M. Huber where it has been on line since 8 May 1986 (Watson, 1994).

Another type of the superconducting magnetic separator is a " reciprocating" device constructed and patented by CARPCO SMS Ltd (Watson 1994). This construction is preferred for technical and economical reasons. The dead time is limited to the time of translocation of the matrix in the filter canal. A construction of this type device on industrial scale is presented in Fig. 9 (Bulletin, 1996).

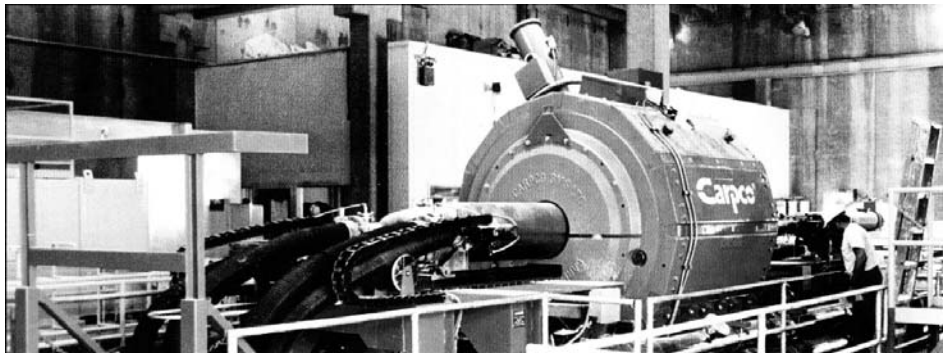

Fig. 9. View of the superconducting magnetic separator ("reciprocating canister" type), built by Carpco SMS Ltd. (Bulletin, 1996)

SYSTEMS COOPERATING WITH A SUPERCONDUCTING MAGNETIC SEPARATOR

The use and operation of superconducting electromagnets as a source magnetic field in magnetic separators and filters is much more complicated than with conventional ones owing to the existence of strong magnetic fields, high energies accumulated in windings, low temperatures and a vacuum present. Superconductor electromagnets should be equipped with installations that comply with requirements and rules of cryogenic and vacuum technologies; also, they must respect characteristic conditions necessary for an electromagnet to operate, such as: cryostat and winding cooling, feeding of the winding, normal operation conditions, and emergency states during the operation. In Fig. 10 a block diagram of a system is presented which enables the operation of a superconducting electromagnet.

The operation cycle of the superconducting separator consists of four following in succession phases: 1 - cooling of the cryostat, 2 - supplying with electrical power, 3 - stable work under rated current (separation cycle), 4 - switching off the supply and heating of the cryostat.

Some exemplary curves $T = f(t)$ and $B = f(t)$ for the operation cycle of the separator are presented in Fig. 11. The temperature change during cooling of the cryostat is presented (as magnified characteristic). The noticeable increase of temperature results from exchange of the vessel for liquid helium.

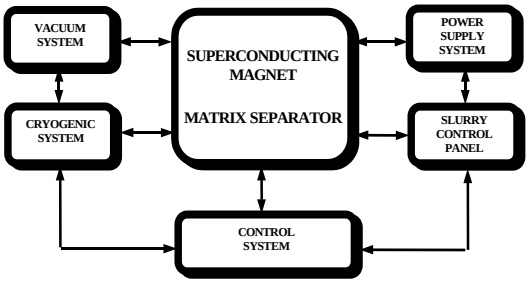

Fig. 10. Functional relations among systems co-operating with superconductor electromagnet (Cieśla, 2003)

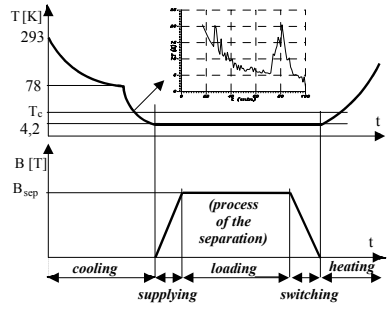

Fig. 11. Operation cycle of superconductor separator (Cieśla, 2003)

LABORATORY SUPERCONDUCTOR SEPARATOR AT AGH

A scheme of a laboratory superconductor magnetic separator at AGH - University of Science and Technology is presented in Fig. 12. Its technical data: $B_{max} = 6$ T (in the centre of the separator canal), volume of the matrix = $1{,}5 \cdot 10^{-3}$ m^3, diameter of the magnet canal = $5.4 \cdot 10^{-2}$ m.

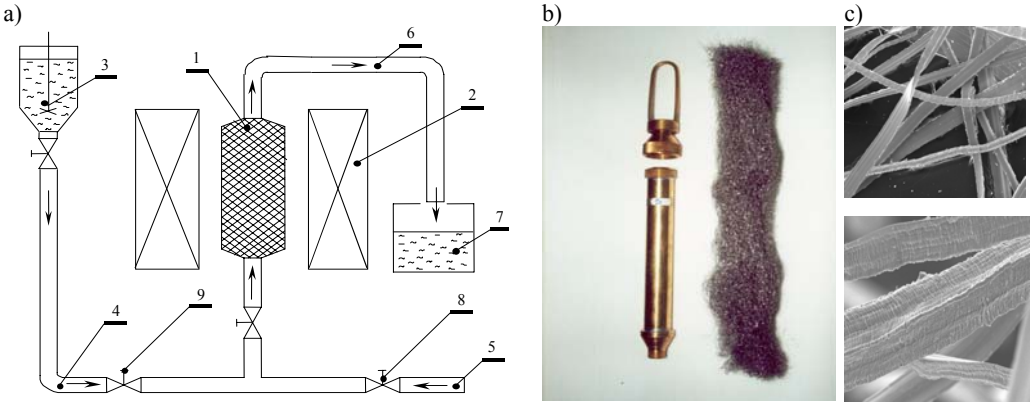

Fig. 12. Superconducting separator for HGMS: a) scheme separator, b) matrix separator, c) filling matrix with stainless steel magnetic wool (wool seen with a magnifier) 1 – matrix of separator, 2 – winding of superconducting magnet, 3 - container for feed to be separated, 4 – stream of feed, 5 – stream of rinse water, 6 – stream of separation product, 7 – container for separation product, 8, 9 – valves (Cieśla, 2003)

CONCLUSIONS

The high force separation capabilities of superconducting magnets and their application for the most difficult separation problems of paramagnetic or low susceptibility materials are now recognised. The advances made in superconducting technology over the recent years have meant that this technology, at one time limited to the research, can now truly enter the industrial processing environment with confidence.

To promote new applications for superconductor magnetic separation, the fusion of science and technology from diverse areas is required. It can be executed through the interchange and co-operation of researches working in different fields: including superconductivity, electrical engineering, and mechanical engineering for equipment improvement, chemical engineering and applied chemistry for separation system and environmental, sanitation, and resource engineering for practical utilization of these systems (Fig. 13). Organizations that promote the exchange of research information from different technical fields and collaboration are very desirable.

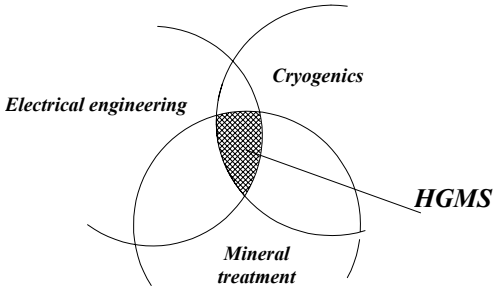

Fig. 13. HGMS process
as a complex issue of separation

REFERENCES

BREVIS T. (1996): *Magnetic Separation,* Mining Magazine, Vol. 175, No. 4, 192 -202.

BULLETIN (1996) *Bulletin No 9621 – 7KDP ©CARPCO, INC.*, 1996.

CIEŚLA A. (1996): *The analysis of the matrix separator operating states with the superconductor magnet constituting a source of field*, (in Polish): Wyd. AGH, ser.: Dissertations, Monographs, No 44.

CIEŚLA A. (2000): *Superconductor Magnetic Filter: Industrial Construction*, Proc. Third International Conference Electromagnetic Devices and Processes in Environment Protection ELMECO 2000, Nałęczów, 4 – 6 June 2000, pp. 174 – 182.

CIEŚLA A. (2003): *Use of the Superconductor magnet to the magnetic separation. Some selected problems of exploitation*, to be published in: International Journal of Applied Electromagnetics and Mechanics, 18 (2003).

OHARA T. et al.: (2001): *Magnetic separation using superconducting magnets*, Physica C 357 – 360, pp. 1272 – 1280.

RICHARDS D. et al.: (1997): *Commercial acceptance of superconducting magnetic separation.* Proceedings of the XX IMPC – Aachen, 21 - 26 September 1997, pp. 638 - 648.

SVOBODA J.(1987): *Magnetic Methods for the Treatment of Minerals.* Elsevier Science Publishers B.V.

WATSON J.H.P.(1994): *Status of Superconducting Magnetic Separation in the Mineral Industry*. Minerals Engineering, 7**,** No 5/6, pp. 737 – 746.

ACKNOWLEDGEMENT

The work presented in this paper was supported by the Polish State Committee for Scientific Research, Warsaw, in the frame of project Internal Research ("Badania własne"), Kraków, 2003.

Cieśla A., *Praktyczne aspekty wysokogradientowej separacji magnetycznej z zastosowaniem magnesów nadprzewodnikowych,* Physicochemical Problems of Mineral Processing, 37 (2003) 169-181 (w jęz. ang.)

Nową metodą wzbogacania, rozwijaną od kilku lat w świecie, jest metoda magnetycznej separacji wysokogradientowej (High Gradient Magnetic Separation - HGMS) z wykorzystaniem elektromagnesów nadprzewodnikowych jako źródeł pola magnetycznego. Metoda ta stwarza nowe możliwości wydzielania składników zawartych w surowcach, a niedostępnych zarówno dla dotychczas stosowanych technik separacji magnetycznej jak i wszelkich innych fizycznych metod rozdziału. Jedną z odmian konstrukcyjnych separatora wysokogradientowego jest separator matrycowy. W pracy przedstawiono fizyczne podstawy separacji magnetycznej, z których wynika jednoznacznie celowość stosowania nadprzewodnikowych separatorów matrycowych, opisano konkretne instalacje przemysłowe, (np. zbudowane przez firmę CARPCO SMS nadprzewodnikowe urządzenie pod nazwą CRYOFILTER generujące pole o indukcji 5 T, stosowane do separacji bardzo drobnych cząstek m. in. do uszlachetniania kaolinu). Przedstawiono laboratoryjny nadprzewodnikowy separator matrycowy będący w dyspozycji Katedry Elektrotechniki Akademii Górniczo – Hutniczej. W kraju prace nad wdrożeniem separatorów nowej generacji, jakimi bez wątpienia są separatory nadprzewodnikowe, do praktyki przemysłowej przebiegają stosunkowo wolno. Decydują o tym zarówno względy materialne (duże koszty inwestycyjne) jak i psychologiczne (nowa technika, ekstremalne warunki eksploatacji). Argumentem przemawiającym za rozwojem przedstawionego typu konstrukcji separatów będą wyniki uzyskiwane na urządzeniu na skalę laboratoryjną. Muszą one być atrakcyjne zarówno pod względem technicznym jak i ekonomicznym. Dla pełnej oceny skuteczności proponowanego procesu wzbogacania magnetycznego i jego ekonomicznych aspektów konieczne jest przeprowadzenie pełnego cyklu badań technologicznych poczynając od modelowania procesu ekstrakcji ziaren w matrycy separatora wysokogradientowego, poprzez weryfikację eksperymentalną i określenie warunków technicznych możliwości aplikacji tego typu urządzenia w ciągu technologicznym. Ze względu na złożoność problematyki, badania takie muszą być prowadzone przez specjalistów kilku dziedzin nauki i techniki. Problem jest bowiem interdyscyplinarny, łączy m. in. przeróbkę kopalin, elektrotechnikę i kriogenikę.

Our books are available in the foolowing booksohps:
„Politechnika", Wybrzeże Wyspiańskiego 27,
50-370 Wrocław, budynek A-1 PWr, tel. (071) 320 25 34
„Tech", plac Grunwaldzki 13,
50–377 Wrocław, budynek D-1 PWr, tel. (071) 320 32 52
Orders can also be sent by post.

ISSN 0137-1282
Physicochemical Problems of Mineral Processing, 37 (2003)